

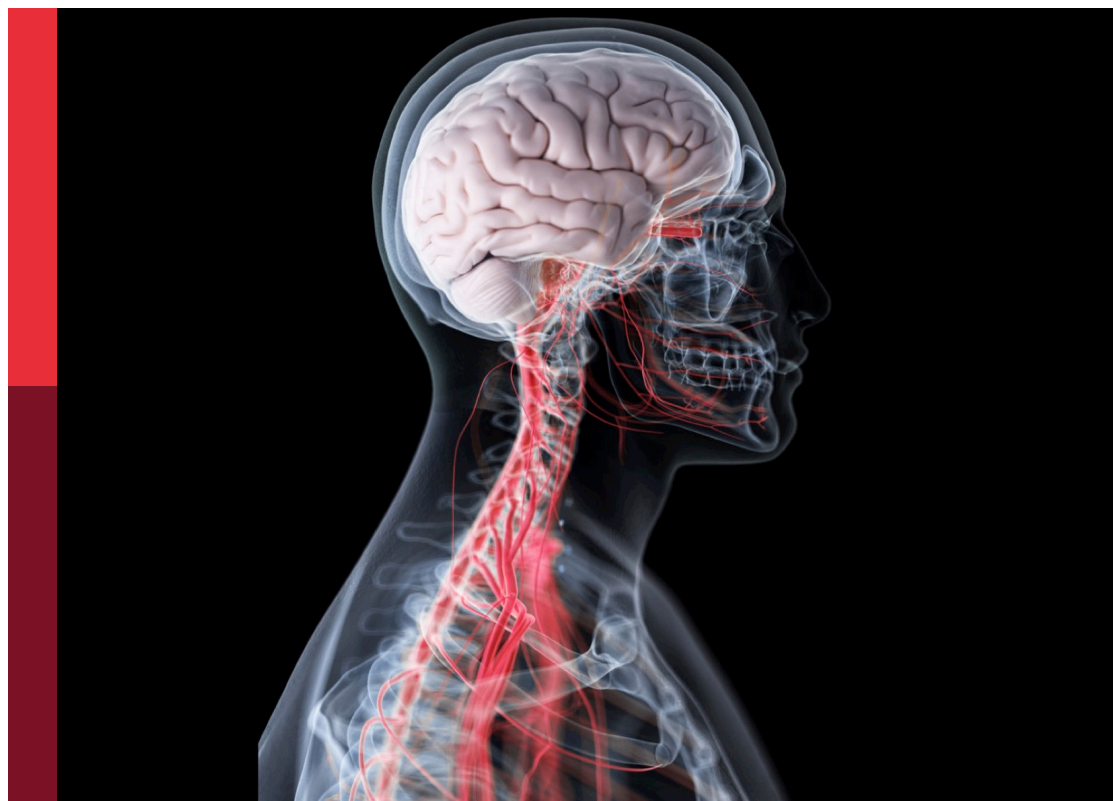
# Multimodal magnetic resonance imaging methods to explore the visual pathway and brain network changes in blindness disease

**Edited by**

Yan Tong, Zhi Wen and Xin Huang

**Published in**

Frontiers in Human Neuroscience



## FRONTIERS EBOOK COPYRIGHT STATEMENT

The copyright in the text of individual articles in this ebook is the property of their respective authors or their respective institutions or funders. The copyright in graphics and images within each article may be subject to copyright of other parties. In both cases this is subject to a license granted to Frontiers.

The compilation of articles constituting this ebook is the property of Frontiers.

Each article within this ebook, and the ebook itself, are published under the most recent version of the Creative Commons CC-BY licence. The version current at the date of publication of this ebook is CC-BY 4.0. If the CC-BY licence is updated, the licence granted by Frontiers is automatically updated to the new version.

When exercising any right under the CC-BY licence, Frontiers must be attributed as the original publisher of the article or ebook, as applicable.

Authors have the responsibility of ensuring that any graphics or other materials which are the property of others may be included in the CC-BY licence, but this should be checked before relying on the CC-BY licence to reproduce those materials. Any copyright notices relating to those materials must be complied with.

Copyright and source acknowledgement notices may not be removed and must be displayed in any copy, derivative work or partial copy which includes the elements in question.

All copyright, and all rights therein, are protected by national and international copyright laws. The above represents a summary only. For further information please read Frontiers' Conditions for Website Use and Copyright Statement, and the applicable CC-BY licence.

ISSN 1664-8714  
ISBN 978-2-83251-604-1  
DOI 10.3389/978-2-83251-604-1

## About Frontiers

Frontiers is more than just an open access publisher of scholarly articles: it is a pioneering approach to the world of academia, radically improving the way scholarly research is managed. The grand vision of Frontiers is a world where all people have an equal opportunity to seek, share and generate knowledge. Frontiers provides immediate and permanent online open access to all its publications, but this alone is not enough to realize our grand goals.

## Frontiers journal series

The Frontiers journal series is a multi-tier and interdisciplinary set of open-access, online journals, promising a paradigm shift from the current review, selection and dissemination processes in academic publishing. All Frontiers journals are driven by researchers for researchers; therefore, they constitute a service to the scholarly community. At the same time, the *Frontiers journal series* operates on a revolutionary invention, the tiered publishing system, initially addressing specific communities of scholars, and gradually climbing up to broader public understanding, thus serving the interests of the lay society, too.

## Dedication to quality

Each Frontiers article is a landmark of the highest quality, thanks to genuinely collaborative interactions between authors and review editors, who include some of the world's best academicians. Research must be certified by peers before entering a stream of knowledge that may eventually reach the public - and shape society; therefore, Frontiers only applies the most rigorous and unbiased reviews. Frontiers revolutionizes research publishing by freely delivering the most outstanding research, evaluated with no bias from both the academic and social point of view. By applying the most advanced information technologies, Frontiers is catapulting scholarly publishing into a new generation.

## What are Frontiers Research Topics?

Frontiers Research Topics are very popular trademarks of the *Frontiers journals series*: they are collections of at least ten articles, all centered on a particular subject. With their unique mix of varied contributions from Original Research to Review Articles, Frontiers Research Topics unify the most influential researchers, the latest key findings and historical advances in a hot research area.

Find out more on how to host your own Frontiers Research Topic or contribute to one as an author by contacting the Frontiers editorial office: [frontiersin.org/about/contact](https://frontiersin.org/about/contact)



# Multimodal magnetic resonance imaging methods to explore the visual pathway and brain network changes in blindness disease

## Topic editors

Yan Tong — Renmin Hospital of Wuhan University, China

Zhi Wen — Renmin Hospital of Wuhan University, China

Xin Huang — Jiangxi Provincial People's Hospital, China

## Citation

Tong, Y., Wen, Z., Huang, X., eds. (2023). *Multimodal magnetic resonance imaging methods to explore the visual pathway and brain network changes in blindness disease*. Lausanne: Frontiers Media SA. doi: 10.3389/978-2-83251-604-1

## Table of contents

- 05 **Editorial: Multimodal magnetic resonance imaging methods to explore the visual pathway and brain network changes in blindness disease**  
Zhi Wen, Yan Tong and Xin Huang
- 07 **Altered Brain Activity in Patients With Comitant Strabismus Detected by Analysis of the Fractional Amplitude of Low-Frequency Fluctuation: A Resting-State Functional MRI Study**  
Meng-Yan Hu, Yi-Cong Pan, Li-Juan Zhang, Rong-Bin Liang, Qian-Min Ge, Hui-Ye Shu, Qiu-Yu Li, Chong-Gang Pei and Yi Shao
- 16 **Abnormal Large-Scale Neuronal Network in High Myopia**  
Yu Ji, Ling Shi, Qi Cheng, Wen-wen Fu, Pei-pei Zhong, Shui-qin Huang, Xiao-lin Chen and Xiao-rong Wu
- 25 **The Predictive Values of Changes in Local and Remote Brain Functional Connectivity in Primary Angle-Closure Glaucoma Patients According to Support Vector Machine Analysis**  
Qiang Fu, Hui Liu and Yu Lin Zhong
- 34 **Altered Intrinsic Regional Spontaneous Brain Activity in Patients With Severe Obesity and Meibomian Gland Dysfunction: A Resting-State Functional Magnetic Resonance Imaging Study**  
Yi Liu, Sheng-Xing Tan, Yu-Kang Wu, Yan-Kun Shen, Li-Juan Zhang, Min Kang, Ping Ying, Yi-Cong Pan, Hui-Ye Shu and Yi Shao
- 46 **Abnormal Fractional Amplitude of Low Frequency Fluctuation Changes in Patients With Dry Eye Disease: A Functional Magnetic Resonance Imaging Study**  
Rong-Bin Liang, Li-Qi Liu, Wen-Qing Shi, Tie Sun, Qian-Min Ge, Qiu-Yu Li, Hui-Ye Shu, Li-Juan Zhang and Yi Shao
- 57 **Altered Homotopic Connectivity in the Cerebellum Predicts Stereopsis Dysfunction in Patients With Comitant Exotropia**  
Fei Chen, Zhirou Hu, Hui Liu, Fangyuan Zhen, Chenlu Liu and Qiuming Li
- 63 **Abnormal Functional Connectivity Between Cerebral Hemispheres in Patients With High Myopia: A Resting fMRI Study Based on Voxel-Mirrored Homotopic Connectivity**  
Yi Cheng, Xiao-Lin Chen, Ling Shi, Si-Yu Li, Hui Huang, Pei-Pei Zhong and Xiao-Rong Wu
- 69 **Alteration of Degree Centrality in Adolescents With Early Blindness**  
Zhi Wen, Yan Kang, Yu Zhang, Huaguang Yang and Baojun Xie
- 76 **Reduction of Interhemispheric Homotopic Connectivity in Cognitive and Visual Information Processing Pathways in Patients With Thyroid-Associated Ophthalmopathy**  
Chen-Xing Qi, Zhi Wen and Xin Huang

- 87 **Altered Temporal Dynamics of the Amplitude of Low-Frequency Fluctuations in Comitant Exotropia Patients**  
Ri-Bo Chen, Shu-Yuan Ye, Chong-Gang Pei and Yu-Lin Zhong
- 94 **Exploration of abnormal dynamic spontaneous brain activity in patients with high myopia *via* dynamic regional homogeneity analysis**  
Yu Ji, Qi Cheng, Wen-wen Fu, Pei-peí Zhong, Shui-qin Huang, Xiao-lin Chen and Xiao-rong Wu
- 102 **Machine learning analysis reveals abnormal functional network hubs in the primary angle-closure glaucoma patients**  
Ri-Bo Chen, Yu-Lin Zhong, Hui Liu and Xin Huang
- 112 **Visually driven functional MRI techniques for characterization of optic neuropathy**  
Sujeevini Sujanthan, Amir Shmuel and Janine Dale Mendola
- 129 **Altered synchronous neural activities in retinal vein occlusion patients: A resting-state fMRI study**  
Yu Mei Xiao, Fan Gan, Hui Liu and Yu Lin Zhong
- 136 **Resting-state functional MRI of the visual system for characterization of optic neuropathy**  
Sujeevini Sujanthan, Amir Shmuel and Janine Dale Mendola
- 144 **Leber's hereditary optic neuropathy companied with multiple-related diseases**  
Ming-ming Sun, Huan-fen Zhou, Qiao Sun, Hong-en Li, Hong-juan Liu, Hong-lu Song, Mo Yang, Da Teng, Shi-hui Wei and Quan-gang Xu



## OPEN ACCESS

EDITED AND REVIEWED BY  
Mingzhou Ding,  
University of Florida, United States

\*CORRESPONDENCE  
Xin Huang  
✉ huangxin5921@126.com

<sup>†</sup>These authors have contributed equally to this work

SPECIALTY SECTION  
This article was submitted to  
Brain Imaging and Stimulation,  
a section of the journal  
Frontiers in Human Neuroscience

RECEIVED 13 January 2023  
ACCEPTED 24 January 2023  
PUBLISHED 03 February 2023

CITATION  
Wen Z, Tong Y and Huang X (2023) Editorial:  
Multimodal magnetic resonance imaging  
methods to explore the visual pathway and  
brain network changes in blindness disease.  
*Front. Hum. Neurosci.* 17:1143465.  
doi: 10.3389/fnhum.2023.1143465

COPYRIGHT  
© 2023 Wen, Tong and Huang. This is an  
open-access article distributed under the terms  
of the [Creative Commons Attribution License](#)  
(CC BY). The use, distribution or reproduction  
in other forums is permitted, provided the  
original author(s) and the copyright owner(s)  
are credited and that the original publication in  
this journal is cited, in accordance with  
accepted academic practice. No use,  
distribution or reproduction is permitted which  
does not comply with these terms.

# Editorial: Multimodal magnetic resonance imaging methods to explore the visual pathway and brain network changes in blindness disease

Zhi Wen<sup>1†</sup>, Yan Tong<sup>2†</sup> and Xin Huang<sup>3\*</sup>

<sup>1</sup>Department of Radiology, Renmin Hospital of Wuhan University, Wuhan, China, <sup>2</sup>Department of Ophthalmology and Visual Sciences, Faculty of Medicine, The Chinese University of Hong Kong, Shatin, Hong Kong SAR, China, <sup>3</sup>Department of Ophthalmology, Jiangxi Provincial People's Hospital, The First Affiliated Hospital of Nanchang Medical College, Nanchang, Jiangxi, China

## KEYWORDS

blindness disease, visual cortex, brain network, fMRI, DTI, ASL

## Editorial on the Research Topic

**Multimodal magnetic resonance imaging methods to explore the visual pathway and brain network changes in blindness disease**

Diseases leading to blindness, such as glaucoma, diabetic retinopathy, optic neuritis and hereditary optic neuropathy, are a global problem. These diseases reduce visual acuity or are related to visual field defects, which results in severe morbidity in affected individuals.

Clinical imaging research related to blindness has shifted from the focus on the orbit to the changes in the structure and function of the brain. According to the symptoms and sensory dysfunctions of many eye diseases, the structure and function of the brain has been affected. FMRI is a non-invasive technique that can reveal these corresponding changes in the brain. It also provides a large amount of evidence of the structural and functional changes of the visual pathway after vision loss, and shows how the visual pathway is affected by eye diseases. More importantly, the development of algorithms and analysis enables us to discover new and valuable biomarkers from the current data. These advanced methods, combined with ophthalmological examination, enable researchers to infer the underlying mechanism of clinical manifestations from different aspects. It might provide new insights into the neuronal characteristics of visual impairment, identify the disease characteristics objectively and accurately, and provide promising therapies on this basis.

In this Research Topic, we collected 16 articles on a broad spectrum of blindness diseases. The authors introduced new imaging indicators, classified them by using machine learning, reviewed the literature and made contributions to this Research Topic. In this editorial, we give an overview of these different articles and group them according to the study design.

## Regional indicators

Hu et al. and Liang et al. explored the fractional amplitude of low-frequency fluctuation (fALFF) changes of patients with comitant exotropia and dry eye disease, respectively, compared to healthy controls (HC). ROC curve showed high diagnostic value of fALFF for distinguishing disease from HC.

Xiao et al. and Liu et al. examined the regional homogeneity (ReHo) changes in patients with retinal vein occlusion and with severe obesity and meibomian gland dysfunction, respectively. Fu et al. applied ReHo and functional connectivity (FC) method to assess the altered local and remote connectivity in primary angle-closure glaucoma (PACG). The accuracy of ReHo to distinguish PACG from HC is good by using the support vector machine (SVM) method.

Chen, Zhong, et al. and Wen et al. used the degree centrality (DC) and SVM method to determine the potential neuropathological mechanism of primary angle-closure glaucoma (PACG) and with early blindness caused by nystagmus, respectively. The accuracy of DC to distinguish PACG from HC is certain.

## Dynamic regional indicators

Ji, Cheng, et al. and Chen, Ye, et al. used ReHo and the amplitude of low-frequency fluctuation (ALFF) combined with sliding window method to evaluate the changes of dynamic neural activity in patients with high myopia and comitant exotropia, respectively, which was helpful to the diagnosis of the diseases. However, by using dALFF map as the classification feature and the SVM method, the discrimination of CE from HC was not good.

## Functional connectivity and large-scale network indicators

Homotopic connectivity as a key feature of the brain, is also a research hotspot. Qi et al., Cheng et al., and Chen, Hu, et al. applied voxel-mirrored homotopic connectivity (VMHC) method to evaluate the changes of FC between hemispheres in patients with thyroid-associated ophthalmopathy, high myopia, and comitant exotropia relative to HC, respectively. Moreover, Qi et al. and Chen, Hu, et al. took the VMHC as the classification feature, SVM method had achieved good performance in distinguishing patients from HC.

Ji, Shi, et al. used independent component analysis (ICA) to detect the changes of FC and functional network connectivity (FNC) within and between resting-state networks (RSNs) in patients with high myopia. It was found that the default mode network and cerebellar dysfunction were related to visual, cognitive and motor balance deficits.

## Literature review

Two literature reviews by Sujanthan et al. reviewed the efforts made by visually-driven fMRI (Sujanthan et al.) and rs-fMRI (Sujanthan et al.) on optic neuropathy, respectively, covered the changes of region activity, FC, and FNC. These papers emphasized the importance of multidimensional representation of optic neuropathy.

Last but not least, Sun et al. reported that clinical, radiologic characteristics of Leber's hereditary optic neuropathy (LHON) associated with multiple-related diseases, especially different subtypes of optic neuritis (ON), which were exhibited with idiopathic orbital inflammatory syndrome (IOIS) and compression optic neuropathy for the first time in this cohort. This condition may be a distinct entity with an unusual clinical and therapeutic profile.

In short, in the current Research Topics, most articles are devoted to describing the characteristics of blindness diseases in a single modality. We imagine that it is possible to integrate the information among multi-dimensional modalities and provide a comprehensive description of a specific disease in future. In addition, with the large-scale data, machine learning and artificial intelligence will help to understand the mechanism, to diagnose accurately, and to optimize treatment of blindness.

## Author contributions

ZW: writing original draft. YT and XH: writing review and editing. All authors contributed to the article and approved the submitted version.

## Funding

This work was supported by the Natural Science Foundation of Jiangxi Province (grant no. 20212BAB216058), Jiangxi Provincial Health Technology Project (grant nos. 202210012 and 202310114), Jiangxi Provincial traditional Chinese Technology Project (grant no. 2022B840), and Fundamental Research Funds for the Central Universities (grant no. 2042018kf0178).

## Conflict of interest

The authors declare that the research was conducted in the absence of any commercial or financial relationships that could be construed as a potential conflict of interest.

## Publisher's note

All claims expressed in this article are solely those of the authors and do not necessarily represent those of their affiliated organizations, or those of the publisher, the editors and the reviewers. Any product that may be evaluated in this article, or claim that may be made by its manufacturer, is not guaranteed or endorsed by the publisher.



# Altered Brain Activity in Patients With Comitant Strabismus Detected by Analysis of the Fractional Amplitude of Low-Frequency Fluctuation: A Resting-State Functional MRI Study

Meng-Yan Hu<sup>†</sup>, Yi-Cong Pan<sup>†</sup>, Li-Juan Zhang, Rong-Bin Liang, Qian-Min Ge, Hui-Ye Shu, Qiu-Yu Li, Chong-Gang Pei\* and Yi Shao\*

## OPEN ACCESS

### Edited by:

Xin Huang,  
Jiangxi Provincial People's Hospital,  
China

### Reviewed by:

Guanghui Liu,  
Fujian Provincial People's Hospital,  
China  
Yuan Liu,  
University of Miami Health System,  
United States

### \*Correspondence:

Yi Shao  
freebee99@163.com  
Chong-Gang Pei  
peichonggang11@163.com

<sup>†</sup>These authors have contributed  
equally to this work

### Specialty section:

This article was submitted to  
Brain Imaging and Stimulation,  
a section of the journal  
Frontiers in Human Neuroscience

**Received:** 12 February 2022

**Accepted:** 21 March 2022

**Published:** 08 April 2022

### Citation:

Hu M-Y, Pan Y-C, Zhang L-J,  
Liang R-B, Ge Q-M, Shu H-Y, Li Q-Y,  
Pei C-G and Shao Y (2022) Altered  
Brain Activity in Patients With  
Comitant Strabismus Detected by  
Analysis of the Fractional Amplitude  
of Low-Frequency Fluctuation:  
A Resting-State Functional MRI  
Study.  
Front. Hum. Neurosci. 16:874703.  
doi: 10.3389/fnhum.2022.874703

Department of Ophthalmology, Jiangxi Province Ocular Disease Clinical Research Center, The First Affiliated Hospital of Nanchang University, Nanchang, China

More and more studies showed that strabismus is not simply an ocular disease, but a neuro-ophthalmology disease. To analyze potential changes in brain activity and their relationship to behavioral performance in comitant strabismus patients and healthy controls. Our study recruited 28 patients with comitant strabismus and 28 people with matched weight, age range, and sex ratio as healthy controls. Using resting-state functional magnetic resonance imaging, we evaluated fALFF to compare spontaneous brain activity between comitant strabismus and healthy controls. We did hospital anxiety and depression scale questionnaires for these patients. We found significantly lower fALFF value in comitant strabismus patients compared with controls in the left frontal superior medial gyrus and the right middle cingulum. In the latter region, fALFF was significantly negatively correlated with the hospital anxiety and depression scale, as well as the duration of disease. Receiver operating characteristic curve analysis indicated that the fALFF method has clear potential for the diagnosis of comitant strabismus patients. These results revealed abnormal spontaneous activity in two brain regions of comitant strabismus patients, which may indicate underlying pathologic mechanisms and may help to advance clinical treatment.

**Keywords:** fractional amplitude of low-frequency fluctuation, comitant strabismus, brain changes, depression and anxiety, resting-state functional magnetic resonance imaging

## INTRODUCTION

Strabismus is an eye disorder characterized by vertical, horizontal or rotational deviation of one eye relative to the other, and can lead to binocular visual impairment and amblyopia, further result in neuropathology outcomes, such as depression and anxiety (Chia et al., 2010; Feng et al., 2015). More and more studies showed that strabismus is not simply an ocular disease, but a neuro-ophthalmology disease (Jackson et al., 2006; Cumurcu et al., 2011; Alpak et al., 2014). According to a meta-analysis, the prevalence of strabismus was about 2.0%, regardless of age or sexual difference (Hashemi et al., 2019). In another study conducted in Eastern China, strabismus prevalence was 5.65% (320 out of 5,667) in preschool students aged 36-72 months, among the 320 strabismus students, 302 were diagnosed as comitant strabismus (CS) (Chen et al., 2016).



Comitant strabismus is the most common type of strabismus characterized by constant angle of strabismus (deviation) in all directions of gaze (Robaei et al., 2006). With either eye used for fixation, the deviation angle remains unchanged. The etiology and pathophysiology of CS is complex and remains unclear. Several risk factors may have contributed to the onset or progress of CS, such as family history, systemic disease, genetic syndrome, dysfunction of extraocular muscles, as well as neuromuscular imbalance (Gunton et al., 2015). Stereopsis impairment and abnormal eye position are the main clinical manifestations of strabismus in adults. Meanwhile, CS children may suffer more severe complication. In addition to disabling diplopia and cosmetic consequence, it may further impair learning ability and result in psychosocial problem (Jackson et al., 2006; Chia et al., 2010). Other studies also showed psychiatric problems in CS patients, such as anxiety and depression (Cumurcu et al., 2011; Alpak et al., 2014). At present, surgical treatment is the most effective method of strabismus correction, which may be important not only for visual correction but also to improve cosmetic and social anxiety, especially in some groups of patients, such as graduates (Estes et al., 2020).

Previous studies showed brain changes in depressed patients, such as enhanced default mode network connectivity with ventral striatum, lower cortical thickness in the left frontal brain regions (Fonseka et al., 2016; Hwang et al., 2016). Another study found declined insular volume in patients with social anxiety (Kawaguchi et al., 2016). As mentioned above, depression and anxiety disorders were also revealed in CS patients, thus brain abnormalities may also exist in CS patients.

In fact, animal studies on strabismus have already revealed functional alterations in the visual cortex and connection changes between brain regions. Studies on strabismic monkeys demonstrated both structural (neuron loss) and functional (reduced metabolic activity) alterations in the primary visual cortex (Crawford and von Noorden, 1979; Adams et al., 2013). Moreover, Schmidt and Lowel (2006) made strabismus animal model via cats, they found that functional maps in area 17 were affected by experience-dependent manipulations, while those in area 18 remain still (Schmidt and Lowel, 2006).

With the development in magnetic resonance imaging technique, we are able to evaluate the human brain changes functionally and anatomically in resting-state (Biswal, 2012). The resting-state functional magnetic resonance imaging (rs-fMRI) method can provide important information about brain activity and it is widely used to investigate spontaneous functional magnetic resonance imaging signals (Zang et al., 2004; Wang et al., 2012; Song et al., 2021). Compared to task-based fMRI, rs-fMRI analyses signal without any specific task or an input, thus patients who have difficulty in accomplishing the task, i.e., pediatric patients, can still undergo rs-fMRI (Smitha et al., 2017).

The amplitude of low-frequency fluctuations (ALFF) is a common rs-fMRI technique used to investigate spontaneous brain activity at rest via measuring the blood-oxygen level-dependent (BOLD) signals (Logothetis et al., 2001; Zuo et al., 2010; Huang et al., 2015; Shao et al., 2015). ALFF reflects the amplitude of signal fluctuations in a single time series per voxel, not unlike the concepts of “power” or “energy”

used in electroencephalogram studies. Statistically, it reflects the mean deviation, standard deviation or variance of signals in a given frequency band, which are all relative values. In contrast, fractional ALFF (fALFF) is a normalized parameter that reflects the contribution of specific low-frequency oscillations relative to the entire frequency range. It is less sensitive to physiological noise than that in ALFF method, indicating that fALFF may detect abnormal brain activities with higher sensitivity and specificity (Zou et al., 2008). The fALFF method has already been applied to study potential neuropathological mechanisms of ophthalmologic diseases such as monocular blindness, different kinds of glaucoma (Li et al., 2014, 2020; Fang et al., 2020; Wang et al., 2021), as well as neurogenic diseases like narcolepsy, idiopathic epilepsy and Parkinson's disease (Qiao and Niu, 2017; Tang et al., 2017; Xiao et al., 2018). But to our knowledge it has not been used in CS. In this study, we used the fALFF method to investigate the relationship between CS and brain activity.

## MATERIALS AND METHODS

### Subjects

Twenty-eight patients with comitant strabismus and another twenty-eight healthy controls were recruited from the First Affiliated Hospital of Nanchang University. The diagnostic criteria of comitant strabismus were: (1) congenital strabismus; (2) stereovision defect (no visual fusion); (3) in the case of alternating strabismus, the strabismus angles were equal; (4) best corrected visual acuities > 1.0 in both eyes.

Twenty-eight healthy controls (HCs) were recruited, matched in terms of age range, sex ratio and education level and with uncorrected or best corrected visual acuity of 1.0 or better.

Participants who met any of the following conditions were excluded from the study: (1) acquired or incomitant strabismus, concealed oblique, and amblyopia, as well as diplopia; (2) history of intraocular or extraocular eye surgery; (3) history of eye diseases (infection, inflammation, ischemic diseases); (4) history of refractive error (myopia higher than  $-1.5D$ , hyperopes or anisometropes); (5) history of mental health disorders (such as anxiety disorder, obsessive-compulsive disorder, depression or schizophrenia), diabetes, cerebral infarction or cardiovascular diseases; (6) history of addictions (alcohol and/or drugs); (7) abnormality of brain parenchyma shown by MRI; (8) contraindication for MRI scanning.

All research methods were approved by the committee of the medical ethics of the First Affiliated Hospital of Nanchang University and were in accordance with the 1964 Helsinki declaration and its later amendments or comparable ethical standards. All subjects were explained the purpose, method, potential risks and signed an informed consent form.

### Administration of Hospital Anxiety and Depression Scale

The Hospital Anxiety and Depression Scale (HADS) is a simple yet reliable tool for assessing anxiety and depression (Snaith, 2003). For participants who were illiterate or were unable to read due to visual impairment, an investigator read the questionnaire

aloud. In all participants, an investigator verbally explained the purpose of the questionnaire and its confidential nature.

## Magnetic Resonance Imaging Scanning

Magnetic resonance imaging scanning was performed using a 3T MR scanner (Trio, Siemens, Munich, Germany). The subjects were in the supine position, wearing earplugs to reduce noise during scanning, and were required to stay awake with eye closed and maintain quiet breathing throughout the scanning period of 15 minutes. The range of head movement during scanning was  $< 3\text{ mm}$ , and the head rotation range was  $< 2.5^\circ$ . The structural images were obtained using single-shot gradient-recalled echo planar imaging sequence with following parameters: repetition time/echo time = 1900/2.26 ms, flip angle =  $9^\circ$ , field of view =  $250 \times 250\text{ mm}$ , matrix =  $256 \times 256$ , slice thickness/gap = 1.0/0.5 mm, images = 176. Besides, each participant underwent three-dimensional metamorphic gradient echo pulse planar imaging with parameters as follows: repetition time/echo time = 2000/40 ms, flip angle =  $90^\circ$ , field of view =  $220 \times 220\text{ mm}$ , matrix =  $64 \times 64$ , slice thickness/gap = 4.0/1.0 mm, images = 240. 30 axial slices were obtained at each time point. The whole scanning time was 8 minutes and no substantial lesions of the brain were found.

## Rs-fMRI Data Processing

For data acquisition and processing, MRICron<sup>1</sup> was employed to classify functional data and eliminate incomplete data. Statistical Parametric Mapping (SPM8)<sup>2</sup> was used to preprocess rs-fMRI images. The processing protocols were as follows: (1) the original data were converted to Neuroimaging Informatics Technology Initiative (NIFTI) format; (2) The first 10 functional images were removed to balance the signal; (3) slice timing and head motion correction; (4) normalization of rs-fMRI images to the standard Montreal Institute of Neurology (MNI) templates and resampled to  $3 \times 3 \times 3\text{ mm}$  voxels; (5) image smoothing with a 6-mm full-width-half-maximum (FWHM) Gaussian to reduce spatial noise; (6) regression of covariates including six head movement parameters, mean framewise displacement, and average signals from white matter, cerebrospinal fluid, and global brain activity; (7) removal of linear trends.

## fALFF Analysis

The fALFF method was used to analyze the fMRI data. The Resting-State fMRI Data Analysis Toolkit (REST)<sup>3</sup> was used to convert time series data into the frequency domain and calculate the power spectrum. The fALFF value was calculated as the ratio of the low-frequency range (0.01–0.08 Hz) to the power spectrum of the entire frequency range (0–0.25 Hz). In addition, the fALFF value was normalized to the whole-brain mean fALFF to reduce inter-subject variability, and a band-pass filtering of 0.01–0.08 Hz was used to minimize deviation from heartbeats and respiratory rhythm.

<sup>1</sup><http://www.nitrc.org/projects/mricron>

<sup>2</sup><http://www.fil.ion.ucl.ac.uk/spm>

<sup>3</sup><http://restfmri.net/forum/REST>

## Statistical Analysis

Brain areas with significant changes in frequency or overall fALFF were selected as regions of interest (ROIs). Two-sample *t*-tests were used to compare fALFF values at the ROIs between the CS and HC groups with sex and age as covariates to control for these factors. Receiver operating characteristic (ROC) curves were also used to assess sensitivity of the discrimination between mean fALFF values in the two groups. In addition, Pearson's correlation was used to assess the relationship between fALFF and both disease duration and HADS score. Analyses were conducted using SPSS version 13.0 statistical software for Windows (SPSS, IBM Corp., United States), and statistical figures were generated by GraphPad Prism 8 software (the GraphPad Software, Inc. La Jolla, CA, United States). \* meant *P* value  $< 0.05$  and was considered statistically significant in all cases.

## RESULTS

### Demographics and Visual Measurements

No significant between-group differences were found (Table 1) in sex ( $p > 0.99$ ), age ( $p = 0.324$ ), weight ( $p = 0.585$ ), handedness ( $p > 0.99$ ), best-corrected VA-DE ( $p = 0.256$ ), or best-corrected VA-FE ( $p = 0.212$ ) between CS and HCs.

### RsfMRI-FALFF Results and Brain Regions

Significantly lower fALFF values were found in the CS compared with HC group in the Frontal\_Sup\_Medial\_L and the Cingulum\_Mid\_R brain regions ( $p = 0.012$  and  $p = 0.039$ , respectively) (Figures 1, 2). Corresponding voxels and coordinate are demonstrated (Table 2).

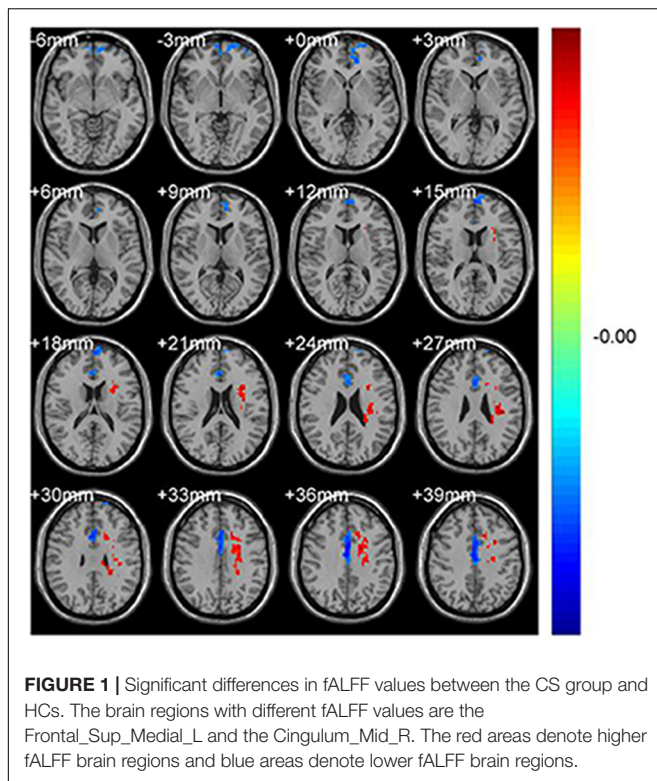
### ROC Curve Analysis

ROC curve analysis was conducted using fALFF values of the two brain regions found to differ between the groups. The areas under the ROC curves were 0.960 ( $p < 0.001$ ; 95% CI: 0.899–1.000) for Frontal\_Sup\_Medial\_L and 0.929 ( $p < 0.001$ ; 95% CI: 0.843–1.000) for the Cingulum\_Mid\_R (Figure 3).

**TABLE 1 |** The conditions of participants included in the study.

Condition	CS	HCS,	t-value	P-value*
Male/female	18/10	18/10	N/A	$> 0.99$
Age (years)	$17.39 \pm 3.56$	$18.68 \pm 2.56$	−1.285	0.365
Weight (kg)	$56.76 \pm 3.66$	$60.59 \pm 3.13$	−0.674	0.576
Handedness	28R	28R	N/A	$> 0.99$
Best-corrected VA-DE	$1.05 \pm 0.10$	$1.15 \pm 0.10$	1.645	0.243
Best-corrected VA-FE	$1.05 \pm 0.15$	$1.15 \pm 0.10$	1.714	0.252
Duration of CTR (days)	$17.39 \pm 3.56$	N/A	N/A	N/A
Esotropia/exotropia	10/18	N/A	N/A	N/A
Angle of strabismus (PD)	$40.25 \pm 11.05$	N/A	N/A	N/A

Independent *t*-tests comparing two groups ( $P < 0.05$  represented statistically significant differences). CS, comitant strabismus; HCs, healthy controls; N/A, not applicable; PD, prism diopter; VA, visual acuity; DE, dominant eye; FE, fellow eye.



## Correlation Analysis of the fALFF Values and Clinical Measurements in Comitant Strabismus Patients

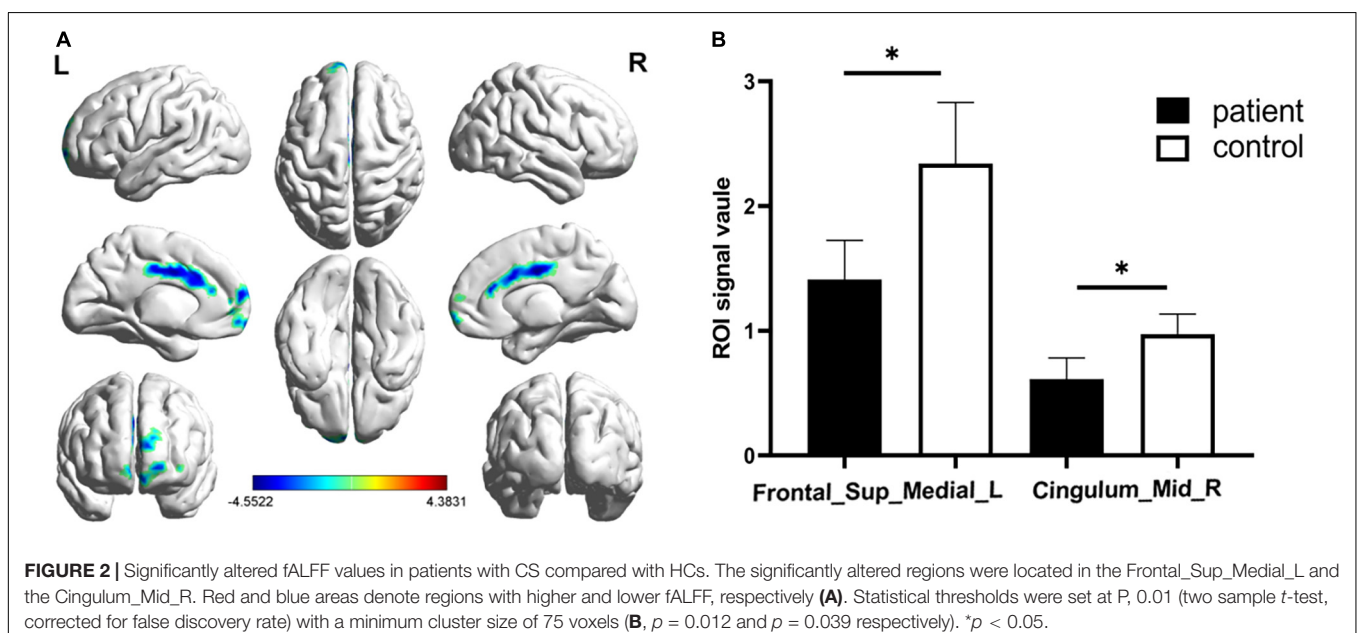
Mean Cingulum\_Mid\_R fALFF values in CS patients were negatively correlated with duration of the disease ( $r = -0.803$ ,  $p < 0.0001$ ) and with HADS score ( $r = -0.829$ ,  $p < 0.0001$ )

(Figures 4A,B). While in the Frontal\_Sup\_Medial\_L, the fALFF values showed no correlation with duration of the disease ( $r = -0.156$ ,  $p = 0.429$ ) or HADS score ( $r = -0.126$ ,  $p = 0.523$ ) (Figures 4C,D).

## DISCUSSION

The fALFF method can provide information about spontaneous brain activity, is considered to represent the process of spontaneity as well as function, and has been successfully applied in patients with ophthalmic and neurogenic diseases (Table 3). To our knowledge, however, this method has not previously been used in patients with comitant strabismus. In the present study, compared with healthy controls, significantly lower fALFF values were found in two brain regions, the left frontal lobe (Frontal\_Sup\_Medial\_L) and the right cingulum (Cingulum\_Mid\_R), in patients with comitant strabismus. In addition, correlation analysis showed significant negative correlation between the fALFF values of the Cingulum\_Mid\_R and the duration of CS, as well as HADS score.

While the fALFF method has not previously been used to assess spontaneous brain activities in patients with comitant strabismus, fMRI has been used with other analysis methods in research on comitant strabismus. Huang et al. used regional homogeneity (ReHo) methods to analyze brain activity in comitant strabismus and found significantly increased ReHo values in several brain areas, including the cingulate gyrus (Huang et al., 2016). In another ALFF study, congenital comitant strabismus patients showed significantly higher ALFF values in some brain regions, while lower values were found in others, such as the frontal gyrus (Tan et al., 2016). Previous research by our group measured degree centrality (DC) values in comitant exotropia strabismus patients and found contrasting changes in different brain regions, such as increased DC values in the



**TABLE 2 |** Brain regions with significant differences in brain activities between CS and HCs.

Brain areas	MNI coordinates			BA	Number of voxels	T- value
	X	Y	Z			
HC > patient						
Frontal Sup Medial L	−12	48	0	31	156	−3.6533
Cingulum Mid R	3	−9	36	34	205	−4.5522

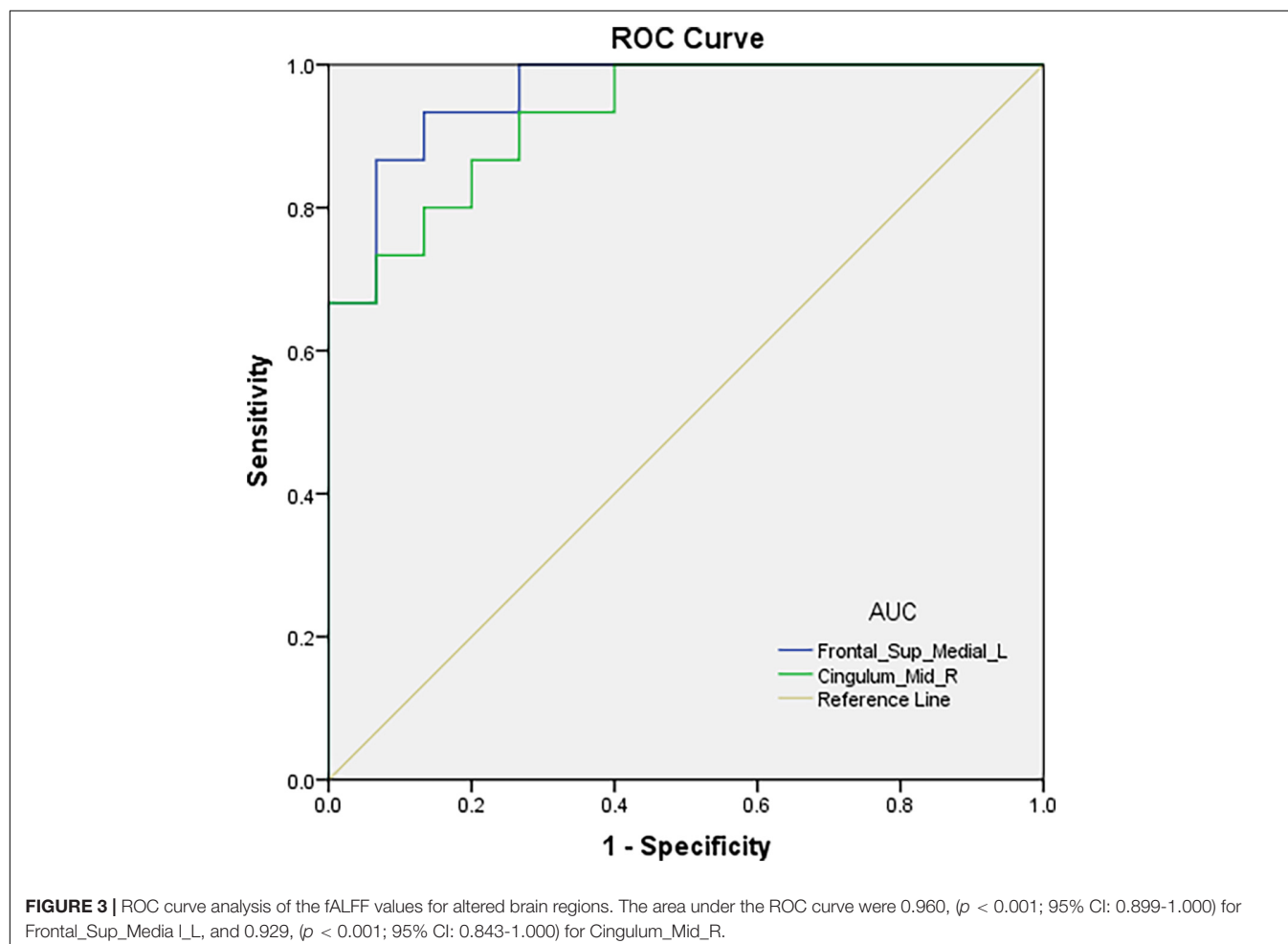
The statistical threshold was set at voxel with  $p < 0.01$  for multiple comparisons using Gaussian random field corrected. MNI, Montreal Neurological Institute; BA, brodmann area.

bilateral anterior cingulate, and decreased values in part of the frontal gyrus (Tan et al., 2018). There are still similar fMRI studies using different methods, such as voxel-based morphometry study, (Ouyang et al., 2017) and pseudo-continuous arterial spin labeling study (Huang et al., 2018), which we may not discuss in detail here. These findings are in broad agreement with those of the present study, with abnormal activity in some brain regions of patients with comitant strabismus.

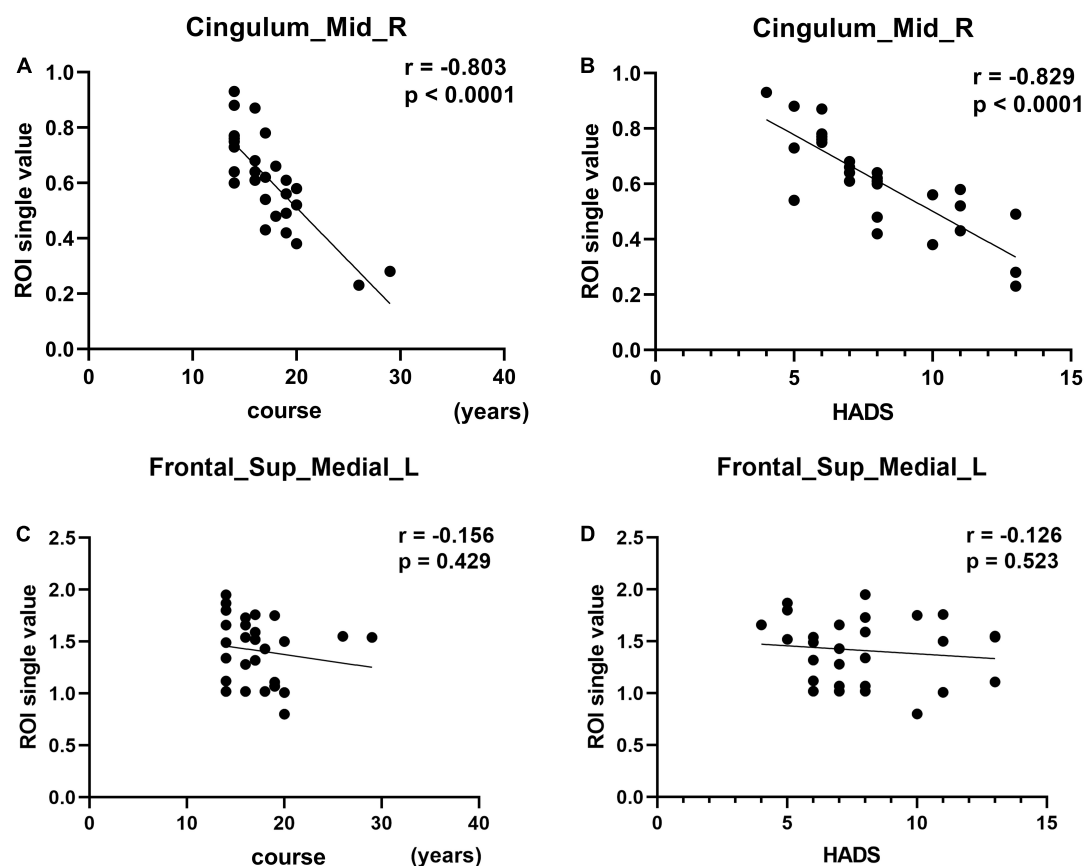
The frontal lobe is a large part of the brain comprising four subcortical circuits. Lesions in each circuit manifest

different disorders, such as voluntary movement, behavioral status, and mental activity disorders (Krudop and Pijnenburg, 2015). Besides, some part of the frontal lobe is important in integrating visual function, the frontal eye field (FEF) is located in the frontal cortex and has the function of triggering eye movements and influencing their accuracy or latency. Previous studies in monkeys have found that the FEF may play an important role in controlling eye movements (Kovelman et al., 2015). In addition, research has shown that the left middle frontal gyrus is associated with strabismus and amblyopia (Thompson et al., 1996). Specifically, lower ALFF values were in the left middle frontal gyrus in strabismic amblyopia than in controls, suggesting abnormal FEF function in this condition. Three brain regions including the Frontal\_Sup\_Medial\_L have been identified as functional candidate hubs in the process of network information transmission (Min et al., 2018). Our finding of significantly lower fALFF value in left Frontal Sup Medial region in comitant strabismus may therefore suggest abnormal network transmission in this condition.

The cingulate cortex, as an important part of the limbic system, has three major divisions. Each division is in charge of different functions: the anterior for emotion states such as







**FIGURE 4 |** Correlation between the fALFF values of the two brain regions and course and HADS. In the CS group, the fALFF value of the Cingulum\_Mid\_R showed a negative correlation with the course (**A**,  $r = -0.803$ ,  $p < 0.0001$ ). The fALFF value of the Cingulum\_Mid\_R showed a negative correlation with the HADS (**B**,  $r = -0.829$ ,  $p < 0.0001$ ). The fALFF values of Frontal\_Sup\_Medial\_L showed no correlation with the course of the disease (**C**,  $r = -0.156$ ,  $p = 0.429$ ) or HADS score (**D**,  $r = -0.126$ ,  $p = 0.523$ ).

depression and anxiety, the middle for decision making and response selection, and the posterior for visuospatial orientation (Vogt, 2019). Shinoura et al. (2013) found improved visual memory after tumorectomy, along with aggravating anxiety disorder. Since the tumors were located just above the right dorsal anterior cingulate cortex (ACC), they speculated the

improvement mainly came from the compression of the right dorsal ACC. In another ReHo study by our group, we found increased ReHo values in cingulate cortex in patients with strabismus and amblyopia (SA), indicating that cingulate gyrus played a compensatory role in the progress of SA (Huang et al., 2016). Meanwhile, contradictory to the studies mentioned above, our present study found reduced fALFF values in the Cingulum\_Mid\_R of patients with comitant strabismus. Since patients in our study all have a normal best-corrected visual acuity (BCVA), which means amblyopia patients were excluded in the study, subject differences may explain the contradiction. Further studies with more grouped patients are needed to clarify our findings. The alteration of these two brain regions and its potential impact were summarized as follow (Table 4).

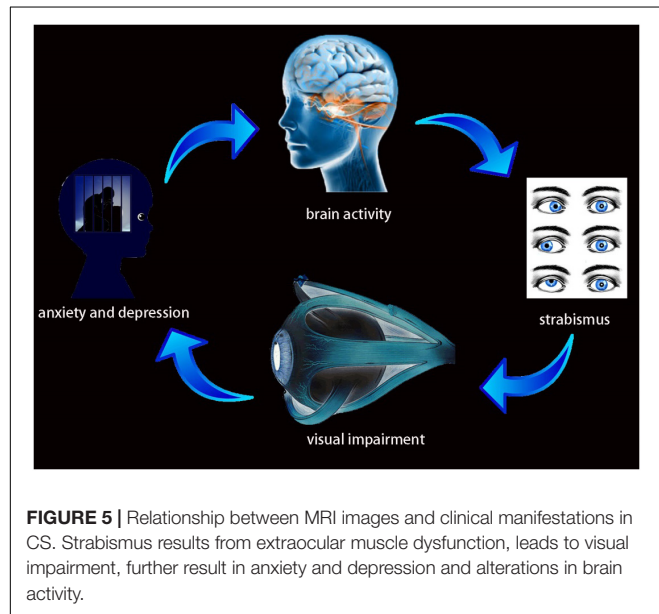
A negative correlation was also found between fALFF values of this region and the HADS score in patients with CS. As is well known, emotion plays an important role in most diseases, and as outlined above this brain region is related to depression, pain, and anxiety. On this basis, we hypothesized that patients with CS have anxiety and depression, and this was confirmed by HADS score analysis.

**TABLE 3 |** fALFF method applied in ophthalmologic and neurogenic disease.

Ophthalmologic disease	Authors and Years	Disease
	Li et al., 2014, 2020; Fang et al., 2020; Wang et al., 2021	Monocular Blindness,
		POAG
		normal-tension glaucoma
Neurogenic disease	Qiao and Niu, 2017; Tang et al., 2017; Xiao et al., 2018	PACG
		Narcolepsy Idiopathic epilepsy
		Parkinson's disease

**TABLE 4 |** Brain regions alternation and its potential impact.

Brain regions	Experimental result	Brain function	Anticipated results
Frontal_Sup_Medial_L	CS < HC.	Information transmission	eye movements
Cingulum_Mid_R.	CS < HC	Executive function, attention and memory	depression, pain, and anxiety



As mentioned above, animal experiments on strabismus displayed primary visual cortex change (Crawford and von Noorden, 1979; Adams et al., 2013). While in our present study, no significant difference was found in primary visual cortex. Since patients in our study all have a normal best-corrected visual acuity (BCVA), which means amblyopia patients were excluded in the study, we thought this may partially explain why no difference was found in primary visual cortex.

Some previous anatomical studies have shown a relationship between the Frontal\_Sup\_Medial\_L and the Cingulum\_Mid\_R (Bubb et al., 2018; Xiao et al., 2018). In the present study, activity in both of these regions was reduced in patients with comitant strabismus. Their relationship suggests the possibility that the frontal lobe injury affected the cingulate gyrus through fibrous connections, causing secondary changes in the latter, and thus triggering symptoms of anxiety and depression. We further speculated that comitant strabismus, resulting from extraocular muscle dysfunction, leads to visual impairment, further contributing to anxiety and depression and alterations in brain activity (Figure 5).

This study has some limitations. First, the sample size was not sufficiently large to subdivide patients into groups representing levels of visual acuity, strabismus angle, periods of disease development, and other variables. Larger sample rsfMRI studies may help better understand the explicit changes in brain activity and CS at different levels of severity or at different categories. Second, strabismus may cause psychological distress related to cosmesis, and this may have some impact on brain activity.

Therefore, psychological factors should be considered to exclude the impact of emotional state. Finally, our study only showed microstructural changes in many brain regions in CS patients. Whether brain activity changes are secondary to strabismus or are the cause of strabismus remains unknown. In the future, larger, more in depth studies may help to address this question.

## CONCLUSION

In conclusion, our study found significant abnormalities in two brain regions (Frontal\_Sup\_Medial\_L and Cingulum\_Mid\_R) in patients with comitant strabismus. ROC analyses indicated high accuracy of the fALFF method for diagnosing CS patients. Correlation analyses demonstrated that changes in Cingulum\_Mid\_R might help the severity of CS and predicted the incidence of depression in the CS patients. In the future, further investigations are needed to form a comprehensive understanding of the neuropathological mechanisms of comitant strabismus.

## DATA AVAILABILITY STATEMENT

The raw data supporting the conclusions of this article will be made available by the authors, without undue reservation.

## ETHICS STATEMENT

The studies involving human participants were reviewed and approved by the committee of the medical ethics of the First Affiliated Hospital of Nanchang University. Written informed consent to participate in this study was provided by the participants' legal guardian/next of kin.

## AUTHOR CONTRIBUTIONS

M-YH, YS, and C-GP designed the current study. Y-CP and L-JZ recruited healthy controls. R-BL and Q-MG performed MRI scanning. H-YS and Q-YL collected and analyzed the data. M-YH wrote the manuscript. All the authors read and approved the final manuscript.

## FUNDING

This research was supported by the Key Research Foundation of Jiangxi Province (Nos. 20203BBG73059 and 20181BBG70004), Excellent Talents Development Project of Jiangxi Province



(20192BCBL23020), Health Development Planning Commission Science Foundation of Jiangxi Province (20175115), and Education Department Youth Scientific Research Foundation (GJJ160122).

## ACKNOWLEDGMENTS

We thank the two reviewers for excellent criticism of the article.

## REFERENCES

- Adams, D. L., Economides, J. R., Sincich, L. C., and Horton, J. C. (2013). Cortical metabolic activity matches the pattern of visual suppression in strabismus. *J. Neurosci.* 33, 3752–3759. doi: 10.1523/JNEUROSCI.3228-12.2013
- Alpak, G., Coskun, E., Erbagci, I., Bez, Y., Okumus, S., Oren, B., et al. (2014). Effects of corrective surgery on social phobia, psychological distress, disease-related disability and quality of life in adult strabismus patients. *Br. J. Ophthalmol.* 98, 876–879. doi: 10.1136/bjophthalmol-2014-304888
- Biswal, B. B. (2012). Resting state fMRI: a personal history. *Neuroimage* 62, 938–944. doi: 10.1016/j.neuroimage.2012.01.090
- Bubb, E. J., Metzler-Baddeley, C., and Aggleton, J. P. (2018). The cingulum bundle: anatomy, function, and dysfunction. *Neurosci. Biobehav. Rev.* 92, 104–127. doi: 10.1016/j.neubiorev.2018.05.008
- Chen, X., Fu, Z., Yu, J., Ding, H., Bai, J., Chen, J., et al. (2016). Prevalence of amblyopia and strabismus in Eastern China: results from screening of preschool children aged 36–72 months. *Br. J. Ophthalmol.* 100, 515–519. doi: 10.1136/bjophthalmol-2015-306999
- Chia, A., Dirani, M., Chan, Y. H., Gazzard, G., Au Eong, K. G., Selvaraj, P., et al. (2010). Prevalence of amblyopia and strabismus in young singaporean chinese children. *Invest. Ophthalmol. Vis. Sci.* 51, 3411–3417. doi: 10.1167/iov.09-4461
- Crawford, M. L., and von Noorden, G. K. (1979). The effects of short-term experimental strabismus on the visual system in *Macaca mulatta*. *Invest. Ophthalmol. Vis. Sci.* 18, 496–505.
- Cumurcu, T., Cumurcu, B. E., Ozcan, O., Demirel, S., Duz, C., Porgali, E., et al. (2011). Social phobia and other psychiatric problems in children with strabismus. *Can. J. Ophthalmol.* 46, 267–270. doi: 10.1016/j.jcjo.2011.05.017
- Estes, K. J., Parrish, R. K., Sinacore, J., Mumby, P. B., and McDonnell, J. F. (2020). Effects of corrective strabismus surgery on social anxiety and self-consciousness in adults. *J. AAPOS* 24, 280.e1–280.e4. doi: 10.1016/j.jaapos.2020.05.017
- Fang, J. W., Yu, Y. J., Tang, L. Y., Chen, S. Y., Zhang, M. Y., Sun, T., et al. (2020). Abnormal Fractional Amplitude of Low-Frequency Fluctuation Changes in Patients with Monocular Blindness: A Functional Magnetic Resonance Imaging (MRI) Study. *Med. Sci. Monit.* 26:e926224. doi: 10.12659/MSM.926224
- Feng, X., Zhang, X., and Jia, Y. (2015). Improvement in fusion and stereopsis following surgery for intermittent exotropia. *J. Pediatr. Ophthalmol. Strabismus.* 52, 52–57. doi: 10.3928/01913913-20141230-08
- Fonseka, B. A., Jaworska, N., Courtright, A., MacMaster, F. P., and MacQueen, G. M. (2016). Cortical thickness and emotion processing in young adults with mild to moderate depression: a preliminary study. *BMC Psychiat.* 16:38. doi: 10.1186/s12888-016-0750-8
- Gunton, K. B., Wasserman, B. N., and DeBenedictis, C. (2015). Strabismus. *Prim. Care* 42, 393–407. doi: 10.1016/j.pop.2015.05.006
- Hashemi, H., Pakzad, R., Heydarian, S., Yekta, A., Aghamirsalim, M., Shokrollahzadeh, F., et al. (2019). Global and regional prevalence of strabismus: a comprehensive systematic review and meta-analysis. *Strabismus* 27, 54–65. doi: 10.1080/09273972.2019.1604773
- Huang, X., Cai, F. Q., Hu, P. H., Zhong, Y. L., Zhang, Y., Wei, R., et al. (2015). Disturbed spontaneous brain-activity pattern in patients with optic neuritis using amplitude of low-frequency fluctuation: a functional magnetic resonance imaging study. *Neuropsychiatr. Dis. Treat.* 11, 3075–3083. doi: 10.2147/NDT.S92497
- Huang, X., Li, S. H., Zhou, F. Q., Zhang, Y., Zhong, Y. L., Cai, F. Q., et al. (2016). Altered intrinsic regional brain spontaneous activity in patients with comitant

## SUPPLEMENTARY MATERIAL

The Supplementary Material for this article can be found online at: <https://www.frontiersin.org/articles/10.3389/fnhum.2022.874703/full#supplementary-material>

**Supplementary Figure 1** | HADS value between CS patients and healthy controls. HCs showed significantly lower HADS scores than that of CS ( $p < 0.0001$ ).

- strabismus: a resting-state functional MRI study. *Neuropsychiatr. Dis. Treat.* 12, 1303–1308. doi: 10.2147/NDT.S105478
- Huang, X., Zhou, S., Su, T., Ye, L., Zhu, P. W., Shi, W. Q., et al. (2018). Resting cerebral blood flow alterations specific to the comitant exophoria patients revealed by arterial spin labeling perfusion magnetic resonance imaging. *Microvasc. Res.* 120, 67–73. doi: 10.1016/j.mvr.2018.06.007
- Hwang, J. W., Xin, S. C., Ou, Y. M., Zhang, W. Y., Liang, Y. L., Chen, J., et al. (2016). Enhanced default mode network connectivity with ventral striatum in subthreshold depression individuals. *J. Psychiat. Res.* 76, 111–120. doi: 10.1016/j.jpsychires.2016.02.005
- Jackson, S., Harrad, R. A., Morris, M., and Rumsey, N. (2006). The psychosocial benefits of corrective surgery for adults with strabismus. *Br. J. Ophthalmol.* 90, 883–888. doi: 10.1136/bjo.2005.089516
- Kawaguchi, A., Nemoto, K., Nakaaki, S., Kawaguchi, T., Kan, H., Arai, N., et al. (2016). Insular Volume Reduction in Patients with Social Anxiety Disorder. *Front. Psychiat.* 7:3. doi: 10.3389/fpsyt.2016.00003
- Kovelman, I., Wagley, N., Hay, J. S., Ugolini, M., Bowyer, S. M., Lajiness-O'Neill, R., et al. (2015). Multimodal imaging of temporal processing in typical and atypical language development. *Ann. N.Y. Acad. Sci.* 1337, 7–15. doi: 10.1111/nyas.12688
- Krudop, W. A., and Pijnenburg, Y. A. (2015). Historical evolution of the frontal lobe syndrome. *Psychopathology* 48, 222–229. doi: 10.1159/000381986
- Li, H. L., Chou, X. M., Liang, Y., Pan, T., Zhou, Q., Pei, C. G., et al. (2020). Use of rsfMRI-fALFF for the detection of changes in brain activity in patients with normal-tension glaucoma. *Acta Radiol.* 62:284185120926901. doi: 10.1177/0284185120926901
- Li, T., Liu, Z., Li, J., Liu, Z., Tang, Z., Xie, X., et al. (2014). Altered amplitude of low-frequency fluctuation in primary open-angle glaucoma: a resting-state FMRI study. *Invest. Ophthalmol. Vis. Sci.* 56, 322–329. doi: 10.1167/iov.14-14974
- Logothetis, N. K., Pauls, J., Augath, M., Trinath, T., and Oeltermann, A. (2001). Neurophysiological investigation of the basis of the fMRI signal. *Nature* 412, 150–157. doi: 10.1038/35084005
- Min, Y. L., Su, T., Shu, Y. Q., Liu, W. F., Chen, L. L., Shi, W. Q., et al. (2018). Altered spontaneous brain activity patterns in strabismus with amblyopia patients using amplitude of low-frequency fluctuation: a resting-state FMRI study. *Neuropsychiatr. Dis. Treat.* 14, 2351–2359. doi: 10.2147/NDT.S171462
- Ouyang, J., Yang, L., Huang, X., Zhong, Y. L., Hu, P. H., Zhang, Y., et al. (2017). The atrophy of white and gray matter volume in patients with comitant strabismus: evidence from a voxel-based morphometry study. *Mol. Med. Rep.* 16, 3276–3282. doi: 10.3892/mmr.2017.7006
- Qiao, P. F., and Niu, G. M. (2017). Resting-State fMRI findings in patients with first-episode idiopathic epilepsy before and after treatment. *Neurosciences* 22, 316–319. doi: 10.17712/nsj.2017.4.20160650
- Robaei, D., Rose, K. A., Kifley, A., Cosstick, M., Ip, J. M., and Mitchell, P. (2006). Factors associated with childhood strabismus: findings from a population-based study. *Ophthalmology* 113, 1146–1153. doi: 10.1016/j.ophtha.2006.02.019
- Schmidt, K. F., and Lowe, S. (2006). The layout of functional maps in area 18 of strabismic cats. *Neuroscience* 141, 1525–1531. doi: 10.1016/j.neuroscience.2006.04.056
- Shao, Y., Cai, F. Q., Zhong, Y. L., Huang, X., Zhang, Y., Hu, P. H., et al. (2015). Altered intrinsic regional spontaneous brain activity in patients with optic neuritis: a resting-state functional magnetic resonance imaging study. *Neuropsychiatr. Dis. Treat.* 11, 3065–3073. doi: 10.2147/NDT.S92968
- Shinoura, N., Yamada, R., Tabei, Y., Shiode, T., Itoi, C., Saito, S., et al. (2013). The right dorsal anterior cingulate cortex may play a role in anxiety disorder and visual function. *Neurol. Res.* 35, 65–70. doi: 10.1179/1743132812Y.0000000101

- Smitha, K. A., Akhil Raja, K., Arun, K. M., Rajesh, P. G., Thomas, B., Kapilamoorthy, T. R., et al. (2017). Resting state fMRI: a review on methods in resting state connectivity analysis and resting state networks. *Neuroradiol. J.* 30, 305–317. doi: 10.1177/1971400917697342
- Snaith, R. P. (2003). The Hospital Anxiety And Depression Scale. *Health Qual. Life Outcomes.* 1:29. doi: 10.1186/1477-7525-1-29
- Song, K., Li, J., Zhu, Y., Ren, F., Cao, L., and Huang, Z. G. (2021). Altered Small-World Functional Network Topology in Patients with Optic Neuritis: A Resting-State fMRI Study. *Dis Markers.* 2021:9948751. doi: 10.1155/2021/9948751
- Tan, G., Dan, Z. R., Zhang, Y., Huang, X., Zhong, Y. L., Ye, L. H., et al. (2018). Altered brain network centrality in patients with adult comitant exotropia strabismus: a resting-state fMRI study. *J. Int. Med. Res.* 46, 392–402. doi: 10.1177/0300060517715340
- Tan, G., Huang, X., Zhang, Y., Wu, A. H., Zhong, Y. L., Wu, K., et al. (2016). A functional MRI study of altered spontaneous brain activity pattern in patients with congenital comitant strabismus using amplitude of low-frequency fluctuation. *Neuropsychiatr. Dis. Treat.* 12, 1243–1250. doi: 10.2147/NDT.S104756
- Tang, Y., Meng, L., Wan, C. M., Liu, Z. H., Liao, W. H., Yan, X. X., et al. (2017). Identifying the presence of Parkinson's disease using low-frequency fluctuations in BOLD signals. *Neurosci. Lett.* 645, 1–6. doi: 10.1016/j.neulet.2017.02.056
- Thompson, K. G., Hanes, D. P., Bichot, N. P., and Schall, J. D. (1996). Perceptual and motor processing stages identified in the activity of macaque frontal eye field neurons during visual search. *J. Neurophysiol.* 76, 4040–4055. doi: 10.1152/jn.1996.76.6.4040
- Vogt, B. A. (2019). Cingulate cortex in the three limbic subsystems. *Handb. Clin. Neurol.* 166, 39–51. doi: 10.1016/B978-0-444-64196-0.00003-0
- Wang, L., Shen, H., Tang, F., Zang, Y., and Hu, D. (2012). Combined structural and resting-state functional MRI analysis of sexual dimorphism in the young adult human brain: an MVPA approach. *Neuroimage* 61, 931–940. doi: 10.1016/j.neuroimage.2012.03.080
- Wang, R., Tang, Z., Liu, T., Sun, X., Wu, L., and Xiao, Z. (2021). Altered spontaneous neuronal activity and functional connectivity pattern in primary angle-closure glaucoma: a resting-state fMRI study. *Neurol. Sci.* 42, 243–251. doi: 10.1007/s10072-020-04577-1
- Xiao, F. L., Lu, C., Zhao, D. J., Zou, Q. H., Zhang, W., Zhang, J., et al. (2018). Recursive Partitioning Analysis of Fractional Low-Frequency Fluctuations in Narcolepsy With Cataplexy. *Front. Neurol.* 9:936. doi: 10.3389/fneur.2018.00936
- Zang, Y., Jiang, T., Lu, Y., He, Y., and Tian, L. (2004). Regional homogeneity approach to fMRI data analysis. *Neuroimage* 22, 394–400. doi: 10.1016/j.neuroimage.2003.12.030
- Zou, Q. H., Zhu, C. Z., Yang, Y., Zuo, X. N., Long, X. Y., Cao, Q. J., et al. (2008). An improved approach to detection of amplitude of low-frequency fluctuation (ALFF) for resting-state fMRI: fractional ALFF. *J. Neurosci. Methods* 172, 137–141. doi: 10.1016/j.jneumeth.2008.04.012
- Zuo, X. N., Di Martino, A., Kelly, C., Shehzad, Z. E., Gee, D. G., Klein, D. F., et al. (2010). The oscillating brain: complex and reliable. *Neuroimage* 49, 1432–1445. doi: 10.1016/j.neuroimage.2009.09.037

**Conflict of Interest:** The authors declare that the research was conducted in the absence of any commercial or financial relationships that could be construed as a potential conflict of interest.

**Publisher's Note:** All claims expressed in this article are solely those of the authors and do not necessarily represent those of their affiliated organizations, or those of the publisher, the editors and the reviewers. Any product that may be evaluated in this article, or claim that may be made by its manufacturer, is not guaranteed or endorsed by the publisher.

Copyright © 2022 Hu, Pan, Zhang, Liang, Ge, Shu, Li, Pei and Shao. This is an open-access article distributed under the terms of the Creative Commons Attribution License (CC BY). The use, distribution or reproduction in other forums is permitted, provided the original author(s) and the copyright owner(s) are credited and that the original publication in this journal is cited, in accordance with accepted academic practice. No use, distribution or reproduction is permitted which does not comply with these terms.



# Abnormal Large-Scale Neuronal Network in High Myopia

Yu Jit, Ling Shi†, Qi Cheng, Wen-wen Fu, Pei-pei Zhong, Shui-qin Huang, Xiao-lin Chen and Xiao-rong Wu\*

Department of Ophthalmology, The First Affiliated Hospital of Nanchang University, Nanchang, China

## OPEN ACCESS

### Edited by:

Xin Huang,  
Jiangxi Provincial People's Hospital,  
China

### Reviewed by:

Tianming Huo,  
Wuhan University, China  
Fei Chen,  
First Affiliated Hospital of Zhengzhou  
University, China

### \*Correspondence:

Xiao-rong Wu  
wxr98021@126.com

† These authors have contributed  
equally to this work

### Specialty section:

This article was submitted to  
Brain Imaging and Stimulation,  
a section of the journal  
Frontiers in Human Neuroscience

Received: 06 February 2022

Accepted: 14 March 2022

Published: 15 April 2022

### Citation:

Ji Y, Shi L, Cheng Q, Fu W-w,  
Zhong P-p, Huang S-q, Chen X-l and  
Wu X-r (2022) Abnormal Large-Scale  
Neuronal Network in High Myopia.  
Front. Hum. Neurosci. 16:870350.  
doi: 10.3389/fnhum.2022.870350

**Aim:** Resting state functional magnetic resonance imaging (rs-fMRI) was used to analyze changes in functional connectivity (FC) within various brain networks and functional network connectivity (FNC) among various brain regions in patients with high myopia (HM).

**Methods:** rs-fMRI was used to scan 82 patients with HM (HM group) and 59 healthy control volunteers (HC group) matched for age, sex, and education level. Fourteen resting state networks (RSNs) were extracted, of which 11 were positive. Then, the FCs and FNCs of RSNs in HM patients were examined by independent component analysis (ICA).

**Results:** Compared with the HC group, FC in visual network 1 (VN1), dorsal attention network (DAN), auditory network 2 (AN2), visual network 3 (VN3), and sensorimotor network (SMN) significantly increased in the HM group. FC in default mode network 1 (DMN1) significantly decreased. Furthermore, some brain regions in default mode network 2 (DMN2), default mode network 3 (DMN3), auditory network 1 (AN1), executive control network (ECN), and significance network (SN) increased while others decreased. FNC analysis also showed that the network connection between the default mode network (DMN) and cerebellar network (CER) was enhanced in the HM group.

**Conclusion:** Compared with HCs, HM patients showed neural activity dysfunction within and between specific brain networks, particularly in the DMN and CER. Thus, HM patients may have deficits in visual, cognitive, and motor balance functions.

**Keywords:** high myopia, resting state network, independent component analysis, functional connectivity, functional network connectivity

## 1. INTRODUCTION

High myopia refers to myopia of  $-6$  diopter or worse, a common eye disease worldwide (Morgan et al., 2012). By 2050, the estimated number of individuals with myopia or HM will reach 4.758 billion (49.8% of the total population) (Holden et al., 2016). In the past two decades, the incidence of HM has been increasing worldwide, particularly in Asia (Morgan et al., 2018). There are many reasons for HM, including genetic factors, environmental factors, and birth season (Wu et al., 2016); environmental factors can be divided into outdoor activities, close work, education, sex,

age, and urban environment (Xiang and Zou, 2020). The typical pathological features of HM include diffuse or patchy chorioretinal atrophy, posterior staphyloma, varicella fissure, Fuchs spot, chorioretinal neovascularization, fovea (Ohno-Matsui et al., 2015), and ocular shape changes; the most important pathological changes are ocular shape changes, which can affect the optical power of the eye (Huang et al., 2018). Importantly, these pathological changes often lead to gradual decline in vision (Saw, 2006). In addition, the foveal avascular area increases in HM patients, while the vascular density decreases; these changes are closely related to fundus lesions (Min et al., 2020). HM can also induce various specific complications, including cataract formation, peripheral retinal tear-induced retinal detachment, myopic foveoschisis, macular hole with or without retinal detachment, peripapillary deformation, dome-shaped macula, choroidal/scleral thinning, myopic choroidal neovascularization, glaucoma, and potential blindness (Ikuno, 2017). Although the current ophthalmic examination enables a clear diagnosis of HM and its complications, there have been few studies of whether myopia can lead to changes in brain activity. In addition, Zhang X. W. et al. (2020) reported that HM patients had different amplitude of low-frequency fluctuations and default mode networks (DMNs), implying that cognitive function is influenced by HM. However, the pathophysiological mechanism by which HM causes changes in cognitive function remains unclear.

In recent years, resting state functional magnetic resonance imaging (rs-fMRI) has been widely used to analyze changes in brain network function among HM patients. Functional magnetic resonance imaging (fMRI) uses blood oxygen level-dependent (BOLD) signals that measure blood oxygen levels in the brain, which are determined by the amounts of oxygenated and deoxygenated hemoglobin. By measuring the strengths of these signals, fMRI can reflect the excitation states of neurons in the brain (Azeez and Biswal, 2017). The main advantage of rs-fMRI is that the signal can be repeatedly captured in a short period of time because BOLD signals do not require an external tracer; they provide comparisons of changes in the concentrations of oxygenated and deoxygenated hemoglobin during functional hyperemia (Hyder and Rothman, 2012). Although rs-fMRI is a non-interventional technique, it can accurately and reliably locate specific cortical areas of brain activity in space and time; it can simultaneously perform repeated scans of the target and track signal changes in real time. Using this technology, Zhai et al. (2016) demonstrated that FC was significantly reduced between the ventral attention and frontoparietal control networks in HM patients. Nelles et al. (2010) demonstrated that frontoparietal network activation was greater in ametropic patients than in normal controls. In a previous study, we showed that the low-frequency fluctuation amplitude was significantly reduced in the bilateral inferior frontal gyrus of HM patients, implying that HM patients have language comprehension and attention control disorders (Huang et al., 2016). However, the above studies have not performed sufficiently comprehensive neuroimaging analyses of spontaneous neural activity and brain network function changes in HM patients.

Independent component analysis (ICA) is a mathematical tool that can separate a series of mutually independent source signals from an observed mixture of unknown source signals, thereby solving the blind source separation problem. Electroencephalogram signals meet most assumptions of ICA (Urrestarazu and Iriarte, 2005); thus, ICA is particularly suitable for analyses of changes in brain network function among HM patients. In recent years, ICA technology has been widely used in studies of neuropsychiatric diseases, including brain network research in patients with stroke, Parkinson's disease, and other diseases (Zhu et al., 2014, 2021). To our knowledge, the present study represents the first use of ICA to study spontaneous brain activity in HM patients, then to explore the relationship of spontaneous brain activity with behavioral performance in those patients.

## 2. PARTICIPANTS AND METHODS

### 2.1. Participants

This study included 82 HM patients and 59 healthy controls (HCs) who underwent examinations from August 2021 to December 2021 in the Department of Ophthalmology at the First Affiliated Hospital of Nanchang University. All participants were matched for age, sex, and education level. Individuals with brain diseases were excluded on the basis of medical history and physical examination findings. All participants underwent examinations in the same setting, and provided written informed consent to be included in the study. All procedures were performed in accordance with the Declaration of Helsinki; ethical approval was obtained from the Medical Ethics Committee of the First Affiliated Hospital of Nanchang University (Jiangxi Province, China).

The inclusion criteria for HM patients were: binocular vision of  $-6$  diopters or worse; corrected visual acuity better than 1.0; and the completion of MRI-related examinations, optical coherence tomography, ultrasonography, and other ophthalmic examinations. The exclusion criteria for HM patients were: binocular vision of better than  $-6$  diopters; history of ocular trauma or ophthalmic surgery; and/or neurological disorders and cerebral infarction.

Healthy controls were randomly selected from Nanchang City on the basis of their age, sex, and education level. All HCs met the following requirements: no eye diseases; no major diseases, such as neurological disorders or cerebral infarction; uncorrected vision or visual acuity better than 1.0; and the completion of MRI-related examinations, optical coherence tomography, ultrasonography, and other ophthalmic examinations.

### 2.2. fMRI Data Acquisition

All MRI data were obtained using a 3-TeslaTrio magnetic resonance imaging scanner system (Trio Tim, Siemens Medical Systems, Erlangen, Germany). These data included conventional T2-weighted imaging (T2WI) and fluid-attenuated inversion recovery (FLAIR) imaging for diagnostic and radiological assessment, along with high-resolution T1-weighted imaging



(T1WI) for cortical surface complexity analyses. In this study, three-dimensional high-resolution T1WI parameters were as follows: repetition time/echo time = 1900/2.26 ms; field of view =  $215 \times 230$  mm; matrix =  $240 \times 256$ ; and 176 sagittal slices with thickness of 1.0 mm. Turbo spin echo-imaging sequence for T2WI scans was performed using the following parameters: repetition time/echo time = 5100/117 ms; field of view =  $240 \times 240$  mm; matrix =  $416 \times 416$ ; number of excitations = 3; echo train length = 11; and 22 axial slices with thickness of 6.5 mm. FLAIR imaging was performed using the following parameters: repetition time/echo time/inversion time = 7000/79/2500 ms; 50 slices;  $240 \times 217$  matrix; and  $0.43 \times 0.43 \times 2$  mm<sup>3</sup> voxels.

## 2.3. fMRI Data Processing

Statistical parameter mapping (SPM 12)<sup>1</sup> was performed using the brain imaging data processing and analysis toolbox (DPABI<sup>2</sup>). Raw data were preprocessed as follows. First, the initial 10 time points of fMRI data were deleted to maintain the signal balance. Second, images were converted from DICOM format to NIFTI format. Third, slice timing correction, head motion correction, and interference covariate removal were performed for the remaining data. During preconditioning, if the participant's head movement showed x-axis, y-axis, or z-axis rotation of  $>2.5^\circ$  or  $>2.5$  mm, the participant was excluded. Fourth, a single three-dimensional Bravo image was registered to the fMRI mean data; T1-weighted images were analyzed using the exponential Lie Algebra (DARTEL) toolbox to improve the spatial accuracy of fMRI data standardization. Fifth, the standardized data were resliced at a resolution of  $3 \times 3 \times 3$  mm within the Montreal Neurological Institute (MNI) space. Finally, an isotropic Gaussian kernel of  $6 \times 6 \times 6$  mm full width at half maximum was used for spatial smoothing to reduce spatial noise and errors caused by spatial standardization.

## 2.4. Independent Component Analysis

Using group ICA of fMRI toolbox [GIFT (Calhoun et al., 2001)] software<sup>3</sup> (version 3.0b), ICA was conducted to convert the preprocessed data into independent components. The process was as follows. First, the software estimated 36 independent components and calculated the spatial correlation of BOLD signals by using the minimum description length criterion. Second, all data for each participant were simplified. The compressed data set of each participant was joined into a group; the aggregated data set was dimensionally reduced using principal component analysis. Third, the independent components of each participant were reverse-reconstructed by ICA at the group level. Fourth, components of the brain network were screened using the following criteria: the spatial coordinates of the peak value of the brain network were located in the gray matter of the brain; there were no obvious blood vessels in the distribution of the brain network; and the brain network signal was a low frequency signal (0.1–0.25 Hz).

<sup>1</sup> <http://www.fil.ion.ucl.ac.uk>

<sup>2</sup> <http://www.rfmri.org/dpabi>

<sup>3</sup> <http://icatb.sourceforge.net/>

Seven RSNs were identified in this study: VN, AN, DMN, SN, DAN, SMN, and ECN.

## 2.5. Statistical Analysis

SPSS version 20.0 software (SPSS Inc., Chicago, IL, United States) was used for statistical analysis. The means and standard deviations of sex, age, and axial length were determined in the HM and HC groups.

## 3. RESULTS

### 3.1. Demographics and Visual Measurements

This study included 89 HM patients (41 men and 48 women, mean age  $26.23 \pm 5.462$  years) and 59 HCs (24 men and 35 women, mean age  $25.78 \pm 3.102$  years). Demographic characteristics are shown in Table 1.

### 3.2. Spatial Pattern of Resting State Networks in Each Group

Figure 1 shows the typical spatial pattern in each RSN in the HM group. The visual network (VN) comprised the middle occipital gyrus, superior occipital gyrus, temporal-occipital regions, and fusiform gyrus; the auditory network (AN) comprised the bilateral middle and superior temporal gyrus. The cerebellar network (CER) comprised the cortex and medulla (parietal nucleus, intermediate nucleus, and dentate nucleus); the DMN comprised the posterior cingulate cortex, precuneus, medial prefrontal cortex, inferior parietal lobule, and lateral temporal cortex. The sensorimotor network (SMN) comprised the precentral gyrus, postcentral gyrus, and supplementary motor area; the salience network (SN) comprised the anterior insula and dorsal anterior cingulate cortex. The executive control network (ECN) comprised the dorsolateral frontal cortex and posterior cingulate cortex; the dorsal attention network (DAN) comprised the inferior parietal cortex, frontal eye motor area, auxiliary motor area, insular lobe, and dorsolateral prefrontal cortex.

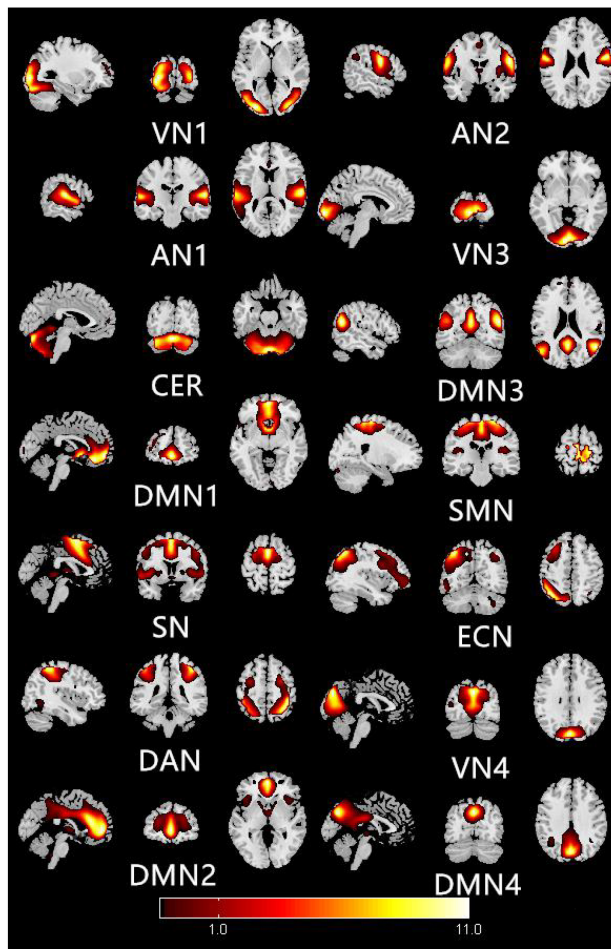
### 3.3. Resting State Network Changes in the High Myopia Group

Figure 2 shows the functional connectivity in each RSN in HM group. In VN1, the functional connectivity of the right middle occipital gyrus increased; in AN1, the functional connectivity of the left middle temporal gyrus decreased, while the functional

**TABLE 1 |** Demographic and clinical characteristics of HM and HC groups.

Characteristic	HM	HC
Men/women	41/48	24/35
Age (years)	$26.23 \pm 5.462$	$25.78 \pm 3.102$
ALM (OD)	$26.67 \pm 0.874$	$23.90 \pm 0.971$
ALM (OS)	$26.58 \pm 0.985$	$23.74 \pm 0.693$

Abbreviations: HM, high myopia; HC, healthy control; ALM, axial length; OD, oculus dexter; OS, oculus sinister.



**FIGURE 1 |** Typical spatial patterns of each RSN in HM group: visual network (VN), auditory network (AN), cerebellar network (CER), default mode network (DMN), sensorimotor network (SMN), saliency network (SN), executive control network (ECN), and dorsal attention network (DAN).

connectivity of the left superior temporal gyrus increased. In DMN1, the functional connectivities of the left caudate nucleus and right anterior cingulate gyrus both decreased. In SN, the functional connectivity of the left middle occipital gyrus decreased, while the functional connectivity of the left insula increased. In DAN, the functional connectivity of the left parietal inferior gyrus region increased. In DMN2, the functional connectivities of the right medial superior frontal gyrus and right middle cingulate gyrus increased, while the functional connectivity of the left middle cingulate gyrus decreased. In AN2, the functional connectivity of the left central posterior gyrus region increased; in VN3, the functional connectivity of the right talar fissure region increased. In DMN3, the functional connectivity of the left precuneus region decreased, while the functional connectivities of the left angular gyrus and right precuneus region both increased. In SMN, the functional connectivities of the left posterior central gyrus and right anterior central gyrus both increased. In ECN, the functional

connectivity of the right middle temporal gyrus decreased, while the functional connectivities of the left middle frontal gyrus, left inferior parietal gyrus, and left medial superior frontal gyrus all increased. The changes of RSN in HM group are shown in Table 2.

### 3.4. Analysis of Functional Network Connections in the High Myopia Group

Figure 3 shows that functional connections of brain networks in HM group were analyzed by FNC technique. Network connections between DMN and CER were enhanced in the HM group ( $P < 0.05$ ).

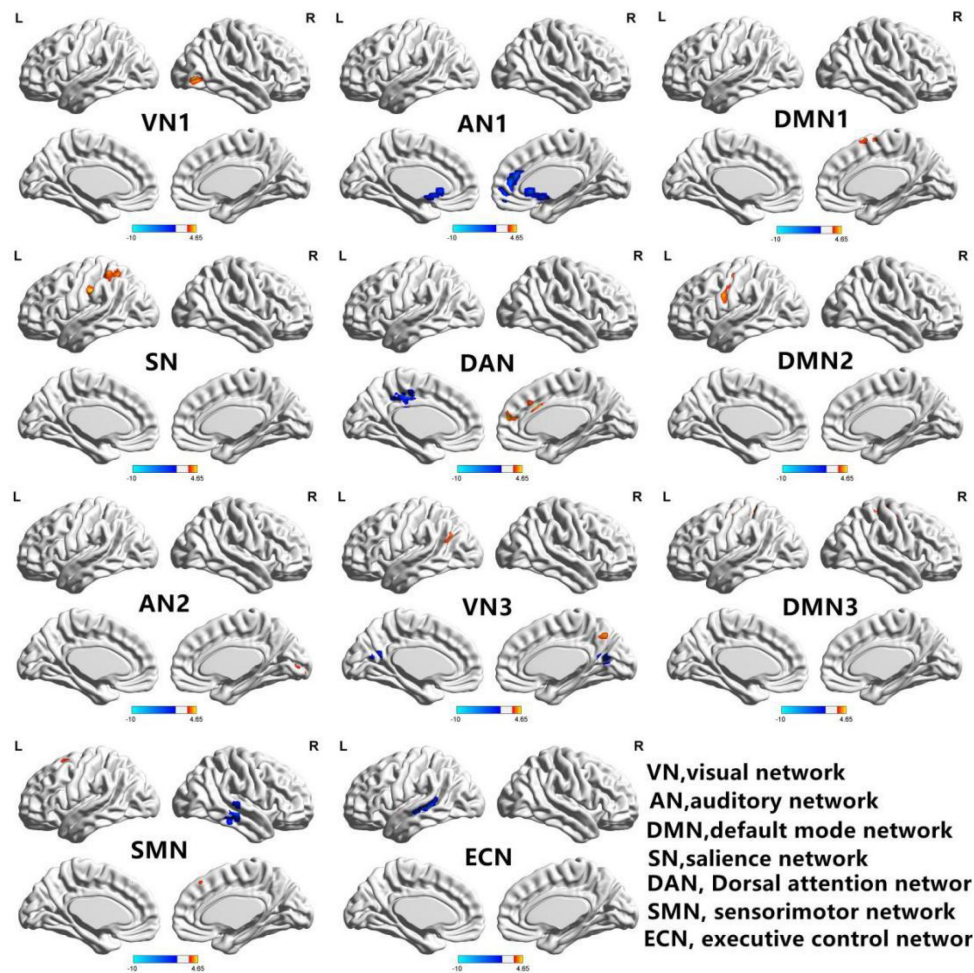
## 4. DISCUSSION

To our knowledge, this is the first exploration of the changes and clinical characteristics of FC and FNC in the RSNs of HM patients. We found that, in HM patients, FC levels increased in VN1, AN2, DMN1, DMN2, DMN3, and SN; FC levels decreased in AN1 and ECN; and FC levels in DAN, VN3, and SMN both increased and decreased. Furthermore, the FNC of HM patients increased between DMN, AN, VN, SN, DAN, and SMN.

The VN is located in the occipital cortex at the temporal lobo-occipital junction, which has an important role in visual information processing (Wang et al., 2008). The main pathological changes in the VN of HM patients are excessive increase in ALM, the presence of posterior staphyloma, and multiple retinal and choroidal lesions (Liu et al., 2010; Ohno-Matsui et al., 2015). In addition, HM patients exhibit abnormalities in the visual cortex (Mirzajani et al., 2011). Zhang et al. (2021) reported that the response to spatial frequency visual stimuli was significantly reduced in HM patients; moreover, the resting state FC density between the superior limbic gyrus and the anterolateral prefrontal cortex was significantly reduced. Cheng et al. (2020) showed that FC density in the posterior cingulate cortex/anterior lobe region was significantly reduced in HM patients. Zou et al. (2021) demonstrated increased FC density between the VN and AN in patients with chronic migraine. Here, we found increased FC density in the right middle occipital gyrus and right talus fissure in HM patients. Taken together, the current and previous results show that long-term HM may lead to changes in FC density in the VN. Therefore, we speculate that HM patients have impaired visual function.

The AN is located in the temporal lobe and has an important role in auditory information processing. There is increasing clinical evidence that HM patients have impaired hearing function. Zhai et al. (2016) showed that FC density in the inferior temporal gyrus significantly decreased in HM patients. In addition, MRI analysis of chronic migraine patients showed that FC decreased in the AN, resulting in auditory disorders such as speech phobia (Moseley and Vlaeyen, 2015; Cordier and Diers, 2018). Zhou et al. (2019) demonstrated that FC density between the right inferior temporal gyrus and the right anterior central gyrus was enhanced in patients with tinnitus, while the right middle frontal gyrus showed a decrease in FC density between





**FIGURE 2 |** In the HM group, 11 brain regions of RSNs were significantly different ( $P < 0.01$ ; GRF correction, cluster-level  $P < 0.05$ ): visual network 1 (VN1), auditory network 1 (AN1), default mode network 1 (DMN1), significance network (SN), dorsal attention network (DAN), default mode network 2 (DMN2), auditory network 2 (AN2), visual network 3 (VN3), default mode network 3 (DMN3), sensorimotor network (SMN), and executive control network (ECN). BrainNet Viewer images show increased (warm colors) and decreased (cool colors) FC connectivities in the HM group.

the bilateral cingulate gyrus and the left anterior central gyrus. Furthermore, we found showed that FC density in the left middle temporal gyrus of AN1 decreased in HM patients, while the FC density in the left superior temporal gyrus increased; additionally, FC density increased in the left postcentral gyrus region of AN2. Therefore, we speculate that HM patients have problems with auditory function. The specific underlying neural mechanism is unclear; we plan to investigate it in future studies.

The DMN consists of multiple brain regions, including the medial prefrontal cortex, posterior cingulate cortex, inferior parietal cortex, and anterior lobe (Raichle, 2015). The DMN has been linked to a wide range of neuropsychiatric disorders, including Alzheimer's disease, autism, schizophrenia, and epilepsy. The DMN has an important role in self-referential thinking and reflection because it shows consistently high blood oxygen-dependent activity during rest (Raichle et al., 2001). There is increasing evidence that disorders of the central nervous system can lead to DMN abnormalities. Zuo et al. (2018) reported

that when the brain shifts from a resting state to a low load state, FC density increases in the DMN; the VN also strengthens its interactions with other brain networks. Zhu et al. (2017b) showed that FC density in front of the DMN decreased in arc-dependent patients. Here, we found that FC density in the left caudate nucleus and the right angular gyrus of DMN1 decreased in HM patients; in DMN2, the FC density in the right medial superior frontal gyrus and the middle region of the right cingulate gyrus both increased, while the FC density in the middle region of the left cingulate gyrus decreased. Additionally, the FC density in the left angular gyrus and the right precuneus region of DMN3 increased, whereas the FC density in the left precuneus region decreased. Therefore, we speculate that HM patients have cognitive function impairment.

The SN, located in the dorsal anterior cingulate gyrus and anterior insula, guides behavior by participating in recognition of the most relevant stimuli (Menon and Uddin, 2010); it has an important role in the detection and location of explicit

**TABLE 2 |** Intranetwork FCs of RSNs in the HM group.

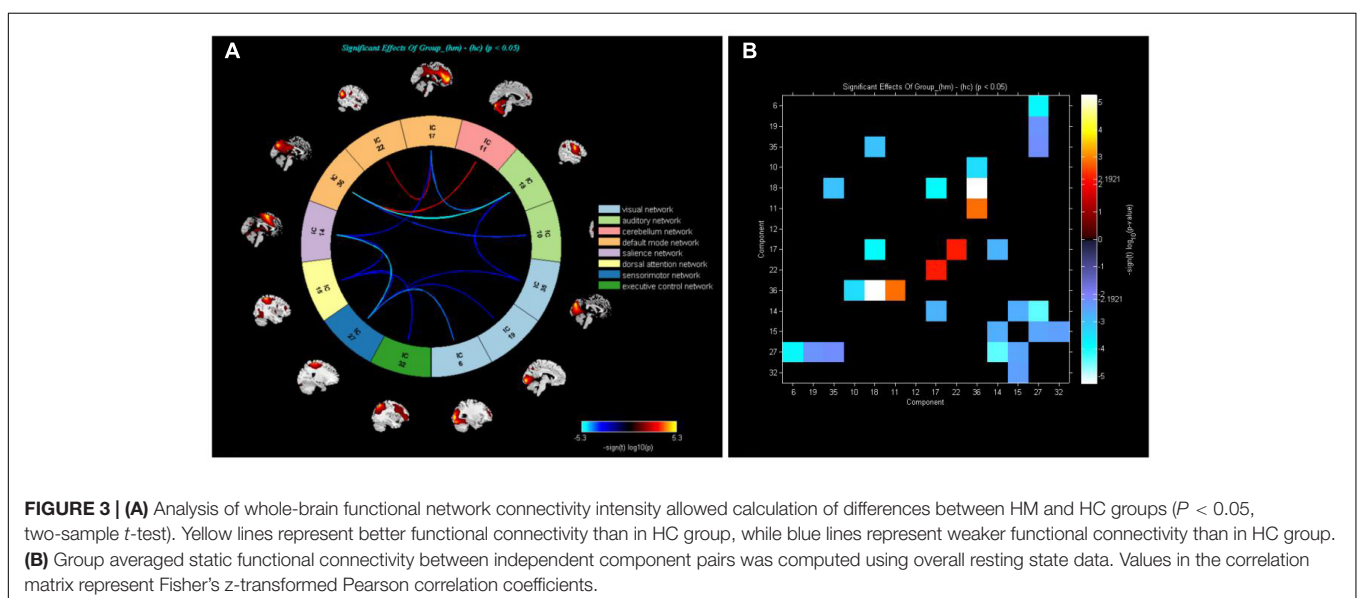
RSN	Brain region	BA	Peak t-score	MNI coordinates (x, y, z)	Cluster size (voxels)
VN1	R-MOG	19	4.6526	45, -75, 3	109
AN1	L-MTG	—	-4.4648	-42, -36, 0	64
	L-STG	42	4.1556	-63, -18, 9	108
DMN1	L-CAU	24	-4.4368	6, 21, -3	96
	R-ACC	—	-4.367	9, 42, 12	95
SN	L-INS	—	4.8092	-42, -18, 15	42
	L-MOG	—	-4.3905	-33, -81, 21	37
DAN	L-IPG	—	4.9254	-54, -21, 36	244
DMN2	R-SFGmed	—	5.5267	12, 48, 15	187
	R-MCC	32	5.2192	3, 21, 30	95
	L-MCC	—	-3.9378	-6, -24, 39	60
AN2	L-PoCG	—	4.6387	-36, -18, 45	186
VN3	R-CAL	17	3.3681	15, -81, 6	74
DMN3	L-PCNU	—	-4.1643	-6, -57, 18	52
	L-ANG	—	4.3362	-57, -54, 21	40
	R-PCNU	7	4.1531	6, -63, 42	59
SMN	L-PoCG	4	4.8034	-42, -15, 54	221
	R-PreCG	6	4.4296	24, -18, 57	244
ECN	R-MTG	21	-5.1214	66, -27, 0	47
	L-MFG	6	4.2445	-24, 12, 60	84
	L-IPG	—	3.4223	-45, -39, 48	32
	L-SFGmed	—	3.5085	0, 36, 45	41

The statistical threshold was set at the voxel level with  $P < 0.01$  for multiple comparisons using Gaussian random field theory (voxel-level  $P < 0.01$ , GRF correction, cluster-level  $P < 0.05$ ). The t-score represents the statistical value of peak voxels showing differences in FC between the two groups. Abbreviations: MOG, middle occipital gyrus; MTG, middle temporal gyrus; STG, superior temporal gyrus; CAU, caudate nucleus; ACC, anterior cingulate and paracingulate gyri; INS, insula; IPG, inferior parietal; SFGmed, superior frontal gyrus, medial; MCC, median cingulate and paracingulate gyri; PoCG, postcentral gyrus; CAL, calcarine fissure and surrounding cortex; PCNU, precuneus; ANG, angular gyrus; PreCG, precentral gyrus; MFG, middle frontal gyrus; R, right; L, left; BA, brodmann area; MNI, montreal neurologic institute.

inputs and task control (Zhou et al., 2018). Zhang et al. (2019) demonstrated that the cortisol stress response level is associated with increasing FC density in the SN. The SN is also a key network for the detection of behavior-related stimuli, as well as the coordination of responses to such stimuli. Wang et al. (2016) reported that FC density in the SN decreases in schizophrenic patients, while the time of internal connection in the SN increases in a dynamic manner. Therefore, SN dysfunction may be caused by the reduction of internal connection stability in the network. We found that FC density increased in the left insular region of the SN and decreased in the left middle occipital gyrus region of the SN in HM patients. Overall, the current and previous results indicate that long-term neurological disease may lead to changes in FC density in the SN. Therefore, we speculate that HM patients have impaired attention and working memory function.

The SMN is composed of subcortical areas such as the cerebellum, basal ganglia, and thalamus (Middleton and Strick, 2000), which can regulate bilateral body balance and control movement (Serrien et al., 2002). Liu et al. (2016) showed that movement disorders in stroke patients are related to abnormal FC density in the SMN or sensorimotor cortex. Acupuncture in stroke patients can increase FC density between the DMN and SMN (Cai et al., 2018). Zhang et al. (2018) reported that FC density in the SMN decreased in patients with lower limb amputation; FC changes in the brain revealed subcortical SMN abnormalities after amputation, highlighting the role of subcortical areas in SMN reorganization after lower limb amputation. In the present study, we found that FC density in the left postcentral gyrus and right precentral gyrus regions of the SMN increased in HM patients. Therefore, we speculate that HM patients have poor body balance and exhibit motor control disorders.

The DAN is composed of connected areas among the bilateral intraparietal sulcus, central anterior sulcus, and superior



frontal sulcus (i.e., frontal eye movement area), which can provide top-down attention orientation. Thus, when the DAN is activated in daily life, it supports focused and efficient work. Xia et al. (2015) reported that FC density in the DAN of type 2 diabetes mellitus patients increased or decreased among regions, reflecting neurobehavioral defects in such patients. Wang et al. (2019) showed that FC density in the DAN decreased in patients with Alzheimer's disease and mild cognitive impairment. Functional interactions between the DAN and DMN are dynamic at all stages of life; changes in FC density in the DAN may affect DMN function. Here, we found that FC density in the left inferior parietal gyrus of DAN increased in HM patients. Therefore, we speculate that HM patients exhibit impaired concentration and attention orientation.

The ECN is composed of the medial prefrontal cortex, cingulate gyrus, and posterior parietal cortex; these areas participate in activity inhibition and emotion, as well as multiple higher cognitive tasks, including adaptive cognitive control (Seeley et al., 2007). Zhu et al. (2018) demonstrated that FC density in the ECN decreased in patients who abstain from alcohol for an extended period; this FC density provided critical information for identifying alcoholism. Zhang Z. et al. (2020) showed that FC density in the right ECN decreased in patients with right frontal lobe epilepsy, while the FC density in the left ECN increased. These results suggest that repeated seizures and sustained epilepsy-related damage may lead to interaction disorders of core brain regions in the ECN, affecting network stability and consistency; these changes may lead to overall functional decline. Our study found that FC density in the left middle frontal gyrus, left inferior parietal gyrus, and left medial superior frontal gyrus of the ECN increased in HM patients, while the FC density in the right middle temporal gyrus decreased. Therefore, we speculate that HM patients experience obstacles to adaptive cognitive control.

Traditionally, HM is regarded as a visual impairment disorder; however, our FNC analysis showed that the network connection between the DMN and CER is enhanced in HM patients, indicating that visual impairment in HM patients may cause impairments in cognitive and balance functions. Zhang D. et al. (2020) showed that the network connection between the DMN and CER was weakened in patients with type 2 diabetes mellitus; this particularly affected the network connection between the bilateral cerebellar region IX and the right wedge/precuneus. The precuneus is the key hub of the DMN, with a vital role in emotional management (Sheline et al., 2009); the CER is also involved in emotional management. An abnormal connection between the left cerebellum and the posterior cortex/anterior lobe of the cingulate gyrus may be predictive of suicidal behavior in depressed adolescents (Zhang et al., 2016). Wang et al. (2017) studied the resting states of the cerebellar hemisphere and its subregions in 228 healthy adults; they found that network connections in various parts of the cerebellum were related to the DMN. Previous studies have shown that patients with alcoholism have weakened connections within the DMN, as well as

between the DMN and other networks (including the CER) (Müller-Oehring et al., 2015; Zhu et al., 2017a). Wang et al. (2014) showed that visual loss can cause changes in high-level cognitive networks. Based on the above findings, we speculate that HM patients experience difficulty with cognitive and balance functions.

There were some limitations in this study. First, it constituted a small experimental analysis; we could not conclusively determine whether HM patients have non-visual dysfunctions (e.g., cognitive and balance functions); additional studies are needed to investigate these relationships. Second, although all participants underwent fMRI in the absence of any task requirement, the direct flow signals were presumably affected by physiological noise. Third, HM patients may have visual impairment complications (e.g., omental detachment, macular hole, and macular hemorrhage), which may cause changes in brain function that could influence the results of fMRI.

## 5. CONCLUSION

Through analyses of the FC within each brain network and the FNC between brain networks of HM patients and HCs, we found that HM patients may have defects in visual, cognitive, and motor balance functions, suggesting that abnormalities in FC may contribute to clinical symptoms in HM patients. Our results provide new insights concerning the pathophysiological mechanisms in HM. Furthermore, our report may support the use of rs-fMRI as a valuable, non-invasive examination of HM patients in regular clinical practice.

## DATA AVAILABILITY STATEMENT

The raw data supporting the conclusions of this article will be made available by the authors, without undue reservation.

## ETHICS STATEMENT

The studies involving human participants were reviewed and approved by the Institutional Review Board of the First Affiliated Hospital of Nanchang University. Written informed consent to participate in this study was provided by the participants' legal guardian/next of kin. Written informed consent was obtained from the individual(s) for the publication of any potentially identifiable images or data included in this article.

## AUTHOR CONTRIBUTIONS

YJ, LS, and X-RW designed the study and oversaw all clinical aspects of study conduct and manuscript preparation. All authors contributed to data collection, statistical analyses, wrote the manuscript, designed the protocol, contributed to the MRI analysis, and approved the submitted version.



## FUNDING

We acknowledge the assistance provided by the National Nature Science Foundation of China (Grant Nos. 82160207, 81760179, and 81360151), Health Development Planning

Commission Science Foundation of Jiangxi Province (No. 20185118), Key research plan of Jiangxi Provincial Science and Technology Department (No. 20192BBG70042), Key projects of Jiangxi Youth Science Fund (No. 20202ACBL216008).

## REFERENCES

- Azeez, A. K., and Biswal, B. B. (2017). A review of resting-state analysis methods. *Neuroimag. Clin. N. Am.* 27, 581–592. doi: 10.1016/j.nic.2017.06.001
- Cai, R. L., Shen, G. M., Wang, H., and Guan, Y. Y. (2018). Brain functional connectivity network studies of acupuncture: a systematic review on resting-state fMRI. *J. Integr. Med.* 16, 26–33. doi: 10.1016/j.joim.2017.12.002
- Calhoun, V. D., Adali, T., Pearlson, G. D., and Pekar, J. J. (2001). A method for making group inferences from functional MRI data using independent component analysis. *Hum. Brain Mapp.* 14, 140–151. doi: 10.1002/hbm.1048
- Cheng, Y., Huang, X., Hu, Y. X., Huang, M. H., Yang, B., Zhou, F. Q., et al. (2020). Comparison of intrinsic brain activity in individuals with low/moderate myopia versus high myopia revealed by the amplitude of low-frequency fluctuations. *Acta Radiol.* 61, 496–507. doi: 10.1177/0284185119867633
- Cordier, L., and Diers, M. (2018). Learning and unlearning of pain. *Biomedicine* 6:67. doi: 10.3390/biomedicine6020067
- Holden, B. A., Fricke, T. R., Wilson, D. A., Jong, M., Naidoo, K. S., Sankaridurg, P., et al. (2016). Global prevalence of myopia and high myopia and temporal trends from 2000 through 2050. *Ophthalmology* 123, 1036–1042. doi: 10.1016/j.ophtha.2016.01.006
- Huang, X., Hu, Y., Zhou, F., Xu, X., Wu, Y., Jay, R., et al. (2018). Altered whole-brain gray matter volume in high myopia patients: a voxel-based morphometry study. *Neuroreport* 29, 760–767. doi: 10.1097/WNR.0000000000001028
- Huang, X., Zhou, F. Q., Hu, Y. X., Xu, X. X., Zhou, X., Zhong, Y. L., et al. (2016). Altered spontaneous brain activity pattern in patients with high myopia using amplitude of low-frequency fluctuation: a resting-state fMRI study. *Neuropsychiatr. Dis. Treat.* 12, 2949–2956. doi: 10.2147/NDT.S118326
- Hyder, F., and Rothman, D. L. (2012). Quantitative fMRI and oxidative neuroenergetics. *Neuroimage* 62, 985–994. doi: 10.1016/j.neuroimage.2012.04.027
- Ikuno, Y. (2017). Overview of the complications of high myopia. *Retina* 37, 2347–2351. doi: 10.1097/IAE.0000000000001489
- Liu, H. H., Xu, L., Wang, Y. X., Wang, S., You, Q. S., and Jonas, J. B. (2010). Prevalence and progression of myopic retinopathy in Chinese adults: the Beijing Eye Study. *Ophthalmology* 117, 1763–1768. doi: 10.1016/j.ophtha.2010.01.020
- Liu, H., Tian, T., Qin, W., Li, K., and Yu, C. (2016). Contrasting evolutionary patterns of functional connectivity in sensorimotor and cognitive regions after stroke. *Front. Behav. Neurosci.* 10:72. doi: 10.3389/fnbeh.2016.00072
- Menon, V., and Uddin, L. Q. (2010). Saliency, switching, attention and control: a network model of insula function. *Brain Struct. Funct.* 214, 655–667. doi: 10.1007/s00429-010-0262-0
- Middleton, F. A., and Strick, P. L. (2000). Basal ganglia and cerebellar loops: motor and cognitive circuits. *Brain Res. Brain Res. Rev.* 31, 236–250. doi: 10.1016/S0165-0173(99)00040-5
- Min, C. H., Al-Qattan, H. M., Lee, J. Y., Kim, J. G., Yoon, Y. H., and Kim, Y. J. (2020). Macular microvasculature in high myopia without pathologic changes: an optical coherence tomography angiography study. *Korean J. Ophthalmol.* 34, 106–112. doi: 10.3341/kjo.2019.0113
- Mirzajani, A., Sarlaki, E., Kharazi, H. H., and Tavan, M. (2011). Effect of lens-induced myopia on visual cortex activity: a functional MR imaging study. *AJNR Am. J. Neuroradiol.* 32, 1426–1429. doi: 10.3174/ajnr.A2551
- Morgan, I. G., French, A. N., Ashby, R. S., Guo, X., Ding, X., He, M., et al. (2018). The epidemics of myopia: aetiology and prevention. *Prog. Retin. Eye Res.* 62, 134–149. doi: 10.1016/j.preteyeres.2017.09.004
- Morgan, I. G., Ohno-Matsui, K., and Saw, S. M. (2012). Myopia. *Lancet* 379, 1739–1748. doi: 10.1016/S0140-6736(12)60272-4
- Moseley, G. L., and Vlaeyen, J. W. S. (2015). Beyond nociception: the imprecision hypothesis of chronic pain. *Pain* 156, 35–38. doi: 10.1016/j.pain.0000000000000014
- Müller-Oehring, E. M., Jung, Y. C., Pfefferbaum, A., Sullivan, E. V., and Schulte, T. (2015). The resting brain of alcoholics. *Cereb. Cortex* 25, 4155–4168. doi: 10.1093/cercor/bhu134
- Nelles, G., Pscherer, A., de Greiff, A., and Esser, J. (2010). Brain activation of eye movements in subjects with refractive error. *Eye Brain* 2, 57–62. doi: 10.2147/eb.s9823
- Ohno-Matsui, K., Kawasaki, R., Jonas, J. B., Cheung, C. M., Saw, S. M., Verhoeven, V. J., et al. (2015). META-analysis for Pathologic Myopia (META-PM) Study Group. International photographic classification and grading system for myopic maculopathy. *Am. J. Ophthalmol.* 159, 877–883. doi: 10.1016/j.ajo.2015.01.022
- Raichle, M. E. (2015). The brain's default mode network. *Annu. Rev. Neurosci.* 38, 433–447. doi: 10.1146/annurev-neuro-071013-014030
- Raichle, M. E., MacLeod, A. M., Snyder, A. Z., Powers, W. J., Gusnard, D. A., and Shulman, G. L. (2001). A default mode of brain function. *Proc. Natl. Acad. Sci. USA* 98, 676–682. doi: 10.1073/pnas.98.2.676
- Saw, S. M. (2006). How blinding is pathological myopia? *Br. J. Ophthalmol.* 90, 525–526. doi: 10.1136/bjo.2005.087999
- Seeley, W. W., Menon, V., Schatzberg, A. F., Keller, J., Glover, G. H., Kenna, H., et al. (2007). Dissociable intrinsic connectivity networks for salience processing and executive control. *J. Neurosci.* 27, 2349–2356. doi: 10.1523/JNEUROSCI.5587-06.2007
- Serrien, D. J., Strens, L. H., Oliviero, A., and Brown, P. (2002). Repetitive transcranial magnetic stimulation of the supplementary motor area (SMA) degrades bimanual movement control in humans. *Neurosci. Lett.* 328, 89–92. doi: 10.1016/S0304-3940(02)00499-8
- Sheline, Y. I., Barch, D. M., Price, J. L., Rundle, M. M., Vaishnavi, S. N., Snyder, A. Z., et al. (2009). The default mode network and self-referential processes in depression. *Proc. Natl. Acad. Sci. USA* 106, 1942–1947. doi: 10.1073/pnas.0812686106
- Urrestarazu, E., and Iriarte, J. (2005). El análisis de componentes independientes (ICA) en el estudio de señales electroencefalográficas [Independent Components Analysis (ICA) in the study of electroencephalographic signals]. *Neurología* 20, 299–310.
- Wang, D., Qin, W., Liu, Y., Zhang, Y., Jiang, T., and Yu, C. (2014). Altered resting-state network connectivity in congenital blind. *Hum. Brain Mapp.* 35, 2573–2581. doi: 10.1002/hbm.22350
- Wang, J., Liu, J., Wang, Z., Sun, P., Li, K., and Liang, P. (2019). Dysfunctional interactions between the default mode network and the dorsal attention network in subtypes of amnesic mild cognitive impairment. *Aging* 11, 9147–9166. doi: 10.18632/aging.102380
- Wang, K., Jiang, T., Yu, C., Tian, L., Li, J., Liu, Y., et al. (2008). Spontaneous activity associated with primary visual cortex: a resting-state FMRI study. *Cereb. Cortex* 18, 697–704. doi: 10.1093/cercor/bhm105
- Wang, X., Zhang, W., Sun, Y., Hu, M., and Chen, A. (2016). Aberrant intrasaliency network dynamic functional connectivity impairs large-scale network interactions in schizophrenia. *Neuropsychologia* 93, 262–270. doi: 10.1016/j.neuropsychologia.2016.11.003
- Wang, Y., Tang, W., Fan, X., Zhang, J., Geng, D., Jiang, K., et al. (2017). Resting-state functional connectivity changes within the default mode network and the salience network after antipsychotic treatment in early-phase schizophrenia. *Neuropsychiatr. Dis. Treat.* 13, 397–406. doi: 10.2147/NDT.S123598
- Wu, X., Gao, G., Jin, J., Hua, W., Tao, L., Xu, S., et al. (2016). Housing type and myopia: the mediating role of parental myopia. *BMC Ophthalmol.* 16:151. doi: 10.1186/s12886-016-0324-z
- Xia, W., Wang, S., Rao, H., Spaeth, A. M., Wang, P., Yang, Y., et al. (2015). Disrupted resting-state attentional networks in T2DM patients. *Sci. Rep.* 5:11148. doi: 10.1038/srep11148
- Xiang, Z. Y., and Zou, H. D. (2020). Recent epidemiology study data of myopia. *J. Ophthalmol.* 2020:4395278. doi: 10.1155/2020/4395278

- Zhai, L., Li, Q., Wang, T., Dong, H., Peng, Y., Guo, M., et al. (2016). Altered functional connectivity density in high myopia. *Behav. Brain Res.* 303, 85–92. doi: 10.1016/j.bbr.2016.01.046
- Zhang, D., Qi, F., Gao, J., Yan, X., Wang, Y., Tang, M., et al. (2020). Altered cerebellar-cerebral circuits in patients with type 2 diabetes mellitus. *Front. Neurosci.* 14:571210. doi: 10.3389/fnins.2020.571210
- Zhang, J., Zhang, Y., Wang, L., Sang, L., Li, L., Li, P., et al. (2018). Brain functional connectivity plasticity within and beyond the sensorimotor network in lower-limb amputees. *Front. Hum. Neurosci.* 12:403. doi: 10.3389/fnhum.2018.00403
- Zhang, S., Chen, J. M., Kuang, L., Cao, J., Zhang, H., Ai, M., et al. (2016). Association between abnormal default mode network activity and suicidality in depressed adolescents. *BMC Psychiatry* 16:337. doi: 10.1186/s12888-016-1047-7
- Zhang, T., Jiang, Q., Xu, F., Zhang, R., Liu, D., Guo, D., et al. (2021). Alternation of resting-state functional connectivity between visual cortex and hypothalamus in guinea pigs with experimental glucocorticoid enhanced myopia after the treatment of electroacupuncture. *Front. Neuroinform.* 14:579769. doi: 10.3389/fninf.2020.579769
- Zhang, W., Hashemi, M. M., Kaldewaij, R., Koch, S. B. J., Beckmann, C., Klumpers, F., et al. (2019). Acute stress alters the 'default' brain processing. *Neuroimage* 189, 870–877. doi: 10.1016/j.neuroimage.2019.01.063
- Zhang, X. W., Dai, R. P., Cheng, G. W., Zhang, W. H., and Long, Q. (2020). Altered amplitude of low-frequency fluctuations and default mode network connectivity in high myopia: a resting-state fMRI study. *Int. J. Ophthalmol.* 13, 1629–1636. doi: 10.18240/ijo.2020.10.18
- Zhang, Z., Zhou, X., Liu, J., Qin, L., Ye, W., and Zheng, J. (2020). Aberrant executive control networks and default mode network in patients with right-sided temporal lobe epilepsy: a functional and effective connectivity study. *Int. J. Neurosci.* 130, 683–693. doi: 10.1080/00207454.2019.1702545
- Zhou, G. P., Shi, X. Y., Wei, H. L., Qu, L. J., Yu, Y. S., Zhou, Q. Q., et al. (2019). Disrupted intraregional brain activity and functional connectivity in unilateral acute tinnitus patients with hearing loss. *Front. Neurosci.* 13:1010. doi: 10.3389/fnins.2019.01010
- Zhou, Y., Friston, K. J., Zeidman, P., Chen, J., Li, S., and Razi, A. (2018). The hierarchical organization of the default, dorsal attention and salience networks in adolescents and young adults. *Cereb. Cortex.* 28, 726–737. doi: 10.1093/cercor/bhx307
- Zhu, D., Chang, J., Freeman, S., Tan, Z., Xiao, J., Gao, Y., et al. (2014). Changes of functional connectivity in the left frontoparietal network following aphasic stroke. *Front. Behav. Neurosci.* 8:167. doi: 10.3389/fnbeh.2014.00167
- Zhu, J., Zeng, Q., Shi, Q., Li, J., Dong, S., Lai, C., et al. (2021). Altered brain functional network in subtypes of parkinson's disease: a dynamic perspective. *Front. Aging Neurosci.* 13:710735. doi: 10.3389/fnagi.2021.710735
- Zhu, X., Cortes, C. R., Mathur, K., Tomasi, D., and Momenan, R. (2017a). Model-free functional connectivity and impulsivity correlates of alcohol dependence: a resting-state study. *Addict. Biol.* 22, 206–217. doi: 10.1111/adb.12272
- Zhu, X., Du, X., Kerich, M., Lohoff, F. W., and Momenan, R. (2018). Random forest based classification of alcohol dependence patients and healthy controls using resting state MRI. *Neurosci. Lett.* 676, 27–33. doi: 10.1016/j.neulet.2018.04.007
- Zhu, X., Zhu, Q., Jiang, C., Shen, H., Wang, F., Liao, W., et al. (2017b). Disrupted resting-state default mode network in betel quid-dependent individuals. *Front. Psychol.* 8:84. doi: 10.3389/fpsyg.2017.00084
- Zou, Y., Tang, W., Qiao, X., and Li, J. (2021). Aberrant modulations of static functional connectivity and dynamic functional network connectivity in chronic migraine. *Quant. Imag. Med. Surg.* 11, 2253–2264. doi: 10.21037/qims-20-588
- Zuo, N., Yang, Z., Liu, Y., Li, J., and Jiang, T. (2018). Core networks and their reconfiguration patterns across cognitive loads. *Hum. Brain Mapp.* 39, 3546–3557. doi: 10.1002/hbm.24193

**Conflict of Interest:** The authors declare that the research was conducted in the absence of any commercial or financial relationships that could be construed as a potential conflict of interest.

**Publisher's Note:** All claims expressed in this article are solely those of the authors and do not necessarily represent those of their affiliated organizations, or those of the publisher, the editors and the reviewers. Any product that may be evaluated in this article, or claim that may be made by its manufacturer, is not guaranteed or endorsed by the publisher.

Copyright © 2022 Ji, Shi, Cheng, Fu, Zhong, Huang, Chen and Wu. This is an open-access article distributed under the terms of the Creative Commons Attribution License (CC BY). The use, distribution or reproduction in other forums is permitted, provided the original author(s) and the copyright owner(s) are credited and that the original publication in this journal is cited, in accordance with accepted academic practice. No use, distribution or reproduction is permitted which does not comply with these terms.



# The Predictive Values of Changes in Local and Remote Brain Functional Connectivity in Primary Angle-Closure Glaucoma Patients According to Support Vector Machine Analysis

Qiang Fu<sup>1</sup>, Hui Liu<sup>2</sup> and Yu Lin Zhong<sup>2\*</sup>

## OPEN ACCESS

### Edited by:

Yan Tong,  
Renmin Hospital of Wuhan University,  
China

### Reviewed by:

Chen-Xing Qi,  
Renmin Hospital of Wuhan University,  
China

Yu-Chen Chen,  
Nanjing Medical University, China  
Zhi Wen,  
Renmin Hospital of Wuhan University,  
China

### \*Correspondence:

Yu Lin Zhong  
804722489@qq.com

### Specialty section:

This article was submitted to  
Brain Imaging and Stimulation,  
a section of the journal  
Frontiers in Human Neuroscience

**Received:** 01 April 2022

**Accepted:** 26 April 2022

**Published:** 19 May 2022

### Citation:

Fu Q, Liu H and Zhong YL (2022)  
The Predictive Values of Changes  
in Local and Remote Brain Functional  
Connectivity in Primary Angle-Closure  
Glaucoma Patients According  
to Support Vector Machine Analysis.  
*Front. Hum. Neurosci.* 16:910669.  
doi: 10.3389/fnhum.2022.910669

<sup>1</sup> Department of Emergency, Jiangxi Provincial People's Hospital, The First Affiliated Hospital of Nanchang Medical College, Nanchang, China, <sup>2</sup> Department of Ophthalmology, Jiangxi Provincial People's Hospital, The First Affiliated Hospital of Nanchang Medical College, Nanchang, China

**Purpose:** The primary angle-closure glaucoma (PACG) is an irreversible blinding eye disease in the world. Previous neuroimaging studies demonstrated that PACG patients were associated with cerebral changes. However, the effect of optic atrophy on local and remote brain functional connectivity in PACG patients remains unknown.

**Materials and Methods:** In total, 23 patients with PACG and 23 well-matched Health Controls (HCs) were enrolled in our study and underwent resting-state functional magnetic resonance imaging (rs-fMRI) scanning. The regional homogeneity (ReHo) method and functional connectivity (FC) method were used to evaluate the local and remote brain functional connectivity. Moreover, support vector machine (SVM) method was applied to constructing PACG classification model.

**Results:** Compared with the HC, PACG patients showed increased ReHo values in right cerebellum (CER)\_8, left CER\_4-5, and right CER\_8. In contrast, PACG patients showed decreased ReHo values in the bilateral lingual gyrus (LING)/calcarine (CAL)/superior occipital gyrus (SOG) and right postcentral gyrus (PostCG). The ReHo value exhibited an accuracy of 91.30% and area under curve (AUC) of 0.95 for distinguishing the PACG patients from HC.

**Conclusion:** Our study demonstrated that the PACG patients showed abnormal ReHo value in the cerebellum, visual cortex, and supplementary motor area, which might be reflect the neurological mechanisms underlying vision loss and eye pain in PACG patients. Moreover, the ReHo values can be used as a useful biomarker for distinguishing the PACG patients from HCs.

**Keywords:** primary angle-closure glaucoma, functional magnetic resonance imaging, regional homogeneity, functional connectivity, support vector machine



## INTRODUCTION

Glaucoma is the second leading cause of blindness globally; the number of patients with glaucoma is expected to increase to 79.6 million by 2020 (Quigley and Broman, 2006). Patients with glaucoma exhibit high intraocular pressure and optic atrophy. Glaucoma can be stratified into open-angle and closed-angle types. The risk factors for glaucoma include genetic (Wiggs and Pasquale, 2017) and environmental components (Lowe, 1972). Although medications and surgical procedures are the primary treatments for glaucoma, there is no effective treatment for advanced glaucoma. Neuroimaging studies have increasingly shown that the glaucoma causes optic nerve atrophy and damage to the visual pathway, including the visual cortex (Gupta et al., 2006; Gupta and Yucel, 2007).

The loss of retinal ganglion cells (RGCs) is the most important pathological change in PACG. The optic atrophy leads to transsynaptic neurodegenerative changes in visual pathways (Nucci et al., 2015; Mancino et al., 2018). Functional magnetic resonance imaging (fMRI) methods have been extensively used to detect abnormalities in brain structure and function in glaucoma patients. Wang et al. demonstrated that PACG patients had significantly lower fractional amplitude of low-frequency fluctuation (fALFF) values in the left cuneus, middle temporal gyrus, and right precentral gyrus; they had higher fALFF values in the bilateral superior frontal gyrus (Wang Q. et al., 2021). Chen et al. reported that the PACG patients showed increased short-range functional connectivity density (FCD) in the left inferior frontal gyrus (IFG)/insula/parahippocampal gyrus and right IFG/insula; they had decreased short-range FCD in the occipital lobe/cuneus/precuneus/superior parietal lobe/postcentral lobe (Chen et al., 2019). In an analysis of high-tension glaucoma patients, Wang et al. found the decreased functional connectivity (FC) within the visual network (Wang et al., 2020a). Moreover, Wang et al. demonstrated that primary open-angle glaucoma (POAG) patients had reduced cerebral blood flow (CBF)-functional connectivity strength (FCS) coupling and an altered CBF/FCS ratio in the visual cortex, salience network, default mode network (DMN), and dorsal attention network (Wang R. et al., 2021). Thus, glaucoma mainly causes abnormal function in the visual cortex. Additionally, glaucoma is accompanied by changes in brain structure. Wang et al. reported that high-tension glaucoma patients showed morphological reductions in visual and non-visual areas throughout the brain (Wang et al., 2020b). Furlanetto et al. reported that glaucoma patients had smaller optic nerve dimensions and shorter lateral geniculate nuclei compared to healthy controls (HCs) (Furlanetto et al., 2018). To our knowledge, the previous neuroimaging studies demonstrated that the glaucoma patients were accompanied by vision and vision-related brain region dysfunction. There have been few studies regarding the synchrony of neural activity changes in PACG patients. Thus, we assume that the PACG patients might be associated with abnormal local and remote brain functional connectivity.

The resting human brain exhibits homogeneous neural activity, which has an important role in visual function (Costa et al., 2017). Recently, fMRI has been used to investigate

the changes in spontaneous neural activity in the human brain. Regional homogeneity (ReHo) analysis can be used to investigate the homogeneity of neural activity by measuring the functional coherence or synchronization of a particular voxel with its nearest voxels (Zang et al., 2004). ReHo analysis has revealed changes in the homogeneity of neural activity in vision-related diseases such as iridocyclitis (Tong et al., 2021) and dysthyroid optic neuropathy (Jiang et al., 2021). In addition to its high spatial and temporal resolution, ReHo analysis provides robust repeatability. In contrast to other fMRI technologies, ReHo method is data-driven technology without preliminary assumption. Moreover, the ReHo method can reflect the neural activity of the whole brain. Thus, ReHo analysis is suitable for non-invasive exploration of changes in neural activity within the brain. In recent years, the combined development of MRI and machine learning technology has provided powerful diagnostic tools. MRI-related machine learning has been successfully applied for accurate clinical classification and diagnosis of many diseases (Han et al., 2019; Niu et al., 2021). Support vector machine (SVM) is a popular tool for fMRI data analysis. SVM can provide a unique solution with a good out-of-sample generalization and an implicit implementation of non-linear classification using the kernel technique. SVM has been used to perform supervised classifications of specific brain functional states/disorders in a variety of task conditions. However, to our knowledge, there have been few studies concerning MRI-related machine learning in PACG patients.

Thus, the present study was performed to investigate the changes in the homogeneity of neural activity in PACG patients. We have investigated the changes in remote FC in PACG patients by region of interest (ROI) analysis by means of the ReHo technique. Moreover, a SVM method was used to determine whether aberrant ReHo could reliably distinguish PACG patients from HCs.

## MATERIALS AND METHODS

### Participants

In total, 23 patients with PACG (10 men and 13 women) were enrolled from the Department of Ophthalmology, Jiangxi Provincial People's Hospital. The diagnostic criteria of PACG were: (1) the intraocular pressure is greater than 21 mmHg in both eyes; (2) optic disc/cup area > 0.6; (3) typical vision field defect (paracentric obscure, arcuate obscure, nasal ladder, fan-shaped field defect, and peripheral field defect); (4) without any other ocular diseases (high myopia, optic neuritis, strabismus, amblyopia, cataracts, and retinal degeneration). The diagnosis of PACG was conducted by two experienced ophthalmologists. All glaucoma patients underwent anterior chamber angiography to make sure the front corner is open. The exclusion criteria of PACG were: (1) advanced PACG patients are associated with severe eye pain; (2) PACG patients with history of surgery; (3) PACG patients with glaucoma-related eye complications such as neovascular glaucoma POAG, secondary glaucoma cataracts, eye atrophy, and corneal edema.

Twenty-three patients' healthy controls (HCs) (10 men and 13 women) were also recruited for this study. The inclusion criteria: (1) without any ocular disease with uncorrected visual acuity (VA)  $> 1.0$ ; (2) no cardiovascular system diseases and no psychiatric disorders.

## Ethical Statement

All research methods were followed the Declaration of Helsinki and were approved by the Ethical Committee for Medicine of Jiangxi Provincial People's Hospital. Participants were enrolled in the study of their own accord and were informed of the purpose, methods, as well as potential risks before signing an informed consent form.

## Clinical Evaluation

The VA of all subjects was measured using the logMAR table and intraocular pressure was assessed by the automatic intraocular pressure measurement. The best-corrected VA and intraocular pressure of both eyes were measured in the each group.

## Magnetic Resonance Imaging Data Acquisition

The MRI scanning was performed on a 3-Tesla MR scanner (750W GE Healthcare, Milwaukee, WI, United States) with an eight-channel head coil. All participants were required to close their eyes without falling asleep when undergoing MRI scanning. The subjects should be keep calm and not engage in specific thoughts. The T1 parameters (repetition time = 8.5 ms, echo time = 3.3 ms, thickness = 1.0 mm, gap = 0 mm, acquisition matrix =  $256 \times 256$ , field of view =  $240 \times 240 \text{ mm}^2$ , and flip angle =  $12^\circ$ ) and 240 functional images parameters (repetition time = 2,000 ms, echo time = 25 ms, thickness = 3.0 mm, gap = 1.2 mm, acquisition matrix =  $64 \times 64$ , field of view =  $240 \times 240 \text{ mm}^2$ , flip angle =  $90^\circ$ , voxel size =  $3.6 \times 3.6 \times 3.6 \text{ mm}^3$ , and 35 axial slices) covering the whole brain were obtained.

## Data Pre-processing

All preprocessing was performed using the toolbox for Data Processing and Analysis of Brain Imaging (DPABI<sup>1</sup>) (Yan et al., 2016) and briefly following the steps: (1) The first 10 volumes of each subject were removed. (2) Slice timing and head motion correction were conducted. (3) Normalized fMRI data were re-sliced with a resolution of  $3 \times 3 \times 3 \text{ mm}^3$ . (4) Data detrends. (5) Linear regression analysis was applied to regress out several covariates (mean frame-wise displacement, global brain signal, and averaged signal from cerebrospinal fluid and white matter). (6) Temporal band-pass filtering was performed (0.01–0.08 Hz).

## Regional Homogeneity Analysis

The ReHo index was calculated by the DPABI software. All ReHo maps of each voxel were  $z$ -transformed with Fisher's  $r$ -to- $z$  transformation to reduce the influence of individual variation for group statistical comparisons.

## Functional Connectivity Analysis

The seed-based FC was used to investigate the remote FC ROI in different ReHo-related brain regions between two groups. Then we calculated the Pearson's correlation coefficient between the representative time series of each seed ROI and every other voxel in the whole brain in the voxel-wise method. Finally, the generated correlations-coefficient maps were converted to  $Z$  values with Fisher's  $r$ -to- $z$  transformation to reduce the impacts of individual variations for group statistical comparisons.

## Support Vector Machine Analysis

The SVM algorithm was performed using the Pattern Recognition for Neuroimaging Toolbox (PRoNTTo) software Cyclotron Research Centre, University of Liège, Belgium (Schrouff et al., 2013). The following steps were followed: (1) dataset specification, (2) the ReHo maps served as a classification feature, (3) Then, the leave-one-out cross-validation (LOOCV) technique was applied to perform SVM classifier validation for model estimation. In each LOOCV fold, FC data from  $n - 1$  samples were selected as the training dataset to train the classification model. (4) The total accuracy, specificity, sensitivity, and area under the receiver operating characteristic curve (AUC) were calculated.

## Statistical Analysis

The independent sample  $t$ -test was used to investigate the clinical features between the two groups.

The one-sample  $t$ -test was conducted to assess the group mean of ReHo maps. The two-sample  $t$ -test was used to compare the two group differences in the ReHo and FC maps using the Gaussian random field (GRF) method (two-tailed, voxel-level  $p < 0.01$ , GRF correction, and cluster-level  $p < 0.05$ ).

## RESULTS

### Demographics and Disease Characteristics

There were no statistically significant differences between the PACG and HC groups in gender ( $p > 0.999$ ), education ( $p = 0.506$ ), or age ( $p = 0.470$ ), but significant differences in BCVA of right eye ( $p < 0.001$ ) and left eye ( $p < 0.001$ ). The results of these data were listed in Table 1.

### Comparisons of Regional Homogeneity Between Patients With Primary Angle-Closure Glaucoma and Health Control

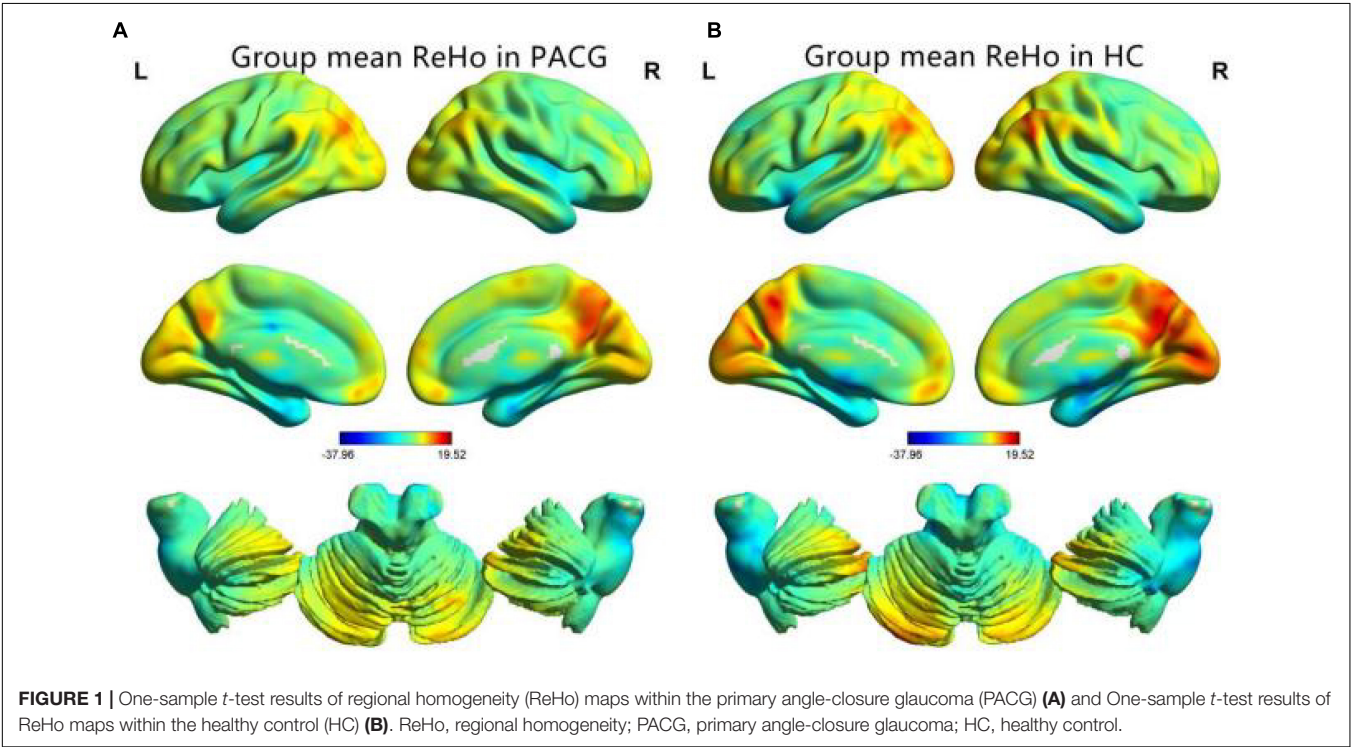
The group means of ReHo maps of the PACG and HC are shown in Figures 1A,B. Compared with the HCs, PACG patients showed significantly increased ReHo values in the right cerebellum (CER)\_8 and left CER\_4-5. Meanwhile, PACG patients showed decreased ReHo values in the bilateral lingual gyrus (LING)/calcarine (CAL)/superior occipital gyrus (SOG) and right postcentral gyrus (PostCG) (Table 2 and Figure 2A).

<sup>1</sup><http://www.rfmri.org/dpabi>

**TABLE 1 |** Demographic and clinical measurements between patients with primary angle-closure glaucoma (PACG) and healthy controls (HCs).

Condition	PACG group	HC group	T-value	P-value
Age (years)	50.96 ± 4.85	50.82 ± 6.76	0.727	0.470
Sex (male/female)	10/13	10/13	N/A	>0.999
Education (years)	12.61 ± 5.88	11.46 ± 6.86	0.670	0.506
BCVA-OD	0.15 ± 0.10	1.18 ± 0.12	0.626	<0.001
BCVA-OS	0.30 ± -0.12	1.14 ± 0.10	0.538	<0.001
Handedness	23 R	23 R	N/A	N/A

Chi-square test for sex. Independent t-test was used for other normally distributed continuous data. Data are displayed as mean ± standard deviation. HC, healthy control; BCVA, best-corrected visual acuity; OD, oculus dexter; OS, oculus sinister; N/A, not applicable; R, right.



**TABLE 2 |** Significant differences in the regional homogeneity (ReHo) between two groups.

Condition	Brain regions	MNI			Peak T-scores	Cluster size (voxels)
		x	y	z		
PACG > HC	R_CER_8	−12	−60	−63	6.4017	645
PACG > HC	L_CER_4-5	−12	−30	−27	4.5909	539
PACG > HC	R_CER_8	15	−21	−51	5.6261	143
PACG < HC	B_LING/CAL/SOG	−9	−102	18	−4.5399	738
PACG < HC	R_PostCG	39	−36	66	−4.7791	514

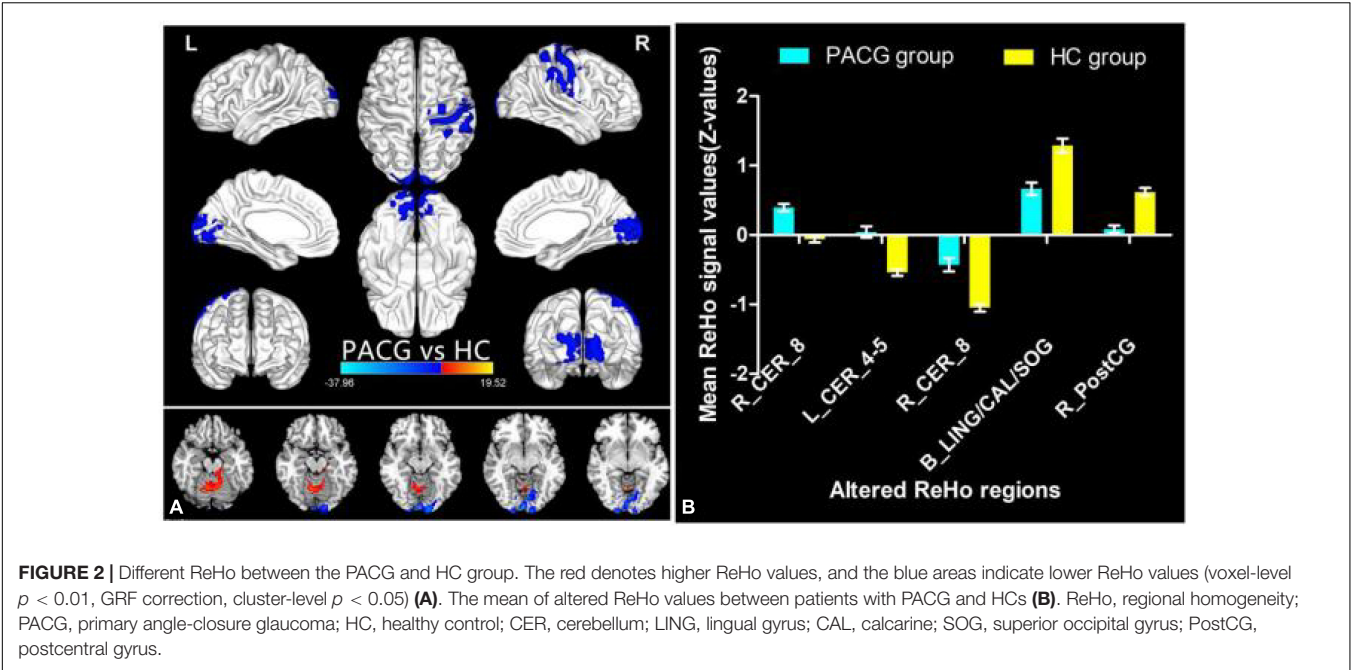
x, y, and z are the locations of the peak voxels in standard MNI coordinates. ReHo, regional homogeneity; PACG, primary angle-closure glaucoma; HC, healthy control; MNI, Montreal Neurological Institute; CER, Cerebellum; LING, Lingual Gyrus; CAL, Calcarine; SOG, Superior Occipital Gyrus; PostCG, Postcentral Gyrus; R, right; L, left; B, bilateral.

The mean values of altered ReHo values were shown with a histogram (Figure 2B).

Differences in Functional Connectivity

The seed-based FC was used to investigate the remote FC between two groups with ROI in the five different ReHo

brain regions: (1) ROI in R\_CER\_8, the PACG patients showed decreased FC between the R\_CER\_8 and R\_IPL, L\_IFG, R\_SFG (Table 3 and Figure 3A). (2) ROI in L\_CER\_4-5, the PACG patients showed decreased FC between the L\_CER\_4-5 and R\_CER\_8, R\_CER\_4\_5, L\_MFG, R\_MFG, L\_PreCUN (Table 3 and Figure 3B). (3) ROI in R\_CER\_8,



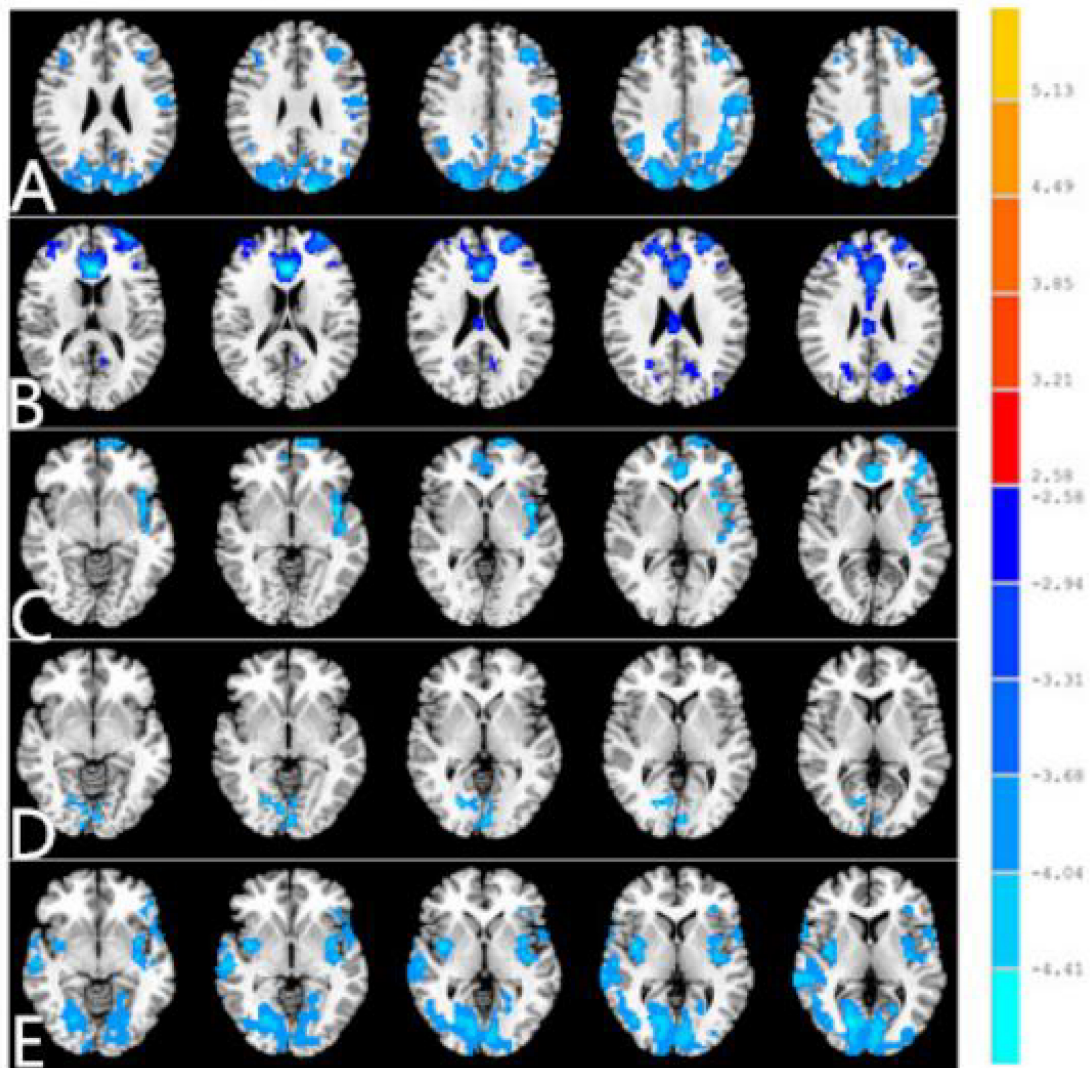
**TABLE 3 |** Significant differences in the functional connectivity (FC) between two groups.

Condition	Brain regions	MNI			Peak <i>T</i> -scores	Cluster size (voxels)
		x	y	z		
ROI in R_CER_8						
PACG < HC	R_IPL	45	−54	42	−5.3942	7070
PACG < HC	L_IFG	−51	39	−9	−3.7121	196
PACG < HC	R_SFG	18	−3	57	−4.2058	485
ROI in L_CER_4-5						
PACG < HC	R_CER_8	15	−54	−60	−4.858	1990
PACG > HC	R_CER_4_5	15	−21	−24	5.1884	653
PACG < HC	L_MFG	−39	60	12	−4.5478	1076
PACG < HC	R_MFG	39	45	15	−3.2698	57
PACG < HC	L_PreCUN	−9	−66	42	−5.0912	4947
ROI in R_CER_8						
PACG < HC	L_INS	−42	3	0	−4.4446	723
PACG < HC	L_ACC	3	39	9	−4.1039	652
PACG < HC	R_ANG	21	−60	45	−4.4087	477
PACG < HC	L_PreCUN	−12	−63	39	−4.7861	988
ROI in B_LING/CAL/SOG						
PACG < HC	R_CER	18	−39	−60	−4.3662	469
PACG < HC	L_CAL	18	−96	−15	−3.3303	171
PACG < HC	R_PostCG	30	−33	54	−4.4334	4396
ROI in R_PostCG						
PACG < HC	L_STG	-30	15	−36	−3.6386	44
PACG < HC	L_INS	−36	−15	−12	−4.5824	593
PACG < HC	L_IFG	−51	39	−9	−3.5894	73
PACG < HC	R_CAL	18	−78	9	−5.1517	6779
PACG < HC	L_IFG	−33	33	3	−3.4947	48

*x, y, and z are the locations of the peak voxels in standard MNI coordinates. FC, functional connectivity; PACG, primary angle-closure glaucoma; HC, healthy control; MNI, Montreal Neurological Institute; CER, Cerebellum; LING, Lingual Gyrus; CAL, Calcarine; SOG, Superior Occipital Gyrus; PostCG, Postcentral Gyrus; IPL, Inferior Parietal Lobule; IFG, Inferior Frontal Gyrus; SFG, Superior Frontal Gyrus; MFG, Middle Frontal Gyrus; PreCUN, Precuneus; INS, Insula; ACC, Anterior Cingulate Gyrus; ANG, Angular Gyrus; PostCG, Precentral Gyrus; STG, Superior Temporal Gyrus; IFG, Inferior Frontal Gyrus; R, right; L, left; B, bilateral.*

the PACG patients showed decreased FC between the L\_INS, and L\_ACC, R\_ANG, L\_PreCUN (Table 3 and Figure 3C). (4) ROI in B\_LING/CAL/SOG, the PACG patients showed decreased FC between the B\_LING/CAL/SOG and R\_CER, L\_CAL, R\_PostCG (Table 3 and Figure 3D). (5) ROI in R\_PostCG, the PACG patients showed decreased FC between the





**FIGURE 3 |** Different FC between two groups with region of interest (ROI) in R\_CER\_8 (A). Different functional connectivity (FC) between two groups with ROI in L\_CER\_4-5 (B). Different FC between two groups with ROI in R\_CER\_8. (C) Different FC between two groups with ROI in B\_LING/CAL/SOG (D). Different FC between two groups with ROI in R\_PostCG (E). The red denotes higher FC signal values, and the blue areas indicate lower FC signal values (voxel-level  $p < 0.01$ , GRF correction, cluster-level  $p < 0.01$ ). FC, functional connectivity; PACG, primary angle-closure glaucoma; HC, healthy control; CER, cerebellum; LING, lingual gyrus; CAL, calcarine; SOG, superior occipital gyrus; PostCG, postcentral gyrus.

R\_PostCG and L\_STG, L\_INS, L\_IFG, R\_CAL, L\_IFG (Table 3 and Figure 3E).

### Support Vector Machine Results

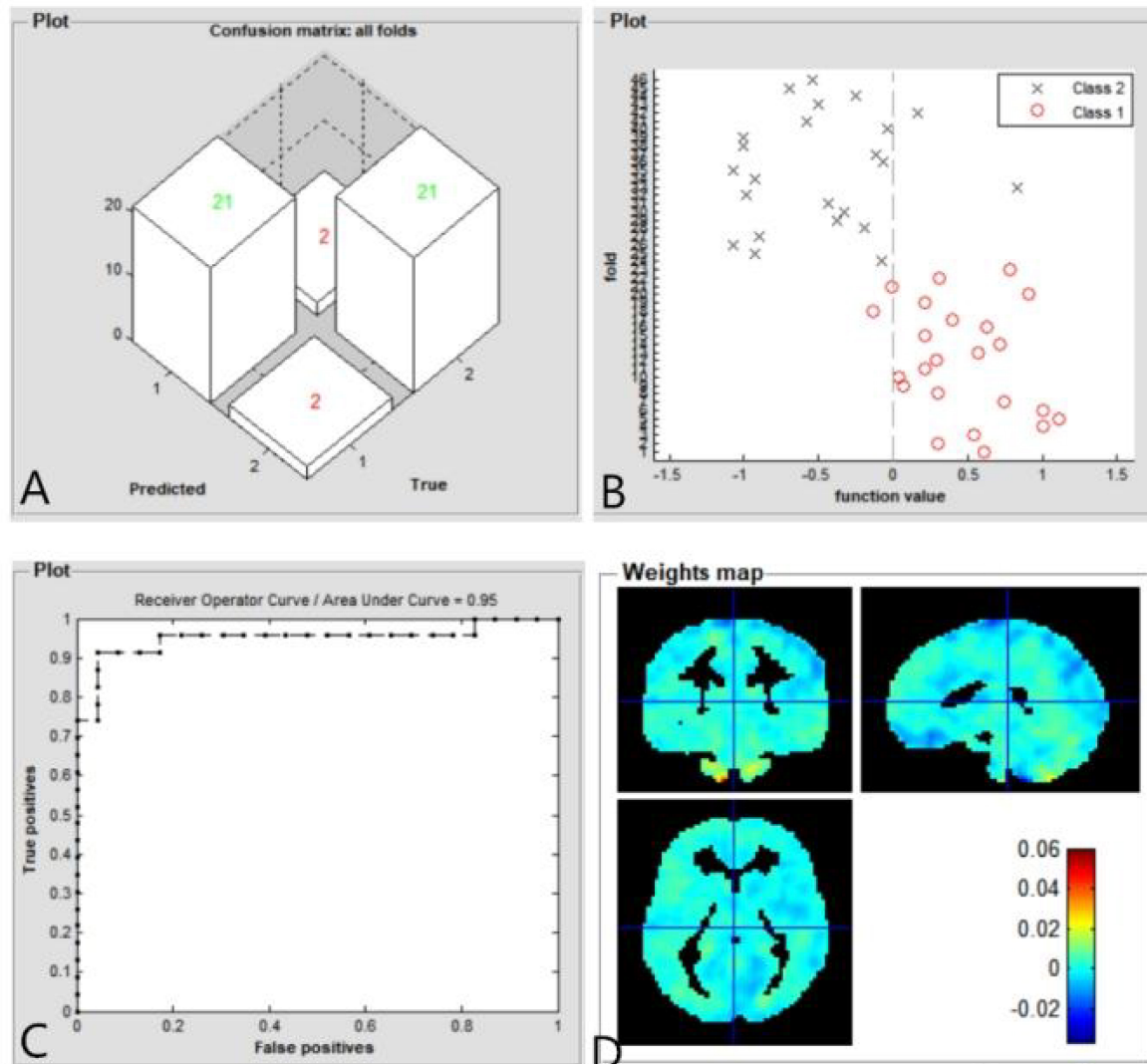
The SVM classification reaches a total accuracy of 91.30%. Classification results using machine learning analysis were based on the ReHo values. Three-dimensional confusion matrices from machine learning analysis (Figure 4A). Function values of two groups (class 1: PACG group; class 2: HC group) (Figure 4B). The ROC curve of the SVM classifier with an AUC value of 0.95 (Figure 4C). Weight maps for SVM models. The weight in each voxel corresponding to its contribution to the model's prediction (Figure 4D).

### DISCUSSION

In this study, compared with HCs, PACG patients had significantly greater ReHo values in the right cerebellum (CER)\_8 and left CER\_4-5. PACG patients also showed decreased ReHo values in the bilateral lingual gyrus (LING)/calcarine (CAL)/SOG and right PostCG. Moreover, PACG patients showed abnormal remote FC within the cerebellar network, visual network, DMN, and sensorimotor network (SMN). Notably, the SVM classifier exhibited overall accuracy of 91.30% and an AUC of 0.95 based on ReHo values.

As noted above, PACG patients had significantly greater ReHo values in the right CER\_8 and left CER\_4-5, compared with the





**FIGURE 4 |** Classification results using machine learning analysis based on ReHo values. Three-dimensional confusion matrices from machine learning analysis (A). Function values of two groups (class 1: PACG group; class 2: HC group) (B). The ROC curve of the SVM classifier with an AUC value of 0.95 (C). Weight maps for SVM models. The weight in each voxel corresponding to its contribution to the model's prediction (D).

values in HCs. The cerebellum has important roles in motor control and body balance (Doya, 2000; Morton and Bastian, 2004), as well as higher cognitive function (Middleton and Strick, 1994). The cerebellum also has important roles in visual attention and working memory (Dai et al., 2013; Brissenden et al., 2018; van Es et al., 2019). Thus, the cerebellum participates in visual information processing. Dai et al. demonstrated that POAG patients had increased FC between V1 and the cerebellum (Dai et al., 2013). Song et al. also reported that POAG patients had increased ReHo values in the cerebellum (Song et al., 2014). In the present study, we found that increased ReHo in the cerebellum of PACG patients, which might reflect impaired visual attention in such patients.

Importantly, PACG patients had decreased ReHo values in the bilateral LING/CAL/SOG, which is located in the primary

visual cortex. Furthermore, we found that PACG patients had decreased remote FC between the visual cortex and the CER, CAL, and PostCG. High intraocular pressure in PACG patients can lead to RGC loss, which results in decreased transmission of visual signals into the visual cortex. Furthermore, the previous neuroimaging studies demonstrated the visual pathway atrophy in glaucoma patients (Hernowo et al., 2011; Haykal et al., 2021). Other studies demonstrated that PACG patients had abnormal cortical thickness in the visual cortex (Yu et al., 2013; Bogorodzki et al., 2014). Thus, we found that the ReHo was decreased in the primary visual cortex of PACG patients, which might indicate abnormal visual information processing in the visual cortex.

In this study, we found that PACG patients had decreased ReHo values in the right PostCG. The PostCG has an important role in sensorimotor function (Zlatkina et al., 2016). The PostCG

dysfunction might induce motor control impairment (Kato and Izumiyama, 2015). Vivek Trivedi et al. reported that visuomotor coordination might be impaired in glaucoma patients (Trivedi et al., 2019). Furthermore, the visual field defect might lead to slow movement and falls in PACG patients; glaucoma patients showed impairments in both visual and somatosensory function, compared to HCs (Black et al., 2008; Kotecha et al., 2012). Consistent with these findings, our study demonstrated that the PACG patients had decreased ReHo values in the PostCG, which might reflect sensorimotor dysfunction. Additionally, the PostCG is important for pain sensory processing. In our study, PACG patients showed symptoms of acute eye pain. The PostCG is also involved in pain information processing. The previous neuroimaging studies demonstrated that the eye pain-related diseases might induce PostCG dysfunction (Tang et al., 2018). Thus, we speculate that the impaired visuomotor coordination and acute eye pain contribute to PostCG dysfunction in PACG patients.

Finally, a machine learning technique (i.e., an SVM classifier) was used to determine whether aberrant ReHo values could reliably distinguish PACG patients from HCs. In our study, the SVM classifier accuracy was 91.30%. The ROC curve of the SVM classifier revealed an AUC of 0.95. Our findings indicate that the ReHo values can be used to reliably distinguish PACG patients from HCs. Therefore, the combination of ReHo analysis and machine learning can be used for disease classification and diagnosis, support the use of these methods in future clinical practice. Thus, SVM model showed high sensitive classification and diagnosis ability using ReHo as a feature. In the future, SVM model could be used for early diagnosis of glaucoma.

## LIMITATIONS

First, the sample size was small. Second, ReHo and FC values on the basis of blood oxygenation level-dependent signals would still

be affected by physiological noise, such as cardiac and respiratory activity and scanning noise. Thirds, PACG patients have an inconsistent course of disease, which might be bad impact on the results of the study.

## CONCLUSION

Our results showed that PACG patients had abnormal homogeneity of neural activities such as cerebellum, visual cortex, and sensorimotor cortex, which might indicate the neural mechanism of visual field defect in patients with PACG. Moreover, ReHo map could be sensitive biomarkers for distinguishing patients with PACG from HCs.

## DATA AVAILABILITY STATEMENT

The raw data supporting the conclusions of this article will be made available by the authors, without undue reservation.

## ETHICS STATEMENT

The studies involving human participants were reviewed and approved by Ethical Committee for Medicine of Jiangxi Provincial People's Hospital. The patients/participants provided their written informed consent to participate in this study.

## AUTHOR CONTRIBUTIONS

QF, HL, and YZ contributed to data collection, statistical analyses, wrote the manuscript, designed the protocol, MRI analysis, designed the study, oversaw all clinical aspects of study conduct, and manuscript preparation. All authors contributed to the article and approved the submitted version.

## REFERENCES

- Black, A. A., Wood, J. M., Lovie-Kitchin, J. E., and Newman, B. M. (2008). Visual impairment and postural sway among older adults with glaucoma. *Optom. Vis. Sci.* 85, 489–497. doi: 10.1097/OPX.0b013e31817882db
- Bogorodzki, P., Piatkowska-Janko, E., Szaflik, J., Szaflik, J. P., Gacek, M., and Grieb, P. (2014). Mapping cortical thickness of the patients with unilateral end-stage open angle glaucoma on planar cerebral cortex maps. *PLoS One* 9:e93682. doi: 10.1371/journal.pone.0093682
- Brissenden, J. A., Tobyne, S. M., Osher, D. E., Levin, E. J., Halko, M. A., and Somers, D. C. (2018). Topographic Cortico-cerebellar Networks Revealed by Visual Attention and Working Memory. *Curr. Biol.* 28, 3364–3372e5. doi: 10.1016/j.cub.2018.08.059
- Chen, L., Li, S., Cai, F., Wu, L., Gong, H., Pei, C., et al. (2019). Altered functional connectivity density in primary angle-closure glaucoma patients at resting-state. *Quant. Imaging Med. Surg.* 9, 603–614. doi: 10.21037/qims.2019.04.13
- Costa, G. N., Duarte, J. V., Martins, R., Wibril, M., and Castelo-Branco, M. (2017). Interhemispheric Binding of Ambiguous Visual Motion Is Associated with Changes in Beta Oscillatory Activity but Not with Gamma Range Synchrony. *J. Cogn. Neurosci.* 29, 1829–1844. doi: 10.1162/jocn\_a\_01158
- Dai, H., Morelli, J. N., Ai, F., Yin, D., Hu, C., Xu, D., et al. (2013). Resting-state functional MRI: functional connectivity analysis of the visual cortex in primary open-angle glaucoma patients. *Hum. Brain Mapp.* 34, 2455–2463. doi: 10.1002/hbm.22079
- Doya, K. (2000). Complementary roles of basal ganglia and cerebellum in learning and motor control. *Curr. Opin. Neurobiol.* 10, 732–739. doi: 10.1016/s0959-4388(00)00153-7
- Furlanetto, R. L., Teixeira, S. H., Gracitelli, C. P. B., Lottenberg, C. L., Emori, F., and Michelan, M. (2018). Structural and functional analyses of the optic nerve and lateral geniculate nucleus in glaucoma. *PLoS One* 13:e0194038. doi: 10.1371/journal.pone.0194038
- Gupta, N., Ang, L. C., de Tilly, L., Noel, Bidaisee, L., and Yucel, Y. H. (2006). Human glaucoma and neural degeneration in intracranial optic nerve, lateral geniculate nucleus, and visual cortex. *Br. J. Ophthalmol.* 90, 674–678. doi: 10.1136/bjo.2005.086769
- Gupta, N., and Yucel, Y. H. (2007). What changes can we expect in the brain of glaucoma patients? *Surv. Ophthalmol.* 52, S122–S126. doi: 10.1016/j.survophthal.2007.08.006
- Han, K. M., De Berardis, D., Fornaro, M., and Kim, Y. K. (2019). Differentiating between bipolar and unipolar depression in functional and structural MRI studies. *Prog. Neuropsychopharmacol. Biol. Psychiatry* 91, 20–27. doi: 10.1016/j.pnpbp.2018.03.022
- Haykal, S., Jansonius, N. M., and Cornelissen, F. W. (2021). Progression of Visual Pathway Degeneration in Primary Open-Angle Glaucoma: a Longitudinal

- Study. *Front. Hum. Neurosci.* 15:630898. doi: 10.3389/fnhum.2021.630898
- Hernowo, A. T., Boucard, C. C., Jansonius, N. M., Hooymans, J. M., and Cornelissen, F. W. (2011). Automated morphometry of the visual pathway in primary open-angle glaucoma. *Invest. Ophthalmol. Vis. Sci.* 52, 2758–2766. doi: 10.1167/iops.10-5682
- Jiang, Y. P., Yang, Y. C., Tang, L. Y., Ge, Q. M., Shi, W. Q., Su, T., et al. (2021). Altered spontaneous brain activity patterns in dysthyroid optic neuropathy: a resting-state fMRI study. *J. Integr. Neurosci.* 20, 375–383. doi: 10.31083/jin2002037
- Kato, H., and Izumiyama, M. (2015). Impaired motor control due to proprioceptive sensory loss in a patient with cerebral infarction localized to the postcentral gyrus. *J. Rehabil. Med.* 47, 187–190. doi: 10.2340/16501977-1900
- Kotecha, A., Richardson, G., Chopra, R., Fahy, R. T., Garway-Heath, D. F., and Rubin, G. S. (2012). Balance control in glaucoma. *Invest. Ophthalmol. Vis. Sci.* 53, 7795–7801. doi: 10.1167/iops.12-10866
- Lowe, R. F. (1972). Primary angle-closure glaucoma. *Br. J. Ophthalmol.* 56, 13–20.
- Mancino, R., Martucci, A., Cesareo, M., Giannini, C., Corasaniti, M. T., Bagetta, G., et al. (2018). Glaucoma and Alzheimer Disease: one Age-Related Neurodegenerative Disease of the Brain. *Curr. Neuropharmacol.* 16, 971–977. doi: 10.2174/1570159X16666171206144045
- Middleton, F. A., and Strick, P. L. (1994). Anatomical evidence for cerebellar and basal ganglia involvement in higher cognitive function. *Science* 266, 458–461. doi: 10.1126/science.7939688
- Morton, S. M., and Bastian, A. J. (2004). Cerebellar control of balance and locomotion. *Neuroscientist* 10, 247–259. doi: 10.1177/1073858404263517
- Niu, C., Wang, Y., Cohen, A. D., Liu, X., Li, H., Lin, P., et al. (2021). Machine learning may predict individual hand motor activation from resting-state fMRI in patients with brain tumors in perirolandic cortex. *Eur. Radiol.* 31, 5253–5262. doi: 10.1007/s00330-021-07825-w
- Nucci, C., Martucci, A., Cesareo, M., Garaci, F., Morrone, L. A., Russo, R., et al. (2015). Links among glaucoma, neurodegenerative, and vascular diseases of the central nervous system. *Prog. Brain Res.* 221, 49–65. doi: 10.1016/bs.pbr.2015.04.010
- Quigley, H. A., and Broman, A. T. (2006). The number of people with glaucoma worldwide in 2010 and 2020. *Br. J. Ophthalmol.* 90, 262–267. doi: 10.1136/bjo.2005.081224
- Schrouff, J., Rosa, M. J., Rondina, J. M., Marquand, A. F., Chu, C., Ashburner, J., et al. (2013). PRoNTTo: pattern recognition for neuroimaging toolbox. *Neuroinformatics* 11, 319–337. doi: 10.1007/s12021-013-9178-1
- Song, Y., Mu, K., Wang, J., Lin, F., Chen, Z., Yan, X., et al. (2014). Altered spontaneous brain activity in primary open angle glaucoma: a resting-state functional magnetic resonance imaging study. *PLoS One* 9:e89493. doi: 10.1371/journal.pone.0089493
- Tang, L. Y., Li, H. J., Huang, X., Bao, J., Sethi, Z., Ye, L., et al. (2018). Assessment of synchronous neural activities revealed by regional homogeneity in individuals with acute eye pain: a resting-state functional magnetic resonance imaging study. *J. Pain Res.* 11, 843–850. doi: 10.2147/JPR.S156634
- Tong, Y., Huang, X., Qi, C. X., and Shen, Y. (2021). Disrupted Neural Activity in Individuals With Iridocyclitis Using Regional Homogeneity: a Resting-State Functional Magnetic Resonance Imaging Study. *Front. Neurol.* 12:609929. doi: 10.3389/fneur.2021.609929
- Trivedi, V., Bang, J. W., Parra, C., Colbert, M. K., O'Connell, C., and Arshad, A. (2019). Widespread brain reorganization perturbs visuomotor coordination in early glaucoma. *Sci. Rep.* 9:14168. doi: 10.1038/s41598-019-50793-x
- van Es, D. M., van der Zwaag, W., and Knapen, T. (2019). Topographic Maps of Visual Space in the Human Cerebellum. *Curr. Biol.* 29, 1689–1694e3. doi: 10.1016/j.cub.2019.04.012
- Wang, Y., Lu, W., Xie, Y., Zhou, J., Yan, T., Han, W., et al. (2020a). Functional Alterations in Resting-State Visual Networks in High-Tension Glaucoma: an Independent Component Analysis. *Front. Hum. Neurosci.* 14:330. doi: 10.3389/fnhum.2020.00330
- Wang, Y., Wang, X., Zhou, J., Qiu, J., Yan, T., Xie, Y., et al. (2020b). Brain morphological alterations of cerebral cortex and subcortical nuclei in high-tension glaucoma brain and its associations with intraocular pressure. *Neuroradiology* 62, 495–502. doi: 10.1007/s00234-019-02347-1
- Wang, Q., Qu, X., Chen, W., Wang, H., Huang, C., Li, T., et al. (2021). Altered coupling of cerebral blood flow and functional connectivity strength in visual and higher order cognitive cortices in primary open angle glaucoma. *J. Cereb. Blood Flow Metab.* 41, 901–913. doi: 10.1177/0271678X20935274
- Wang, R., Tang, Z., Liu, T., Sun, X., Wu, L., and Xiao, Z. (2021). Altered spontaneous neuronal activity and functional connectivity pattern in primary angle-closure glaucoma: a resting-state fMRI study. *Neurol. Sci.* 42, 243–251. doi: 10.1007/s10072-020-04577-1
- Wiggs, J. L., and Pasquale, L. R. (2017). Genetics of glaucoma. *Hum. Mol. Genet.* 26, R21–R27. doi: 10.1001/jama.2019.16161
- Yan, C. G., Wang, X. D., Zuo, X. N., and Zang, Y. F. (2016). DPABI: data Processing & Analysis for (Resting-State) Brain Imaging. *Neuroinformatics* 14, 339–351. doi: 10.1007/s12021-016-9299-4
- Yu, L., Xie, B., Yin, X., Liang, M., Evans, A. C., Wang, J., et al. (2013). Reduced cortical thickness in primary open-angle glaucoma and its relationship to the retinal nerve fiber layer thickness. *PLoS One* 8:e73208. doi: 10.1371/journal.pone.0073208
- Zang, Y., Jiang, T., Lu, Y., He, Y., and Tian, L. (2004). Regional homogeneity approach to fMRI data analysis. *Neuroimage* 22, 394–400. doi: 10.1016/j.neuroimage.2003.12.030
- Zlatkina, V., Amiez, C., and Petrides, M. (2016). The postcentral sulcal complex and the transverse postcentral sulcus and their relation to sensorimotor functional organization. *Eur. J. Neurosci.* 43, 1268–1283. doi: 10.1111/ejn.13049

**Conflict of Interest:** The authors declare that the research was conducted in the absence of any commercial or financial relationships that could be construed as a potential conflict of interest.

**Publisher's Note:** All claims expressed in this article are solely those of the authors and do not necessarily represent those of their affiliated organizations, or those of the publisher, the editors and the reviewers. Any product that may be evaluated in this article, or claim that may be made by its manufacturer, is not guaranteed or endorsed by the publisher.

Copyright © 2022 Fu, Liu and Zhong. This is an open-access article distributed under the terms of the Creative Commons Attribution License (CC BY). The use, distribution or reproduction in other forums is permitted, provided the original author(s) and the copyright owner(s) are credited and that the original publication in this journal is cited, in accordance with accepted academic practice. No use, distribution or reproduction is permitted which does not comply with these terms.



# Altered Intrinsic Regional Spontaneous Brain Activity in Patients With Severe Obesity and Meibomian Gland Dysfunction: A Resting-State Functional Magnetic Resonance Imaging Study

## OPEN ACCESS

### Edited by:

Xin Huang,  
Jiangxi Provincial People's Hospital,  
China

### Reviewed by:

Hua Wang,  
Central South University, China  
Melis Palamar,  
Ege University, Turkey

### \*Correspondence:

Yi Shao  
freebee99@163.com

<sup>†</sup> These authors have contributed  
equally to this work

### Specialty section:

This article was submitted to  
Brain Imaging and Stimulation,  
a section of the journal  
Frontiers in Human Neuroscience

**Received:** 19 February 2022

**Accepted:** 11 April 2022

**Published:** 19 May 2022

### Citation:

Liu Y, Tan S-X, Wu Y-K, Shen Y-K,  
Zhang L-J, Kang M, Ying P, Pan Y-C,  
Shu H-Y and Shao Y (2022) Altered  
Intrinsic Regional Spontaneous Brain  
Activity in Patients With Severe  
Obesity and Meibomian Gland  
Dysfunction: A Resting-State  
Functional Magnetic Resonance  
Imaging Study.  
Front. Hum. Neurosci. 16:879513.  
doi: 10.3389/fnhum.2022.879513

Yi Liu<sup>††</sup>, Sheng-Xing Tan<sup>††</sup>, Yu-Kang Wu<sup>1</sup>, Yan-Kun Shen<sup>1</sup>, Li-Juan Zhang<sup>2</sup>, Min Kang<sup>2</sup>,  
Ping Ying<sup>2</sup>, Yi-Cong Pan<sup>2</sup>, Hui-Ye Shu<sup>2</sup> and Yi Shao<sup>2\*</sup>

<sup>1</sup> Department of Gastrointestinal Surgery, The First Affiliated Hospital of Nanchang University, Nanchang, China,

<sup>2</sup> Department of Ophthalmology, The First Affiliated Hospital of Nanchang University, Jiangxi Branch of National Clinical  
Research Center for Ocular Disease, Nanchang, China

**Purpose:** To evaluate potential regional homogeneity (ReHo) cerebrum function lesions in people with severe obesity and meibomian gland dysfunction (SM) and probe the connection between aberrant cerebrum activity and clinical manifestations.

**Patients and Methods:** An aggregation of 12 patients with SM, and 12 healthy controls (HCs) closely matched in age and gender were enrolled. We applied corneal confocal microscopy and fundus angiography to compare imaging distinctions between the two groups. SMs were required to carefully fill out the Hospital Anxiety Depression Scale (HADS) forms, and a correlation analysis was performed. ReHo was also utilized to appraise partial differences in spontaneous cerebrum function. Receiver operating characteristic (ROC) curves were created to partition ReHo values between patients with SM and the HCs.

**Results:** ReHo values for the left cerebellum (LC), right fusiform gyrus (RFG), left inferior temporal gyrus (LITG), left rectus gyrus (LRG), right thalamus (RT), right caudate (RC), left insula (LI), and left thalamus (LT) of subjects with SM were notably higher than those of the HCs ( $P < 0.05$ ). ReHo values of the right middle frontal gyrus (RMFG) in subjects with SM were decreased notably compared to the HCs ( $P < 0.05$ ). ReHo values for the RMFG showed a negative correlation with the anxiety scores (ASs;  $r = -0.961$ ,  $P < 0.001$ ) and ReHo values for the RFG showed a positive correlation with the depression scores (DSs;  $r = 0.676$ ,  $P = 0.016$ ). The areas under the ROC curve were 1.000 ( $P < 0.001$ ) for the RMFG, LC, LITG, LRG, RC, LI, and LT and 0.993 ( $P < 0.001$ )



for the RFG and RT. The results from the ROC curve analysis indicated that changes in the ReHo values of some brain regions may help diagnose SM.

**Conclusion:** Our research emphasized that patients with SM had lesions in synchronized neural activity in many encephalic areas. Our discoveries may provide beneficial information for exploring the neuromechanics of SM.

**Keywords:** severe obesity, meibomian gland dysfunction, regional homogeneity, resting state, functional magnetic resonance imaging, Hospital Anxiety Depression Scale

## INTRODUCTION

Adult obesity signifies body mass index (BMI) greater than or equal to 30, and severe obesity (SO) is defined as BMI greater than or equal to 35 (Hales et al., 2020). Obesity is now an epidemic disease and its complications include type 2 diabetes (Stein and Colditz, 2004) and increased risk for cardiovascular, musculoskeletal, and tumor diseases (D'Abbondanza et al., 2020). Apart from these widely known systemic diseases, SO gives rise to cognizance injures, and it is also a hazardous factor for vascular dementia. Some study have pointed out that the changes in cerebrum structure and function related to obesity may be the cause of cognitive and emotional dysfunctions in SO patients (Zeighami et al., 2021).

The meibomian gland (MG) is a sebaceous gland in the eyelid. It can produce a tarsal plate and is the lipid component of the tear film. The plate gland is very crucial for delaying tear film evaporation, which can prevent dry eyes (Osae et al., 2019). The MG has the ability to reduce surface tension, which contributes to diffusion of the tear film on the ocular surface (Millar and Schuett, 2015). Due to the MG being able to produce lipids that make up the meibomian, and the blood and meibomian contour have attributes in common, some studies have reported that dyslipidemia, such as SO, can bring about meibomian gland dysfunction (MGD), including changes in the meibomian lipid component (Mudgil, 2014). An abnormality of the lipid component may lead to inflammation, which is an underlying cause of blepharitis and can eventually impact the regular excretory capabilities of the MG (Pietiläinen et al., 2007). This may generate degraded tear film quality and stabilization, eventually leading to ophthalmic surface inflammation in patients with MGD (Knop et al., 2011). A study showed that there was a strong positive correlation between dyslipidemia and MGD (Kuriakose and Braich, 2018). In the studied cases in our institution, we observed that all patients with SO had MGD. Due to the particularity of the anatomy of the MG, routine examination and diagnosis mainly rely on corneal confocal microscopy and fundus anatomy (Figure 1).

fMRI is a sophisticated non-invasive technique that is used to study the complexity of the brain-behavior relationship (García-García et al., 2019). Compared with traditional MRI technology, its main advantages include high dimensional resolution and the ability to disclose microstructure changes (Zhang et al., 2018). fMRI studies have reported differences in cerebrum activity levels between thin and obese people in different static state networks, including the default pattern network, significance network, and

temporal lobe network (Val-Laillet et al., 2015). It is an essential tool for the study of cerebrum changes and the corresponding behavioral pathological basis in patients with SM.

The regional homogeneity (ReHo) method is a resting pattern functional magnetic resonance surveying method that has been used to assess lesions of the cerebrum (Guo et al., 2020). The ReHo method can measure the similarity of a time series of specific voxels and their nearest neighbors (Ding et al., 2020). These signals have previously been utilized to detect changes in nerve actions in sufferers of multifarious neural diseases, including Alzheimer's disease, depressive disorder, schizophrenia, and attention deficit (Zhang Y. et al., 2019).

In this study, we utilized the ReHo method to study the cerebrum functions of patients with SM, to confirm lesions of cerebrum, and probe into the latent pathological mechanisms. To our knowledge, this is the first study on SM utilizing this approach.

## MATERIALS AND METHODS

### Subjects

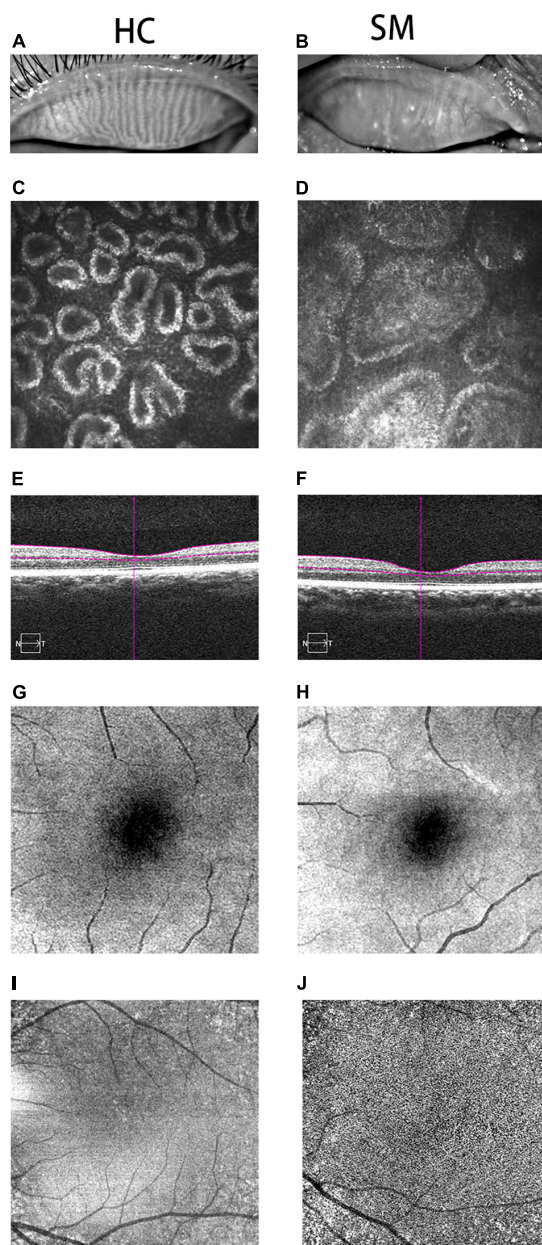
An aggregation of 12 patients with SM (4 men and 8 women) were enlisted from the Ophthalmology Department of the Nanchang University's First Adjunctive Hospital. Indications for SM patients were as follows: (1) BMI  $\geq 35$ ; (2) male waistline  $\geq 90$  cm and female waistline  $\geq 85$  cm; (3) capable of being scanned with an MRI (no heart pacemaker or embedded metallic installations); and (4) no mental disturbance (major depression and/or anxiety disorders); (5) suffering from MGD. The elimination standard for SM included the following criteria: (1) SO caused by receiving massive hormones in a short period of time; (2) no painkillers before the fMRI scan; (3) history of diabetes; and (4) suffering from family inherited diseases.

Twelve (6 males and 6 females) subjects acted as healthy controls (HCs) and they were similarly aligned with SM sufferers in terms of age and gender. Every HC was conformed with the following standards: (1)  $24 \geq \text{BMI} \geq 20$ ; (2) could participate in an MRI scan; (3) head MRI showed normal brain parenchyma; (4) no history of MGD or other eye diseases; and (5) no mental illness.

### Ethical Approval and Consent to Participate

The study methods and protocols were approved by the Medical Ethics Committee of the First Affiliated Hospital of Nanchang





**FIGURE 1 |** Typical pictures of HC and SM groups. We photographed the changes of MGs in HC group (A) and SM group (B). We can obviously observed that the MG in HC group is clearer than that in SM group. At the same time, we took pictures of the two groups of MGs with corneal confocal microscope, and we could observe the typical differences between the two groups of MGs. The MG in SM group was obviously blocked, and it was widened at the same time (D). Meanwhile, we could observe the normal MG in HC group (C). Therefore, it could be speculated that severe obesity may lead to tarsal gland blockage and degeneration. According to the cross-sectional observation image of retinal thickness in the control group, we could observe that the choroidal thickness in the SM group (F) was significantly thinner than that in the HC group (E). According to the fundus angiography images we obtained, we also observed that the capillaries in HC group (G,I) were more developed than those in SM group (H,J), indicating that severe obesity may reduce the thickness of choroid and fundus blood supply, and may further cause fundus disease. HCs, healthy controls; SM, severe obesity and meibomian gland dysfunction; MG, meibomian gland.

University (Nanchang, China) and followed the principles of the Declaration of Helsinki. All subjects were notified of the objectives and content of the study and latent risks, and then provided written informed consent to participate.

## MRI Parameters

MRI scanning was operated on a 3-Tesla MR scanner (Trio, Siemens, Munich, Germany). High-distinguishability T1-weighted graphics were attained with a triaxial spoiled grads-duplicated sequence in an axial orientation: replication time = 1,900 ms, echo time = 2.26 ms, thickness = 1.0 mm, interval = 0.5 mm, collection matrix =  $256 \times 256$ , visual field =  $250 \times 250$  mm, rollover angle =  $9^\circ$ . Definitely, 240 functional graphics (replication time = 2,000 ms, echo time = 30 ms, thickness = 4.0 mm, interval = 1.2 mm, collection matrix =  $64 \times 64$ , rollover angle =  $90^\circ$ , visual field =  $220 \times 220$  mm, 30 axial sections with grads-duplicated echo-plane image formation pulse array) overlaying the entire cerebrum were attained.

## fMRI Data Analysis

All functional data were handled by a software percolator<sup>1</sup> and statistical parameter graphing was operated with SPM8 (The MathWorks, Inc., Natick, MA, United States) and rs-fMRI DPARSFA<sup>2</sup> software data conducting coadjutants. The primary procedures of pretreatment included slice timing, head motion rectification, exerting Friston six-head motion parameters to eliminate head motion influences, dimensional standardization with normal echo planar picture templates to achieve Neurology Montreal Institute (MNI) standards, and smoothening with a Gaussian kernel of  $6 \text{ mm} \times 6 \text{ mm} \times 6 \text{ mm}$  full-width at half-maximum (FW-HM). REST software (State Key Laboratory of Cognitive Neuroscience and Learning, Beijing Normal University, Beijing, China) was utilized to compute ReHo. The basal technique of assessment was to analyze Kendall

<sup>1</sup>[www.MRIcro.com](http://www.MRIcro.com)

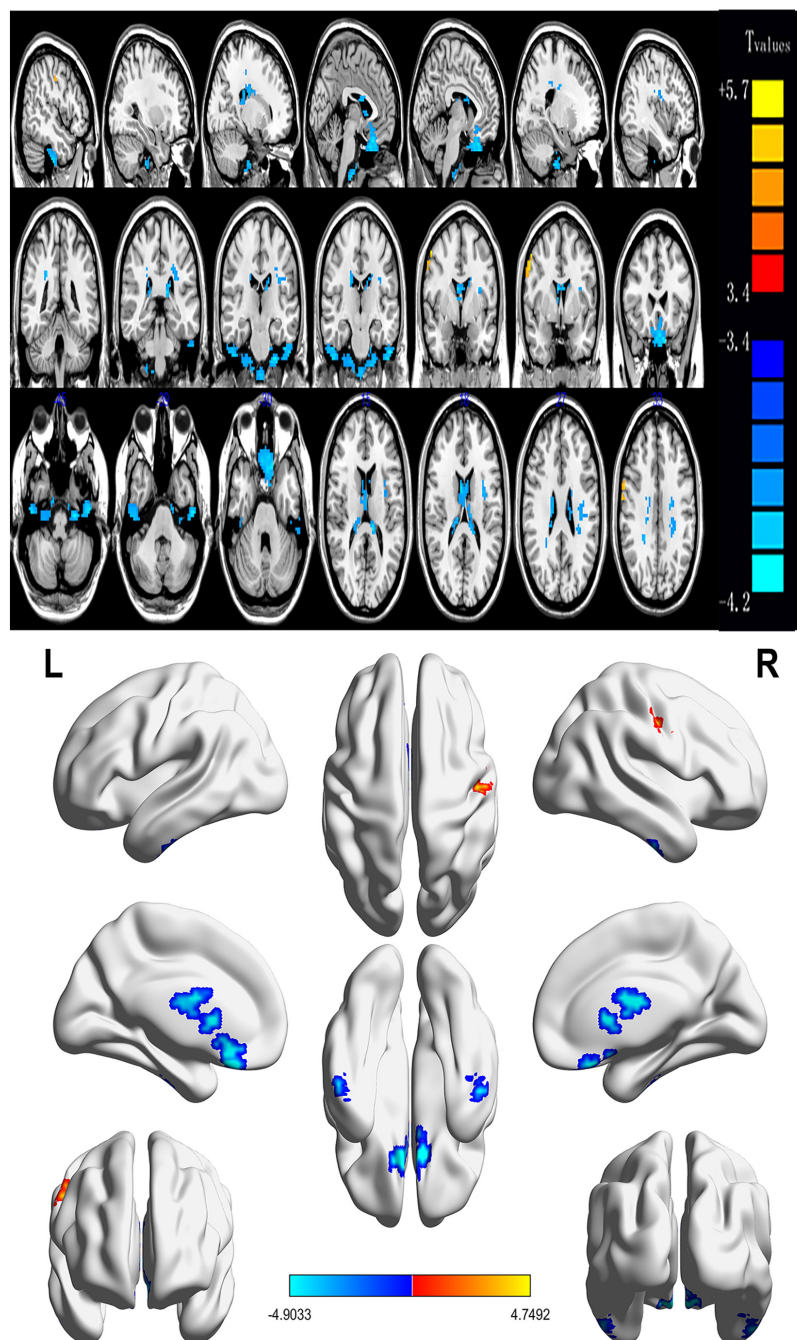
<sup>2</sup><http://rfmri.org/DPARSF>

**TABLE 1 |** Basic information of participants in the study.

Condition	SM	HC	t	P-value
Male/female	4/8	6/6	N/A	0.430
Age (years)	$34.25 \pm 7.07$	$31.67 \pm 5.98$	0.925	0.365
Weight (kg)	$111.92 \pm 13.33$	$66.08 \pm 10.41$	8.986	<0.01
Handedness	12R	12R	N/A	>0.99
Initial visual acuity-left eye (log Mar)	$0.80 \pm 0.16$	$0.58 \pm 0.09$	3.742	<0.01
Initial visual acuity-right eye (log Mar)	$0.83 \pm 0.22$	$0.62 \pm 0.13$	2.813	<0.05
Daily life score	$90.92 \pm 6.53$	$100.00 \pm 0.00$	4.617	<0.01
MMSE	$21.42 \pm 4.37$	$27.83 \pm 2.41$	4.266	<0.01

Independent t-tests comparing the two groups ( $p < 0.05$  represented statistically significant differences). Data presented as mean  $\pm$  SD.

HC, healthy control; SM, severe obesity and meibomian gland dysfunction; MMSE, mini-mental state examination.



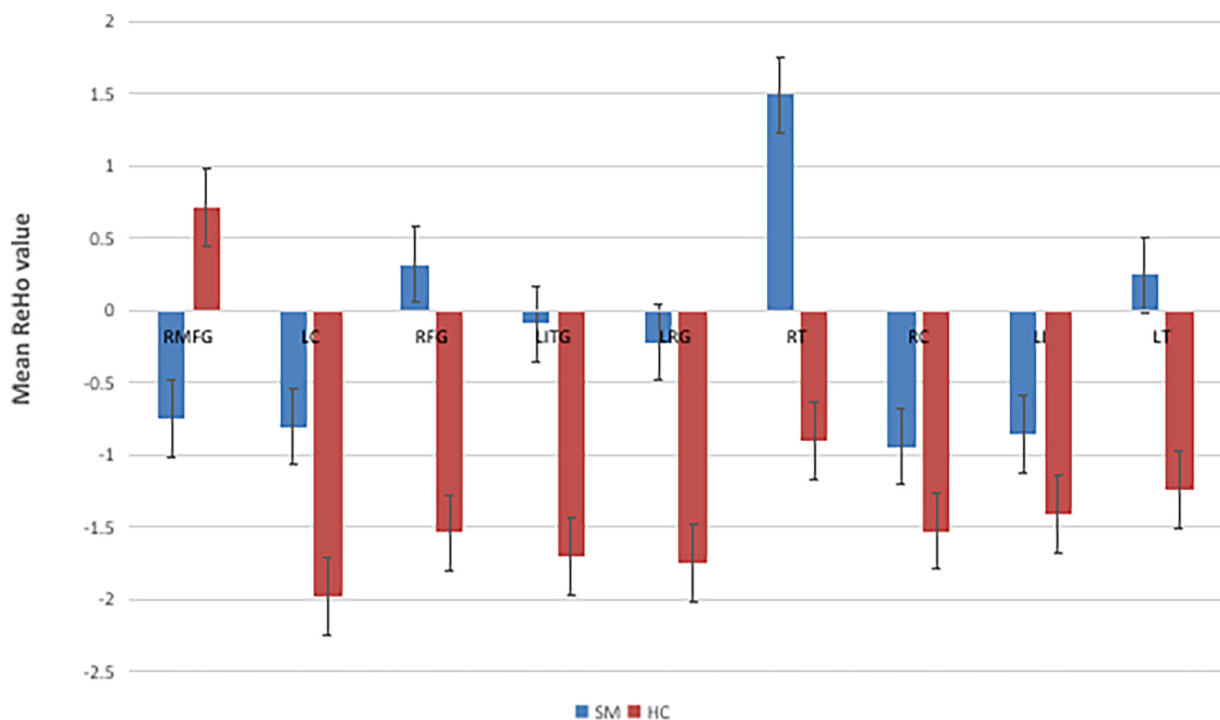
**FIGURE 2 |** Spontaneous brain activity in patients with severe obesity and meibomian gland dysfunction. Red regions (left cerebellum, right fusiform gyrus, left inferior temporal gyrus, left rectus gyrus, right thalamus, right caudate, left insula, and left thalamus) indicate higher ReHo values, while blue regions (right middle frontal gyrus) represent lower ReHo values ( $P < 0.05$ ; AlphaSim-corrected; cluster size,  $> 40$ ). ReHo, regional homogeneity; R, right; L, left.

consistency coefficients (KCC) of a given voxel and the adjacent voxel time series.

## Statistical Analysis

To probe the set differentiates in the ReHo values between patients with SM and the healthy, fMRI data were fitted with a general linear model (GLM) with the SPM9 toolkit.

$P < 0.05$  was regarded as statistically crucial and rectified with random field (Gaussian random field) principle with minimum  $z > 2.3$ . Two-sample Student's  $t$ -test was utilized for consecutive data for behavioral manifestations. All statistical analyses were accomplished with the IBM SPSS Statistics 20.0 software (IBM Corporation, Armonk, NY, United States).



**FIGURE 3 |** The mean single ReHo value between the SMs group and HCs. RMFG, right middle frontal gyrus; LC, left cerebellum; RFG, right fusiform gyrus; LITG, left inferior temporal gyrus; LRG, left rectus gyrus; RT, right thalamus; RC, right caudate; LI, left insula; LT, left thalamus; ReHo, regional homogeneity; HCs, healthy controls; SM, severe obesity and meibomian gland dysfunction.

## Brain–Behavior Correlation Analysis

In accordance with the ReHo computation consequences, some disparate cerebrum areas portrayed different semaphores between SM groups and HCs. For each area, the medial ReHo values was computed by meaning over all voxels. The connection between the average ReHo value and their clinical distinctions was computed utilizing the correlation analysis ( $P < 0.001$  was deemed as statistically essential).

## Clinical Data Analysis

The accumulative clinical measured values, including the initial visual acuity, daily life scores and mini-mental state examinations were documented and analyzed in the research with standalone sample  $t$ -test ( $P < 0.05$  as significantly different).

## Ocular Surface and Meibomian Gland Dysfunction Evaluations

We applied Keratograph ocular surface comprehensive analyzer to analyze the ocular surface. At the same time, we utilized MG evaluator and MG imaging technology to observe and evaluate the MG structure. According to the results of MG imaging, we scored and recorded the upper and lower eyelids of each patients' eye, respectively. We scored according to the range of MG loss. Asian Dry Eye Association China Branch Score Standard: 0: no loss of MG; 1 point: the proportion of MG missing  $<1/3$ ; 2 points: the proportion of missing MG is  $1/3$ – $2/3$ ; 3 points: the proportion of MG loss is  $>2/3$ . 1 or more is abnormal.

## RESULTS

### Demographics and Visual Measurements

No remarkable differentiations in age ( $P = 0.365$ ) and gender ( $P = 0.430$ ) between SM subjects and HCs were identified. The distinctions observed between the two groups in initial visual acuity with binoculars, daily life scores, and mini-mental state examinations were statistically significant ( $P < 0.05$ ; Table 1).

### ReHo Differences Between SM Patients and HCs

Contrasted with HCs, SM sufferers manifested observably increased ReHo values in the left cerebellum, right fusiform gyrus, left inferior temporal gyrus, left rectus gyrus, right thalamus, right caudate, left insula, left thalamus, and reduced ReHo values in the right middle frontal gyrus (Figures 2, 3 and Table 2).

### Regional Homogeneity Values of Severe Obesity and Meibomian Gland Dysfunction Brain Regions and Hospital Anxiety Depression Scale Scores

In the SM group, a negative correlation was found between the ReHo values at the right middle frontal gyrus (RMFG) and the anxiety scores (AS) ( $r = -0.961$ ,  $P < 0.001$ ; Figure 4A). ReHo



values at the right fusiform gyrus (RFG) portrayed a positive correlation with the depression scores (DSs;  $r = 0.676$ ,  $P = 0.016$ ; **Figure 4B**).

## Receiver Operating Characteristic Curve

There was an immense difference in the ReHo values between the SM group and the HCs. Therefore, we hypothesized that the ReHo values could be used to distinguish SM patients from the HCs. To test this hypothesis, we created an receiver operating characteristic (ROC) curve to investigate the medial

ReHo values of disparate cerebrum areas. The area under curve (AUC) denoted the diagnosis rate. A value of 0.5–0.7 signified low accuracy, 0.7–0.9 signified medium accuracy, and  $>0.9$  signified high accuracy. The areas below the ROC curve were 1.000 ( $P < 0.001$ ; 95% CI: 1.000–1.000) for the RMFG, left cerebellum (LC), left inferior temporal gyrus (LITG), left rectus gyrus (LRG), right caudate (RC), left insula (LI), left thalamus (LT); 0.993 ( $P < 0.001$ ; 95% CI: 0.971–1.000) for the RFG, and right thalamus (RT; **Figure 5**). Collectively, these results indicated that the ReHo values of disparate cerebrum areas might be used in the diagnosis of SM. In addition, ROC curves showed that the ReHo values of the RMFG, LC, LITG, LRG, RC, LI, and LT were more clinically relevant than the RFG and RT.

**TABLE 2 |** Brain regions with significant differences in ReHo between the HC and SM groups.

ReHo	Brain areas	MNI coordinates			BA	Peak voxels	t-Value
		X	Y	Z			
HC > SO							
1	RMFG	54	0	51	6	85	7.28
HC < SO							
2	LC	−27	−21	−45		256	−9.61
3	RFG	51	−18	−45	20	108	−7.78
4	LITG	−54	−18	−39	20	107	−8.74
5	LRG	−12	24	−30	25	266	−9.38
6	RT	6	3	18		109	−8.87
7	RC	24	−42	33		109	−6.72
8	LI	−36	−21	27	13	97	−5.91
9	LT	−12	−33	15		80	−8.25

For fMRI data, two-sample t-test was performed to examine the voxel-wise difference between the SM and HC groups using the REST toolbox. The statistical threshold was set at the voxel level with  $P < 0.05$ , FDR corrected, and cluster size  $>100$  voxels for multiple comparison. These voxels were regarded as the regions of interest showing significant difference between the two groups.

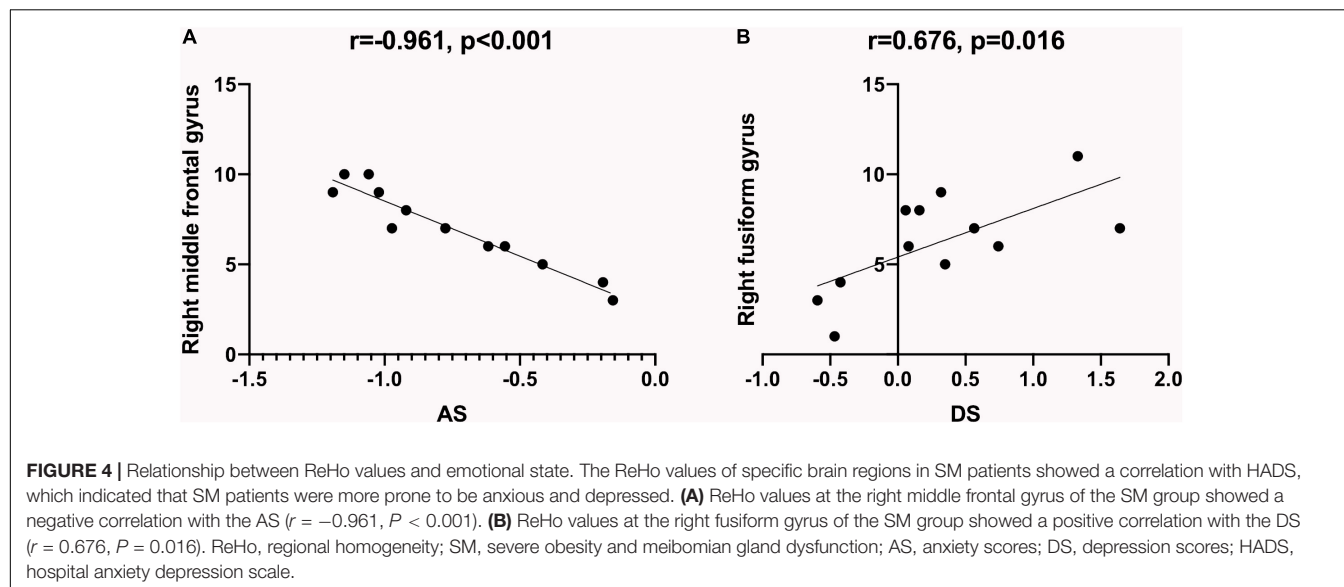
ReHo, regional homogeneity; HCs, healthy controls; SM, severe obesity and meibomian gland dysfunction; RMFG, right middle frontal gyrus; LC, left cerebellum; RFG, right fusiform gyrus; LITG, left inferior temporal gyrus; LRG, left rectus gyrus; RT, right thalamus; RC, right caudate; LI, left insula; LT, left thalamus.

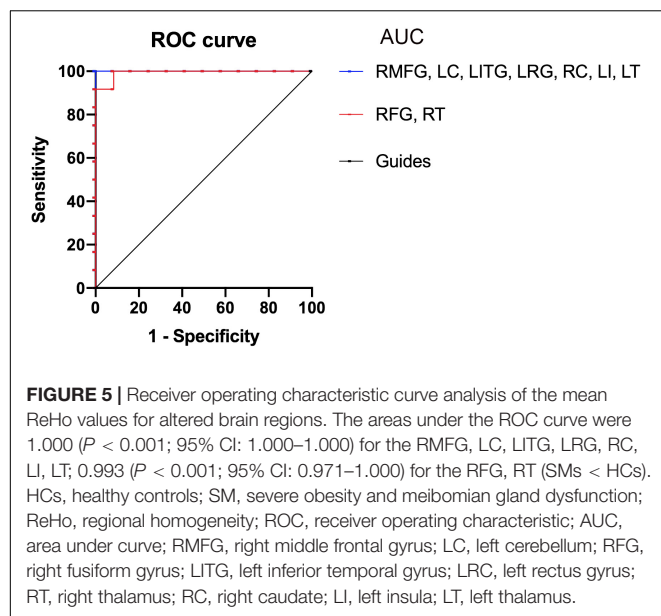
## Meibomian Gland Dysfunction Evaluation

We observed and evaluated the MG structure of SM group by MG imaging to determine the extent and degree of MG tissue loss. The results were: five people (one male, four female) one point; four people (one male, three female) two points; three people (two men, one woman) three points.

## DISCUSSION

Nowadays, obesity has become an epidemic. According to research statistics, nearly 2.1 billion people in the world are overweight or obese (Smith and Smith, 2016). SO is often coupled with hyperlipidemia (D'Abbondanza et al., 2020), which is characterized by elevated blood lipid levels (causing atherosclerosis), such as cholesterol, triglycerides, and low-density lipoproteins, and decreased high-density lipoproteins (Butovich, 2008; Butovich, 2010; Green-Church et al., 2011). On the one hand, an abnormality of the lipid component will affect the structure of MG and make MG hypertrophy (Osae et al., 2020). On the other hand, it may lead to inflammation, which is an underlying cause of blepharitis and can eventually impact the regular excretory capabilities of the MG





**TABLE 3 |** Regional homogeneity method applied in systemic and neurogenic diseases.

	References	Disease
Systemic diseases	Liu et al., 2018	Systemic lupus erythematosus
	Zhang J. et al., 2019	Hypertension
	Zeighami et al., 2021	Hyperlipidemia
Neurogenic diseases	Xing et al., 2018	Primary Sjögren syndrome
	Ji et al., 2020	Schizophrenia
	Hu et al., 2020	Dementia
	Zhang et al., 2021	Diabetes
	Shen et al., 2020	Generalized anxiety disorder

ReHo, regional homogeneity.

(Pietiläinen et al., 2007). This may generate degraded tear film quality and stabilization, eventually leading to ophthalmic surface inflammation in patients with MGD (Knop et al., 2011).

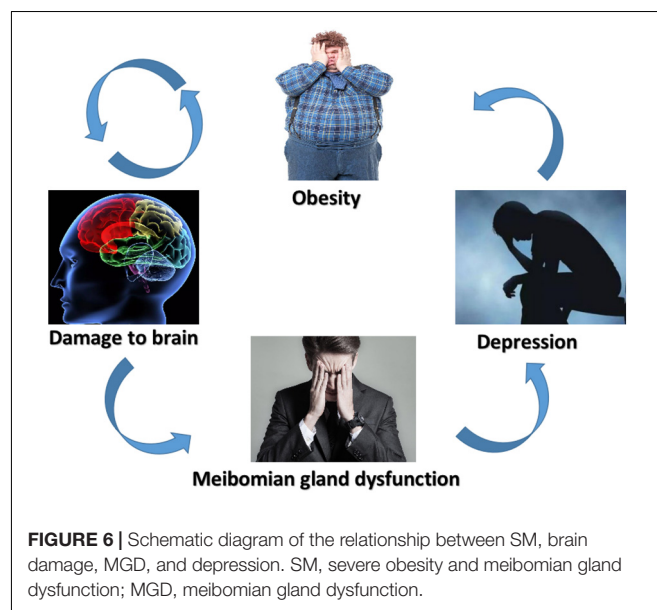
Obstructive sleep apnea hypopnea syndrome (OSAHS) is a common complication in obese patients. It is characterized by recurrent apnea and hypopnea during sleep, resulting in chronic intermittent hypoxia and hypercapnia (De Backer, 2013). Long term chronic intermittent hypoxia in patients with OSAHS will cause chronic inflammatory response and immune changes (Maniaci et al., 2021). Long term hypoxia and persistent inflammation lead to apoptosis of goblet cells and keratoconjunctival epithelial cells on the ocular surface and damage the ocular surface (Liu et al., 2022). In addition, this long-term intermittent hypoxia can not only directly damage the MG, but also indirectly cause MGD by causing the increase of matrix metalloproteinase, the decrease of elastic fibers and the relaxation of eyelids (Reins et al., 2018; Liu et al., 2022). The mechanism is that the MG cannot excrete normally due to the loss of eyelid support and extrusion, and MG obstruction develops into MGD (Pihlblad and Schaefer, 2013).

To the best of our knowledge, this was the first investigation to assess the influences of SM on resting-state cerebrum motions

**TABLE 4 |** Brain regions alternations and its potential impact.

Brain regions	Experimental result	Brain function	Anticipated results
Right middle frontal gyrus	SMs < HCs	Continuous attention, emotional processing, sleep stability	Attention disorder, depression, primary insomnia
Left cerebellum	SMs > HCs	Emotional control, cognitive processing, motion control	Emotional and behavioral disorder
Right fusiform gyrus	SMs > HCs	Cognitive functions	Pure alexia, face blindness
Left inferior temporal gyrus	SMs > HCs	Mentality, visual word processing	Chronic schizophrenia, language barrier
Bilateral thalamus	SMs > HCs	Postural control, somatosensory and motor	Postural disorders, motor sensory dysfunction
Right caudate	SMs > HCs	Cognitive performance, memory, mental stability	Cognitive deficits, memory impairment
Left insula	SMs > HCs	Language expression, audiovisual perception, emotional control	Language barrier, audiovisual impairment, depression

HCs, healthy controls; SM, severe obesity and meibomian gland dysfunction.



utilizing the ReHo method. The ReHo technique has been used to study multiple systemic and neural diseases with success and it possesses massive potentiality for future studies (Table 3). In this research, we discovered that the SM group had reduced ReHo in the RMFG, and elevated ReHo in the LC, RFG, LITG, LRG, RT, RC, LI, and LT (Table 4). We also verified that the lesions in the internal connection patterns of SM patients' brains were associated with a series of emotional and behavioral disorders including depression (Figure 6).

The MFG is an area on the ventral side of the medial prefrontal cortex and it is thought to participate in emotional processing and automatic or implicit regulation of emotion



(Jiang and Zuo, 2016). Moreover, it is responsible for many cognitive functions, such as top-down regulation in working memory, decision-making, attention processing, and emotional processing (Kupfer et al., 2012; Xu et al., 2020). In one study, researchers utilized amplitude of low-frequency fluctuations (ALFFs) measurements to study entire brain activity in patients with anxiety and depression. The outcomes showed the ALFF value in the MFG was decreased in anxious depressed patients. Therefore, the decrease in ALFF values in the MFG and its significant negative correlation with hysteresis factor scores indicated that the MFG is involved in the pathological process of anxious depression (Beevers et al., 2015). The decrease in MFG activity may also show the following comprehensive side effects: decreased cognitive function, reduced ability to change amygdala's fear stimulus response by using emotion regulation strategies, thus weakening emotion regulation and increasing suicide possibilities (Japee et al., 2015). As is known, chronic attention deficit is a feature of many neurological diseases. fMRI has shown that the MFG is active in attention tasks and event analysis, indicating its importance in sustained attention (Zhao et al., 2020). In addition, interference from the right MFG can promote network associations with other areas to elevate persistent attentiveness. Another study emphasized that MFG acts an essential part of the kinematic network lesions involving attention conduction, especially the adjustment in persistent attention (van Heeringen et al., 2017). As one of the most common health problems, primary insomnia usually manifests as difficulty in starting and maintaining sleep (Neale et al., 2015). Research by Song et al. (2019) compared insomniacs with HCs and primary insomnia patients had reduced GM volume in several cerebrum regions, including the MFG. In another study, researchers evaluated the effects of 36 h of acute sleep deprivation on the functional connections between the PC and other areas of the brain. The results showed that 36 h after acute sleep deprivation, the connection between the right precuneus and the right MFG was markedly weakened (Morin et al., 2011). The authors suggested the right MFG acts as a significant factor in sustained attention, and damage to the right MFG may cause insomnia.

According to clinical observations and neuroanatomical research, the cerebellum is a structure closely connected with motor control as well as motor learning (Xie et al., 2020). The anatomic datum portrayed that the cerebellum had heterolateral connections with plentiful cortical regions of the bilateral hemispheres, including the motor area (D'Angelo et al., 2016; Li et al., 2020). One study have shown that sensory movement mainly activates the anterior lobule, and there are secondary manifestations in lobules VIIa and VIIb. In one study, healthy subjects were asked to reach out and grasp an object. During this process, the researchers detected the excitation of cerebellar lobules VI and VIIb (Bernard and Seidler, 2013). Recent studies have shown that, besides motor functions, the cerebellum also contributes to the stability of behavioral cognitive, emotional, and social functions (Bostan and Strick, 2018). These different functions can be activated because the cerebellum has obvious interconnections with different cortical areas. In addition, the

prefrontal cortex-cerebellar circuit also exists and participates in the regulation of cognitive-emotional processes. Due to this versatility, cerebellar dysfunction and pathology can lead to cognitive and affective symptoms (Abdelgabar et al., 2019); for example, the skin pick-up disorder (SPD), which is a specific type of repetitive behavior of body focusing that can cause bodily harm. There have been reports that patients scratched their skin unconsciously until they noticed that they were scratching because of pain or bleeding (Van Overwalle et al., 2014). One study suggested that mood disorders were a core pathological mechanism of SPD. Before skin manipulation, the patient would feel a nervous or negative emotional state. By picking-up, the intensity of these disturbing states was at least temporarily reduced (Schmahmann and Sherman, 1998). Damage to the LC may cause negative emotions in SM patients, which may cause symptoms similar to the SPD.

Patients with pure aphasia show serious character recognition impairments. One study have shown that patients with dyslexia, after the damage to the RFG, are impaired not only in word recognition but also in recognition of numbers, objects, and even faces (Grant et al., 2012). Generally speaking, facial perception impairment refers to the inability to recognize previously seen faces (Roberts et al., 2013). This perception function is mediated by a well-defined and widely distributed hierarchical nervous system. The core of this system is composed of bilateral occipitotemporal regions of the striate extracorporeal visual cortex, the most significant of which is the RFG (Behrmann and Plaut, 2014). Therefore, damage to the RFG may lead to severe facial agnosia. In this research, we also discovered SM patients featured elevated ReHo values in the RFG region, suggesting that SM may be related to recognition impairment.

The inferior temporal gyrus is situated on the lateral and inferior surface of the temporal lobe (Susilo and Duchaine, 2013). Previous functional neuroimaging studies have shown that the inferior temporal gyrus is involved in a variety of cognitive processes, as well as the integration of vision and multimodal sensations (Cabeza and Nyberg, 2000; Conklin et al., 2002). These results indicated that sufferers with schizophrenia had a decline in gray matter volume in the bilateral inferior temporal gyrus (Herath et al., 2001). Furthermore, language fluency is one of the most commonly used neuropsychological measurement methods for language ability and executive function, requiring candidates to generate as many words as possible according to given category clues or letter clues within a preset time (Mesulam, 1998). Contrasted with the HCs, sufferers with left temporal region lesions spoke fewer words in the semantic fluency task (Onitsuka et al., 2004). Therefore, the lesion of the LITG in SM patients may cause mental instability and some language barriers.

The thalamus is not merely a simple relay function, it has a significant integration function, especially in vestibular processing. Peripheral organ fibers are mainly projected through the morphological specific thalamic nucleus, such as the external geniculate nucleus and medial geniculate nucleus of the optical system and the aural system, and then projected to the respective cortex or subcortical target area. This organization, together with the orderly corticothalamic feedback mechanism,

turns the thalamus into a modulating character in sensorial processing (Shao et al., 2014). Therefore, for the vestibular system, the thalamus is a unique subcortical site of multi-sensory integration. These vestibular thalamic loops may construct functional passages that conform the signals of the vestibule with other signals in the thalamus (Luckhurst and Lloyd-Jones, 2001). Vestibular hemispatial neglect is a central disorder of the features of aberrant perception (Sherman, 2007). fMRI of these sufferers during vestibular stimulation augmented the blood oxygen level-dependent signals in the thalamus were different from those of the healthy and migraine patients (Wijesinghe et al., 2015). Such observations indicated that the thalamus played an indispensable role in the production of vestibular perception, and the anomalies of the thalamus might be the cause of the distortions observed in some clinical conditions. The thalamic nucleus that receives the vestibular afferent is also concerned with handling messages from other sensorial systems. Thus, the thalamus may be regarded as an essential locus for sensory conformity. Studies have compared apoplexy patients with a certain extent of sensory loss with normal controls. The results showed that the interaction between vestibular and sensory messages relied on the functionality of the thalamus (Stolte et al., 2015). In addition, psychophysical studies have shown that the impairment of multisensory integration in patients suffering from Parkinson's disease may be due to the lack of facilitation of the ascending cholinergic system, which leads to thalamic dysfunction (Russo et al., 2014). Moreover, a study of two Parkinson's disease patients, after continuous cerebrum stimulation of the subthalamic nucleus, showed that subjective vertical changes in vision, a characteristic usually related to vestibular dysfunction, also indicated the interaction between vestibule and thalamus (Barra et al., 2010). The increased bilateral thalamic ReHo values associated with SM may cause migraine and motor-sensory dysfunction related to vestibular dysfunction.

The head of the caudate nucleus is part of the dorsolateral prefrontal circuit (DLPFC). Disruption of the DLPFC may lead to cognitive deficits in the prefrontal lobe and impaired memory (Müller et al., 2013). Lesions in the head of the caudate nucleus can lead to dysfunctional performance syndrome, attention deficits, and impaired short-term and long-term memory (Mike et al., 2009). Cognizant lesions in Parkinson's disease patients impact multiple domains, such as attention, visual space, and memory (Leh et al., 2007). This may be due to the important function of the caudate nucleus as a message center, and dopaminergic degeneration of the caudate nucleus in Parkinson's disease can lead to damage to the caudate nucleus (Apostolova et al., 2010). In one study, researchers found that the betweenness centrality of the RC nucleus of Parkinson's disease patients was positively correlated with the Montreal cognitive assessment score (Bartels and Leenders, 2009). Through PET imaging, some have reported relevance between the RC nucleus and cognizant ability: they applied the Stroop test in sufferers with early Parkinson's disease and found that the decline in the dopamine of the RC nucleus was associated with slow time processing and cognitive impairment (Bell et al., 2015; Wright et al., 2020). Therefore, damage to the RC of SM patients may cause cognitive and memory impairment.

The LI is located behind the frontal lobe, temporal lobe, and capillary cortex (Brück et al., 2001). Although overlying merely 2% of the cerebral cortex, the insula is like a multitudinous functional expressway involving a mass of cognitive and emotional courses. These include: visceral movement, visceral sensory function, body movement, motor correlation, eye movement, language system, and aural function, and it also covers cognitive domains, including physical awareness and emotion (Ko et al., 2017). The insula plays an important role in the language network. Guenot et al. (2004) carried out a meta-analysis of expressive language tasks and showed that the former island was the core part of activating language function. Recently, high-resolution fiber tract imaging studies have reported associations between the insula and the visually related regions of the parietal and temporal lobes in humans (Nieuwenhuys, 2012). In terms of visual function, the insula is considered to be a cross-modal cortical integrator that stimulates perception and visual awareness (Lu et al., 2016). Therefore, we speculated that SM and MGD might cause brain dysfunction (Table 4). Major depression is a persistent and debilitating emotional disorder characterized by negative emotions, difficulty sleeping, loss of appetite, and inattention (Chang et al., 2013). There has been evidence that the insula was an area related to emotional saliency and attention distribution during emotional tasks (Fletcher et al., 2015). Some data have shown that the insula was a pivotal brain structure for depression, emotional prominence, and mutual perception. Linear regression showed that abnormal LI thickness can significantly increase the risk of major depression (American Psychiatric Association, 2013). Therefore, the significant increase in the ReHo value of the LI may lead to speech and hearing impairment and depression.

In summary, evaluating the ReHo values of SM patients through fMRI is an efficient technique to probe into the connection between SM and lesions in cerebrum functions. We detected aberrant spontaneous activities in certain cerebrum regions of SM sufferers, which might be associated with the neurological mechanisms of SM. However, our research has a few limitations; for example, the sample size was too small, and all subjects were from the same institution. The general representation is, therefore, relatively poor. In addition, the scan time was too long for some participants, so their motions might have affected the results.

Also, our study lacked a detailed ocular surface assessment in SM patients. This may lead us to overlook the possible combination of obesity with other important eye diseases. Future research will expand the sample size, institutional sources, standardize the scanning procedures and mostly importantly, add detailed ocular surface assessments so as to obtain more representative and profound research results for SM.

## DATA AVAILABILITY STATEMENT

The raw data supporting the conclusions of this article will be made available by the authors, without undue reservation.

## ETHICS STATEMENT

The study methods and protocols were approved by the Medical Ethics Committee of The First Affiliated Hospital of Nanchang University and followed the principles of the Declaration of Helsinki. All subjects were notified of the objectives and content of the study and latent risks, and then provided written informed consent to participate.

## AUTHOR CONTRIBUTIONS

YL, S-XT, and Y-KW analyzed the data and drafted the manuscript. Y-KS, L-JZ, and MK assisted with data interpretation and figure composing. PY, Y-CP, and H-YS

collected the data. YS conceived, designed, and directed the study, and revised and approved the manuscript. All authors contributed to the article and approved the submitted version.

## FUNDING

This work was supported by National Natural Science Foundation (No: 82160195); Central Government Guides Local Science and Technology Development Foundation (No: 20211ZDG02003); Key Research Foundation of Jiangxi Province (Nos: 20181BBG70004 and 20203BBG73059); Excellent Talents Development Project of Jiangxi Province (No: 20192BCBL23020); and Natural Science Foundation of Jiangxi Province (No: 20181BAB205034).

## REFERENCES

- Abdelgabar, A. R., Suttrup, J., Broersen, R., Bhandari, R., Picard, S., Keyers, C., et al. (2019). Action perception recruits the cerebellum and is impaired in patients with spinocerebellar ataxia. *Brain* 142, 3791–3805. doi: 10.1093/brain/awz337
- American Psychiatric Association (2013). *Diagnostic and Statistical Manual of Mental Disorders*, 5th Edn. Arlington, VA: American Psychiatric Publishing.
- Apostolova, L. G., Beyer, M., Green, A. E., Hwang, K. S., Morra, J. H., Chou, Y. Y., et al. (2010). Hippocampal, caudate, and ventricular changes in Parkinson's disease with and without dementia. *Mov. Disord* 25, 687–695. doi: 10.1002/mds.22799
- Barra, J., Marquer, A., Joassin, R., Reymond, C., Metge, L., Chauvineau, V., et al. (2010). Humans use internal models to construct and update a sense of verticality. *Brain* 133(Pt 12), 3552–3563. doi: 10.1093/brain/awq311
- Bartels, A. L., and Leenders, K. L. (2009). Parkinson's disease: the syndrome, the pathogenesis and pathophysiology. *Cortex* 45, 915–921. doi: 10.1016/j.cortex.2008.11.010
- Beevers, C. G., Clasen, P. C., Enock, P. M., and Schnyer, D. M. (2015). Attention bias modification for major depressive disorder: effects on attention bias, resting state connectivity, and symptom change. *J. Abnorm. Psychol.* 124, 463–475. doi: 10.1037/abn0000049
- Behrmann, M., and Plaut, D. C. (2014). Bilateral hemispheric processing of words and faces: evidence from word impairments in prosopagnosia and face impairments in pure alexia. *Cereb. Cortex* 24, 1102–1118. doi: 10.1093/cercor/bhs390
- Bell, P. T., Gilat, M., O'Callaghan, C., Copland, D. A., Frank, M. J., Lewis, S. J., et al. (2015). Dopaminergic basis for impairments in functional connectivity across subdivisions of the striatum in Parkinson's disease. *Hum. Brain Mapp.* 36, 1278–1291. doi: 10.1002/hbm.22701
- Bernard, J. A., and Seidler, R. D. (2013). Cerebellar contributions to visuomotor adaptation and motor sequence learning: an ALE meta-analysis. *Front. Hum. Neurosci.* 7:27. doi: 10.3389/fnhum.2013.00027
- Bostan, A. C., and Strick, P. L. (2018). The basal ganglia and the cerebellum: nodes in an integrated network. *Nat. Rev. Neurosci.* 19, 338–350. doi: 10.1038/s41583-018-0002-7
- Brück, A., Portin, R., Lindell, A., Laihin, A., Bergman, J., Haaparanta, M., et al. (2001). Positron emission tomography shows that impaired frontal lobe functioning in Parkinson's disease is related to dopaminergic hypofunction in the caudate nucleus. *Neurosci. Lett.* 311, 81–84. doi: 10.1016/s0304-3940(01)02124-3
- Butovich, I. A. (2008). On the lipid composition of human meibum and tears: comparative analysis of nonpolar lipids. *Invest. Ophthalmol. Vis. Sci.* 49, 3779–3789. doi: 10.1167/iovs.08-1889
- Butovich, I. A. (2010). Fatty acid composition of cholesteryl esters of human meibomian gland secretions. *Steroids* 75, 726–733. doi: 10.1016/j.steroids.2010.04.011
- Cabeza, R., and Nyberg, L. (2000). Imaging cognition II: An empirical review of 275 PET and fMRI studies. *J. Cogn. Neurosci.* 12, 1–47. doi: 10.1162/08989290051137585
- Chang, L. J., Yarkoni, T., Khaw, M. W., and Sanfey, A. G. (2013). Decoding the role of the insula in human cognition: functional parcellation and large-scale reverse inference. *Cereb. Cortex* 23, 739–749. doi: 10.1093/cercor/bhs065
- Conklin, H. M., Calkins, M. E., Anderson, C. W., Dinzeo, T. J., and Iacono, W. G. (2002). Recognition memory for faces in schizophrenia patients and their first-degree relatives. *Neuropsychologia* 40, 2314–2324. doi: 10.1016/s0028-3932(02)00091-x
- D'Abbondanza, M., Ministrini, S., Pucci, G., Nulli Migliola, E., Martorelli, E. E., Gandolfo, V., et al. (2020). Very low-carbohydrate ketogenic diet for the treatment of severe obesity and associated non-alcoholic fatty liver disease: the role of sex differences. *Nutrients* 12:2748. doi: 10.3390/nu12092748
- D'Angelo, E., Mapelli, L., Casellato, C., Garrido, J. A., Luque, N., Monaco, J., et al. (2016). Distributed circuit plasticity: new clues for the cerebellar mechanisms of learning. *Cerebellum* 15, 139–151. doi: 10.1007/s12311-015-0711-7
- De Backer, W. (2013). Obstructive sleep apnea/hypopnea syndrome. *Panminerva Med* 55, 191–195.
- Ding, Y., Ji, G., Li, G., Zhang, W., Hu, Y., Liu, L., et al. (2020). Altered Interactions among resting-state networks in individuals with obesity. *Obesity (Silver Spring)* 28, 601–608. doi: 10.1002/oby.22731
- Fletcher, P. D., Downey, L. E., Golden, H. L., Clark, C. N., Slattery, C. F., Paterson, R. W., et al. (2015). Auditory hedonic phenotypes in dementia: A behavioural and neuroanatomical analysis. *Cortex* 67, 95–105. doi: 10.1016/j.cortex.2015.03.021
- García-García, I., Michaud, A., Dadar, M., Zeighami, Y., Neseliler, S., Collins, D. L., et al. (2019). Neuroanatomical differences in obesity: meta-analytic findings and their validation in an independent dataset. *Int. J. Obes. (Lond)*. 43, 943–951. doi: 10.1038/s41366-018-0164-4
- Grant, J. E., Odlaug, B. L., Chamberlain, S. R., Keuthen, N. J., Lochner, C., and Stein, D. J. (2012). Skin picking disorder. *Am. J. Psychiatry* 169, 1143–1149. doi: 10.1176/appi.ajp.2012.12040508
- Green-Church, K. B., Butovich, I., Willcox, M., Borchman, D., Paulsen, F., Barabino, S., et al. (2011). The international workshop on meibomian gland dysfunction: report of the subcommittee on tear film lipids and lipid-protein interactions in health and disease. *Invest. Ophthalmol. Vis. Sci.* 52, 1979–1993. doi: 10.1167/iovs.10-6997d
- Guenot, M., Isnard, J., and Sindou, M. (2004). Surgical anatomy of the insula. *Adv. Tech. Stand Neurosurg.* 29, 265–288. doi: 10.1007/978-3-7091-0558-0\_7
- Guo, P., Zhao, P., Lv, H., Su, Y., Liu, M., Chen, Y., et al. (2020). Abnormal regional spontaneous neural activity in nonarteritic anterior ischemic optic neuropathy: a resting-state functional MRI study. *Neural Plast* 2020:8826787. doi: 10.1155/2020/8826787
- Hales, C. M., Carroll, M. D., Fryar, C. D., and Ogden, C. L. (2020). Prevalence of obesity and severe obesity among adults: United States, 2017–2018. *NCHS Data Brief* 360, 1–8.



- Herath, P., Kinomura, S., and Roland, P. E. (2001). Visual recognition: evidence for two distinctive mechanisms from a PET study. *Hum Brain Mapp.* 12, 110–119. doi: 10.1002/1097-0193(200102)12:2<110::aid-hbm1008>3.0.co;2-0
- Hu, T., Hou, Y., Wei, Q., Yang, J., Luo, C., Chen, Y., et al. (2020). Patterns of brain regional functional coherence in cognitive impaired ALS. *Int. J. Neurosci.* 130, 751–758. doi: 10.1080/00207454.2019.1705806
- Japee, S., Holiday, K., Satyshur, M. D., Mukai, I., and Ungerleider, L. G. (2015). A role of right middle frontal gyrus in reorienting of attention: a case study. *Front Syst. Neurosci.* 9:23. doi: 10.3389/fnsys.2015.00023
- Ji, L., Meda, S. A., Tamminga, C. A., Clementz, B. A., Keshavan, M. S., Sweeney, J. A., et al. (2020). Characterizing functional regional homogeneity (ReHo) as a B-SNP psychosis biomarker using traditional and machine learning approaches. *Schizophr. Res.* 215, 430–438. doi: 10.1016/j.schres.2019.07.015
- Jiang, L., and Zuo, X. N. (2016). Regional homogeneity: a multimodal, multiscale neuroimaging marker of the human connectome. *Neuroscientist* 22, 486–505. doi: 10.1177/1073858415595004
- Knop, E., Knop, N., Millar, T., Obata, H., and Sullivan, D. A. (2011). The international workshop on meibomian gland dysfunction: report of the subcommittee on anatomy, physiology, and pathophysiology of the meibomian gland. *Invest. Ophthalmol. Vis. Sci.* 52, 1938–1978. doi: 10.1167/iovs.10-6997c
- Ko, J. H., Katakao, A., Aljuaid, M., Goertzen, A. L., Borys, A., Hobson, D. E., et al. (2017). Alzheimer's disease neuroimaging initiative. distinct brain metabolic patterns separately associated with cognition, motor function, and aging in parkinson's disease dementia. *Neurobiol. Aging* 60, 81–91. doi: 10.1016/j.neurobiolaging.2017.08.020
- Kupfer, D. J., Frank, E., and Phillips, M. L. (2012). Major depressive disorder: new clinical, neurobiological, and treatment perspectives. *Lancet* 379, 1045–1055. doi: 10.1016/S0140-6736(11)60602-8
- Kuriakose, R. K., and Braich, P. S. (2018). Dyslipidemia and its association with meibomian gland dysfunction: a systematic review. *Int. Ophthalmol.* 38, 1809–1816. doi: 10.1007/s10792-017-0633-0
- Leh, S. E., Pfito, A., Chakravarty, M. M., and Strafella, A. P. (2007). Fronto-striatal connections in the human brain: a probabilistic diffusion tractography study. *Neurosci. Lett.* 419, 113–118. doi: 10.1016/j.neulet.2007.04.049
- Li, B., Zhang, L., Zhang, Y., Chen, Y., Peng, J., Shao, Y., et al. (2020). Decreased functional connectivity between the right precuneus and middle frontal gyrus is related to attentional decline following acute sleep deprivation. *Front Neurosci.* 14:530257. doi: 10.3389/fnins.2020.530257
- Liu, S., Cheng, Y., Xie, Z., Lai, A., Lv, Z., Zhao, Y., et al. (2018). Conscious resting State fMRI Study in SLE patients without major neuropsychiatric manifestations. *Front Psychiatry* 9:677. doi: 10.3389/fpsy.2018.00677
- Liu, S., Li, S., Li, M., Zeng, S., Chen, B., and Zhang, L. (2022). Evaluation of the ocular surface and meibomian gland in obstructive sleep apnea hypopnea syndrome. *Front Med (Lausanne)*. 9:832954. doi: 10.3389/fmed.2022.832954
- Lu, C., Long, Y., Zheng, L., Shi, G., Liu, L., Ding, G., et al. (2016). Relationship between Speech Production and Perception in People Who Stutter. *Front Hum. Neurosci.* 10:224. doi: 10.3389/fnhum.2016.00224
- Luckhurst, L., and Lloyd-Jones, T. J. (2001). A selective deficit for living things after temporal lobectomy for relief of epileptic seizures. *Brain Lang* 79, 266–296. doi: 10.1006/brln.2001.2485
- Maniaci, A., Iannella, G., Cocuzza, S., Vicini, C., Magliulo, G., Ferlito, S., et al. (2021). Oxidative stress and inflammation biomarker expression in obstructive sleep apnea patients. *J. Clin. Med* 10:277. doi: 10.3390/jcm10020277
- Mesulam, M. M. (1998). From sensation to cognition. *Brain* 121(Pt 6), 1013–1052. doi: 10.1093/brain/121.6.1013
- Mike, A., Balas, I., Varga, D., Janszky, J., Nagy, F., and Kovacs, N. (2009). Subjective visual vertical may be altered by bilateral subthalamic deep brain stimulation. *Mov. Disord* 24, 1556–1557. doi: 10.1002/mds.22605
- Millar, T. J., and Schuett, B. S. (2015). The real reason for having a meibomian lipid layer covering the outer surface of the tear film - a review. *Exp. Eye Res.* 137, 125–138. doi: 10.1016/j.exer.2015.05.002
- Morin, C. M., LeBlanc, M., Bélanger, L., Ivers, H., Mérette, C., and Savard, J. (2011). Prevalence of insomnia and its treatment in Canada. *Can. J. Psychiatry* 56, 540–548. doi: 10.1177/070674371105600905
- Mudgil, P. (2014). Antimicrobial role of human meibomian lipids at the ocular surface. *Invest. Ophthalmol. Vis. Sci.* 55, 7272–7277. doi: 10.1167/iovs.14-15512
- Müller, M. L., Albin, R. L., Kotagal, V., Koeppe, R. A., Scott, P. J., Frey, K. A., et al. (2013). Thalamic cholinergic innervation and postural sensory integration function in Parkinson's disease. *Brain* 136(Pt 11), 3282–3289. doi: 10.1093/brain/awt247
- Neale, C., Johnston, P., Hughes, M., and Scholey, A. (2015). Functional activation during the rapid visual information processing task in a middle aged cohort: an fMRI study. *PLoS One* 10:e0138994. doi: 10.1371/journal.pone.0138994
- Nieuwenhuys, R. (2012). The insular cortex: a review. *Prog. Brain Res.* 195, 123–163. doi: 10.1016/B978-0-444-53860-4.00007-6
- Onitsuka, T., Shenton, M. E., Salisbury, D. F., Dickey, C. C., Kasai, K., Toner, S. K., et al. (2004). Middle and inferior temporal gyrus gray matter volume abnormalities in chronic schizophrenia: an MRI study. *Am. J. Psychiatry* 161, 1603–1611. doi: 10.1176/appi.ajp.161.9.1603
- Osae, E. A., Bullock, T., Chintapalati, M., Brodesser, S., Hanlon, S., Redfern, R., et al. (2020). Obese mice with dyslipidemia exhibit meibomian gland hypertrophy and alterations in meibum composition and aqueous tear production. *Int. J. Mol. Sci.* 21:8772. doi: 10.3390/ijms21228772
- Osae, E. A., Steven, P., Redfern, R., Hanlon, S., Smith, C. W., Rumbaut, R. E., et al. (2019). Dyslipidemia and meibomian gland dysfunction: utility of lipidomics and experimental prospects with a diet-induced obesity mouse model. *Int. J. Mol. Sci.* 20:3505. doi: 10.3390/ijms20143505
- Pietiläinen, K. H., Sysi-Aho, M., Rissanen, A., Seppänen-Laakso, T., Yki-Järvinen, H., Kaprio, J., et al. (2007). Acquired obesity is associated with changes in the serum lipidomic profile independent of genetic effects—a monozygotic twin study. *PLoS One* 2:e218. doi: 10.1371/journal.pone.0000218
- Pihlblad, M. S., and Schaefer, D. P. (2013). Eyelid laxity, obesity, and obstructive sleep apnea in keratoconus. *Cornea* 32, 1232–1236. doi: 10.1097/ICO.0b013e318281e755
- Reins, R. Y., Lema, C., Courson, J., Kunnen, C. M. E., and Redfern, R. L. (2018). MyD88 deficiency protects against dry eye-induced damage. *Invest. Ophthalmol. Vis. Sci.* 59, 2967–2976. doi: 10.1167/iovs.17-23397
- Roberts, S., O'Connor, K., and Bélanger, C. (2013). Emotion regulation and other psychological models for body-focused repetitive behaviors. *Clin. Psychol. Rev.* 33, 745–762. doi: 10.1016/j.cpr.2013.05.004
- Russo, A., Marcelli, V., Esposito, F., Corvino, V., Marcuccio, L., Giannone, A., et al. (2014). Abnormal thalamic function in patients with vestibular migraine. *Neurology* 82, 2120–2126. doi: 10.1212/WNL.0000000000000496
- Schmahmann, J. D., and Sherman, J. C. (1998). The cerebellar cognitive affective syndrome. *Brain* 121(Pt 4), 561–579. doi: 10.1093/brain/121.4.561
- Shao, Z., Janse, E., Visser, K., and Meyer, A. S. (2014). What do verbal fluency tasks measure? Predictors of verbal fluency performance in older adults. *Front Psychol.* 22:772. doi: 10.3389/fpsyg.2014.00772
- Shen, Z., Zhu, J., Ren, L., Qian, M., Shao, Y., Yuan, Y., et al. (2020). Aberrant amplitude low-frequency fluctuation (ALFF) and regional homogeneity (ReHo) in generalized anxiety disorder (GAD) and their roles in predicting treatment remission. *Ann. Transl. Med* 8:1319. doi: 10.21037/atm-20-6448
- Sherman, S. M. (2007). The thalamus is more than just a relay. *Curr. Opin. Neurobiol.* 17, 417–422. doi: 10.1016/j.conb.2007.07.003
- Smith, K. B., and Smith, M. S. (2016). Obesity statistics. *Prim. Care* 43, 121–135. doi: 10.1016/j.jpop.2015.10.001
- Song, P., Lin, H., Liu, C., Jiang, Y., Lin, Y., Xue, Q., et al. (2019). Transcranial magnetic stimulation to the middle frontal gyrus during attention modes induced dynamic module reconfiguration in brain networks. *Front Neuroinform.* 13:22. doi: 10.3389/fninf.2019.00022
- Stein, C. J., and Colditz, G. A. (2004). The epidemic of obesity. *J. Clin. Endocrinol. Metab.* 89, 2522–2525. doi: 10.1210/jc.2004-0288
- Stolte, B., Holle, D., Naegel, S., Diener, H. C., and Obermann, M. (2015). Vestibular migraine. *Cephalalgia* 35, 262–270. doi: 10.1177/0333102414535113
- Susilo, T., and Duchaine, B. (2013). Dissociations between faces and words: comment on Behrmann and Plaut. *Trends Cogn. Sci.* 17:545. doi: 10.1016/j.tics.2013.09.005
- Val-Lailliet, D., Aarts, E., Weber, B., Ferrari, M., Quaresima, V., Stoeckel, L. E., et al. (2015). Neuroimaging and neuromodulation approaches to study eating behavior and prevent and treat eating disorders and obesity. *Neuroimage Clin.* 8, 1–31. doi: 10.1016/j.nicl.2015.03.016

- van Heeringen, K., Wu, G. R., Vervaeke, M., Vanderhasselt, M. A., and Baeken, C. (2017). Decreased resting state metabolic activity in frontopolar and parietal brain regions is associated with suicide plans in depressed individuals. *J. Psychiatr. Res.* 84, 243–248. doi: 10.1016/j.jpsychires.2016.10.011
- Van Overwalle, F., Baetens, K., Mariën, P., and Vandekerckhove, M. (2014). Social cognition and the cerebellum: a meta-analysis of over 350 fMRI studies. *Neuroimage* 86, 554–572. doi: 10.1016/j.neuroimage.2013.09.033
- Wijesinghe, R., Protti, D. A., and Camp, A. J. (2015). Vestibular Interactions in the Thalamus. *Front Neural Circuits* 9:79. doi: 10.3389/fncir.2015.00079
- Wright, N., Alhindi, A., Millikin, C., Modirrousta, M., Udow, S., Borys, A., et al. (2020). Elevated caudate connectivity in cognitively normal Parkinson's disease patients. *Sci. Rep.* 10:17978. doi: 10.1038/s41598-020-75008-6
- Xie, D., Qin, H., Dong, F., Wang, X., Liu, C., Xue, T., et al. (2020). Functional connectivity abnormalities of brain regions with structural deficits in primary insomnia patients. *Front Neurosci.* 14:566. doi: 10.3389/fnins.2020.00566
- Xing, W., Shi, W., Leng, Y., Sun, X., Guan, T., Liao, W., et al. (2018). Resting-state fMRI in primary Sjögren syndrome. *Acta. Radiol.* 59, 1091–1096. doi: 10.1177/0284185117749993
- Xu, W., Chen, S., Xue, C., Hu, G., Ma, W., Qi, W., et al. (2020). Functional MRI-Specific alterations in executive control network in mild cognitive impairment: an ale meta-analysis. *Front. Aging Neurosci.* 12:578863. doi: 10.3389/fnagi.2020.578863
- Zeighami, Y., Iceta, S., Dadar, M., Pelletier, M., Nadeau, M., Biertho, L., et al. (2021). Spontaneous neural activity changes after bariatric surgery: a resting-state fMRI study. *Neuroimage* 241:118419. doi: 10.1016/j.neuroimage.2021.118419
- Zhang, J., Cai, X., Wang, Y., Zheng, Y., Qu, S., Zhang, Z., et al. (2019). Different brain activation after acupuncture at combined acupoints and single acupoint in hypertension patients: an rs-fMRI study based on reho analysis. *Evid. Based Complement Alternat Med* 2019:5262896. doi: 10.1155/2019/5262896
- Zhang, R., Beyer, F., Lampe, L., Luck, T., Riedel-Heller, S. G., Loeffler, M., et al. (2018). White matter microstructural variability mediates the relation between obesity and cognition in healthy adults. *Neuroimage* 172, 239–249. doi: 10.1016/j.neuroimage.2018.01.028
- Zhang, Y., Ji, G., Li, G., Hu, Y., Liu, L., Jin, Q., et al. (2019). Ghrelin reductions following bariatric surgery were associated with decreased resting state activity in the hippocampus. *Int. J. Obes. (Lond)*. 43, 842–851. doi: 10.1038/s41366-018-0126-x
- Zhang, Y., Zhang, X., Ma, G., Qin, W., Yang, J., Lin, J., et al. (2021). Neurovascular coupling alterations in type 2 diabetes: a 5-year longitudinal MRI study. *BMJ Open Diabetes Res. Care* 9:e001433. doi: 10.1136/bmjdr-2020-001433
- Zhao, P., Yan, R., Wang, X., Geng, J., Chattun, M. R., Wang, Q., et al. (2020). Reduced resting state neural activity in the right orbital part of middle frontal gyrus in anxious depression. *Front Psychiatry* 10:994. doi: 10.3389/fpsy.2019.00994

**Conflict of Interest:** The authors declare that the research was conducted in the absence of any commercial or financial relationships that could be construed as a potential conflict of interest.

**Publisher's Note:** All claims expressed in this article are solely those of the authors and do not necessarily represent those of their affiliated organizations, or those of the publisher, the editors and the reviewers. Any product that may be evaluated in this article, or claim that may be made by its manufacturer, is not guaranteed or endorsed by the publisher.

Copyright © 2022 Liu, Tan, Wu, Shen, Zhang, Kang, Ying, Pan, Shu and Shao. This is an open-access article distributed under the terms of the Creative Commons Attribution License (CC BY). The use, distribution or reproduction in other forums is permitted, provided the original author(s) and the copyright owner(s) are credited and that the original publication in this journal is cited, in accordance with accepted academic practice. No use, distribution or reproduction is permitted which does not comply with these terms.





# Abnormal Fractional Amplitude of Low Frequency Fluctuation Changes in Patients With Dry Eye Disease: A Functional Magnetic Resonance Imaging Study

## OPEN ACCESS

### Edited by:

Xin Huang,  
Jiangxi Provincial People's Hospital,  
China

### Reviewed by:

Yan Zhang,  
Jilin University, China  
Yanhui Bai,  
The First Affiliated Hospital of  
Zhengzhou University, China

### \*Correspondence:

Yi Shao  
freebee99@163.com

<sup>†</sup>These authors have contributed  
equally to this work

### Specialty section:

This article was submitted to  
Brain Imaging and Stimulation,  
a section of the journal  
Frontiers in Human Neuroscience

**Received:** 20 March 2022

**Accepted:** 28 April 2022

**Published:** 24 May 2022

### Citation:

Liang R-B, Liu L-Q, Shi W-Q, Sun T,  
Ge Q-M, Li Q-Y, Shu H-Y, Zhang L-J  
and Shao Y (2022) Abnormal  
Fractional Amplitude of Low  
Frequency Fluctuation Changes in  
Patients With Dry Eye Disease: A  
Functional Magnetic Resonance  
Imaging Study.  
Front. Hum. Neurosci. 16:900409.  
doi: 10.3389/fnhum.2022.900409

Rong-Bin Liang<sup>†</sup>, Li-Qi Liu<sup>†</sup>, Wen-Qing Shi, Tie Sun, Qian-Min Ge, Qiu-Yu Li, Hui-Ye Shu,  
Li-Juan Zhang and Yi Shao\*

Department of Ophthalmology, The First Affiliated Hospital of Nanchang University, Jiangxi Center of National Ocular Disease  
Clinical Research, Nanchang, China

**Purpose:** To investigate spontaneous brain activity in patients with dry eye (DE) and healthy control (HC) using the fractional amplitude of low frequency fluctuation (fALFF) technique with the aim of elucidating the relationship between the clinical symptoms of DE and changes in brain function.

**Material and Methods:** A total of 28 patients with DE and 28 matched healthy volunteers (10 males and 18 females in each group) were enrolled. Resting-state functional magnetic resonance imaging scans were performed in both groups. Then all subjects were required to complete a comprehensive Hospital Anxiety and Depression Scale (HADS). Receiver operating characteristic (ROC) curve analysis was used to evaluate the differences in fALFF values between the two groups and their diagnostic value. Linear correlations between HADS and fALFF values in different brain regions of DE patients were analyzed using the *Pearson* correlation coefficient.

**Results:** Patients with DE had significantly higher fALFF values in the left calcarine sulcus (CS) than the HC group, while fALFF values in the bilateral middle frontal gyrus (MFG) and right MFG/right inferior frontal gyrus (IFG) were significantly lower in DE patients than in HC group. fALFF values had a high diagnostic value for differentiating patients with DE from the HC group ( $P < 0.001$ ). Right MFG and right MFG/IFG were significantly correlated with HADS values.

**Conclusion:** Our study found that DE mainly involved functional disorders in the brain areas of the left CS, bilateral MFG and right MFG/right IFG, which helped us to find possible clinical features of DE disease and reflected the potential pathological mechanism of DE.

**Keywords:** dry eye, fractional amplitude of low frequency fluctuation, anxiety, depression, brain function

## INTRODUCTION

Dry eye (DE) is a multifactorial chronic ocular surface disorder commonly encountered in ophthalmology. The prevalence of DE ranges from 5% to 50% and can be as high as 75% in adults over the age of 40, with women being one of the most commonly affected groups (Stapleton et al., 2017). The etiology of DE is complex and the causative mechanisms are not yet fully elucidated. Common risk factors include advanced age, female sex, low humidity environment, systemic medication, and autoimmune diseases. The prevalence of DE is higher in people working at video terminals and in those exposed to harsh environments, such as high altitude, low air pressure, hypoxia, wind, and strong ultraviolet light, for long periods of time. Diabetes, keratoconus surgery, pterygium, allergic conjunctivitis, dry syndrome, and ocular surface drug abuse are strong risk factors for the development of DE (Jiang et al., 2017). DE can seriously affect the ability to perform daily activities, such as reading, using a computer, and driving, resulting in reduced quality of life and increased social burden.

Individuals with DE are more likely than those without the condition to have a visual impairment, neuropathic pain, anxiety, depression, and other symptoms (Weatherby et al., 2019). The mechanism underlying the development of these symptoms and whether they are related to brain dysfunction is not fully understood. Hence, it is important to explore whether abnormal changes occur in the brains of patients with DE relative to healthy controls.

Functional magnetic resonance imaging (fMRI) is a very mainstream, non-invasive, and safe imaging technique that is commonly used to detect some brain diseases and neurological abnormalities (Khosla et al., 2019). We can use fMRI to examine the functional metabolism of the brain in DE patients to further understand the mechanisms of abnormal brain function in DE patients. In recent years, more and more scholars have studied the abnormal alterations in the brain of DE, and the study of DE from central nervous system functionalism is called for, thus using fMRI technology provides us with an effective means to explore the central changes in DE patients. Yan et al. (2020) detected abnormal limbic-cortical circuit ReHo values in patients with DE using resting-state MRI. Many past researches have shown that in patients with Sjögren's syndrome using fMRI, abnormalities in brain function have been found in the white matter (Lauvsnes et al., 2014), cerebellar gray matter (Tzarouchi et al., 2011), the hippocampal region (Zhang et al., 2020), and the frontoparietal and visual cortex regions (Xing et al., 2018). Until now, there are few studies on the changes in brain function in patients with DE. Resting-state MRI can noninvasively assess the functional status of the brain at the visual cortex and visual pathway levels. Therefore, in this study, we used fractional amplitude of low frequency fluctuation (fALFF) in patients with severe dry eye to explore changes in the functional activity of various brain regions in patients with DE, with a view to further understanding the neuropathological mechanisms of DE.

## MATERIALS AND METHODS

### Subjects

We recruited patients with DE ( $N = 28$ ; 18 females and 10 males) who attended the Ophthalmology Department of the First Affiliated Hospital of Nanchang University. The diagnostic criteria for DE were as follows: (1) patients complained of one of the subjective symptoms, including ocular dryness, foreign body sensation, burning sensation, fatigue, discomfort, blurred vision, or eye pain; and (2) a score of  $\geq 7$  on the Chinese Dry Eye Questionnaire scale or an Ocular Surface Disease Index (OSDI) score of  $\geq 13$ ; and tear film rupture time  $< 5$  s or Schirmer I test (without anesthesia)  $\leq 5$  mm/5 min (Figure 1).

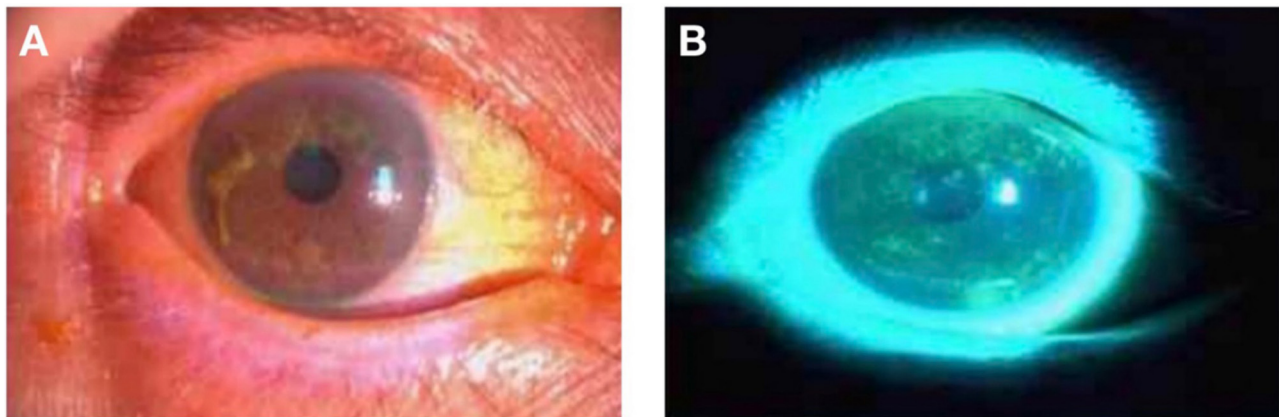
Inclusion criteria for patients with DE were as follows: (1) met the diagnostic criteria for DE; and (2) were between 40 and 60 years of age. Exclusion criteria were as follows: (1) ocular anomalies, such as conjunctival scarring, atresia of the lacrimal gland opening, or complete atrophy of accessory lacrimal glands; (2) other ocular diseases associated with other conjunctiva, cornea, or iris; (3) pregnant or lactating women; (4) suspected or confirmed history of substance abuse; (5) systemic diseases such as Sjögren's syndrome, Stephens-Johnson syndrome, systemic lupus erythematosus; (6) presence of metallic foreign bodies in the body, such as pacemakers; (7) suffering from a neurological or psychological disorder; and (8) factors that may affect the study results, such as a history of alcohol consumption or smoking, claustrophobia, etc.

We also recruited 28 healthy volunteers as the HC group (18 females and 10 males) who were matched to DE patients in terms of age, gender, and other demographic parameters. HC group met the following criteria: (1) no brain parenchymal abnormalities on MRI; (2) no other ocular diseases and corrected visual acuity; (3) no abnormalities on neurological examination; and (4) no contraindications to MRI.

All study procedures followed the Declaration of Helsinki, were in accordance with the principles of medical ethics, and were approved by the Medical Ethics Committee of the First Affiliated Hospital of Nanchang University. All subjects signed the relevant informed consent forms before the examination and were informed of the study objectives, methods, and associated risks.

### Hospital Anxiety and Depression Scale (HADS) Score Acquisition

All subjects were assessed by the same professionally trained and highly experienced psychological nurse. The first step was to ensure that the assessment was completed independently, with calm mental activity, and in the most realistic way possible. If the subject had a literacy impairment, the nurse completed it for them by describing the meaning of the questions in detail. The HADS scale consists of a total of 14 questions, including two subscales consisting of anxiety (Group A questions) and depression (Group D questions). The values in front of the four options represent the final score for the question change (Jones et al., 2017).



**FIGURE 1 |** Photographs of the anterior segment of a DE patient taken using slit-lamp microscopy. Panels (A,B) are photographs of the preocular segment of the same patient under slit lamp microscopy, and (B) is a photograph after sodium fluorescein staining. Abbreviations: DE, dry eye.

## MRI Data Acquisition

MRI was performed with a 3-Tesla magnetic resonance scanner (Magnetom Trio; Siemens, Munich, Germany). Subjects were instructed to keep their eyes closed but remain awake and relaxed until the end of the scan. Data were obtained with a 3D spoiled gradient-recalled echo sequence. The imaging parameters of the T1-weighted and T2-weighted image sequences (176 images) were as follows: repetition time (TR) = 1,900 ms, echo time (TE) = 2.26 ms, thickness = 1.0 mm, gap = 0.5 mm, acquisition matrix =  $256 \times 256$ , the field of view =  $250 \times 250$  mm, and flip angle =  $9^\circ$ . Imaging parameters for the 240 functional images were as follows: TR = 2,000 ms, TE = 30 ms, thickness = 4.0 mm, gap = 1.2 mm, acquisition matrix =  $64 \times 64$ , flip angle =  $90^\circ$ , field of view =  $220 \times 220$  mm, and 29 axials. Scanning times were 5 and 10 min, respectively.

## fALFF Analysis

The fALFF value was calculated on the trend data by REST software. REST had a built-in fast Fourier transform function that converts time series data into the frequency domain and calculates the power spectrum. Using the ratio of each frequency in the low-frequency range (0.01–0.08 Hz) to the power in the whole frequency range (0–0.25 Hz), fALFF was obtained.

## Functional Magnetic Resonance Data Analysis

The fALFF values of the DE and HC group were made more normally distributed by Fisher Z-transformation. The fALFF values were analyzed by independent two-sample *t*-test using SPM8-based REST software, and the False Discovery Rate (FDR) correction method was used to perform multiple testing hypothesis corrections. The width at half height (FWHM) was set to  $4 \text{ mm} \times 4 \text{ mm} \times 4 \text{ mm}$  and set  $Q < 0.01$ .

## Correlation Analysis

All patients were asked to complete the HADS, and the resulting data were analyzed for correlation with fALFF values using GraphPad Prism8 (GraphPad Software, Inc. La Jolla, CA, USA), and correlation graphs generated based on the results.

## Statistical Analysis

We used SPSS 22.0 (SPSS, IBM Corporation, USA) software to perform independent sample *t*-tests and chi-squared tests to determine the differences between the data of this experiment. The 2-sample *t*-test was applied to determine the difference in mean fALFF values between DE patients and the HC group; receiver operating characteristic (ROC) curves were used to determine the diagnostic value of fALFF values in each brain region for DE patients. *Pearson* correlation coefficient analysis was applied to explore the relationship between the mean fALFF values of each brain region and their clinical behaviors in the DE group. In all our statistical analyses, *p*-values  $< 0.05$  considered that the differences were statistically significant.

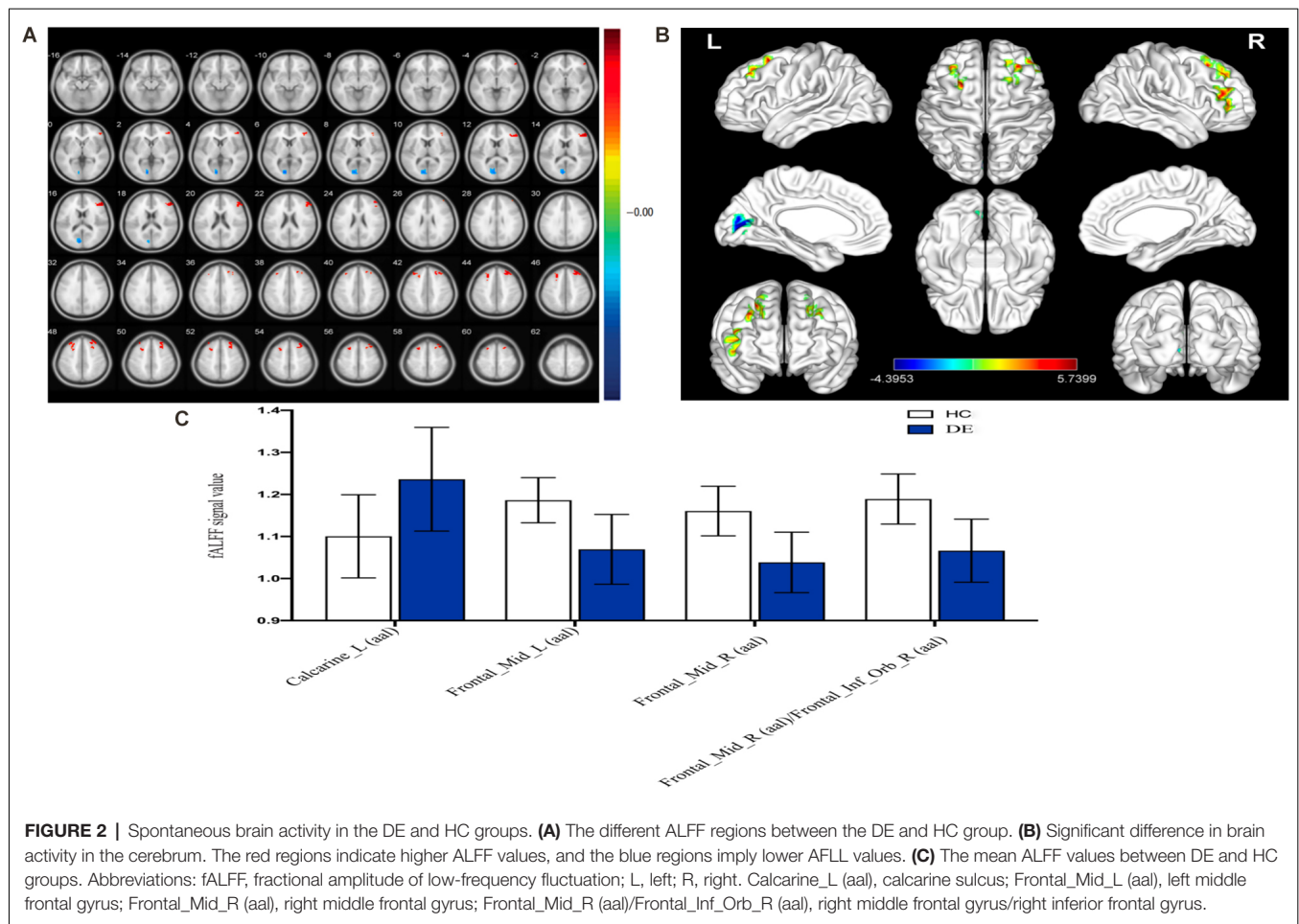
## RESULTS

### Demographic Information and Visual Measurements

There were no significant differences in age ( $p = 0.674$ ), weight ( $p = 0.628$ ), height ( $p = 0.138$ ), body mass index ( $p = 0.111$ ), or years of education ( $p = 0.940$ ) between patients with DE and HC (Table 1).

### Differences in fALFF Values Between Patients With DE and HC

As shown in Figure 2 and Table 2, the fALFF values in the left calcarine sulcus (CS) were significantly higher in patients with DE than in the HC group, whereas fALFF values in the bilateral middle frontal gyrus (MFG) and right MFG/right inferior frontal



gyrus (IFG) were significantly lower in patients with DE than in the HC group.

## ROC Curve Analysis

Given that fMRI can detect abnormal activity in certain brain regions, we investigated the diagnostic value of fALFF values in patients with DE by ROC curve analysis. As shown in **Figure 3**, the AUC value for the left CS was 0.8022 (95% confidence interval(CI): 0.681–0.924;  $p < 0.0001$ ), that for the left MFG was 0.8763 (95% CI: 0.786–0.966;  $p < 0.0001$ ), that for the right MFG was 0.9134 (95% CI: 0.842–0.985;

$p < 0.0001$ ), and the AUC value of the right MFG/right IFG was 0.8909 (95% CI: 0.802–0.980;  $p < 0.0001$ ). These results suggest that fALFF values in these brain regions exhibit good accuracy and are valuable for differentiating patients with DE from HC.

## Correlation Analysis

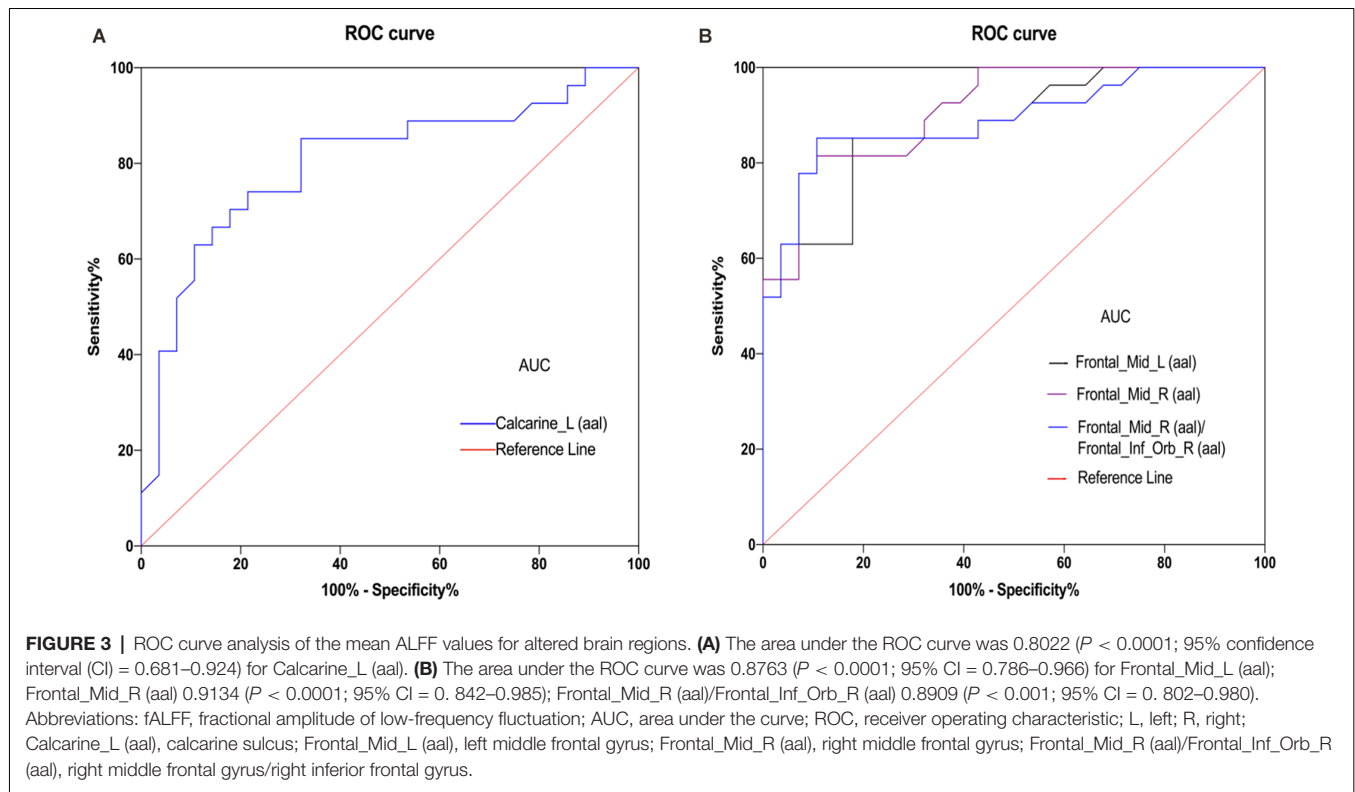
The results of *Pearson* correlation coefficient analysis in **Figure 4** and **Table 3** showed that fALFF values in right MFG ( $r = -0.7286$ ,  $P < 0.0001$ ) and right MFG/right IFG ( $r = -0.5447$ ,

**TABLE 1 |** Clinical characteristics of patients between DE and HC group.

Characteristics	DE	HC	t-value	p-values
Male/female	10\18	10\18	NA	NA
Age (years)	49.07 ± 4.45	48.78 ± 4.25	0.423	0.674
Weight (kg)	58.29 ± 3.65	58.75 ± 3.33	−0.488	0.628
Height (cm)	167.50 ± 7.07	164.93 ± 5.38	1.504	0.138
BMI (kg/m <sup>2</sup> )	20.87 ± 2.03	21.57 ± 1.34	−1.619	0.111
Years of education (years)	10.29 ± 1.61	10.25 ± 1.90	0.076	0.940

Notes: Independent *t*-tests comparing the two groups ( $P < 0.05$ ) represented statistically significant differences). Abbreviation: DE, dry eye; HC, healthy control; NA, not applicable; BMI, body mass index.





$P = 0.0027$ ) were significantly and negatively correlated with HADS values.

## DISCUSSION

The global prevalence of DE is estimated to be 5%–50%, with a prevalence of approximately 5.7% in women under 50 years of age, increasing to 9.8% in postmenopausal women (Verjee et al., 2020). DE can cause eye discomfort, visual disturbances, neuropathic pain, anxiety, and depression, among other symptoms. Further, DE has a long chronic onset and can progress without intervention, seriously affecting the quality of life and increasing social burden (Matossian et al., 2019). To date, although fALFF has been studied in neurological disorders, very few studies have applied fALFF in the investigation of DE. The fMRI is an emerging imaging technique that is widely

used in the study of neurological diseases. Currently, fMRI has been used in a variety of ophthalmic and neurological diseases (Table 4). The purpose of this study was to explore the changes in spontaneous brain activity in patients with DE using fALFF, with the aim of providing new evidence regarding the neuropathological mechanisms underlying the condition and its diagnosis.

Compared with the HC group, patients with DE had significantly higher fALFF values in the left CS and significantly lower fALFF values in the bilateral MFG and right MFG/right IFG. Figure 5 shows the abnormal brain regions.

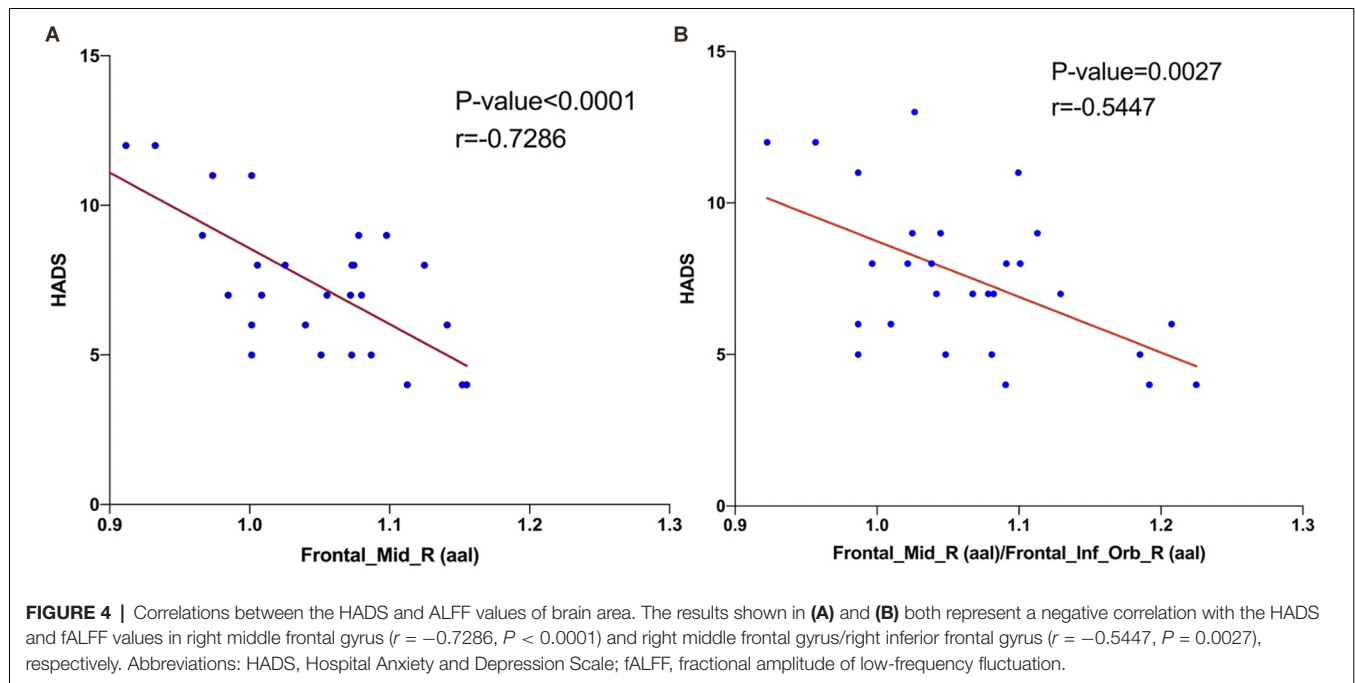
## Analysis of Elevated fALFF Values in Patients With DE

The occipital lobe is a relatively small part of the posterior end of the cerebral hemisphere, containing the visual cortex

**TABLE 2 |** Brain regions with significant differences in fALFF values between DE and HC group.

Brain areas	MNI coordinates			Number of voxels	T-value
	X	Y	Z		
HC>DE					
Frontal_Mid_R (aal)/Frontal_Inf_Orb_R (aal)	51	36	15	93	5.7399
Frontal_Mid_R (aal)	30	39	45	99	5.6994
Frontal_Mid_L (aal)	−24	18	57	65	4.7412
HC<DE					
Calcarine_L (aal)/brodmann area 17/brodmann area 18	−6	−81	15	86	−4.3953

Note: The statistical threshold was set at the voxel level with  $P < 0.05$  for multiple comparisons using False Discovery Rate ( $Q < 0.01$  and cluster size  $> 15$ ). Abbreviations: fALFF, fractional amplitude of low-frequency fluctuation; L, left; DE, dry eye; HC, healthy control; MNI, Montreal Neurological Institute; R, right; Calcarine\_L (aal), calcarine sulcus; FrontalMidL (aal), left middle frontal gyrus; FrontalMidR (aal), right middle frontal gyrus; FrontalMidR (aal)/FrontalInfOrbR (aal), right middle frontal gyrus/right inferior frontal gyrus.



and primary visual areas. In humans, the primary visual cortex (V1) is mainly located in the occipital cortex (Brodmann area 17/Brodmann area 18) above and below the CS, which receives impulses from the upper retina, below the CS, which receives impulses from the lower retina, and below the posterior lower 1/3 of the CS, which receives impulses from the macula (De Moraes, 2013). V1 receives visual information from the lateral geniculate body and is responsible for the perception of natural scenes and color signals (Weliky et al., 2003). Impaired optic nerve function can lead to dysfunction of the visual cortex, and the connections between neurons in the

visual cortex are reduced in blind people (Fox and Raichle, 2007). In a study by Williamson et al. (1992), patients with abnormal occipital lobe discharges were found to experience hallucinations, episodic blackouts, abnormal eye movements, visual field defects, and other disorders. Further, a study by Rossion et al. (2003) determined that damage to the occipital lobe can result in reduced recognition of faces, and abnormalities in the functional connectivity of primary visual cortical areas have been reported in studies of refractive parametric amblyopia (Ding et al., 2013), strabismus (Yan et al., 2019), and glaucoma (Wang et al., 2017). In the

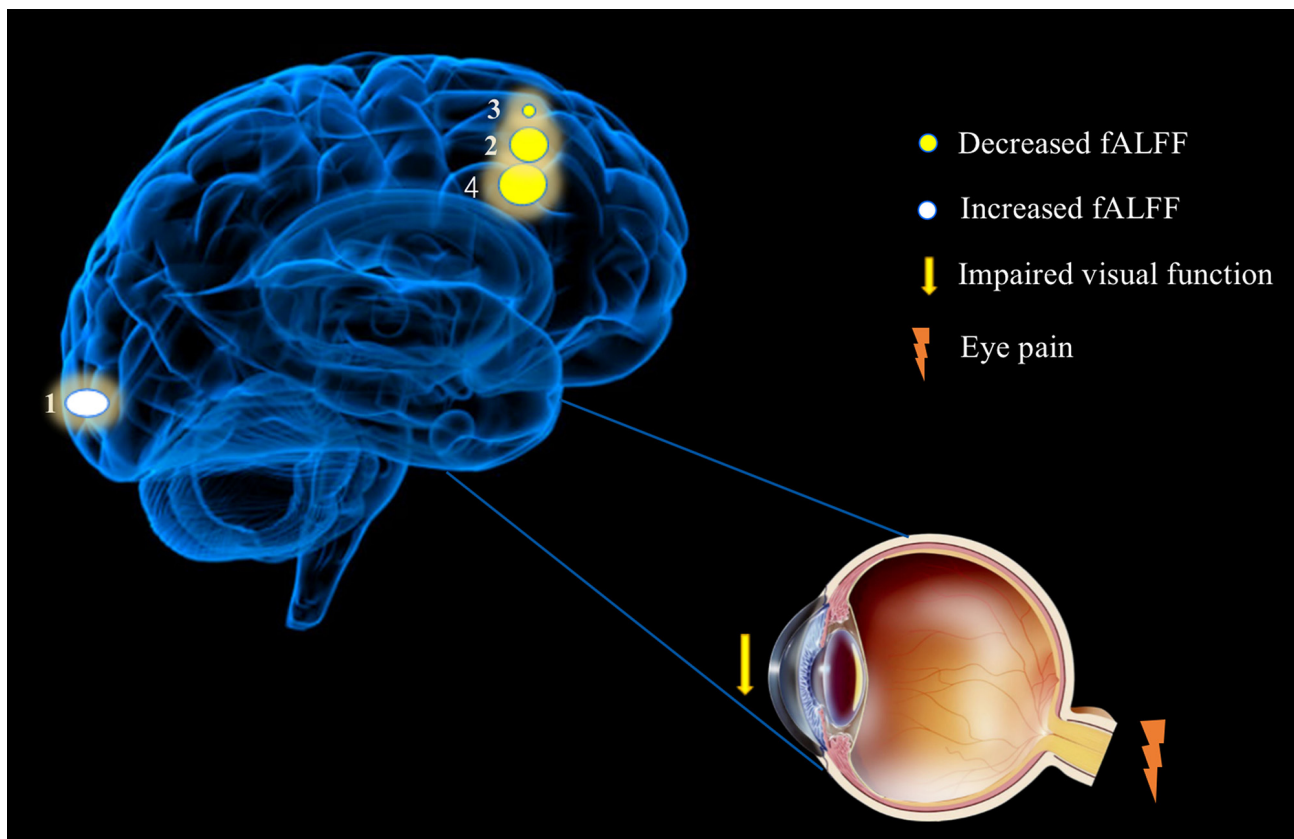
**TABLE 3 |** Pearson correlations analysis.

Brain regions	fALFF value (mean $\pm$ SD)	HADS (mean $\pm$ SD)	r-value	P-value
Calcarine_L (aal)	1.2363 $\pm$ 0.1232	7.5357 $\pm$ 2.4854	-0.2641	0.1744
Frontal_Mid_L (aal)	1.0694 $\pm$ 0.0831		-0.3661	0.0553
Frontal_Mid_R (aal)	1.0384 $\pm$ 0.0720		-0.7286	<0.0001
Frontal_Mid_R (aal)/Frontal_Inf_Orb_R (aal)	1.0663 $\pm$ 0.0750		-0.5447	0.0027

Note: fALFF, fractional amplitude of low-frequency fluctuation; SD, standard deviation.

**TABLE 4 |** Application of fALFF in ophthalmology and other diseases.

Author	Year	Disease	References
<b>Ophthalmological diseases</b>			
Wen-Feng Liu et al.	2019	Exophthalmos of Primary Hyperthyroidism	Liu et al. (2019)
Rong Wang et al.	2021	Primary angle-closure glaucoma	Wu et al. (2020)
Zhu F et al.	2019	Corneal ulcer	Zhu et al. (2019)
Shi WQ et al.	2019	Monocular blindness	Shi et al. (2019)
<b>Neurogenic diseases</b>			
Natalia Egorova et al.	2017	Post-stroke	Egorova et al. (2017)
Liu Yang et al.	2018	Alzheimer Spectrum	Yang et al. (2018)
Anny Reyes et al.	2016	Epilepsy	Reyes et al. (2016)



**FIGURE 5 |** Significant differences in spontaneous brain activity between the DE and HC groups. Different brain regions that were observed: (1) Calcarine\_L (aal); (2) Frontal\_Mid\_R(aal); (3) Frontal\_Mid\_L(aal); (4) and Frontal\_Mid\_R(aal)/Frontal\_Inf\_Orb\_R (aal). The white areas present brain regions with increased fALFF values and the yellow areas are brain regions with decreased fALFF values. Abbreviations: fALFF, fractional amplitude of low-frequency fluctuation; L, left; R, right; Calcarine\_L (aal), calcarine sulcus; Frontal\_Mid\_L (aal), left middle frontal gyrus; Frontal\_Mid\_R (aal), right middle frontal gyrus; Frontal\_Mid\_R (aal)/Frontal\_Inf\_Orb\_R (aal), right middle frontal gyrus/right inferior frontal gyrus.

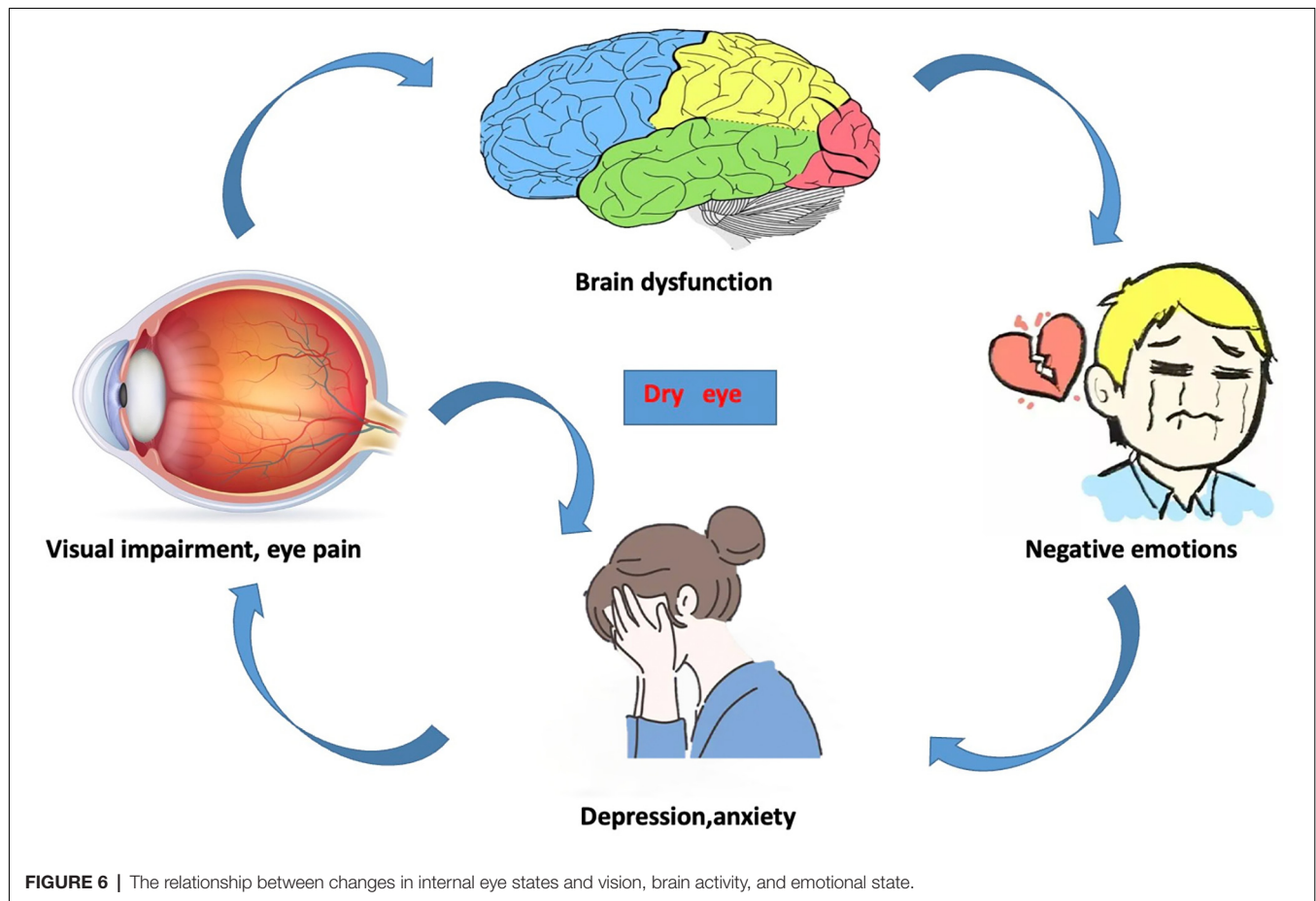
present study, fALFF values from the left CS were significantly increased in patients with DE compared with the HC group, suggesting that activity of this brain region is enhanced in patients with DE, which improves visual information processing. As DE can cause damage to patients' vision, we speculate that the increase in fALFF values in the CS visual cortex may be a compensatory result for the visual damage caused by DE.

### Analysis of Reduced fALFF Values in Patients With DE

The MFG is located in the anterior part of the brain and is responsible for language processing, stress response (Carter et al., 2006), cognitive function (Achiron et al., 2013), and attention control (Japee et al., 2015). Many disorders are associated with MFG dysfunction; for example, attention deficit hyperactivity disorder (ADHD; Tafazoli et al., 2013) and schizophrenia (Quan et al., 2013). Patients with depression also show significant MFG dysfunction (Andersson et al., 2009). The MFG is involved in the regulation of downstream nociception, and dysfunction of this circuit can lead to

pain (Mylius et al., 2006); for example, reduced gray matter in the MFG was found in patients with cluster headaches (Absinta et al., 2012). Sprenger et al. (2007) used [18F]-fluorodeoxyglucose positron emission tomography to measure significantly reduced frontal lobe glucose metabolism in patients with cluster headache, which indicated dysfunction in pain modulation regions. In the present study, we found that the fALFF values from bilateral MFG were significantly lower in patients with DE, suggesting abnormal MFG function. Therefore, we hypothesize that MFG dysfunction may be associated with the occurrence of ocular pain, anxiety, and depression in patients with DE.

The IFG is closely related to emotional (Tabei, 2015) and attention (Ochsner et al., 2012) regulation and is also involved in the protection of memory (Lin et al., 2017). In children with autism spectrum disorders, sleep deprivation is associated with an increase in negative affect and a decrease in positive affect and psychomotor performance, and brain function analysis revealed alterations in several brain regions, including a decrease in the connection between the IFG and the thalamus (Li et al., 2021). Further, IFG white matter connectivity



was significantly reduced in patients with compulsive disorder (Goncalves et al., 2015). Coordination between vision and movement relies on the frontoparietal network, which receives visual and proprioceptive inputs, and the IFG is involved in the integrated processing of visual-motor sensory information (Papadelis et al., 2016). In terms of molecular mechanisms, IFG  $\gamma$ -aminobutyric acid type A receptor binding affinity is associated with cognitive impairment and  $\gamma$ -aminobutyric acid type A receptor binding affinity is positively associated with sustained visual attention (Kasagi et al., 2018). In the present study, we found that the fALFF values from the IFG were significantly lower in patients with DE than in the HC group, which may be related to the negative emotions associated with visual impairment and chronic ocular discomfort in patients with DE.

Numerous previous studies have reported clear correlations between dry eyes and anxiety and depression, where patients with DE have reduced tear film stability, intense ocular discomfort, and greater susceptibility to adverse mood (van der Vaart et al., 2015). A population-based cross-sectional study in Beijing, China that scored depression in 1,456 patients with DE found that depression was markedly more prevalent in patients with DE than in those without (Labbe et al., 2013). In a study of patients with moderate to severe depression, cognitive deficits in depressed patients were associated with primary visual cortex function at the CS (Desseilles et al., 2011). A voxel-based morphometric study found significant reductions in gray matter volume in the MFG, IFG, and middle temporal gyrus regions in patients with major depression (Kandilarova et al., 2019). In a study based on regional homogeneity (ReHo),

**TABLE 5 |** Brain regions alteration and its potential impact.

Brain regions	Experimental	Brain function	Anticipated results
Calcarine sulcus	DE>HC	Natural scene coding Color signal perception.	Visual impairment, identify obstacles, etc.
Middle frontal gyrus	DE<HC	Processing of language cognitive function, and Pain perception.	Depression, headaches, poor concentration, etc.
Inferior frontal gyrus	DE<HC	Visual processing, emotional processing.	Visual impairment, dementia, etc.

Note: DE, dry eye; HC, healthy control.



depressed patients had lower ReHo in the right MFG and left precentral gyrus (Geng et al., 2019). IFG is an indirect inhibitor of the amygdala, and a study of 137 anxious patients found significantly impaired IFG function, which was associated with a weaker reciprocal excitatory connection between the IFG and vmPFC (Cha et al., 2016). The reality of our findings (Figure 4) is that the fALFF value of right MFG ( $r = -0.7286$ ,  $P < 0.0001$ ) and the right MFG/right IFG value ( $r = -0.5447$ ,  $P = 0.0027$ ) were significantly and negatively correlated with the HADS value. This suggests a potential association between the changes in brain function occurring in DE patients and their greater susceptibility to anxiety and depression.

In our study, we found that the fALFF values in the vicinity of the CS of patients with DE were significantly higher than those in the HC group, while the fALFF values at the MFG and IFG in patients with DE were significantly lower than those in the HC group. Visual impairment, chronic neuropathic pain, ocular discomfort, and reduced emotional regulation caused by brain dysfunction in patients with DE are associated with neuropathy mechanisms underlying anxiety and depression (Bai et al., 2020).

In conclusion, long-term DE brings negative emotions and reduces the quality of life of patients, we found that the fALFF values of CS, MFG, and IFG of DE patients are abnormal compared with those of the HC group by resting-state MRI. ROC curve analysis of left CS, left MFG, right MFG and right MFG/right IFG involved in this study have high differential diagnosis significance indicating that the fALFF values of MFG and IFG combined can be used as a potential imaging biomarker to discriminate between DE and HC groups. We speculate that DE may cause brain dysfunction (Table 5, Figure 6). The neurological basis for the pathophysiology of the dry eye provided by the present study may lead to a new field of research to define this basis more precisely with the aim of providing a new idea for the diagnosis and treatment of patients with DE.

There are some limitations to this study; first, our study sample size was relatively small, which may directly lead to less reliable results, and in order to validate our findings, we need to conduct the study in a larger population. Then, we did not group the degree of disease of DE, and at a later stage, we need to further group the severity of DE on the basis of a large sample for comparison.

## REFERENCES

- Absinta, M., Rocca, M. A., Colombo, B., Falini, A., Comi, G., Filippi, M., et al. (2012). Selective decreased grey matter volume of the pain-matrix network in cluster headache. *Cephalalgia* 32, 109–115. doi: 10.1177/0333102411431334
- Achiron, A., Chapman, J., Tal, S., Bercovich, E., Gil, H., Achiron, A., et al. (2013). Superior temporal gyrus thickness correlates with cognitive performance in multiple sclerosis. *Brain Struct. Funct.* 218, 943–950. doi: 10.1007/s00429-012-0440-3
- Andersson, M., Ystad, M., Lundervold, A., and Lundervold, A. J. (2009). Correlations between measures of executive attention and cortical thickness of

## DATA AVAILABILITY STATEMENT

The original contributions presented in the study are included in the article, further inquiries can be directed to the corresponding author.

## ETHICS STATEMENT

The studies involving human participants were reviewed and approved by Medical Ethics Committee of the First Affiliated Hospital of Nanchang University. The patients/participants provided their written informed consent to participate in this study.

## AUTHOR CONTRIBUTIONS

YS guarantees the integrity of the whole learning and the approval of the final version of the manuscript. R-BL is responsible for learning concepts, research design, and manuscript draft. L-QL is responsible for literature research, data analysis/interpretation. W-QS and TS are responsible for clinical experimental research, data collection, and statistical analysis. Q-MG, Q-YL, H-YS, and L-JZ are responsible for manuscript editing and original revision/review. All authors contributed to the article and approved the submitted version.

## FUNDING

This study was supported in part by grants from The Central Government Guides Local Science and Technology Development Foundation (No.: 20211ZDG02003); Key Research Foundation of Jiangxi Province (No.: 20181BBG70004, 20203BBG73059); Excellent Talents Development Project of Jiangxi Province (No.: 20192BCBL23020); Natural Science Foundation of Jiangxi Province (No.: 20181BAB205034); Grassroots Health Appropriate Technology “Spark Promotion Plan” Project of Jiangxi Province (No.: 20188003); Health Development Planning Commission Science Foundation of Jiangxi Province (No.: 20201032, 202130210); Health Development Planning Commission Science TCM Foundation of Jiangxi Province (No.: 2018A060, 2020A0087); Education Department Foundation of Jiangxi Province (No.: GJJ200157, GJJ200159, GJJ200169).

- left posterior middle frontal gyrus - a dichotic listening study. *Behav. Brain Funct.* 5:41. doi: 10.1186/1744-9081-5-41
- Bai, Y. M., Chen, M. H., Hsu, J. W., Huang, K. L., Tu, P. C., Chang, W. C., et al. (2020). A comparison study of metabolic profiles, immunity and brain gray matter volumes between patients with bipolar disorder and depressive disorder. *J. Neuroinflammation*. 17:42. doi: 10.1186/s12974-020-1724-9
- Carter, R. M., O'Doherty, J. P., Seymour, B., Koch, C., and Dolan, R. J. (2006). Contingency awareness in human aversive conditioning involves the middle frontal gyrus. *Neuroimage* 29, 1007–1012. doi: 10.1016/j.neuroimage.2005.09.011
- Cha, J., DeDora, D., Nedic, S., Ide, J., Greenberg, T., Hajcak, G., et al. (2016). Clinically anxious individuals show disrupted feedback between inferior

- frontal gyrus and prefrontal-limbic control circuit. *J. Neurosci.* 36, 4708–4718. doi: 10.1523/JNEUROSCI.1092-15.2016
- De Moraes, C. G. (2013). Anatomy of the visual pathways. *J. Glaucoma* 22, S2–S7. doi: 10.1097/IJG.0b013e3182934978
- Desseilles, M., Schwartz, S., Dang-Vu, T. T., Sterpenich, V., Anseau, M., Maquet, P., et al. (2011). Depression alters “top-down” visual attention: a dynamic causal modeling comparison between depressed and healthy subjects. *Neuroimage* 54, 1662–1668. doi: 10.1016/j.neuroimage.2010.08.061
- Ding, K., Liu, Y., Yan, X., Lin, X., and Jiang, T. (2013). Altered functional connectivity of the primary visual cortex in subjects with amblyopia. *Neural Plast.* 2013:612086. doi: 10.1155/2013/612086
- Egorova, N., Veldsman, M., Cumming, T., and Brodtmann, A. (2017). Fractional amplitude of low-frequency fluctuations (fALFF) in post-stroke depression. *Neuroimage Clin.* 16, 116–124. doi: 10.1016/j.nicl.2017.07.014
- Fox, M. D., and Raichle, M. E. (2007). Spontaneous fluctuations in brain activity observed with functional magnetic resonance imaging. *Nat. Rev. Neurosci.* 8, 700–711. doi: 10.1038/nrn2201
- Geng, J., Yan, R., Shi, J., Chen, Y., Mo, Z., Shao, J., et al. (2019). Altered regional homogeneity in patients with somatic depression: a resting-state fMRI study. *J. Affect Disord.* 246, 498–505. doi: 10.1016/j.jad.2018.12.066
- Goncalves, O. F., Sousa, S., Maia, L., Carvalho, S., Leite, J., Ganho, A., et al. (2015). Inferior frontal gyrus white matter abnormalities in obsessive-compulsive disorder. *Neuroreport* 26, 495–500. doi: 10.1097/WNR.0000000000000377
- Japee, S., Holiday, K., Satyshur, M. D., Mukai, I., and Ungerleider, L. G. (2015). A role of right middle frontal gyrus in reorienting of attention: a case study. *Front. Syst. Neurosci.* 9:23. doi: 10.3389/fnsys.2015.00023
- Jiang, N., Ye, L. H., Ye, L., Yu, J., Yang, Q. C., Yuan, Q., et al. (2017). Effect of mistletoe combined with carboxymethyl cellulose on dry eye in postmenopausal women. *Int. J. Ophthalmol.* 10, 1669–1677. doi: 10.18240/ijo.2017.11.06
- Jones, L., Downie, L. E., Korb, D., Benitez-Del-Castillo, J. M., Dana, R., Deng, S. X., et al. (2017). TFOS DEWS II management and therapy report. *Ocul. Surf.* 15, 575–628. doi: 10.1016/j.jtos.2017.05.006
- Kandilarova, S., Stoyanov, D., Sirakov, N., Maes, M., and Specht, K. (2019). Reduced grey matter volume in frontal and temporal areas in depression: contributions from voxel-based morphometry study. *Acta Neuropsychiatr.* 31, 252–257. doi: 10.1017/neu.2019.20
- Kasagi, M., Motegi, T., Narita, K., Fujihara, K., Suzuki, Y., Tagawa, M., et al. (2018).  $\Gamma$ -Aminobutyric acid type A receptor binding affinity in the right inferior frontal gyrus at resting state predicts the performance of healthy elderly people in the visual sustained attention test. *Int. Psychogeriatr.* 30, 1385–1391. doi: 10.1017/S1041610217002988
- Khosla, M., Jamison, K., Ngo, G. H., Kuceyeski, A., and Sabuncu, M. R. (2019). Machine learning in resting-state fMRI analysis. *Magn. Reson. Imaging* 64, 101–121. doi: 10.1016/j.mri.2019.05.031
- Labbe, A., Wang, Y. X., Jie, Y., Baudouin, C., Jonas, J. B., Xu, L., et al. (2013). Dry eye disease, dry eye symptoms and depression: the Beijing Eye Study. *Br. J. Ophthalmol.* 97, 1399–1403. doi: 10.1136/bjophthalmol-2013-303838
- Lauvnes, M. B., Beyer, M. K., Appenzeller, S., Greve, O. J., Harboe, E., Goransson, L. G., et al. (2014). Loss of cerebral white matter in primary Sjogren's syndrome: a controlled volumetric magnetic resonance imaging study. *Eur. J. Neurol.* 21, 1324–1329. doi: 10.1111/ene.12486
- Li, B. Z., Cao, Y., Zhang, Y., Chen, Y., Gao, Y. H., Peng, J. X., et al. (2021). Relation of decreased functional connectivity between left thalamus and left inferior frontal gyrus to emotion changes following acute sleep deprivation. *Front. Neurol.* 12:642411. doi: 10.3389/fneur.2021.642411
- Lin, F., Ren, P., Lo, R. Y., Chapman, B. P., Jacobs, A., Baran, T. M., et al. (2017). Insula and inferior frontal gyrus' activities protect memory performance against alzheimer's disease pathology in old age. *J. Alzheimers Dis.* 55, 669–678. doi: 10.3233/JAD-160715
- Liu, W. F., Shu, Y. Q., Zhu, P. W., Li, B., Shi, W. Q., Lin, Q., et al. (2019). The cerebellum posterior lobe associates with the exophthalmos of primary hyperthyroidism: a resting-state fmri study. *Int. J. Endocrinol.* 2019:8135671. doi: 10.1155/2019/8135671
- Matossian, C., McDonald, M., Donaldson, K. E., Nichols, K. K., MacIver, S., Gupta, P. K., et al. (2019). Dry eye disease: consideration for women's health. *J. Womens Health (Larchmt)* 28, 502–514. doi: 10.1089/jwh.2018.7041
- Mylius, V., Reis, J., Kunz, M., Beyer, T. F., Oertel, W. H., Rosenow, F., et al. (2006). Modulation of electrically induced pain by paired pulse transcranial magnetic stimulation of the medial frontal cortex. *Clin. Neurophysiol.* 117, 1814–1820. doi: 10.1016/j.clinph.2006.04.013
- Ochsner, K. N., Silvers, J. A., and Buhle, J. T. (2012). Functional imaging studies of emotion regulation: a synthetic review and evolving model of the cognitive control of emotion. *Ann. N Y Acad. Sci.* 1251, E1–E24. doi: 10.1111/j.1749-6632.2012.06751.x
- Papadelis, C., Arfeller, C., Erla, S., Nollo, G., Cattaneo, L., and Braun, C. (2016). Inferior frontal gyrus links visual and motor cortices during a visuomotor precision grip force task. *Brain Res.* 1650, 252–266. doi: 10.1016/j.brainres.2016.09.011
- Quan, M., Lee, S. H., Kubicki, M., Kikinis, Z., Rath, Y., Seidman, L. J., et al. (2013). White matter tract abnormalities between rostral middle frontal gyrus, inferior frontal gyrus and striatum in first-episode schizophrenia. *Schizophr. Res.* 145, 1–10. doi: 10.1016/j.schres.2012.11.028
- Reyes, A., Thesen, T., Wang, X., Hahn, D., Yoo, D., Kuzniecky, R., et al. (2016). Resting-state functional MRI distinguishes temporal lobe epilepsy subtypes. *Epilepsia* 57, 1475–1484. doi: 10.1111/epi.13456
- Rossion, B., Caldara, R., Seghier, M., Schuller, A. M., Lazeyras, F., Mayer, E., et al. (2003). A network of occipito-temporal face-sensitive areas besides the right middle fusiform gyrus is necessary for normal face processing. *Brain* 126, 2381–2395. doi: 10.1093/brain/awg241
- Shi, W. Q., He, Y., Li, Q. H., Tang, L. Y., Li, B., Lin, Q., et al. (2019). Central network changes in patients with advanced monocular blindness: a voxel-based morphometric study. *Brain Behav.* 9:e01421. doi: 10.1002/brb3.1421
- Sprenger, T., Ruether, K. V., Boecker, H., Valet, M., Berthele, A., Pfaffenrath, V., et al. (2007). Altered metabolism in frontal brain circuits in cluster headache. *Cephalalgia* 27, 1033–1042. doi: 10.1111/j.1468-2982.2007.01386.x
- Stapleton, F., Alves, M., Bunya, V. Y., Jalbert, I., Lekhanont, K., Malet, F., et al. (2017). TFOS DEWS II epidemiology report. *Ocul. Surf.* 15, 334–365. doi: 10.1016/j.jtos.2017.05.003
- Tabei, K. (2015). Inferior frontal gyrus activation underlies the perception of emotions, while precuneus activation underlies the feeling of emotions during music listening. *Behav. Neurol.* 2015:529043. doi: 10.1155/2015/529043
- Tafazoli, S., O'Neill, J., Bejjani, A., Ly, R., Salamon, N., McCracken, J. T., et al. (2013). 1H MRSI of middle frontal gyrus in pediatric ADHD. *J. Psychiatr. Res.* 47, 505–512. doi: 10.1016/j.jpsychires.2012.11.011
- Tzarouchi, L. C., Tsietsaki, N., Konitsiotis, S., Zikou, A., Astrakas, L., Drosos, A., et al. (2011). CNS involvement in primary Sjogren Syndrome: assessment of gray and white matter changes with MRI and voxel-based morphometry. *Am. J. Roentgenol.* 197, 1207–1212. doi: 10.2214/AJR.10.5984
- van der Vaart, R., Weaver, M. A., Lefebvre, C., and Davis, R. M. (2015). The association between dry eye disease and depression and anxiety in a large population-based study. *Am. J. Ophthalmol.* 159, 470–474. doi: 10.1016/j.ajo.2014.11.028
- Verjee, M. A., Brissette, A. R., and Starr, C. E. (2020). Dry eye disease: early recognition with guidance on management and treatment for primary care family physicians. *Ophthalmol. Ther.* 9, 877–888. doi: 10.1007/s40123-020-00308-z
- Wang, J., Li, T., Zhou, P., Wang, N., Xian, J., He, H., et al. (2017). Altered functional connectivity within and between the default model network and the visual network in primary open-angle glaucoma: a resting-state fMRI study. *Brain Imaging Behav.* 11, 1154–1163. doi: 10.1007/s11682-016-9597-3
- Weatherby, T. J. M., Raman, V. R. V., and Agius, M. (2019). Depression and dry eye disease: a need for an interdisciplinary approach? *Psychiatr. Danub.* 31, 619–621.
- Weliky, M., Fiser, J., Hunt, R. H., and Wagner, D. N. (2003). Coding of natural scenes in primary visual cortex. *Neuron* 37, 703–718. doi: 10.1016/s0896-6273(03)00022-9
- Williamson, P. D., Thadani, V. M., Darcey, T. M., Spencer, D. D., Spencer, S. S., Mattson, R. H., et al. (1992). Occipital lobe epilepsy: clinical characteristics, seizure spread patterns and results of surgery. *Ann. Neurol.* 31, 3–13. doi: 10.1002/ana.410310103

- Wu, Y. Y., Wang, S. F., Zhu, P. W., Yuan, Q., Shi, W. Q., Lin, Q., et al. (2020). Altered intrinsic functional connectivity of the primary visual cortex in patients with neovascular glaucoma: a resting-state functional magnetic resonance imaging study. *Neuropsychiatr. Dis. Treat.* 16, 25–33. doi: 10.2147/NDT.S228606
- Xing, W., Shi, W., Leng, Y., Sun, X., Guan, T., Liao, W., et al. (2018). Resting-state fmri in primary sjogren syndrome. *Acta Radiol.* 59, 1091–1096. doi: 10.1177/0284185117749993
- Yan, H., Shan, X., Wei, S., Liu, F., Li, W., Lei, Y., et al. (2020). Abnormal spontaneous brain activities of limbic-cortical circuits in patients with dry eye disease. *Front. Hum. Neurosci.* 14:574758. doi: 10.3389/fnhum.2020.574758
- Yan, X., Wang, Y., Xu, L., Liu, Y., Song, S., Ding, K., et al. (2019). Altered functional connectivity of the primary visual cortex in adult comitant strabismus: a resting-state functional MRI study. *Curr. Eye Res.* 44, 316–323. doi: 10.1080/02713683.2018.1540642
- Yang, L., Yan, Y., Wang, Y., Hu, X., Lu, J., Chan, P., et al. (2018). Gradual disturbances of the amplitude of low-frequency fluctuations (ALFF) and fractional ALFF in Alzheimer spectrum. *Front. Neurosci.* 12:975. doi: 10.3389/fnins.2018.00975
- Zhang, X. D., Zhao, L. R., Zhou, J. M., Su, Y. Y., Ke, J., Cheng, Y., et al. (2020). Altered hippocampal functional connectivity in primary Sjogren syndrome: a resting-state fMRI study. *Lupus* 29, 446–454. doi: 10.1177/0961203320908936
- Zhu, F., Tang, L., Zhu, P., Lin, Q., Yuan, Q., Shi, W., et al. (2019). Resting-state functional magnetic resonance imaging (fMRI) and functional connectivity density mapping in patients with corneal ulcer. *Neuropsychiatr. Dis. Treat.* 15, 1833–1844. doi: 10.2147/NDT.S210658

**Conflict of Interest:** The authors declare that the research was conducted in the absence of any commercial or financial relationships that could be construed as a potential conflict of interest.

**Publisher's Note:** All claims expressed in this article are solely those of the authors and do not necessarily represent those of their affiliated organizations, or those of the publisher, the editors and the reviewers. Any product that may be evaluated in this article, or claim that may be made by its manufacturer, is not guaranteed or endorsed by the publisher.

Copyright © 2022 Liang, Liu, Shi, Sun, Ge, Li, Shu, Zhang and Shao. This is an open-access article distributed under the terms of the Creative Commons Attribution License (CC BY). The use, distribution or reproduction in other forums is permitted, provided the original author(s) and the copyright owner(s) are credited and that the original publication in this journal is cited, in accordance with accepted academic practice. No use, distribution or reproduction is permitted which does not comply with these terms.



# Altered Homotopic Connectivity in the Cerebellum Predicts Stereopsis Dysfunction in Patients With Comitant Exotropia

Fei Chen<sup>1\*</sup>, Zhirou Hu<sup>1</sup>, Hui Liu<sup>2</sup>, Fangyuan Zhen<sup>1</sup>, Chenlu Liu<sup>1</sup> and Qiuming Li<sup>1\*</sup>

<sup>1</sup> Department of Ophthalmology, The First Affiliated Hospital of Zhengzhou University, Zhengzhou, China, <sup>2</sup> Department of Ophthalmology, Jiangxi Provincial People's Hospital, Nanchang, China

## OPEN ACCESS

### Edited by:

Yan Tong,  
Renmin Hospital of Wuhan University,  
China

### Reviewed by:

Zhi Wen,  
Renmin Hospital of Wuhan University,  
China  
Chen-Xing Qi,  
Renmin Hospital of Wuhan University,  
China

### \*Correspondence:

Fei Chen  
2015283020193@whu.edu.cn  
Qiuming Li  
15838241308@163.com

### Specialty section:

This article was submitted to  
Brain Imaging and Stimulation,  
a section of the journal  
Frontiers in Human Neuroscience

Received: 11 April 2022

Accepted: 09 May 2022

Published: 02 June 2022

### Citation:

Chen F, Hu Z, Liu H, Zhen F, Liu C  
and Li Q (2022) Altered Homotopic  
Connectivity in the Cerebellum  
Predicts Stereopsis Dysfunction  
in Patients With Comitant Exotropia.  
Front. Hum. Neurosci. 16:917769.  
doi: 10.3389/fnhum.2022.917769

**Purpose:** Comitant exotropia (CE) is a common eye disorder characterized by impaired stereoscopic vision and eye deviation. Previous neuroimaging studies demonstrated that patients with CE were accompanied by specific functional and structural abnormalities of the brain. However, the effect of impaired stereoscopic vision and eye deviation on interhemispheric homotopic connectivity remains unknown.

**Methods:** A total of thirty-six patients with CE (25 males and 11 females) and 36 well-matched healthy controls underwent magnetic resonance imaging scanning. The voxel-mirrored homotopic connectivity (VMHC) method was applied to assess the interhemispheric homotopic connectivity changes in patients with CE. Furthermore, the support vector machine method was applied to assess to differentiate patients with CE from healthy controls (HCs) with the VMHC maps as a feature.

**Results:** Compared with HCs, patients with CE showed significantly increased VMHC values in the bilateral cerebellum\_8 and cerebellum\_4\_5. Moreover, we found that the VMHC maps showed an accuracy of 81.94% and an area under the curve of 0.87 for distinguishing the patients with CE from HCs.

**Conclusion:** Our study demonstrates that patients with CE showed interhemispheric homotopic connectivity changes in the cerebellum, which might reflect the neurological mechanisms of impaired stereoscopic vision and eye deviation in patients with CE.

**Keywords:** comitant exotropia, functional magnetic resonance imaging, voxel-mirrored homotopic connectivity, functional connectivity, support vector machine

## INTRODUCTION

Comitant exotropia (CE) is a common eye disease characterized by ocular deviation and stereopsis dysfunction. The prevalence of exotropia is approximately 1% in all children (Govindan et al., 2005). There are several risk factors for the development of strabismus, including myopia (Zhang et al., 2021), anisometropia (Smith et al., 2017), and a family history of strabismus (Taira et al., 2003). Stereopsis dysfunction is a core clinical symptom in patients. Binocular visual function in patients with strabismus can interfere with daily life and work. Moreover, patients with strabismus may also have mental health problems (Lin et al., 2014; Lee et al., 2022). Strabismus



surgery is currently an important tool in the treatment of strabismus. However, some patients are unable to re-establish stereopsis after strabismus surgery. The integration of binocular visual information occurs in the lateral geniculate nucleus; this integration leads to binocular vision and depth perception. However, the neural mechanisms that underlie central nervous system dysfunction in patients with CE remain unclear.

Functional magnetic resonance imaging (fMRI) has been widely used to study changes in brain neural activity in patients with strabismus. Chen et al. (2021a) reported that brain neural activity considerably differed between patients with CE and HCs; affected areas included the middle occipital gyrus and supplementary motor area/precentral gyrus, implying that stereopsis dysfunction was present in patients with CE. Tan et al. (2018) reported that patients with CE exhibited abnormal network activity in various brain regions. Using a voxel-based analysis method, Yan et al. (2010) showed that patients with CE had lower fractional anisotropy values in the right middle occipital gyrus and right supramarginal gyrus. Huang et al. (2018) reported that patients with CE had increased resting cerebral blood flow in the supplementary eye field, cingulate eye field, and frontal eye field. Jin et al. (2022) also found that, compared to healthy controls, patients with CE had abnormalities in the cerebellar, sensorimotor, auditory, and visual networks. Thus, the abovementioned studies demonstrated that patients with CE had abnormalities in vision and eye-motor control regions of the brain (supplementary eye field, cingulate eye field, and frontal eye field). However, the effects of impaired stereopsis and eye deviation on interhemispheric homotopic connectivity remain unclear. The human brain exhibits interhemispheric homotopic connectivity. Homotopic connectivity within the visual cortex participates in visual information processing (Dougherty et al., 2005; Butt et al., 2015). Furthermore, homotopic connectivity may reflect the mechanisms that underlie central nervous system disorders. The voxel-mirrored homotopic connectivity (VMHC) method, first proposed by Zuo et al. (2010), quantifies the homotopic connectivity between individual voxels in one hemisphere and their mirror voxel counterparts in the other hemisphere. Previous studies demonstrated that the VMHC method has a good spatial and temporal resolution (Yang et al., 2019; Chen et al., 2021b; Wu et al., 2021). Although there have been many studies concerning the functional connectivity changes that occur in CE, the effects of impaired stereopsis and eye deviation on interhemispheric homotopic connectivity in patients with CE are still unknown. Furthermore, with the rapid development of machine learning technology, MRI-related machine learning methods are increasingly used in disease classification; such applications can provide sensitive biomarkers for disease diagnosis and prediction. Support vector machine (SVM) methods are supervised machine learning algorithms widely used for MRI data classification; these methods can achieve individual-level classification and detect biomarkers based on neuroimaging data. SVM methods can reduce the high dimensionality of MRI data and improve the level of data generalization. Compared with other machine learning methods, such as random forest, naïve Bayes, and convolutional neural network. SVM methods have been successfully used to

classify diseases, such as iridocyclitis (Tong et al., 2021), primary dysmenorrhea (Gui et al., 2021), and major depressive disorder (Gao et al., 2021). However, no studies have used SVM and VMHC methods to distinguish patients with CE from HCs.

Considering the published findings described above, the purpose of this study was to determine whether patients with CE exhibit interhemispheric homotopic connectivity. Additionally, an SVM method was used to investigate the predictive value of VMHC data for diagnostic classification. Thus, we hypothesized that the patients with CE might be associated with abnormal interhemispheric homotopic connectivity.

## MATERIALS AND METHODS

### Participants

Thirty-six patients with CE (mean age,  $24.25 \pm 1$  years) and 36 healthy controls (HCs; mean age,  $24.46 \pm 1.31$  years) were recruited from the first hospital affiliated with Zhengzhou University and Jiangxi Provincial People's Hospital. The diagnostic criteria of patients with CE were: (1) CE, exodeviation angles between  $15^\Delta$  and  $80^\Delta$ ; (2) without a history of strabismus surgery; The exclusion criteria of CE individuals in the study were: (1) additional ocular-related complications (e.g., cataract, glaucoma, high myopia, or optic neuritis); (2) sensory exotropia, fixed exotropia, secondary exotropia, restricted exotropia, and exotropia with vertical exotropia; and (3) concomitant exotropia were associated with amblyopia.

### Ethics Statement

All research methods followed the Declaration of Helsinki and were approved by the Ethical Committee for Medicine of the first hospital affiliated with Zhengzhou University and Jiangxi Provincial People's Hospital. Participants enrolled in the study of their own accord and were informed of the purpose, methods, as well as potential risks before signing an informed consent form.

### Magnetic Resonance Imaging Acquisition

Magnetic resonance imaging scanning was performed on a 3-tesla magnetic resonance scanner (Discovery MR 750W system; GE Healthcare, Milwaukee, WI, United States), with the eight-channel head coil. Functional images were obtained by using a gradient-echo-planar imaging sequence. All the subjects were asked to keep their eyes closed and relaxed without falling asleep.

### Functional Magnetic Resonance Imaging Data Analysis

All preprocessing was performed using the toolbox for Data Processing and Analysis of Brain Imaging (DPABI)<sup>1</sup> (Yan et al., 2016) which is based on Statistical Parametric Mapping (SPM12)<sup>2</sup> implemented in MATLAB 2013a (MathWorks, Natick, MA, United States) and, briefly, using the following steps: (1) Remove

<sup>1</sup><http://www.rfmri.org/dpabi>

<sup>2</sup><http://www.fil.ion.ucl.ac.uk>

first ten volumes; (2) Slice timing effects, motion-corrected; (3) Normalized data (in Montreal Neurological Institute 152 space) to EPI template were re-sliced at a resolution of  $3 \text{ mm} \times 3 \text{ mm} \times 3 \text{ mm}$ ; (4) Spatial smoothing by convolution with an isotropic Gaussian kernel of  $6 \text{ mm} \times 6 \text{ mm} \times 6 \text{ mm}$  full width at half maximum; (5) The fMRI data with linear trends were removed; (6) Linear regression analysis was applied to regress out several covariates (mean framewise displacement, global brain signal, and averaged signal from cerebrospinal fluid and white matter); and (7) Temporal band-pass was filtered (0.01–0.08 Hz) to reduce the influence of noise.

## Voxel-Mirrored Homotopic Connectivity Analysis

To evaluate the interhemispheric connectivity, the VMHC method was performed using the DPABI toolkit according to previous research (Zuo et al., 2010). The VMHC values for each participant were calculated as the Pearson correlation between each pair of symmetrical interhemispheric voxels' time series.

## Support Vector Machine Analysis

To evaluate whether the VMHC metrics alterations could serve as potential diagnostic metrics for CE, we performed ML analyses using the SVM algorithm with the average VMHC values of all clusters showing significant intragroup differences as the features. The following steps were followed (Schrouff et al., 2013): (1) The VMHC maps of two groups served as a classification feature; and (2) Then, the leave-one-out cross-validation technique was applied to perform SVM classifier validation. This procedure was repeated  $n$  times. For classification, two classes were defined (patients' group and HCs group) and processed using a soft-margin hyper-parameter approach. The soft-margin parameters take the values 0.01, 0.1, 1, 10, 100, and 1,000 in the SVM classifier in the current version of PRoNTo, which make the model obtain the maximum interval hyperplane with the minimum classification error. To quantify the performance of classification methods, accuracy, sensitivity, and specificity were reported. Besides the classification accuracy, the receiver operating characteristic (ROC) curves and the corresponding area under the curve (AUC) were also computed to evaluate the classification efficiency.

## Statistical Analysis

The independent sample  $t$ -test was used to investigate the clinical features of the two groups.

The one-sample  $t$ -test was conducted to assess the group mean of VMCH maps. The two-sample  $t$ -test was used to compare the two group differences in the VMCH maps using the Gaussian random field (GRF) method (two-tailed, voxel-level  $P < 0.01$ , GRF correction, cluster-level  $P < 0.05$ ).

## RESULTS

### Demographics and Disease Characteristics

There were no statistically significant differences between the CE and HC groups in gender or age, the results of these clinical data were summarized in **Table 1**.

### Different Voxel-Mirrored Homotopic Connectivity Values Between Two Groups

The group means of VMHC maps of the CE and HC are shown (**Figures 1A,B**). Compared with the HCs, patients with CE showed significantly increased VMHC values in the bilateral cerebellum\_8 and bilateral cerebellum\_4\_5 (**Table 2** and **Figure 2A**). The mean values of altered VMHC values were shown with a histogram (**Figure 2B**).

### Support Vector Machine Classification Results

To evaluate the classification ability of the SVM model, the accuracy, sensitivity, specificity, and precision were calculated and the ROC curve of the classifier was illustrated in **Figure 3**. Moreover, we found that the VMHC maps showed an accuracy of 81.94% and an AUC of 0.87 for distinguishing the patients with CE from HCs.

## DISCUSSION

Compared to HCs, patients with CE had significantly greater VMHC values in the bilateral cerebellum\_8 and cerebellum\_4\_5. Additionally, the VMHC maps exhibited an accuracy of 81.94% and an AUC of 0.87 for distinguishing patients with CE from HCs.

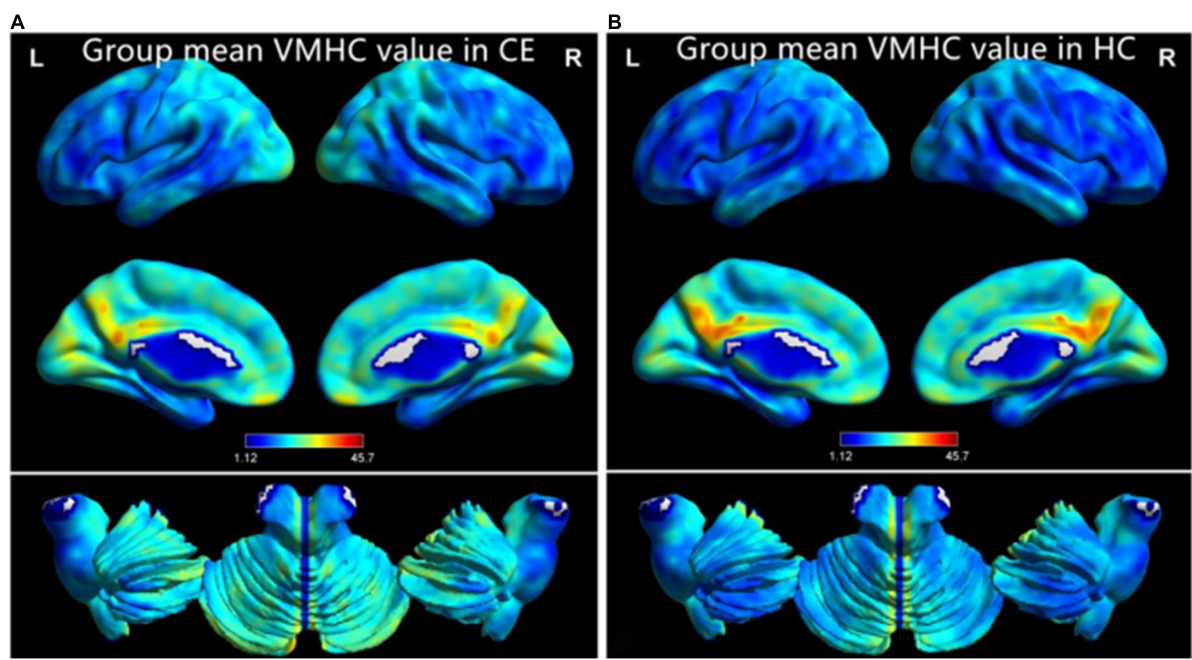
In this study, patients with CE exhibited a significant increase in VMHC values in the cerebellum. The cerebellum plays an important role in balance control and motor function; it is also involved in eye movement and visual perception. Thier and Markanday (2019) demonstrated that the cerebellum plays an

**TABLE 1** | Demographics and visual measurements between two groups.

Condition	CE group	HC group	T-values	P-values
Gender (male/female)	(25/11)	(25/11)	N/A	N/A
Age (years)	15.80 $\pm$ 2.46	16.00 $\pm$ 2.68	-0.240	0.812
Handedness	36 R	36 R	N/A	N/A

Note: Independent  $t$ -test for the other normally distributed continuous data (means  $\pm$  SD).

Abbreviations: CE, comitant exotropia and HC, health control.

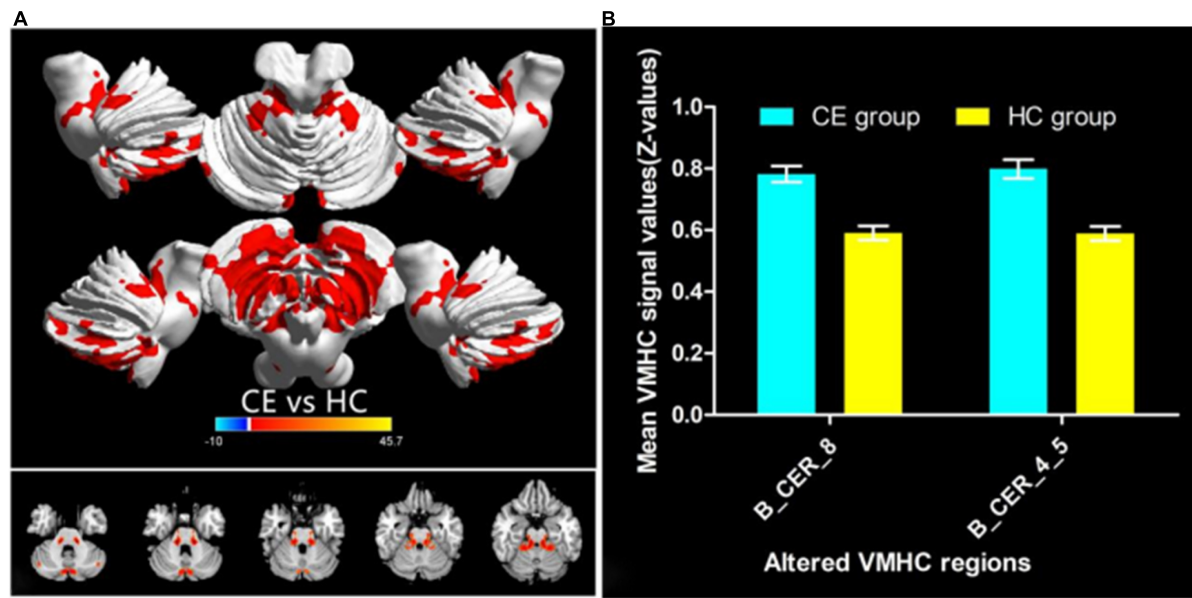


**FIGURE 1 |** One-sample *t*-test results of VMHC maps within comitant exotropia (CE) group **(A)** and HC group **(B)**. Abbreviations: CE, comitant exotropia; HC, health control; and VMHC, voxel-mirrored homotopic connectivity.

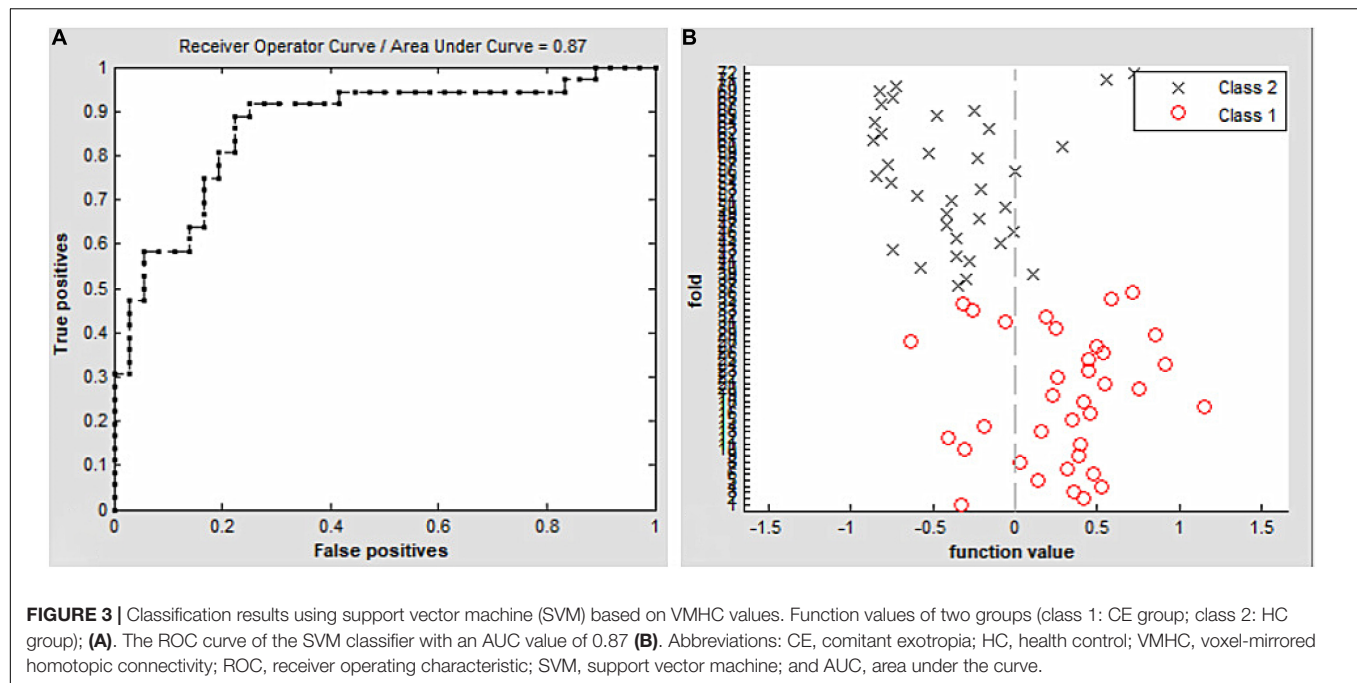
**TABLE 2 |** Different voxel-mirrored homotopic connectivity (VMHC) values between two groups.

Condition	Brain regions	BA	Peak <i>T</i> -scores	MNI coordinates ( <i>x, y, z</i> )	Cluster size (voxels)
CE>HC	Bilateral cerebellum_8	–	4.8927	±6 –63 –51	697
CE>HC	Bilateral cerebellum_4_5	–	4.8512	±12 –33 –30	154

*Note: Different VMHC values between two groups (voxel-level  $P < 0.01$ , GRF correction, cluster-level  $P < 0.05$ ). Abbreviations: CE, comitant exotropia; HC, health control; MNI, Montreal Neurological Institute; and VMHC, voxel-mirrored homotopic connectivity.*



**FIGURE 2 |** Significant VMHC differences in the CE and HC group **(A)**; the mean of altered VMHC values between patients with CE and HCs **(B)**. Abbreviations: CE, comitant exotropia; HC, health control; VMHC, voxel-mirrored homotopic connectivity; and CER, cerebellum.



important role in visually guided eye movements and visual motion perception. Moreover, the cerebellum is responsible for encoding eye movements (Lixenberg et al., 2020). Thus, the vermal cortex to visual motion perception is non-motor and involves cerebellar influence on cortical information processing. Previous neuroimaging studies have shown that strabismus is accompanied by cerebellar dysfunction. Zhu et al. (2018) demonstrated a significant reduction in functional connectivity between the left Brodmann area (BA17) and the left lingual gyrus/posterior cerebellar lobe in patients with CE. Ouyang et al. (2017) found that the left posterior cerebellar gray matter volume (GMV) was decreased in patients with CE. Higher VMHC reflects the increased functional connectivity in both hemispheres indicating the hyperconnectivity of bilateral brain areas. Besides, the higher VMHC value in the cerebellar might reflect the high functional connectivity within the cerebellar network. Consistent with these findings, we found a significant increase in cerebellar VMHC values in patients with CE, which suggests that oculomotor and visual perception dysfunction are present in patients with CE.

Our study showed that using VMHC maps, the SVM method could distinguish patients with CE from HCs with an accuracy of 81.94% and an AUC of 0.87. The SVM method has been widely used in machine learning studies of MRI imaging. To our knowledge, no study has evaluated the combined effect of VMHC and SVM techniques on CE classification. In our study, we investigated whether VMHC maps could be used as a classification feature to distinguish these groups, based on a machine learning approach that used an SVM classifier. We found that good machine classification accuracy could be achieved using VMHC maps. Thus, our results suggest that VMHC maps may be suitable for distinguishing patients with CE from HCs.

However, some limitations should be acknowledged. First, our sample size was small. Second, the clinical course of CE varies among patients; this may have affected the accuracy of our results. Third, the VMHC maps were based on BOLD signals, which may be affected by physiological noise. Finally, we applied the SVM method to assess the sensitivity of the classification; this method might have been affected by the sample size.

## CONCLUSION

Our findings indicate that cerebellar homotopic connectivity is increased in patients with CE, thereby providing insight into the neural mechanism that underlies oculomotor and visual perception dysfunction in patients with CE. Furthermore, VMHC maps may be suitable for distinguishing patients with CE from HCs.

## DATA AVAILABILITY STATEMENT

The original contributions presented in the study are included in the article/supplementary material, further inquiries can be directed to the corresponding authors.

## ETHICS STATEMENT

The studies involving human participants were reviewed and approved by The First Affiliated Hospital of Zhengzhou University, Jiangxi Provincial People's Hospital. The patients/participants provided their written informed consent to participate in this study.



## AUTHOR CONTRIBUTIONS

FC, ZH, and HL contributed to data collection, statistical analyses, and writing the manuscript. FZ and CL designed the

protocol and contributed to the MRI analysis. FC and QL designed the study, oversaw all clinical aspects of study conduct, and manuscript preparation. All authors contributed to the article and approved the submitted version.

## REFERENCES

- Butt, O. H., Benson, N. C., Datta, R., and Aguirre, G. K. (2015). Hierarchical and homotopic correlations of spontaneous neural activity within the visual cortex of the sighted and blind. *Front. Hum. Neurosci.* 9:25. doi: 10.3389/fnhum.2015.00025
- Chen, J., Jin, H., Zhong, Y. L., and Huang, X. (2021a). Abnormal low-frequency oscillations reflect abnormal eye movement and stereovision in patients with Comitant Exotropia. *Front. Hum. Neurosci.* 15:754234. doi: 10.3389/fnhum.2021.754234
- Chen, J., Sun, D., Shi, Y., Jin, W., Wang, Y., Xi, Q., et al. (2021b). Altered static and dynamic voxel-mirrored homotopic connectivity in subacute stroke patients: a resting-state fMRI study. *Brain Imaging Behav.* 15, 389–400. doi: 10.1007/s11682-020-00266-x
- Dougherty, R. F., Ben-Shachar, M., Bammer, R., Brewer, A. A., and Wandell, B. A. (2005). Functional organization of human occipital-callosal fiber tracts. *Proc. Natl. Acad. Sci. U.S.A.* 102, 7350–7355. doi: 10.1073/pnas.0500003102
- Gao, Y., Wang, X., Xiong, Z., Ren, H., Liu, R., Wei, Y., et al. (2021). Abnormal fractional amplitude of low-frequency fluctuation as a potential imaging biomarker for first-episode major depressive disorder: a resting-state fMRI study and support vector machine analysis. *Front. Neurol.* 12:751400. doi: 10.3389/fneur.2021.751400
- Govindan, M., Mohney, B. G., Diehl, N. N., and Burke, J. P. (2005). Incidence and types of childhood exotropia: a population-based study. *Ophthalmology* 112, 104–108. doi: 10.1016/j.ophtha.2004.07.033
- Gui, S. G., Chen, R. B., Zhong, Y. L., and Huang, X. (2021). Machine learning analysis reveals abnormal static and dynamic low-frequency oscillations indicative of long-term menstrual pain in primary dysmenorrhea patients. *J. Pain Res.* 14, 3377–3386. doi: 10.2147/JPR.S332224
- Huang, X., Zhou, S., Su, T., Ye, L., Zhu, P. W., Shi, W. Q., et al. (2018). Resting cerebral blood flow alterations specific to the comitant exophoria patients revealed by arterial spin labeling perfusion magnetic resonance imaging. *Microvasc. Res.* 120, 67–73. doi: 10.1016/j.mvr.2018.06.007
- Jin, H., Chen, R. B., Zhong, Y. L., Lai, P. H., and Huang, X. (2022). Effect of impaired stereoscopic vision on large-scale resting-state functional network connectivity in comitant exotropia patients. *Front. Neurosci.* 16:833937. doi: 10.3389/fnins.2022.833937
- Lee, Y. H., Repka, M. X., Borlik, M. F., Velez, F. G., Perez, C., Yu, F., et al. (2022). Association of strabismus with mood disorders, schizophrenia, and anxiety disorders among children. *JAMA Ophthalmol.* 140, 373–381. doi: 10.1001/jamaophthalmol.2022.0137
- Lin, S., Congdon, N., Yam, J. C., Huang, Y., Qiu, K., Ma, D., et al. (2014). Alcohol use and positive screening results for depression and anxiety are highly prevalent among Chinese children with strabismus. *Am. J. Ophthalmol.* 157, 894–900.e1. doi: 10.1016/j.ajo.2014.01.012
- Lixenberg, A., Yarkoni, M., Botschko, Y., and Joshua, M. (2020). Encoding of eye movements explains reward-related activity in cerebellar simple spikes. *J. Neurophysiol.* 123, 786–799. doi: 10.1152/jn.00363.2019
- Ouyang, J., Yang, L., Huang, X., Zhong, Y. L., Hu, P. H., Zhang, Y., et al. (2017). The atrophy of white and gray matter volume in patients with comitant strabismus: Evidence from a voxel-based morphometry study. *Mol. Med. Rep.* 16, 3276–3282. doi: 10.3892/mmr.2017.7006
- Schrouff, J., Rosa, M. J., Rondina, J. M., Marquand, A. F., Chu, C., Ashburner, J., et al. (2013). PRoNTo: pattern recognition for neuroimaging toolbox. *Neuroinformatics* 11, 319–337. doi: 10.1007/s12021-013-9178-1
- Smith, E. L. III, Hung, L. F., Arumugam, B., Wensveen, J. M., Chino, Y. M., and Harwerth, R. S. (2017). Observations on the relationship between anisometropia, amblyopia and strabismus. *Vision Res.* 134, 26–42. doi: 10.1016/j.visres.2017.03.004
- Taira, Y., Matsuo, T., Yamane, T., Hasebe, S., and Ohtsuki, H. (2003). Clinical features of comitant strabismus related to family history of strabismus or abnormalities in pregnancy and delivery. *Jpn. J. Ophthalmol.* 47, 208–213. doi: 10.1016/s0021-5155(02)00685-8
- Tan, G., Dan, Z. R., Zhang, Y., Huang, X., Zhong, Y. L., Ye, L. H., et al. (2018). Altered brain network centrality in patients with adult comitant exotropia strabismus: a resting-state fMRI study. *J. Int. Med. Res.* 46, 392–402. doi: 10.1177/0300060517715340
- Thier, P., and Markanday, A. (2019). Role of the vermal cerebellum in visually guided eye movements and visual motion perception. *Annu. Rev. Vis. Sci.* 5, 247–268. doi: 10.1146/annurev-vision-091718-015000
- Tong, Y., Huang, X., Qi, C. X., and Shen, Y. (2021). Altered functional connectivity of the primary visual cortex in patients with iridocyclitis and assessment of its predictive value using machine learning. *Front. Immunol.* 12:660554. doi: 10.3389/fimmu.2021.660554
- Wu, L., Wang, C., Liu, J., Guo, J., Wei, Y., Wang, K., et al. (2021). Voxel-mirrored homotopic connectivity associated with change of cognitive function in chronic pontine stroke. *Front. Aging Neurosci.* 13:621767. doi: 10.3389/fnagi.2021.621767
- Yan, C. G., Wang, X. D., Zuo, X. N., and Zang, Y. F. (2016). DPABI: data processing & Analysis for (Resting-State) Brain Imaging. *Neuroinformatics* 14, 339–351.
- Yan, X., Lin, X., Wang, Q., Zhang, Y., Chen, Y., Song, S., et al. (2010). Dorsal visual pathway changes in patients with comitant exotropia. *PLoS One* 5:e10931. doi: 10.1371/journal.pone.0010931
- Yang, H., Wang, C., Ji, G., Feng, Z., Duan, J., Chen, F., et al. (2019). Aberrant interhemispheric functional connectivity in first-episode, drug-naïve major depressive disorder. *Brain Imaging Behav.* 13, 1302–1310. doi: 10.1007/s11682-018-9917-x
- Zhang, X. J., Lau, Y. H., Wang, Y. M., Kam, K. W., Ip, P., Yip, W. W., et al. (2021). Prevalence of strabismus and its risk factors among school aged children: The Hong Kong Children Eye Study. *Sci. Rep.* 11:13820. doi: 10.1038/s41598-021-93131-w
- Zhu, P. W., Huang, X., Ye, L., Jiang, N., Zhong, Y. L., Yuan, Q., et al. (2018). Altered intrinsic functional connectivity of the primary visual cortex in youth patients with comitant exotropia: a resting state fMRI study. *Int. J. Ophthalmol.* 11, 668–673. doi: 10.18240/ijo.2018.04.22
- Zuo, X. N., Kelly, C., and Di Martino, A. (2010). Growing together and growing apart: regional and sex differences in the lifespan developmental trajectories of functional homotopy. *J. Neurosci.* 30, 15034–15043. doi: 10.1523/JNEUROSCI.2612-10.2010

**Conflict of Interest:** The authors declare that the research was conducted in the absence of any commercial or financial relationships that could be construed as a potential conflict of interest.

**Publisher's Note:** All claims expressed in this article are solely those of the authors and do not necessarily represent those of their affiliated organizations, or those of the publisher, the editors and the reviewers. Any product that may be evaluated in this article, or claim that may be made by its manufacturer, is not guaranteed or endorsed by the publisher.

Copyright © 2022 Chen, Hu, Liu, Zhen, Liu and Li. This is an open-access article distributed under the terms of the Creative Commons Attribution License (CC BY). The use, distribution or reproduction in other forums is permitted, provided the original author(s) and the copyright owner(s) are credited and that the original publication in this journal is cited, in accordance with accepted academic practice. No use, distribution or reproduction is permitted which does not comply with these terms.



# Abnormal Functional Connectivity Between Cerebral Hemispheres in Patients With High Myopia: A Resting FMRI Study Based on Voxel-Mirrored Homotopic Connectivity

Yi Cheng<sup>†</sup>, Xiao-Lin Chen<sup>†</sup>, Ling Shi, Si-Yu Li, Hui Huang, Pei-Pei Zhong and Xiao-Rong Wu\*

Department of Ophthalmology, The First Affiliated Hospital of Nanchang University, Nanchang, China

## OPEN ACCESS

### Edited by:

Xin Huang,  
Jiangxi Provincial People's  
Hospital, China

### Reviewed by:

Yu Lin Zhong,  
Jiangxi Provincial People's  
Hospital, China  
Chen-Xing Qi,  
Renmin Hospital of Wuhan  
University, China

### \*Correspondence:

Xiao-Rong Wu  
wxr98021@126.com

<sup>†</sup>These authors have contributed  
equally to this work and share first  
authorship

### Specialty section:

This article was submitted to  
Brain Imaging and Stimulation,  
a section of the journal  
Frontiers in Human Neuroscience

Received: 01 April 2022

Accepted: 19 April 2022

Published: 23 June 2022

### Citation:

Cheng Y, Chen X-L, Shi L, Li S-Y,  
Huang H, Zhong P-P and Wu X-R  
(2022) Abnormal Functional  
Connectivity Between Cerebral  
Hemispheres in Patients With High  
Myopia: A Resting FMRI Study Based  
on Voxel-Mirrored Homotopic  
Connectivity.  
*Front. Hum. Neurosci.* 16:910846.  
doi: 10.3389/fnhum.2022.910846

**Purpose:** To study the changes in functional connections between the left and right hemispheres of patients with high myopia (HM) and healthy controls (HCs) by resting functional magnetic resonance imaging (fMRI) based on voxel-mirrored homotopic connectivity (VMHC). To study the changes in resting-state functional connectivity (rsFC) between the left and right hemispheres of patients with HM and healthy controls (HCS) at rest by using resting functional magnetic resonance imaging (fMRI) based on voxel-mirror homotopy connectivity (VMHC).

**Patients and Methods:** A total of 89 patients with HM (41 men and 48 women) and 59 HCs (24 men and 35 women) were collected and matched according to gender, age, and education level. The VMHC method was used to evaluate the changes in rsFC between cerebral hemispheres, and a correlation analysis was carried out to understand the differences in brain functional activities between the patients with HM and the HCs.

**Results:** Compared with the HCs, the VMHC values of the putamen and fusiform in the HM group were significantly lower (voxel-level  $p < 0.01$ , Gaussian random field correction cluster level  $p < 0.05$ ).

**Conclusion:** This study preliminarily confirmed the destruction of interhemispheric functional connection in some brain regions of the patients with HM and provided effective information for clarifying the neural mechanism of patients with HM.

**Keywords:** high myopia, voxel-mirrored homotopic connectivity, functional magnetic resonance imaging, putamen, fusiform gyrus

## INTRODUCTION

High myopia (HM) is a worldwide health problem that has attracted widespread attention. It seriously affects the quality of life of patients. The rate of incidence is increasing year by year. It affects about 2.9% of the global population (Holden et al., 2015). HM refers to myopia with diopter  $> -6D$ , mostly axial myopia, which is characterized by pathological and degenerative changes in the retina, choroid, and sclera, resulting in visual impairment. Therefore, the harm is great (Hsu et al., 2014). Eyeground structures such as the retina and optic nerve are closely related to the

brain, especially visual-related areas (Wang et al., 2020). One study has shown that the retinal nerve fiber layer of patients with HM becomes thinner and that the optic papilla is deformed (Qu et al., 2018). Zhai et al. (2016) found that the visual function of patients with HM was abnormal, the functional connection of the posterior cingulate cortex/precuneus decreased, and the function of other brain regions changed. Therefore, they believed that abnormal visual experiences would lead to abnormal brain structure and function. In addition, a correlation analysis based on functional connectivity density (FCD) mapping and seeding showed that HM can lead to changes in brain morphology and functional connectivity density (Li et al., 2012; Zhai et al., 2016). Consequently, HM may lead to changes in brain functional activities.

In order to evaluate the changes in brain activity, functional magnetic resonance imaging (fMRI) is increasingly conducted in studies on HM. MRI has the characteristics of multi-sequence, multi parameters, no ionizing radiation, routine imaging, and functional imaging. It can find changes in brain activity and function in patients with HM, and it has a great application value. A recent study used functional magnetic resonance imaging to evaluate the activity of occipital visual cortex in patients with lens induced high myopia (IHM) under different visual stimulation. The results showed that the activity of visual cortex in patients with IHM was significantly lower than that in the normal group (Mirzajani et al., 2017). Patients with HM have certain changes in visual pathway area and limbic system structure (Huang et al., 2018). Homotopic functional connectivity is the connection between mirror regions of the cerebral hemisphere, and it is also one of the most remarkable features of the internal functional structure of the brain (Salvador et al., 2005; Stark et al., 2008). It may reflect that inter-hemispheric communication plays a very important role in integrating brain function based on coherent cognition and behavior. At the same time, it has significant spatial variability related to function and is disturbed by a variety of pathological conditions (Mancuso et al., 2019). Previous studies related to MRI have found that HM affects brain neural activity and functional connection, but the specific mechanism has not been fully clarified.

Voxel-mirrored homotopic connectivity (VMHC) is a method proposed by Stark DE (Stark et al., 2008) to explore the differences in functional connections between voxels in bilateral hemispheric symmetrical systems and evaluate their coordination. It is a functional magnetic resonance imaging technology used to explore brain tissue patterns based on resting functional connections. This method needs to conduct anatomical structure correction to make the bilateral cerebral hemispheres basically symmetrical and calculate the time-series correlation between each voxel and its contralateral hemisphere allele. The lower the VMHC value, the worse the coordination of allelic voxel functional activities between the bilateral cerebral hemispheres. On the contrary, the higher VMHC value, the coordination will be better. Different MRI analysis methods have different emphases in expressing the functional changes of brain regions. VMHC not only directly compares functional connections between cerebral hemispheres in the resting state but also accurately and effectively evaluates changes in functional

connections between cerebral hemispheres related to patients' behavior and cognition. It has certain efficiency, stability, and safety in studies on brain information integration. In recent years, more and more studies have focused on VMHC and found that it is related to a variety of diseases and functional states, and has a good correlation. Kelly et al. found that there is an association between long-term exposure to cocaine and large-scale brain circuit interruption supporting cognitive control through the VMHC method (Kelly et al., 2011). Luo et al. (2018) found that the VMHC value was lower in some brain regions of multi-domain amnesic mild cognitive impairment patients and showed more severe interhemispheric communication defects than that of single-domain amnesic mild cognitive impairment patients. In addition, there were VMHC abnormalities in multiple brain regions of patients with type 2 diabetes, indicating that the functional coordination between the same brain regions was generally impaired (Zhang Y. et al., 2021). In conclusion, rs-fMRI analysis based on VMHC can provide additional information beyond the classical FC index for understanding the neural mechanism of executive function changes between cerebral hemispheres, and VMHC is a reliable neural index for brain function reorganization. Through previous studies, it has also been found that VMHC has been used for the analysis of a variety of eye diseases, such as primary open-angle glaucoma (Liu et al., 2008), monocular blindness (Shao et al., 2018), and strabismus amblyopia (Zhang S. et al., 2021). We speculate that patients with HM, which affects brain visual imaging, may have abnormal brain functional activities. Therefore, this study discusses changes in cerebral hemisphere functional connection in patients with HM by VMHC analysis, to provide a new idea for the neural mechanism of HM.

## MATERIALS AND METHODS

### Participants

Participants were selected from the hospital during the period from September 2018 to September 2020. The cohort included 89 patients with HM and 59 HCs without ametropia. The inclusion criteria for patients with myopia were as follows: (1) aged 18–60 years, (2) meeting the diagnostic criteria of high myopia, (3) right-hand dominance, and (4) no other ophthalmic diseases. The exclusion criteria were: (1) other ophthalmic diseases, (2) unilateral myopia, (3) abnormal brain structure such as tumor or subdural hematoma, (4) mental diseases and unable to cooperate, and (5) complications of HM including HM optic neuropathy and HM macular degeneration. The age, sex, hand advantage, and education level of the HCs were matched with those of the HM group and met the following criteria: (1) no ametropia and other ophthalmic diseases, (2) no mental diseases, and (3) normal routine brain magnetic resonance imaging. All the subjects underwent MRI scanning, and those with incomplete MRI data or excessive head movements were excluded. The study was approved by the medical ethics committee of the First Affiliated Hospital of Nanchang University, and all the participants were informed and agreed.

## MRI Acquisition

All MRI data were collected with a Siemens Trio 3.0T scanner by implementing an 8-channel head coil. MRI scanning was performed on each subject. Whole-brain T1-weighted images were obtained with magnetization-prepared gradient echo image (MPRAGE) with these parameters: repetition time = 1,900 ms, echo time (TE) = 2.26 ms, thickness = 1, no intersection gap, acquisition matrix =  $256 \times 256$ , field of view (FOV) =  $240 \times 240$  mm<sup>2</sup>, and flip angle = 12°. Functional images were obtained using a gradient-echo-planar imaging sequence.

## Data Preprocessing in Functional Magnetic Resonance Imaging

The preprocessing reason brain imaging data processing and analysis toolbox (DPABI, <http://rfmri.org/dpabi>) are completed based on statistical parameter mapping (SPM12), which runs on MATLAB 8.4.0 (MathWorks, Natick, MA, United States). The main preprocessing steps were: discard the first 10 volumes, slice timing, spatial rearrangement, head motion correction, individual registration between high-resolution T1 and EPI images, spatial normalization, and spatial smoothing that can reduce the registration error and increase the normality of statistical data. The RS fMRI data set is registered in the space of Montreal Neurological Institute (MNI) and resampled to a  $3 \times 3 \times 3$  mm<sup>3</sup> cube voxel; head movement data with a maximum translation of more than 2 mm or a maximum rotation of 2° were excluded from the final analysis. The preprocessed data are divided into typical frequency bands (0.01–0.1 Hz). Linear regression is performed on covariates such as head movement, whole-brain parenchyma, and cerebrospinal fluid signals to reduce the impact (including white matter, cerebrospinal fluid, and head movement parameters based on Friston 24 parameter model) (Friston et al., 1996).

## Statistical Analysis of VMHC

The value of VMHC is calculated as the Pearson correlation coefficient between the voxel time series between each pair of mirror hemispheres (Zuo et al., 2010). The REST software was used to calculate the Pearson's correlation between each group of symmetrical alleles in both cerebral hemispheres one by one, and then the fisher-z transform was performed on these correlation values. The results of correlation values formed the VMHC diagram and were used for subsequent group-level analysis. To reduce the difference between different subjects, it is also necessary to standardize the mean of the whole brain VMHC map.

## Statistical Analysis

This study was tested with the SPSS software (version 13.0; SPSS Inc., Chicago, IL, United States). The changes in VMHC z-diagram between the healthy control group and the HM group were evaluated by two-sample *t*-tests. All important clusters were reported on MNI coordinates, and the *T* value of peak voxels was determined (voxel-level  $P < 0.01$ , Gaussian random field [GRF] correction, cluster-level  $P < 0.05$ ).

**TABLE 1 |** General characteristics of the patients.

	Age(years)	Female/Male	ALM(OD)	ALM(OS)
HM	26.235 ± 0.462	48/41	26.670 ± 0.874	26.580 ± 0.985
HCS	25.783 ± 0.102	35/24	23.900 ± 0.971	23.740 ± 0.693

ALM, axial length; HM, high myopia; HCS, healthy controls; OD, oculus dexter; OS, oculus sinister.

## RESULTS

### Basic Information

The basic information of patients with HM and the healthy control group is shown in Table 1.

### VMHC Group Differences

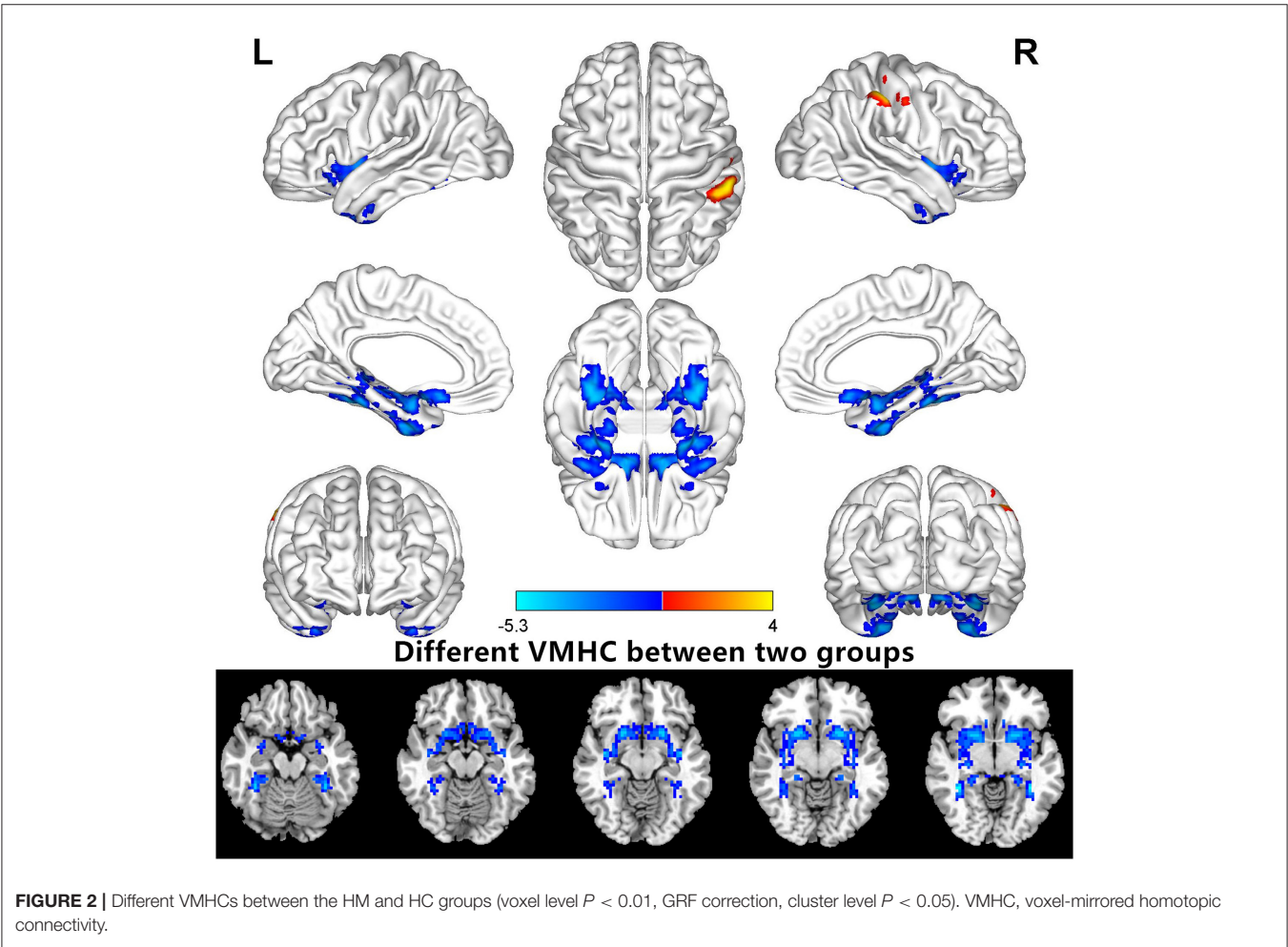
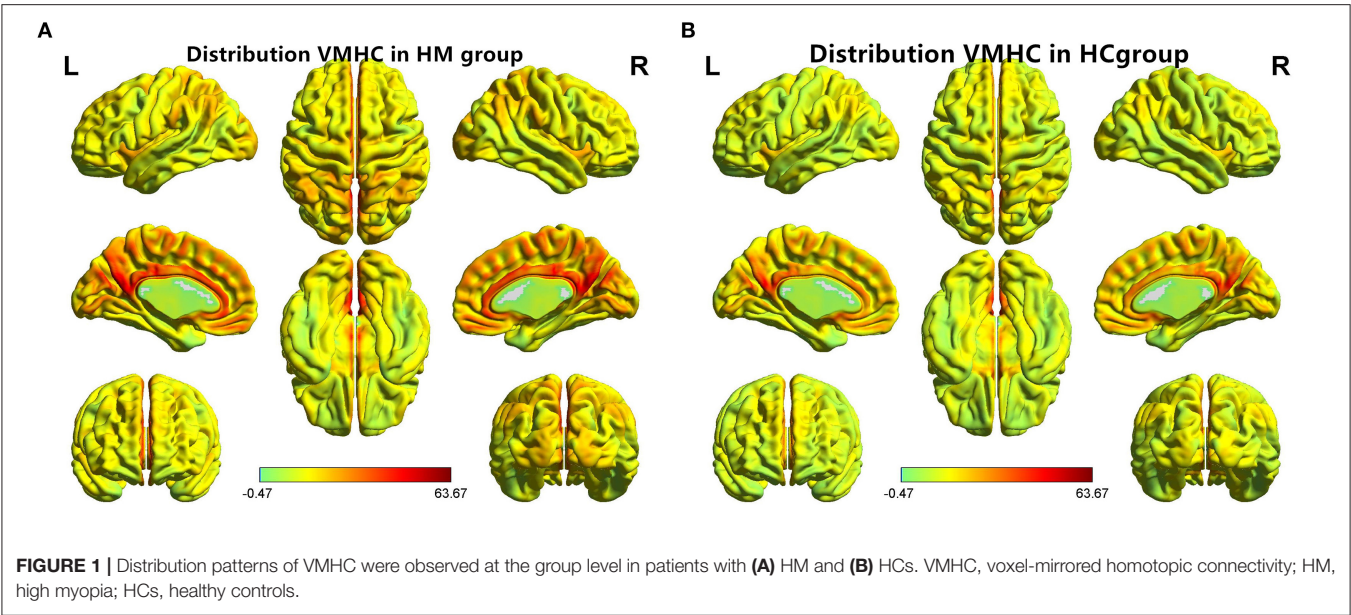
VMHC values changed between the HM group and the HC group (Figure 1); Compared with HCS, the VMHC in the lenticular nucleus and fusiform gyrus decreased in patients with HM (Figure 2, Table 2).

## DISCUSSION

In this study, we evaluated the VMHC difference between the HM group and the HC group. The study found that compared with the HCs, the VMHC values of the putamen and fusiform gyrus of the patients with HM were decreased.

The putamen is a structure located under the cortex and a part of the dorsal striatum of the basal ganglia. It is considered to be related to reinforcement learning, motor control, and language function (Vinas-Guasch and Wu, 2017). Recently, it has been found that the putamen is closely related to processes that visually guided and internally guided force control in humans. A study on changes in visual movement and functional activities in brain regions found that 91% of caudate cells and 65% of putamen cells changed when monkeys performed visual tasks. Therefore, the activity of neurons in the caudate and putamen during a visuomotor task will be activated whether there is motor behavior or not (Romero et al., 2008). Li et al. found that the regional homology (ReHo) of bilateral putamen in patients with idiopathic rapid eye movement sleep behavior disorder (iRBD) was significantly reduced, the tracer uptake of bilateral putamen and left caudate nucleus was also significantly reduced, and abnormal spontaneous brain activity of bilateral putamen in patients with iRBD was detected when studying the correlation between iRBD and the putamen (Li et al., 2019). It can be seen from the above that the change in the putamen is related to the abnormal state of the body. When studying changes in brain structure between patients with HM and HCs, Huang et al. (2018) found that the global gray matter volume (GMV) of the bilateral putamen in patients with HM was increased. The authors speculated that HM may lead to structural changes in the bilateral putamen, to compensate for the motor function of HM. In our study, we found that compared with the HC group, the VMHC value of the putamen in patients with HM was decreased, which may be related to abnormal changes in this area due to the abnormal visual experience and behavior of HM. It is





**TABLE 2 |** Different voxel-mirrored homotopic connectivity (VMHC) values of brain areas between the HM and HC groups (voxel level  $P < 0.01$ , Gaussian random field, GRF, correction).

Conditions	L/R	Brain regions	MIN coordinates			Cluster size	T-value
			X	Y	Z		
HM<HC							
1		Putamen	21	12	±9	664	−4.8082
2		Fusiform	±36	−39	−21	210	−5.2993

*T*: there were significant differences in the statistical values of peak voxels between the two groups. *X*, *Y*, and *Z* are the coordinates of the main peak position in the Montreal Neurological Institute (MNI) space (voxel level  $P < 0.01$ , GRF correction). HM, high myopia; HCs, healthy controls.

consistent with the above research results. Hence, we speculate that HM will lead to disorder in the putamen connection and affect visual function.

The fusiform gyrus is located in the middle and bottom of the visual joint cortex. It is the largest macro-anatomical structure in the advanced visual cortex and has a wide range of functions; however, it is highly controversial (Cohen et al., 2000; Huth et al., 2012; Cukur et al., 2013). At first, it was well-known for its facial-recognition function, but with the deepening of research, it was found that it was more involved in processing high-order visual information, especially related to face, body, and stimuli characterized by high spatial frequency, and was responsible for the recognition of secondary classification of objects (Weiner and Zilles, 2016; Rokem et al., 2017). Moreover, the fusiform gyrus has a special visual processing mechanism for text and objects (Chen et al., 2019). Tanja Kassuba et al. found that the lateral occipital cortex (LO), fusiform gyrus, and intraparietal sulcus (IPS) play an important role in the integration of visual-tactile objects (Kassuba et al., 2014). In addition, a study on the frequency-dependent spontaneous neural activity of primary angle-closure glaucoma found that the ALFF values of multiple brain regions were changed. The ALFF values in the bilateral frontal lobe, right fusiform gyrus, and right posterior cerebellar lobe were higher in slow band 5 than in slow band 4. It was considered that the abnormal spontaneous neural activity of patients with PACG indicates that the cognitive, visual, and emotional functions of these patients are impaired (Jiang et al., 2019). In our study, we found that the VMHC value of the fusiform gyrus in the patients with HM was decreased. We speculated that abnormal visual experience may lead to structural changes in the fusiform gyrus and even affect its functions, such as visual and recognition functions.

However, there are some limitations to this experiment. For example, the sample size is not large enough, and the head movement and cerebrospinal fluid movement effects of the patients during examination have a certain impact on the experiment. However, to minimize such effects, we have strictly selected qualified examination results and eliminated the effects of movement on the brain through statistical methods. In

addition, the results of this study were obtained in the resting state of participants. In future studies, we will also combine the resting-state and task-state fMRI to research the changes of abnormal brain regions in different states. At the same time, we will expand the sample size and improve the applicability and accuracy of the results.

## CONCLUSION

In conclusion, compared with the HCs, VMHC values in different brain regions of the patients with HM have different changes, suggesting that HM may cause changes in functional connections between cerebral hemispheres in some regions, resulting in functional damage, which may become a breakthrough in studying the divine mechanism of changes in visual and motor functions in HM.

## DATA AVAILABILITY STATEMENT

The raw data supporting the conclusions of this article will be made available by the authors, without undue reservation.

## ETHICS STATEMENT

The studies involving human participants were reviewed and approved by The First Affiliated Hospital of Nanchang University. The patients/participants provided their written informed consent to participate in this study.

## AUTHOR CONTRIBUTIONS

X-RW: guidance on the content of this article. X-LC: charts and diagrams graphic typesetting. S-YL, LS, HH, and P-PZ: clinical data collection. All authors contributed to the article and approved the submitted version.

## FUNDING

This work was supported by Key research plan of Jiangxi Provincial Department of Science and Technology (No. 20192BBG70042), Jiangxi Province Education Department Key Foundation (No. GJJ160033), Health Development Planning Commission Science Foundation of Jiangxi Province (No. 20185118), Technology and Science Foundation of Jiangxi Province (No. 20141BBG70027), Jiangxi Province Education Department Scientific Research Foundation (No. GJJ13147), Health and Family Planning Commission Traditional Chinese Medicine Foundation of Jiangxi Province (No. 2017A001), and Basic Health Appropriate Technology Spark Promotion Program of Jiangxi Province (No. 20188007).

## ACKNOWLEDGMENTS

We would like to thank for the support of NSFC, etc.

## REFERENCES

- Chen, Y., Xiang, C., Liu, W., Zhu, P., Ye, L., Li, B., et al. (2019). Application of amplitude of low-frequency fluctuation to altered spontaneous neuronal activity in classical trigeminal neuralgia patients: A resting-state functional MRI study. *Mol. Med. Rep.* 20, 1707–1715. doi: 10.3892/mmr.2019.10404
- Cohen, L., Dehaene, S., Naccache, L., Lehericy, S., Dehaene-Lambertz, G., Henaff, M., et al. (2000). The visual word form area: spatial and temporal characterization of an initial stage of reading in normal subjects and posterior split-brain patients. *Brain*. 123, 291–307. doi: 10.1093/brain/123.2.291
- Cukur, T., Huth, A., Nishimoto, S., and Gallant, J. (2013). Functional subdomains within human FFA. *J. Neurosci.* 33, 16748–16766. doi: 10.1523/JNEUROSCI.1259-13.2013
- Friston, K. J., Williams, S., Howard, R., Frackowiak, R., and Turner, R. (1996). Movement-related effects in fMRI time-series. *Magn. Reson. Med.* 35, 346–355. doi: 10.1002/mrm.1910350312
- Holden, B., Wilson, D., Jong, M., Sankaridurg, P., Fricke, T., Smith, E. L. I., et al. (2015). Myopia: a growing global problem with sight-threatening complications. *Commun. Eye Health*. 28, 35. Available online at: <https://pubmed.ncbi.nlm.nih.gov/26692649/>
- Hsu, C., Chen, S., Li, A., and Lee, F. (2014). Systolic blood pressure, choroidal thickness, and axial length in patients with myopic maculopathy. *J. Chin. Med. Assoc.* 77, 487–491. doi: 10.1016/j.jcma.2014.06.009
- Huang X., Hu, Y., Zhou, F., Wu, Y., Xu, X., Wu, Y., et al. (2018). Altered whole-brain gray matter volume in high myopia patients: a voxel-based morphometry study. *Neuroreport*. 29, 760–767. doi: 10.1097/WNR.0000000000001028
- Huth, A., Nishimoto, S., Vu, A., and Gallant, J. (2012). A continuous semantic space describes the representation of thousands of object and action categories across the human brain. *Neuron*. 76, 1210–1224. doi: 10.1016/j.neuron.2012.10.014
- Jiang, F., Yu, C., Zuo, M., Zhang, C., Wang, Y., Zhou, F., et al. (2019). Frequency-dependent neural activity in primary angle-closure glaucoma. *Neuropsychiatr. Dis. Treat.* 15, 271–282. doi: 10.2147/NDT.S187367
- Kassuba, T., Klinge, C., Holig, C., Roder, B., and Siebner, H. (2014). Short-term plasticity of visuo-haptic object recognition. *Front. Psychol.* 5, 274. doi: 10.3389/fpsyg.2014.00274
- Kelly, C., Zuo, X., Gotimer, K., Cox, C., Lynch, L., Brock, D., et al. (2011). Reduced interhemispheric resting state functional connectivity in cocaine addiction. *Biol. Psychiatry*. 69, 684–692. doi: 10.1016/j.biopsych.2010.11.022
- Li, G., Chen, Z., Zhou, L., Yao, M., Luo, N., Kang, W., et al. (2019). Abnormal intrinsic brain activity of the putamen is correlated with dopamine deficiency in idiopathic rapid eye movement sleep behavior disorder. *Sleep Med.* 75, 73–80. doi: 10.1016/j.sleep.2019.09.015
- Li, Q., Guo, M., Dong, H., Zhang, Y., and Fu, Y., Yin, X. (2012). Voxel-based analysis of regional gray and white matter concentration in high myopia. *Vision. Res.* 58, 45–50. doi: 10.1016/j.visres.2012.02.005
- Liu, T., Zeng, D., Zeng, C., and He, X. (2008). Association between MYOC.mt1 promoter polymorphism and risk of primary open-angle glaucoma: a systematic review and meta-analysis. *Med. Sci. Monit.* 14, A87–A93. Available online at: <https://pubmed.ncbi.nlm.nih.gov/18591929/>
- Luo, X., Li, K., Zeng, Q., Huang, P., Jiaerken, Y., Qiu, T., et al. (2018). Decreased bilateral FDG-PET uptake and inter-hemispheric connectivity in multi-domain amnesic mild cognitive impairment patients: a preliminary study. *Front. Aging. Neurosci.* 10, 161. doi: 10.3389/fnagi.2018.00161
- Mancuso, L., Costa, T., Nani, A., Manuella, J., Liloia, D., Gelmini, G., et al. (2019). The homotopic connectivity of the functional brain: a meta-analytic approach. *Sci. Rep.* 9, 3346. doi: 10.1038/s41598-019-40188-3
- Mirzajani, A., Ghorbani, M., and Rasuli, B., Mahmoud-Pashazadeh, A. (2017). Effect of induced high myopia on functional MRI signal changes. *Phys. Med.* 37, 32–36. doi: 10.1016/j.ejomp.2017.04.004
- Qu, D., Lin, Y., Jiang, H., Shao, Y., Shi, Y., Airen, S., et al. (2018). Retinal nerve fiber layer (RNFL) integrity and its relations to retinal microvasculature and microcirculation in myopic eyes. *Eye Vis.* 5, 25. doi: 10.1186/s40662-018-0120-3
- Rokem, A., Takemura, H., Bock, A., Scherf, K., Behrmann, M., Wandell, B., et al. (2017). The visual white matter: The application of diffusion MRI and fiber tractography to vision science. *J. Vis.* 17, 4. doi: 10.1167/17.2.4
- Romero, M., Bermudez, M., Vicente, A., Perez, R., and Gonzalez, F. (2008). Activity of neurons in the caudate and putamen during a visuomotor task. *Neuroreport*. 19, 1141–1145. doi: 10.1097/WNR.0b013e328307c3fc
- Salvador, R., Suckling, J., Schwarzbauer, C., and Bullmore, E. (2005). Undirected graphs of frequency-dependent functional connectivity in whole brain networks. *Philos. Trans. R. Soc. Lond B Biol. Sci.* 360, 937–946. doi: 10.1098/rstb.2005.1645
- Shao, Y., Bao, J., Huang, X., Zhou, F., Ye, L., Min, Y., et al. (2018). Comparative study of interhemispheric functional connectivity in left eye monocular blindness versus right eye monocular blindness: a resting-state functional MRI study. *Oncotarget*. 9, 14285–14295. doi: 10.18632/oncotarget.24487
- Stark, D., Margulies, D., Shehzad, Z., Reiss, P., Kelly, A., Uddin, L., et al. (2008). Regional variation in interhemispheric coordination of intrinsic hemodynamic fluctuations. *J. Neurosci.* 28, 13754–13764. doi: 10.1523/JNEUROSCI.4544-08.2008
- Vinas-Guasch, N., and Wu, Y. (2017). The role of the putamen in language: a meta-analytic connectivity modeling study. *Brain Struct. Funct.* 222, 3991–4004. doi: 10.1007/s00429-017-1450-y
- Wang, H., Li, S., Chen, X., Wang, Y., Li, J., and Wang, Z. (2020). Cerebral blood flow alterations in high myopia: an arterial spin labeling study. *Neural. Plast.* 2020, 6090262. doi: 10.1155/2020/6090262
- Weiner, K., and Zilles, K. (2016). The anatomical and functional specialization of the fusiform gyrus. *Neuropsychologia*. 83, 48–62. doi: 10.1016/j.neuropsychologia.2015.06.033
- Zhai, L., Li, Q., Wang, T., Dong, H., Peng, Y., Guo, M., et al. (2016). Altered functional connectivity density in high myopia. *Behav. Brain Res.* 303, 85–92. doi: 10.1016/j.bbr.2016.01.046
- Zhang, S., Gao, G., Shi, W., Li, B., Lin, Q., Shu, H., et al. (2021). Abnormal interhemispheric functional connectivity in patients with strabismic amblyopia: a resting-state fMRI study using voxel-mirrored homotopic connectivity. *BMC Ophthalmol.* 21, 255. doi: 10.1186/s12886-021-02015-0
- Zhang, Y., Wang, J., Wei, P., Zhang, J., Zhang, G., Pan, C., et al. (2021). Interhemispheric resting-state functional connectivity abnormalities in type 2 diabetes patients. *Ann. Palliat. Med.* 10, 8123–8133. doi: 10.21037/apm-21-1655
- Zuo, X., Kelly, C., Di Martino, A., Mennes, M., Margulies, D., Bangaru, S., et al. (2010). Growing together and growing apart: regional and sex differences in the lifespan developmental trajectories of functional homotopy. *J. Neurosci.* 30, 15034–15043. doi: 10.1523/JNEUROSCI.2612-10.2010

**Conflict of Interest:** The authors declare that the research was conducted in the absence of any commercial or financial relationships that could be construed as a potential conflict of interest.

**Publisher's Note:** All claims expressed in this article are solely those of the authors and do not necessarily represent those of their affiliated organizations, or those of the publisher, the editors and the reviewers. Any product that may be evaluated in this article, or claim that may be made by its manufacturer, is not guaranteed or endorsed by the publisher.

Copyright © 2022 Cheng, Chen, Shi, Li, Huang, Zhong and Wu. This is an open-access article distributed under the terms of the Creative Commons Attribution License (CC BY). The use, distribution or reproduction in other forums is permitted, provided the original author(s) and the copyright owner(s) are credited and that the original publication in this journal is cited, in accordance with accepted academic practice. No use, distribution or reproduction is permitted which does not comply with these terms.



# Alteration of Degree Centrality in Adolescents With Early Blindness

Zhi Wen<sup>1</sup>, Yan Kang<sup>2,3</sup>, Yu Zhang<sup>1</sup>, Huaguang Yang<sup>1</sup> and Baojun Xie<sup>1\*</sup>

<sup>1</sup> Department of Radiology, Renmin Hospital of Wuhan University, Wuhan, China, <sup>2</sup> State Key Laboratory of Magnetic Resonance and Atomic and Molecular Physics, National Center for Magnetic Resonance in Wuhan, Wuhan Institute of Physics and Mathematics, Innovation Academy for Precision Measurement Science and Technology, Chinese Academy of Sciences, Wuhan, China, <sup>3</sup> University of Chinese Academy of Sciences, Beijing, China

## OPEN ACCESS

### Edited by:

Mingzhou Ding,  
University of Florida, United States

### Reviewed by:

Yu Lin Zhong,  
Jiangxi Provincial People's Hospital,  
China  
Tianming Huo,  
Wuhan University, China

### \*Correspondence:

Baojun Xie  
xiebj@126.com

### Specialty section:

This article was submitted to  
Brain Imaging and Stimulation,  
a section of the journal  
Frontiers in Human Neuroscience

**Received:** 04 May 2022

**Accepted:** 06 June 2022

**Published:** 27 June 2022

### Citation:

Wen Z, Kang Y, Zhang Y, Yang H  
and Xie B (2022) Alteration of Degree  
Centrality in Adolescents With Early  
Blindness.  
*Front. Hum. Neurosci.* 16:935642.  
doi: 10.3389/fnhum.2022.935642

Congenital nystagmus in infants and young children can lead to early blindness (EB). Previous neuroimaging studies have demonstrated that EB is accompanied by alterations in brain structure and function. However, the effects of visual impairment and critical developmental periods on brain functional connectivity at rest have been unclear. Here, we used the voxel-wise degree centrality (DC) method to explore the underlying functional network brain activity in adolescents with EB. Twenty-one patients with EBs and 21 sighted controls (SCs) underwent magnetic resonance imaging. Differences between the two groups were assessed using the DC method. Moreover, the support vector machine (SVM) method was used to differentiate patients with EB patients from the SCs according to DC values. Compared with the SCs, the patients with EB had increased DC values in the bilateral cerebellum\_6, cerebellum vermis\_4\_5, bilateral supplementary motor areas (SMA), and left fusiform gyrus; the patients with EB had decreased DC values in the bilateral rectal gyrus and left medial orbital frontal gyrus. The SVM classification of the DC values achieved an overall accuracy of 70.45% and an area under the curve of 0.86 in distinguishing between the patients with EB and the SCs. Our study may reveal the neuromechanism of neuroplasticity in EB; the findings provide an imaging basis for future development of restorative visual therapies and sensory substitution devices, and future assessments of visual rehabilitation efficacy.

**Keywords:** early blindness, congenital nystagmus (CN), resting-state functional magnetic resonance imaging, degree centrality, neural plasticity

## INTRODUCTION

Blindness affects approximately 500 million people worldwide (WHO, 2017). The total number of registered blind people in China is increasing; it has reached 5.5 million. Although 80% of blindness cases involve individuals aged > 50 years, children and young adults who are blind have fewer educational and employment opportunities, lower earning potential, and worse quality of life than individuals who are not blind.

The overall critical period for vision development is from 0 to 3 years of age; the maturation period is from 6 to 8 years of age (Lewis and Maurer, 2009). Specific aspects of vision have different critical periods of development. For example, visual perception of object shape, which is primarily mediated by the ventral visual flow, develops later than visual perception of motion, which is mediated by the dorsal visual flow. Thus, the overall critical period for vision impairment extends until approximately 10 years of age (Bourne and Rosa, 2006).

Early blindness (EB) is defined as visual deprivation before the age of 12, when most children have not completed the critical period for vision development. Visual deprivation can result in



reorganization of brain function and structure (Reislev et al., 2016). Compared with the control group, the EB group exhibited significantly less gray matter volume in the visual cortex (Pan et al., 2007), although it exhibited increased cortical thickness in the medial visual cortex (Bridge et al., 2009). Voxel-based morphometry (VBM) and diffusion tensor imaging (DTI) studies revealed that visual tracts and radiations were significantly atrophied in patients with EB (Shimony et al., 2006); longer blindness was associated with more extensive impacts on visual radiations (Ptito et al., 2008). In addition to visual pathway damage, functional changes occur in brain regions secondary to EB. A PET study showed that cerebral blood flow to the cerebellum was significantly increased in patients with EB (Uhl et al., 1993). Functional connectivity among the visual cortex, cerebellum, supplementary motor area (SMA), motor cortex, and temporal cortex was weaker in patients with EB than in controls (Yu et al., 2008; Heine et al., 2015). During auditory processing, the functional connectivity between visual and auditory cortices decreases in patients with EB, while the connectivity between occipital and temporal cortices increases (Pelland et al., 2017). Overall, vision-related brain regions in patients with EB undergo extensive neuroplasticity to adapt to the disease environment.

Resting-state functional magnetic resonance imaging (MRI) (rs-fMRI) can detect blood oxygen level-dependent changes at rest; the results reflect brain function under physiological and pathological conditions *in vivo*. In the resting state, brain neurons demonstrate a spontaneous activity, which is transmitted to other neurons; the brain thus forms a complex functional network. Degree centrality (DC), which evaluates voxel centrality by assessing the number of connections between that voxel and other voxels at the whole-brain level, can avoid the influence of subjective seed-site selection (Zuo et al., 2012). To some extent, increase or decrease in DC can explain the coordinating and antagonistic effects of brain networks under disease conditions. The DC method has been widely used to analyze ophthalmic diseases such as glaucoma (Cai et al., 2015) and strabismus (Tan et al., 2018). Here, we hypothesized that patients with EB experience visual deprivation-induced reorganization of the brain; the critical developmental period is important for this process. Congenital nystagmus (CN) occurs in infants and young children with no obvious abnormalities in the eyes or the brain. Its main clinical manifestations are involuntary, rhythmic, and reciprocating eye movements and abnormal visual function; it leads to EB. However, the etiology and pathogenesis of CN are unknown. In this study, we performed rs-fMRI to explore the pattern of DC changes in CN. Additionally, we used the support vector machine (SVM) method to investigate the predictive value of DC for clinical diagnosis.

## MATERIALS AND METHODS

### Participants

This study was approved by the Ethics Committee of Renmin Hospital of Wuhan University. Before undergoing MRI, all the participants or their parents provided written informed consent to participate. Twenty-one patients with EB (10 female patients) and 21 sighted controls (SCs) (11 female patients) aged

15–20 years were enrolled in this study. All the patients with EB were from the School for Blind Children in Wuhan (China); the cause of blindness in all the patients was CN. EB was defined as loss of vision at  $\leq 12$  years of age. The diagnosis of blindness was made by two experienced ophthalmologists who tested each eye separately and measured visual acuity, visual field, and peripheral vision. Loss of vision was characterized as the inability to see light in either eye.

The inclusion criteria for SCs were as follows: right-handedness, age  $< 19$  years, and binocular vision of  $\geq 5$ . The exclusion criteria for patients with EB and SCs were as follows: lesions visible on MRI (e.g., brain tumors and vascular malformations), history of ocular trauma and/or traumatic brain injury, history of neurological diseases and/or mental illness, and/or contraindications for MRI (e.g., claustrophobia or pacemaker implant).

### Magnetic Resonance Imaging Data Acquisition

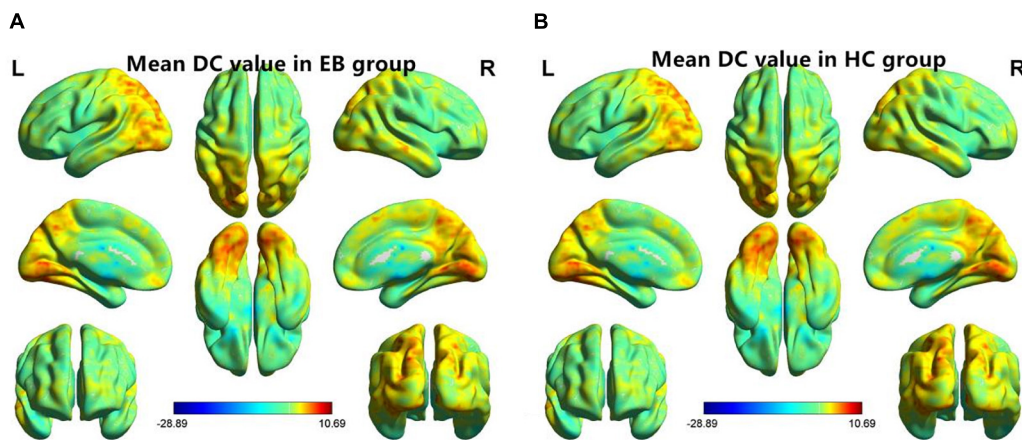
MRI scans were performed using a 3.0T MRI scanner (Discovery 750w; GE Healthcare, Milwaukee, WI, United States) with an 8-channel head coil. Foam pads were placed on both sides of the jaw to limit head movements; earplugs were used to reduce exposure to scanning noise. During data acquisition, all the participants were asked to close their eyes, remain awake, and not think about anything specific. rs-fMRI was performed using a gradient-echo planar imaging sequence, and with the following parameters: TR/TE = 2,000/30 ms, flip angle =  $90^\circ$ , FOV =  $240 \times 240$  mm<sup>2</sup>, data matrix size =  $64 \times 64$ , slice thickness = 4 mm, interleaved axial slices = 40, and volumes = 210. T1-weighted high-resolution magnetization-prepared rapid gradient-echo structural images were also acquired for alignment and tissue segmentation using the following parameters: TR/TE = 8.5/3.2 ms, flip angle =  $9^\circ$ , matrix size =  $256 \times 256$ , voxel size =  $1 \times 1 \times 1$  mm<sup>3</sup>, and sagittal slices = 176. T2WI and T2-FLAIR images were collected to exclude participants with brain lesions.

### Magnetic Resonance Imaging Preprocessing

The rs-fMRI data were preprocessed using the Data Processing & Analysis of Brain Imaging (DPABI) toolbox in the MATLAB software (version 2014a). Preprocessing was performed in the following order: (1) data format conversion, (2) removal of the first 10 volumes for each participant, (3) slice timing; (4) head motion correction and acquisition of head motion parameters for each participant, where participants with head movement  $> 2$  mm or rotation  $> 2^\circ$  were removed, (5) segmentation, (6) removal of linear drift, (7) filtering, and (8) spatial standardization to Montreal Neurological Institute space with a voxel size of  $3 \text{ mm} \times 3 \text{ mm} \times 3 \text{ mm}$ .

### Degree Centrality Processing

Using an individual voxel function network, DC was calculated by counting the number of significant suprathreshold correlations (i.e., the degree of binarized adjacency matrix) among the participants. In this study, DC values with a



**FIGURE 1 |** One-sample *t*-test results of maps in the (A) EB group and the (B) SC group. DC, degree centrality; EB, early blindness; SCs, sighted controls; L, left; and R, right.

correlation number  $r \geq 0.25$  were calculated using the DPABI software. The following equation was used to convert the voxel-wise DC map of each participant to a z-score map:  $Z_i = \frac{DC_i - \text{meanall}}{\text{stdall}}$ , where  $Z_i$  is the z-score of a voxel,  $DC_i$  is the DC value of a voxel, meanall is the average DC value of all voxels in the brain mask, and stdall is the standard deviation of DC values of all voxels in the brain mask.

## Support Vector Machine Analysis

To determine whether changes in DC values could be used as a diagnostic indicator for EB, we performed an ML analysis with the SVM algorithm using the Pattern Recognition for Neuroimaging Toolbox (PRoNTo) software (Schrouff et al., 2013). First, the mean DC values of brain regions that differed between the groups were used as classification features. Then, the leave-one-out cross-validation technique was used to validate the SVM classifier. Accuracy, sensitivity, and specificity were used to quantify the performance of the classification method; receiver operating characteristic curve and corresponding area under the curve values were calculated to assess classification efficacy.

## Statistical Analysis

Two-sample *t*-tests and chi-squared test were performed using the SPSS software (version 22.0) to compare clinical variables between the EB and SC groups. *P*-values  $< 0.05$  were considered statistically significant. Age, sex, and total intracranial volume were used as covariates in a two-sample *t*-test with REST V1.8 (Song et al., 2011) to evaluate differences in voxel-level DC between the groups. The Gaussian random field (GRF) method was used to correct for multiple comparisons (two-tailed, voxel-level  $P < 0.01$ ; GRF correction, cluster-level  $P < 0.05$ ).

## RESULTS

### Demographics and Visual Measurements

There were no significant differences between the EB and SC groups in terms of age ( $P = 0.37$ ), sex ( $P = 0.76$ ), education

level ( $P = 0.28$ ), or handedness ( $P = 0.28$ ). The demographic information of the two groups is shown in Table 1.

### Degree Centrality Differences Between Groups

One-sample *t*-test was performed to extract the DC values across the subjects within each group ( $P < 0.05$ ; Figure 1). Compared with the SCs, the patients with EB had increased DC values in the bilateral cerebellum\_6, cerebellum vermis\_4\_5, bilateral SMAs, and left fusiform gyrus; they had decreased DC values in the bilateral rectal gyri and left medial orbital frontal gyrus (mOFG) (Table 2 and Figures 2, 3).

### Support Vector Machine Classification

The SVM classification of DC values achieved an overall accuracy of 70.45% and an area under the curve of 0.86 in distinguishing between the patients with EB and the SCs (Figure 4).

## DISCUSSION

In this study, we found that early visual deprivation could cause functional reorganization in several brain regions. Compared with the SC group, the patients with EB had increased DC values

**TABLE 1 |** Demographic information of participants in each group and between-group comparisons.

	EB ( $n = 21$ )	SC ( $n = 21$ )	<i>P</i>
Age (years)	$17.95 \pm 1.40$	$17.76 \pm 1.45$	0.37
Sex (female/male)	11/10	10/11	0.76
Education level (years)	$10.33 \pm 1.11$	$10.76 \pm 1.45$	0.28
Handedness	21R	21R	1
Duration of blindness (years)	$10.14 \pm 1.46$	—	—
Nystagmus type	18 Vertical/3 horizontal	—	—

EB, early blindness; SC, sighted controls. Values are expressed as means  $\pm$  standard deviations or frequencies.

**TABLE 2** | Brain regions with significant differences in DC values between the EB and SC groups (Gaussian random field-corrected cluster-level  $P < 0.05$ ).

Specific effects	Identified brain regions	BA	Peak coordinates (MNI)			Side	Peak T	Cluster size (voxels)
			X	Y	Z			
EB > SC	Supplementary motor area	6	0	24	57	B	4.84	59
	Fusiform gyrus	37	−45	−54	−3	L	3.97	83
	Vermis_4_5	—	0	−63	−6	—	3.56	12
	Cerebellum_6	—	−3	−60	−24	B	4.82	1,099
EB < SC	Medial orbital frontal gyrus	10	−3	54	−3	L	−3.76	18
	Rectal gyrus	11	−12	42	−21	L	−3.98	20
		11	0	54	−21	B	−3.56	21

BA, Brodmann area; MNI, Montreal Neurological Institute; EB, early blindness; SCs, sighted controls; L, left; B, bilateral.

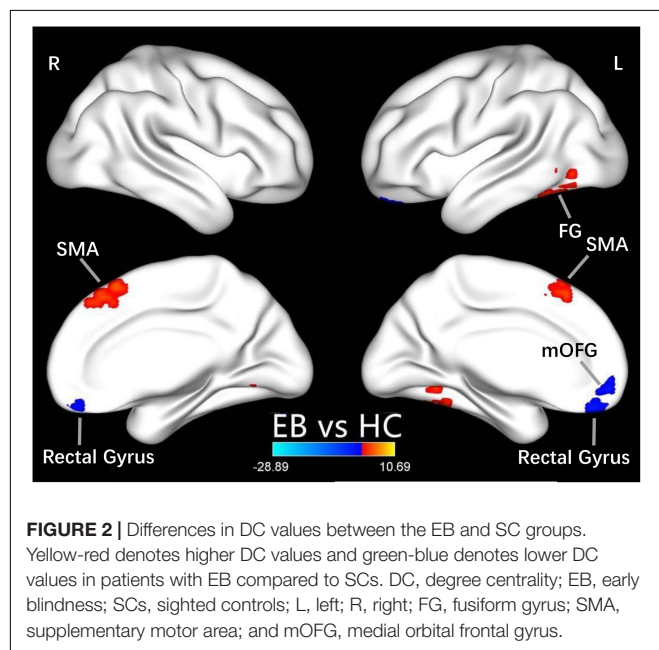
in the bilateral cerebellum\_6, vermis\_4\_5, left fusiform gyrus, and bilateral SMAs, while they had decreased DC values in the bilateral rectus gyri and left mOFG. Additionally, using DC as an indicator, the SVM method could distinguish the patients with EB from the SCs with an accuracy rate of 70.45% and an area under the curve of 0.86.

CN first affects patients during childhood. Abnormalities in eye movements and visual perception lead to further compensation by the brain during the development of visual information processing, which leads to increased activation in some brain areas. The cerebellum is responsible for coding and perceiving eye movements (Thier and Markanday, 2019; Lixenberg et al., 2020). Both saccades and smooth tracking are closely associated with the cerebellum (Buttner and Kremmyda, 2007; Quinet et al., 2020). fMRI studies have shown that in patients with CN, activation of the cerebellar vermis

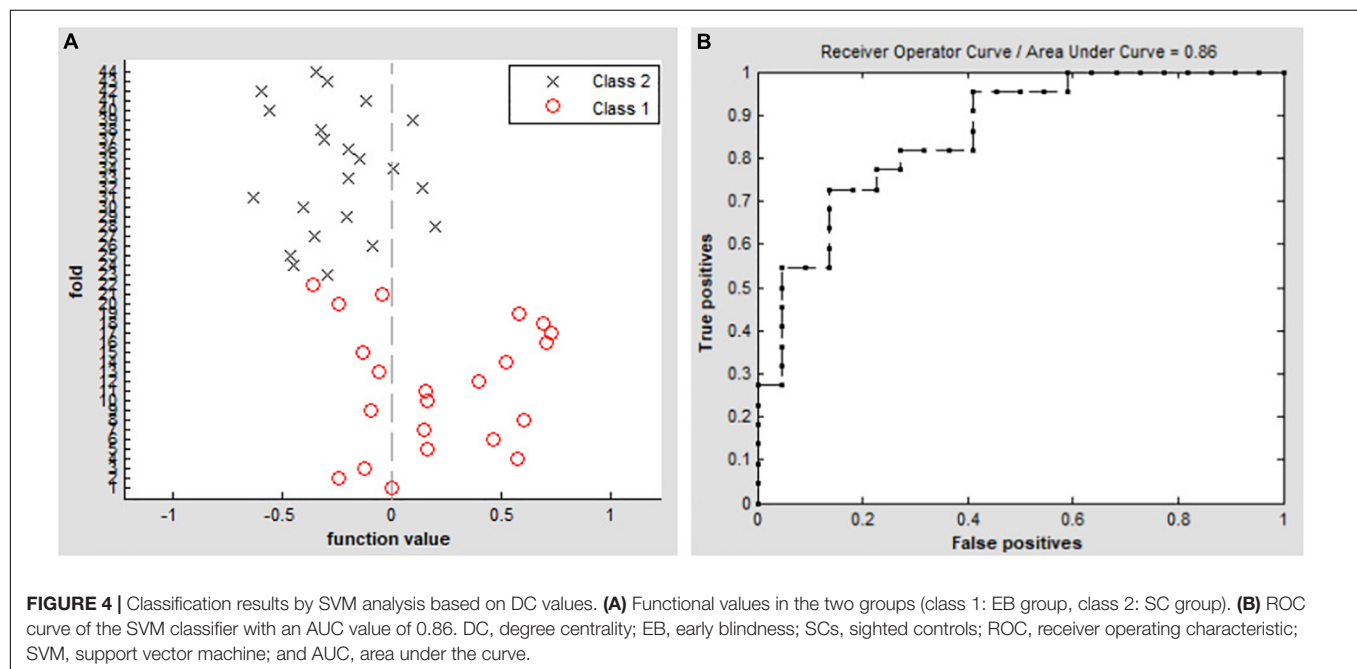
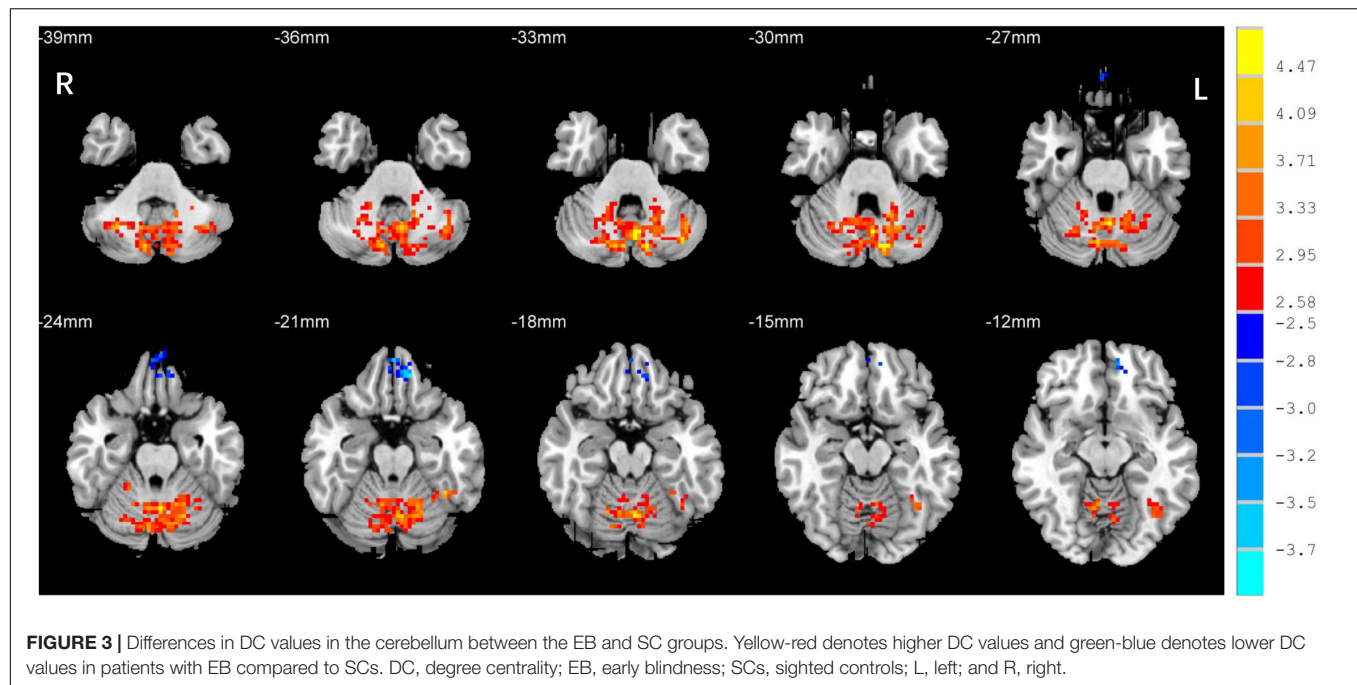
increases during horizontal and vertical visual stimulations; thus, the cerebellar vermis inhibits excessive eye movements (Dieterich et al., 2000). A VBM study showed that hypertrophy of the cerebellar vermis occurs in patients with CN because of repeated attempts to inhibit excessive oscillation (Hufner et al., 2011). In contrast, activation of the cerebellar lobe may be primarily associated with changes in attention that maintain eye movement and gaze (Dieterich et al., 2000). In this study, we found increased DC values in the bilateral cerebellum\_6 and the cerebellar vermis\_4\_5 among the  $P$  patients with EB (Table 2 and Figure 3), which is consistent with the results of previous studies. We presume that the increased DC values in the cerebellum indicate visual and attentional compensations associated with nystagmus.

In our study, compared with the SCs, the patients with EB had increased DC values in bilateral SMAs and decreased DC values in the left mOFG and bilateral rectal gyri (Table 2 and Figure 2). The main cognitive visual pathways include the dorsal and ventral streams (Dutton and Jacobson, 2001). The dorsal stream is responsible for processing the entire input visual scene; this stream includes the occipital, posterior parietal, and frontal cortices. The frontal cortex (including frontal visual areas) produces rapid and accurate eye movements to select targets (Schall, 2004); it is activated at the beginning of eye movements (i.e., voluntary saccades) (Murthy et al., 2007) and pursuit movements (Ono and Mustari, 2009). Motion-related areas receive visual information and generate accurate motion through the visual space. Thus, the frontal eye field, SMA, and medial parietal lobe cooperate during saccade tasks; the frontal eye field, SMA, lateral parietal lobe, and superior/middle temporal gyrus cooperate during pursuit tasks. Our finding that patients with CN had reduced DC values in the left mOFG and bilateral rectal gyri, along with increased DC values in the bilateral SMAs, implies damage to saccadic and pursuit eye movements.

Importantly, we found that DC values in the left fusiform gyrus were higher in patients with EB than in the SCs (Table 2 and Figure 2). The fusiform gyrus is known as the temporo-occipital gyrus; it is involved in object processing in the visual, auditory, tactile modalities, and matching of object-related information across the three sensory modalities







(Kassuba et al., 2011). A recent ALE meta-analysis (Zhang et al., 2019) showed that, compared with SCs, persistent activation of the fusiform gyrus in patients with EB was associated with altered object motor function. Therefore, altered DC values in the left fusiform gyrus are associated with object recognition deficits.

There were several limitations in this study. First, the number of patients included was small. However, Friston (2012) suggested that a sample size of > 16 participants per group is acceptable in rs-fMRI studies, consistent with the requirements for a one-sample *t*-test. Our sample sizes were 21 patients with EB and

21 SCs, which exceeded the threshold of > 16 participants per group. Furthermore, we conducted Gaussian random field correction to properly control for false positives; we confirmed the presence of a statistical DC difference between the EB and SC groups. Second, although the ReHo and ALFF methods are reportedly more stable than DC, these methods do not carry any advantage or disadvantage in terms of solving clinical problems. Our study focused on changes in brain network nodes caused by CN; therefore, the DC method was appropriate. Future large-scale studies and research should be conducted from multiple perspectives.



In summary, we found that resting-state DC values were altered among the patients with CN, in association with deficits in saccadic and pursuit eye movements. Our results provide an imaging basis for future development of restorative visual therapies and sensory substitution devices, and future assessments of visual rehabilitation efficacy.

## DATA AVAILABILITY STATEMENT

The original contributions presented in this study are included in the article/supplementary material, further inquiries can be directed to the corresponding author/s.

## ETHICS STATEMENT

The studies involving human participants were reviewed and approved by the Ethics Committee of Renmin Hospital of

Wuhan University. Written informed consent to participate in this study was provided by the participants' legal guardian/next of kin.

## AUTHOR CONTRIBUTIONS

BX designed the study. ZW, YZ, and HY collected the clinical and MRI data. ZW and YK analyzed the MRI data and drafted the manuscript. YK wrote the protocol. HY contributed to the design of the study. All authors contributed to the article and approved the submitted version.

## FUNDING

This study was supported by the Fundamental Research Funds for the Central Universities (grant no. 2042018kf0178).

## REFERENCES

- Bourne, J. A., and Rosa, M. G. (2006). Hierarchical development of the primate visual cortex, as revealed by neurofilament immunoreactivity: early maturation of the middle temporal area (MT). *Cereb. Cortex* 16, 405–414. doi: 10.1093/cercor/bhi119
- Bridge, H., Cowey, A., Ragge, N., and Watkins, K. (2009). Imaging studies in congenital anophthalmia reveal preservation of brain architecture in 'visual' cortex. *Brain* 132, 3467–3480. doi: 10.1093/brain/awp279
- Buttner, U., and Kremmyda, O. (2007). Smooth pursuit eye movements and optokinetic nystagmus. *Dev. Ophthalmol.* 40, 76–89. doi: 10.1159/000100350
- Cai, F., Gao, L., Gong, H., Jiang, F., Pei, C., Zhang, X., et al. (2015). Network Centrality of Resting-State fMRI in Primary Angle-Closure Glaucoma Before and After Surgery. *PLoS One* 10:e0141389. doi: 10.1371/journal.pone.0141389
- Dieterich, M., Bucher, S. F., Seelos, K. C., and Brandt, T. (2000). Cerebellar activation during optokinetic stimulation and saccades. *Neurology* 54, 148–155. doi: 10.1212/wnl.54.1.148
- Dutton, G. N., and Jacobson, L. K. (2001). Cerebral visual impairment in children. *Semin. Neonatol.* 6, 477–485. doi: 10.1053/siny.2001.0078
- Friston, K. (2012). Ten ironic rules for non-statistical reviewers. *Neuroimage* 61, 1300–1310. doi: 10.1016/j.neuroimage.2012.04.018
- Heine, L., Bahri, M. A., Cavaliere, C., Soddu, A., Laureys, S., Ptito, M., et al. (2015). Prevalence of increases in functional connectivity in visual, somatosensory and language areas in congenital blindness. *Front. Neuroanat.* 9:86. doi: 10.3389/fnana.2015.00086
- Hufner, K., Stephan, T., Flanagan, V. L., Deutschlander, A., Dera, T., Karch, C., et al. (2011). Cerebellar and visual gray matter brain volume increases in congenital nystagmus. *Front. Neurol.* 2:60. doi: 10.3389/fneur.2011.00060
- Kassuba, T., Klinge, C., Holig, C., Menz, M. M., Ptito, M., Roder, B., et al. (2011). The left fusiform gyrus hosts trisensory representations of manipulable objects. *Neuroimage* 56, 1566–1577. doi: 10.1016/j.neuroimage.2011.02.032
- Lewis, T. L., and Maurer, D. (2009). Effects of early pattern deprivation on visual development. *Optom. Vis. Sci.* 86, 640–646. doi: 10.1097/OPX.0b013e3181a7296b
- Lixenberg, A., Yarkoni, M., Botschko, Y., and Joshua, M. (2020). Encoding of eye movements explains reward-related activity in cerebellar simple spikes. *J. Neurophysiol.* 123, 786–799. doi: 10.1152/jn.00363.2019
- Murthy, A., Ray, S., Shorter, S. M., Priddy, E. G., Schall, J. D., and Thompson, K. G. (2007). Frontal eye field contributions to rapid corrective saccades. *J. Neurophysiol.* 97, 1457–1469. doi: 10.1152/jn.00433.2006
- Ono, S., and Mustari, M. J. (2009). Smooth pursuit-related information processing in frontal eye field neurons that project to the NRTF. *Cereb. Cortex* 19, 1186–1197. doi: 10.1093/cercor/bhn166
- Pan, W. J., Wu, G., Li, C. X., Lin, F., Sun, J., and Lei, H. (2007). Progressive atrophy in the optic pathway and visual cortex of early blind Chinese adults: A voxel-based morphometry magnetic resonance imaging study. *Neuroimage* 37, 212–220. doi: 10.1016/j.neuroimage.2007.05.014
- Pelland, M., Orban, P., Dansereau, C., Lepore, F., Bellec, P., and Collignon, O. (2017). State-dependent modulation of functional connectivity in early blind individuals. *Neuroimage* 147, 532–541. doi: 10.1016/j.neuroimage.2016.12.053
- Ptito, M., Schneider, F. C., Paulson, O. B., and Kupers, R. (2008). Alterations of the visual pathways in congenital blindness. *Exp. Brain Res.* 187, 41–49. doi: 10.1007/s00221-008-1273-4
- Quinet, J., Schultz, K., May, P. J., and Gamlin, P. D. (2020). Neural control of rapid binocular eye movements: Saccade-vergence burst neurons. *Proc. Natl. Acad. Sci. U.S.A.* 117, 29123–29132. doi: 10.1073/pnas.2015318117
- Reislev, N. L., Dyrby, T. B., Siebner, H. R., Kupers, R., and Ptito, M. (2016). Simultaneous assessment of white matter changes in microstructure and connectedness in the blind brain. *Neural Plast.* 2016:6029241. doi: 10.1155/2016/6029241
- Schall, J. D. (2004). On the role of frontal eye field in guiding attention and saccades. *Vision Res.* 44, 1453–1467. doi: 10.1016/j.visres.2003.10.025
- Schrouff, J., Rosa, M. J., Rondina, J. M., Marquand, A. F., Chu, C., Ashburner, J., et al. (2013). PRoNTTo: pattern recognition for neuroimaging toolbox. *Neuroinformatics* 11, 319–337. doi: 10.1007/s12021-013-9178-1
- Shimony, J. S., Burton, H., Epstein, A. A., McLaren, D. G., Sun, S. W., and Snyder, A. Z. (2006). Diffusion tensor imaging reveals white matter reorganization in early blind humans. *Cereb. Cortex* 16, 1653–1661. doi: 10.1093/cercor/bhj102
- Song, X. W., Dong, Z. Y., Long, X. Y., Li, S. F., Zuo, X. N., Zhu, C. Z., et al. (2011). REST: a toolkit for resting-state functional magnetic resonance imaging data processing. *PLoS One* 6:e25031. doi: 10.1371/journal.pone.0025031
- Tan, G., Dan, Z. R., Zhang, Y., Huang, X., Zhong, Y. L., Ye, L. H., et al. (2018). Altered brain network centrality in patients with adult comitant exotropia strabismus: A resting-state fMRI study. *J. Int. Med. Res.* 46, 392–402. doi: 10.1177/0300060517715340
- Thier, P., and Markanday, A. (2019). Role of the Vermal Cerebellum in Visually Guided Eye Movements and Visual Motion Perception. *Annu. Rev. Vis. Sci.* 5, 247–268. doi: 10.1146/annurev-vision-091718-015000
- Uhl, F., Franzen, P., Podreka, I., Steiner, M., and Deecke, L. (1993). Increased regional cerebral blood flow in inferior occipital cortex and cerebellum of early blind humans. *Neurosci. Lett.* 150, 162–164.
- WHO (2017). *Visual Impairment and Blindness*. Available online at: <https://www.who.int/en/news-room/fact-sheets/detail/blindness-and-visual-impairment> (Accessed on Feb 05, 2022).
- Yu, C., Liu, Y., Li, J., Zhou, Y., Wang, K., Tian, L., et al. (2008). Altered functional connectivity of primary visual cortex in early blindness. *Hum. Brain Mapp.* 29, 533–543. doi: 10.1002/hbm.20420

- Zhang, C., Lee, T. M. C., Fu, Y., Ren, C., Chan, C. C. H., and Tao, Q. (2019). Properties of cross-modal occipital responses in early blindness: An ALE meta-analysis. *Neuroimage Clin.* 24:102041. doi: 10.1016/j.nicl.2019.102041
- Zuo, X. N., Ehmke, R., Mennes, M., Imperati, D., Castellanos, F. X., Sporns, O., et al. (2012). Network centrality in the human functional connectome. *Cereb. Cortex* 22, 1862–1875. doi: 10.1093/cercor/bhr269

**Conflict of Interest:** The authors declare that the research was conducted in the absence of any commercial or financial relationships that could be construed as a potential conflict of interest.

**Publisher's Note:** All claims expressed in this article are solely those of the authors and do not necessarily represent those of their affiliated organizations, or those of the publisher, the editors and the reviewers. Any product that may be evaluated in this article, or claim that may be made by its manufacturer, is not guaranteed or endorsed by the publisher.

Copyright © 2022 Wen, Kang, Zhang, Yang and Xie. This is an open-access article distributed under the terms of the Creative Commons Attribution License (CC BY). The use, distribution or reproduction in other forums is permitted, provided the original author(s) and the copyright owner(s) are credited and that the original publication in this journal is cited, in accordance with accepted academic practice. No use, distribution or reproduction is permitted which does not comply with these terms.



# Reduction of Interhemispheric Homotopic Connectivity in Cognitive and Visual Information Processing Pathways in Patients With Thyroid-Associated Ophthalmopathy

Chen-Xing Qi<sup>1†</sup>, Zhi Wen<sup>2†</sup> and Xin Huang<sup>3\*</sup>

<sup>1</sup> School of Optometry and Ophthalmology and Eye Hospital, Wenzhou Medical University, Wenzhou, China, <sup>2</sup> Department of Radiology, Renmin Hospital of Wuhan University, Wuhan, China, <sup>3</sup> Department of Ophthalmology, Jiangxi Provincial People's Hospital, The First Affiliated Hospital of Nanchang Medical College, Nanchang University, Nanchang, China

## OPEN ACCESS

### Edited by:

Chien-Han Lai,  
National Yang-Ming University, Taiwan

### Reviewed by:

Xiuxiu Qin,  
Southern Medical University, China  
Xize Jia,  
Hangzhou Normal University, China

### \*Correspondence:

Xin Huang  
334966891@qq.com

<sup>†</sup>These authors have contributed  
equally to this work

### Specialty section:

This article was submitted to  
Brain Imaging and Stimulation,  
a section of the journal  
Frontiers in Human Neuroscience

**Received:** 23 February 2022

**Accepted:** 10 June 2022

**Published:** 30 June 2022

### Citation:

Qi C-X, Wen Z and Huang X (2022)  
Reduction of Interhemispheric  
Homotopic Connectivity in Cognitive  
and Visual Information Processing  
Pathways in Patients With  
Thyroid-Associated Ophthalmopathy.  
Front. Hum. Neurosci. 16:882114.  
doi: 10.3389/fnhum.2022.882114

**Purpose:** Thyroid-associated ophthalmopathy (TAO) is a vision threatening autoimmune and inflammatory orbital disease, and has been reported to be associated with a wide range of structural and functional abnormalities of bilateral hemispheres. However, whether the interhemisphere functional connectivity (FC) of TAO patients is altered still remain unclear. A new technique called voxel-mirrored homotopic connectivity (VMHC) combined with support vector machine (SVM) method was used in the present study to explore interhemispheric homotopic functional connectivity alterations in patients with TAO.

**Methods:** A total of 21 TAO patients (14 males and 7 females) and 21 wellmatched healthy controls (HCs, 14 males and 7 females), respectively, underwent functional magnetic resonance imaging (fMRI) scanning in the resting state. We evaluated alterations in the resting state functional connectivity between hemispheres by applying VMHC method and then selected these abnormal brain regions as seed areas for subsequent study using FC method. Furthermore, the observed changes of regions in the VMHC analysis were chosen as classification features to differentiate patients with TAO from HCs through support vector machine (SVM) method.

**Results:** The results showed that compared with HCs, TAO patients showed significantly lower VMHC values in the bilateral postcentral gyrus, lingual gyrus, calcarine, middle temporal gyrus, middle occipital gyrus and angular. Moreover, significantly decreased FC values were found between the right postcentral gyrus/lingual gyrus/calcarine and left lingual gyrus/cuneus/superior occipital gyrus, left postcentral gyrus/lingual gyrus/calcarine and right lingual gyrus/ middle temporal gyrus, right middle temporal gyrus and left cerebellum-8/lingual gyrus/middle occipital gyrus/supplementary motor area, left middle temporal gyrus and right middle occipital gyrus, right middle occipital gyrus/angular and left middle temporal pole (voxel-level  $p < 0.01$ , Gaussian random field correction, cluster-level  $p < 0.05$ ). The SVM classification model achieved good performance in differentiating TAO patients from HCs (total accuracy: 73.81%; area under the curve: 0.79).

**Conclusion:** The present study revealed that the altered interhemisphere interaction and integration of information involved in cognitive and visual information processing pathways including the postcentral gyrus, cuneus, cerebellum, angular, widespread visual cortex and temporal cortex in patients with TAO relative to HC group. VMHC variability had potential value for accurately and specifically distinguishing patients with TAO from HCs. The new findings may provide novel insights into the neurological mechanisms underlying visual and cognitive disorders in patients with TAO.

**Keywords:** thyroid-associated ophthalmopathy, functional magnetic resonance imaging, voxel-mirrored homotopic connectivity, functional connectivity, support vector machine

## INTRODUCTION

Hyperthyroidism occurs mainly in adults between the ages of 20 and 40 years, with an incidence of ~2% (Reddy et al., 2017). In these patients, thyroid hormone levels inside and outside of the thyroid gland increase for various reasons. Thyroid hormone enters the blood circulation and has systemic effects on tissues and organs, resulting in broadly increased excitability and hypermetabolism (Tu et al., 2020). The most common extrathyroidal complication of hyperthyroidism is thyroid-associated ophthalmopathy (TAO). The clinical course of this disease is generally divided into acute inflammatory and chronic quiescent stages. The most common physical complaints in patients with TAO are exophthalmos, eyelid swelling, lid retraction and impaired visual function (Du et al., 2021). Lesions in the visual pathway are mainly caused by periorbital edema that compresses the optic nerve, retinal ganglion cell damage because of abnormal thyroid hormone levels, and high intraocular pressure (Zah-Bi et al., 2019). TAO is a multifactorial inflammatory and autoimmune orbital disease; thus, affected patients exhibit ocular symptoms, along with affective dysfunction and cognitive deficits (Coulter et al., 2007).

In recent years, the development of functional neuroimaging techniques has enabled the identification of visual and cognitive dysfunction in patients with TAO; these are associated with local structural and functional abnormalities in the corresponding brain regions. For example, a study using diffusion tensor imaging technique found that patients with TAO had significant microstructural changes in optic nerve (Liu et al., 2022). Investigations of neural metabolic activity in the brains of TAO patients showed abnormal metabolic activities in the prefrontal cortex, which were closely associated with poor performance on neuropsychological tests (Bhatara et al., 1998). Wu et al. (2020) reported that patients with TAO exhibited gray matter loss and lower fractional anisotropy in brain regions corresponding to visual and cognitive dysfunction. Graph theoretical analysis showed that structural brain connectome disruption was present in patients with TAO, in relation to psychiatric dysfunction (Wu et al., 2021). In addition to showing structural changes in the brain, patients with TAO have also been reported to have functional disturbances in brain regions. A regional homogeneity algorithm revealed that

hyperthyroidism patients with dysthyroid optic neuropathy had abnormal neural activity in the limbic system (Jiang et al., 2021). Using functional magnetic resonance imaging (fMRI) method, Chen et al. (2021b) found aberrant spontaneous brain activities in regions associated with cognitive and visual deficits in patients with TAO; these findings indicated that careful monitoring is needed for neuropsychological disturbances in such patients during diagnosis and treatment. Thus far, research has consistently shown that patients with TAO have structural and neural function alterations in vision-related and cognition-related brain regions. Nevertheless, it remains unclear whether an abnormal functional interaction exists between the two cerebral hemispheres in patients with TAO.

Research by Foubert et al. (2010) showed that synchronization between cerebral hemispheres is closely associated with the visual experiences. Interhemispheric homotopic connectivity has been proposed as a basic principle of functional architecture that integrates brain functions underlying coherent cognition, visual processing, and consciousness (Zuo et al., 2010). Resting-state fMRI constitutes a noninvasive and repeatable method to directly quantify interhemispheric functional connectivities (FCs). Originating from resting brain symmetrical voxels, voxel-mirrored homotopic connectivity (VMHC) is an index that can be used to measure the synchronization between two hemispheres. The strength of functional connection between a voxel and its corresponding voxels in the contralateral hemisphere is calculated using the VMHC algorithm. Abnormal connections involving multiple symmetrical regions in the two hemispheres can reflect coordinated neuronal activity in the right and left hemispheres. Because it enables characterization of the intrinsic functional architecture of the brain, the VMHC algorithm has recently been used to investigate brain function in common ocular diseases (Foubert et al., 2010; Liang et al., 2017). Seed-based FC in rs-fMRI is a measure of the spatiotemporal synchrony or correlations of the blood oxygenation level-dependent (BOLD) signal among anatomically distinct brain regions. VMHC can only reflect changes in functional connectivity in both hemispheres. The seed-based FC method reflect the region of interests (ROI) to whole brain FC, which indicate the whole brain network communication. In order to comprehensively analyze the changes of brain function in TAO patients, we combined VMHC technology and FC technology in this study.



Machine learning (ML), the core algorithm of artificial intelligence, has provided a systematic approach for using a set of high-dimensional data to make predictions. Furthermore, ML is a promising method in ophthalmology research because of its precision, non-invasiveness, and repeatability; it can be used for the diagnosis of ocular diseases and for the evaluation of therapeutic effects in those diseases. Support vector machine (SVM) is a supervised learning algorithm with a unique ability to classify disease-state and disease-free conditions; it has great potential for finding subtle differences in spatial patterns of structural and functional brain images. Tong et al. (2021) assessed the combined effects of an SVM model and FC analysis to classify iridocyclitis patients and healthy controls (HCs), with a substantial accuracy of 67.31%. Cui et al. (2020) also reported that the SVM approach provided robust accuracy in the classification of patients with generalized anxiety disorder through evaluations of the dynamic alterations of amplitude of low-frequency fluctuations metrics. To our knowledge, this was the first study that applied the SVM technique to VMHC data for predictive investigations in patients with TAO.

Here, we investigated changes in interhemispheric FC among patients with TAO by means of VMHC metrics. Subsequently, we used a seed-based FC method to detect potential alterations in interregional connectivity between regions with abnormal VMHC values and other brain areas. We then used the observed alterations in the VMHC algorithm as classification features to examine whether these alterations could provide substantial accuracy and specificity for differentiating patients with TAO from HCs *via* SVM classification.

## METHODS

### Subjects

The work recruited a total of 21 right-handed patients with TAO (14 males and 7 females, mean age:  $54.17 \pm 4.83$ ) from ophthalmology and endocrinology departments of Jiangxi Provincial People's Hospital. The inclusion criteria of TAO patients into experimental group included the following details: (1) these patients were all in the acute inflammatory stage of TAO with vision loss and definite ocular symptoms (i.e., clear evidence of impaired visual function, swelling of eyelids, lid retraction and exophthalmos); (2) ability to complete the fMRI scanning (no cardiac pacemaker, implanted metal devices or insulin pump); (3) no history or clinical evidence of any other diseases including cardiovascular diseases, neurological diseases, psychiatric disorders, brain parenchyma diseases and systematic diseases. Subjects were excluded in the research if they presented as one of the following conditions: (1) other ocular diseases besides TAO (glaucoma, vitreous hemorrhage, high myopia, strabismus, etc.); (2) previous history of ocular surgery and eye trauma; (3) breastfeeding and pregnant women.

During the same period, 21 HCs (14 males and 7 females, mean age:  $55.17 \pm 5.37$ ) matched with similar age, sex, handedness and academic years were recruited to participate the study. And the subjects must presented with no eye disease, no brain neurological disease or systematic disease, no alcohol or

drug addiction and no contraindications for fMRI scanning—details of the study participants were the same as our previous work (Qi et al., 2021).

This cross-sectional, retrospective study was approved by the institutional review board of Jiangxi Provincial People's Hospital and all research methods strictly adhered to the Declaration of Helsinki. Participants enrolled in the study of their own accord and were informed of the purpose, methods, as well as potential risks before signing an informed consent form.

### MRI Data Acquisition

MRI scanning was performed on a 3-Tesla MR scanner (GE Healthcare, Milwaukee, WI, USA) with an eight-channel head coil. All participants were required to close their eyes without falling asleep when undergoing MRI scanning. The T1 parameters (repetition time = 8.5 ms, echo time = 3.3 ms, thickness = 1.0 mm, gap = 0 mm, acquisition matrix =  $256 \times 256$ , field of view =  $240 \times 240 \text{ mm}^2$  and flip angle =  $12^\circ$ ) and 240 functional images parameters (repetition time = 2000 ms, echo time = 25 ms, thickness = 3.0 mm, gap = 1.2 mm, acquisition matrix =  $64 \times 64$ , field of view =  $240 \times 240 \text{ mm}^2$ , flip angle =  $90^\circ$ , voxel size =  $3.6 \times 3.6 \times 3.6 \text{ mm}^3$  and 35 axial slices) covering the whole brain for all participants were obtained.

### fMRI Data Pre-processing

All preprocessing was performed using the toolbox for Data Processing & Analysis of Brain Imaging-Version4.1 (DPABI, <http://www.rfmri.org/dpabi>), which is based on Statistical Parametric Mapping (SPM8) (<http://www.fil.ion.ucl.ac.uk>) implemented in MATLAB 2013a (MathWorks, Natick, MA, USA) and briefly following the steps: (1) The first 10 volumes of each subject were removed for the signal reaching equilibrium. (2) Slice timing and head motion correction were conducted. For head motion parameters, more than 2 mm in any direction of x, y, and z or for whom rotation exceeded  $2^\circ$  of any angle during scanning were excluded. (3) Individual 3D-BRAVO images were registered to the mean fMRI data, then resulting aligned T1-weighted images were segmented using the Diffeomorphic Anatomical Registration Through Exponentiated Lie Algebra (DARTEL) approach normalized to the Montreal Neurological Institute (MNI) space. (4) Linear regression analysis was applied to regress out several covariates (Friston-24 head motion parameters, global brain signal, and averaged signal from cerebrospinal fluid and white matter). (5) The fMRI data with linear trend were removed, and temporal band-pass was filtered (0.01–0.08 Hz) to reduce the influence of noise.

### VMHC Analysis

To evaluate the interhemispheric connectivity, VMHC method was performed using the DPABI toolkit according to a previous research (Zuo et al., 2010). Briefly, T1 structural images of all participants were normalized to generate a symmetrical template of left and right hemispheres to reduce the geometric difference between brain hemispheres. Then, the same transformation of the T1 images was performed on the preprocessed functional images.

The VMHC values were calculated for each pair of symmetrical interhemispheric voxel's time series (Pearson's correlation) at each voxel as interhemispheric resting-state homotopic connectivity (VMHC). Moreover, this symmetric T1 template did not include the brain midline ( $X = 0$ ) area. Finally, the generated correlation values were performed with Fisher's  $z$  transformation to obtain the zVMHC maps for further analysis and help to improve normality.

## Seed-Based FC Analysis

The DPABI toolkit was also applied to define the regions of interest (ROI) so as to investigate whether abnormal FC existed between the brain regions with altered VMHC values and other brain regions. We defined the center of regions with altered VMHC as the seed point and set the radius of the sphere ROI as 3 mm to compute FC signal values. For each participant, we first averaged the time series of voxels within each ROI, and next computed the Pearson's correlation coefficient for the subjects between the representative time series of the ROIs and the time series of other cerebrum regions. Finally, to minimize the influence of individual differences on statistical comparison, we applied Fisher's  $z$  transformation for converting the generated correlations-coefficient maps to zFC values.

## Statistical Analysis

The cumulative clinical measurements were analyzed in this study using SPSS 20.0 (SPSS Inc, Chicago, IL, USA). Chi-square test was adopted to evaluate categorical variables, while Independent two-sample  $t$ -test was applied to analyse continuous variables. A  $p$  value  $< 0.05$  was considered statistically significant.

A two-sample  $t$ -test was used to investigate the difference in the zVMHC maps and  $z$ -value FC maps between the two groups with DPABI toolkit after controlling for the effects of age and sex. Gaussian random field (GRF) method was used to correct for multiple comparisons of VMHC and FC differences between the two groups (two-tailed, voxel-level  $p < 0.01$ , GRF correction, cluster-level  $p < 0.05$ ).

## SVM Analysis

To evaluate whether the VMHC metrics alterations could serve as potential diagnostic metrics for TAO, we performed ML analyses using SVM algorithm with the average VMHC values of all clusters showing significant intragroup differences as the features.

Mapping nonlinear data to a high dimension feature space and finding a linear separating hyperplane to separate the two-group data are the core idea of SVM algorithm. In this study, we used the Gaussian radial basis function kernel SVM, implement in the LIBSVM software package (<http://www.csie.ntu.edu.tw/~cjlin/libsvm/>), to investigate the potential diagnostic of dynamic metrics. The  $C$  in the SVM was set to 1 and radial basis function kernel parameter  $\gamma$  was optimized among the values of  $2N$  ( $N$  from 4 to 4), and a leave-one-out cross-validation (LOOCV) was applied to validate the performance of our proposed approach. It involved excluding a participant from each group for test and training the classifier using the remaining participants. This procedure was repeated for each

**TABLE 1 |** Characteristics of participants included in the study.

Condition	TAO group	HC group	$t$	$P$ -value*
Gender (male/female)	14/7	14/7	N/A	$>0.999$
Age (years)	$54.17 \pm 4.83$	$55.17 \pm 5.37$	$-0.348$	$0.745$
Duration (months)	$11.25 \pm 4.42$	N/A	N/A	N/A
BCVA-OD	$0.67 \pm 0.35$	$1.14 \pm 0.15$	$-4.462$	$0.026$
BCVA-OS	$0.64 \pm 0.29$	$1.06 \pm 0.23$	$-4.297$	$0.023$
IOP	$25.63 \pm 3.36$	$14.45 \pm 1.07$	$5.532$	$<0.001$
Education	$11.17 \pm 2.64$	$11.42 \pm 1.95$	$-0.269$	$0.861$

Independent samples  $t$ -test for the other normally distributed continuous data (means  $\pm$  SD). \* $p < 0.05$  indicated significant differences.

TAO, thyroid-associated ophthalmopathy; HC, healthy control; N/A, not applicable; BCVA, best corrected visual acuity; OD, oculus dexter; OS, oculus sinister; IOP, intraocular pressure.

participant to assess the overall accuracy of the SVM. To quantify the performance of classification methods, accuracy, sensitivity and specificity were reported. Besides the classification accuracy, the receiver operating characteristic (ROC) curves and the corresponding area under the curve (AUC) were also computed to evaluate the classification efficiency.

## RESULTS

### Demographics and Disease Characteristics

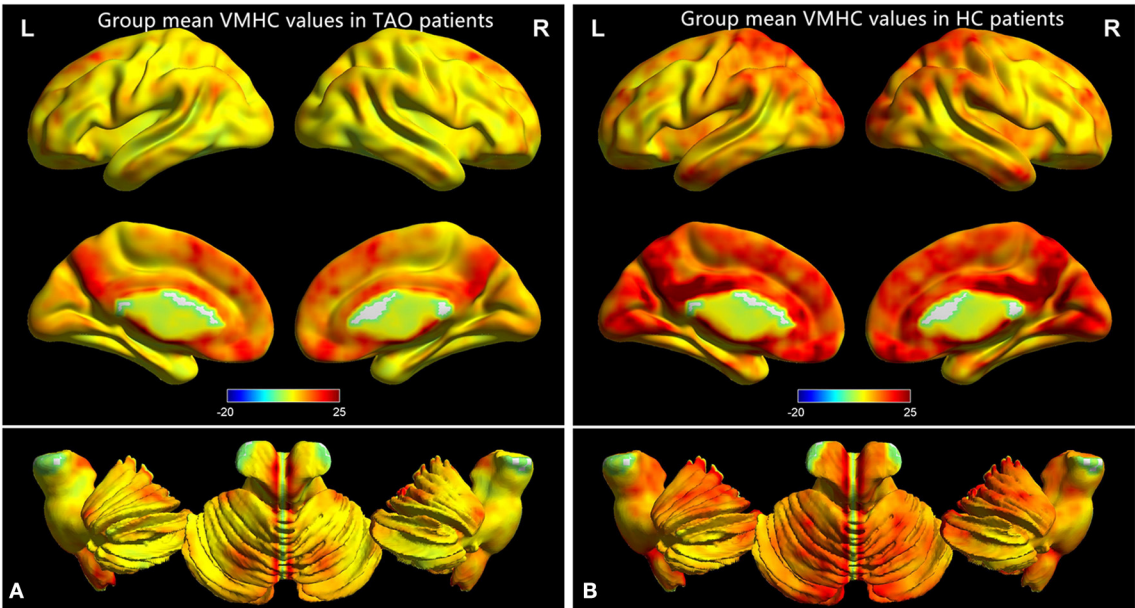
There were no statistically significant differences between the TAO and HC groups in gender ( $P > 0.999$ ) or age ( $P = 0.745$ ), but significant differences in best corrected visual acuity of left eye ( $p = 0.023$ ), right eye ( $p = 0.026$ ), and intraocular pressure ( $p < 0.001$ ). The results of these clinical data were summarized in Table 1.

### Comparisons of VMHC Between Patients With TAO and HCs

Figure 1 showed the spatial distribution of global VMHC maps of the TAO and HCs within each group. Compared with the HCs, patients with TAO showed significantly lower VMHC values in the bilateral postcentral gyrus (PostCG), lingual gyrus (LING), calcarine (CAL), middle temporal gyrus (MTG), middle occipital gyrus (MOG) and angular (ANG) (voxel-level  $p < 0.01$ , GRF correction, cluster-level  $p < 0.05$ ). Detailed information for these brain areas with altered VMHC values between the two groups was shown in Table 2 and Figure 2.

### Differences in FC

A total of six seed ROIs (three per hemisphere) were applied for further FC analysis, which were derived from those regions showing significant differences in the VMHC values. We finally found TAO patients exhibited decreased FC values between the right PostCG/LING/CAL and left LING/cuneus (CUN)/superior occipital gyrus(SOG), left PostCG/LING/CAL and right LING/MTG, right MTG and left cerebellum-8 (CER-8)/LING/MOG/supplementary motor area (SMA), left MTG and right MOG, right MOG/ANG and left middle temporal pole



**FIGURE 1 |** One-sample t-test results of VMHC maps within TAO group (A) and HC group (B). TAO, thyroid-associated ophthalmopathy; VMHC, voxel-mirrored homotopic connectivity; HC, healthy control.

(MTP) (voxel-level  $p < 0.01$ , GRF correction, cluster-level  $p < 0.05$ ), which were illustrated in Table 3 and Figure 3. But the left MOG/ANG of TAO patients didn't shown significantly higher or lower FC values with other brain regions than that of HCs.

SVM Classification Results

To evaluate the classification ability of the SVM model, the accuracy, sensitivity, specificity and precision were calculated and the ROC curve of the classifier were illustrated in Figure 4. The performance of the classifier achieved an accuracy of 73.81% and AUC of 0.79 for TAO vs HCs. Moreover, the SVM was applied to asses the classification ability of FC values (Supplementary Document).

DISCUSSION

To our knowledge, this is the first study to use the VMHC method combined with seed-based FC to explore interhemispheric functional coordination in patients with TAO and HCs. Compared with HCs, TAO patients showed significantly lower VMHC values in the bilateral PostCG/LING/CAL, MTG, and MOG/ANG. These reductions indicated extensive disruption of interhemispheric FC in patients with TAO. Furthermore, TAO patients exhibited decreased FC values between the right PostCG/LING/CAL and left LING/CUN/SOG, left PostCG/LING/CAL and right LING/MTG, right MTG and left CER-8/LING/MOG/ SMA, left MTG and right MOG, right MOG/ANG and left MTP (voxel-level  $p < 0.01$ , GRF correction, cluster-level  $p < 0.05$ ). The performance of the SVM classifier achieved an accuracy of 73.81% and AUC of 0.79 for TAO vs HCs.

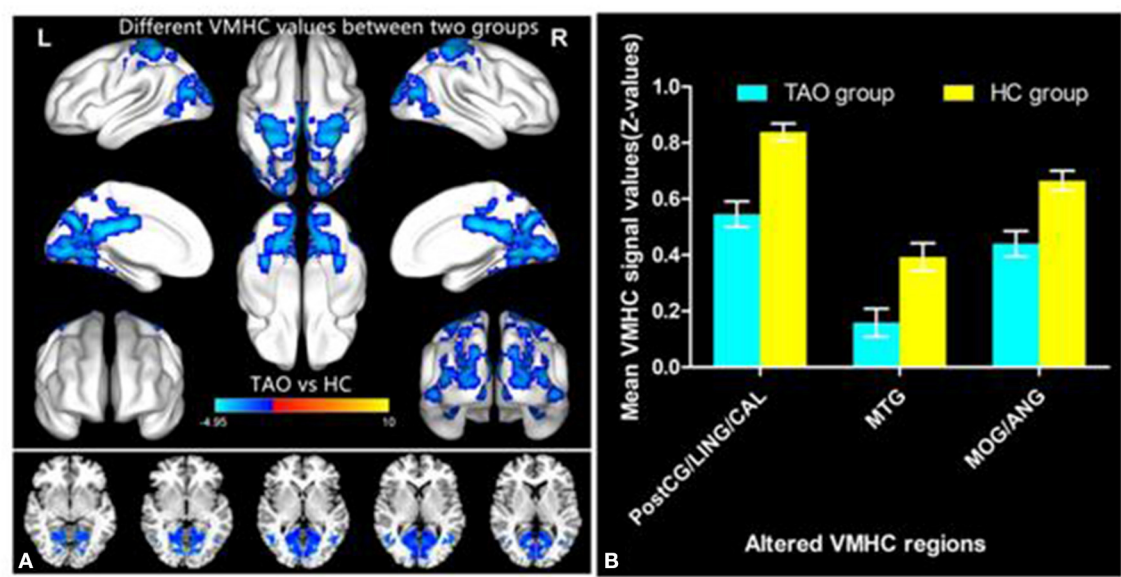
**TABLE 2 |** Brain areas with significantly altered VMHC values between two groups.

Regions	Cluster size	Brodmann's areas	MNI coordination			T value
			X	Y	Z	
R/L-PostCG/LING/CAL	2,243	3/4/18/19	± 3	−21	27	−4.9477
R/L-MTG	13	-	± 39	−63	3	−3.0776
R/L-MOG/ANG	27	19/39	± 45	−78	33	−3.3491

TAO, thyroid-associated ophthalmopathy; MNI, Montreal Neurological Institute; VMHC, voxel-mirrored homotopic connectivity; PostCG, postcentral gyrus; LING, lingual gyrus; CAL, calcarine; MTG, middle temporal gyrus; MOG, middle occipital gyrus; ANG, angular gyrus.

The occipital lobe contains most anatomical areas of the visual cortex, including the three Brodmann areas (Flores, 2002; Teng et al., 2018; Qi et al., 2021) associated with vision. The occipital lobe is associated with visual information processing; it has a critical role in the perception of facial emotion (Flores, 2002; Teng et al., 2018). BA19, the MOG, is regarded as a component of the dorsal visual stream, which has an important role in visual spatial processing (Tu et al., 2013; Chen et al., 2019a). The CAL is the most reliable anatomic landmark of the medial part of the occipital lobe; it contains the primary visual area. Lesions of the CAL are reportedly associated with visual field defects and the perception of phosphenes (Zhang et al., 2018; El Mohamad et al., 2019). The LING, located in the second visual area, receives strong feedforward connections from the CAL; the LING is also a crucial component of the dorsal visual pathway for visual processing and spatial memory





**FIGURE 2 |** Significant VMHC differences in the TAO and HC group **(A)**; The mean of altered VMHC values between patients with TAO and HCs **(B)**. TAO, thyroid-associated ophthalmopathy; HC, healthy control; VMHC, voxel-mirrored homotopic connectivity; PostCG, postcentral gyrus; LING, lingual gyrus; CAL, calcarine; MTG, middle temporal gyrus; MOG, middle occipital gyrus; ANG, angular gyrus.

(Klaver et al., 2015). The CUN is a wedge-shaped cortical region located inside the occipital lobe, posterior to the parietal occipital fissure and superior to the CAL. The CUN consists of both striatal and extrastriatal visual cortex; it receives direct input from the lateral geniculate body (Leopold, 2012; Meylakh and Henderson, 2022). Chen et al. (2021a) reported that patients with active TAO exhibited significantly decreased spontaneous brain activity in the MOG; this decreased activity was associated with visual deficits. Additionally, Tu et al. (2020) found abnormal FC density between the left precuneus and occipital gyrus in patients with dysthyroid optic neuropathy. The research revealed that dynamic abnormalities in thyroid hormone levels can lead to structural and functional abnormalities in the visual cortex. There is increasing neuroimaging evidence that patients with impaired vision have abnormal brain activity within the occipital cortex (Liang et al., 2017; Huang et al., 2019; Qi et al., 2021). Consistent with these findings, our study found that patients with TAO had significantly decreased interhemispheric FC in the MOG, LING, CAL, SOG and CUN; these results suggested the presence of disrupted interhemispheric functional synchronization in the visual network of TAO cohort, which corresponded to impaired visual function.

In addition to VMHC alterations in the visual brain network, we found that interhemispheric FC in the sensorimotor network was lower in patients with TAO than in HCs. The PostCG, a region in the parietal lobe, is the location of the primary somatosensory cortex; it is responsible for sensory functions such as the encoding of touch and pain (Shao et al., 2018; Chen et al., 2019b). Moreover, the PostCG is considered a component of the dorsal visual pathway and is involved in modulating vision (Zhu et al., 2016). Patients

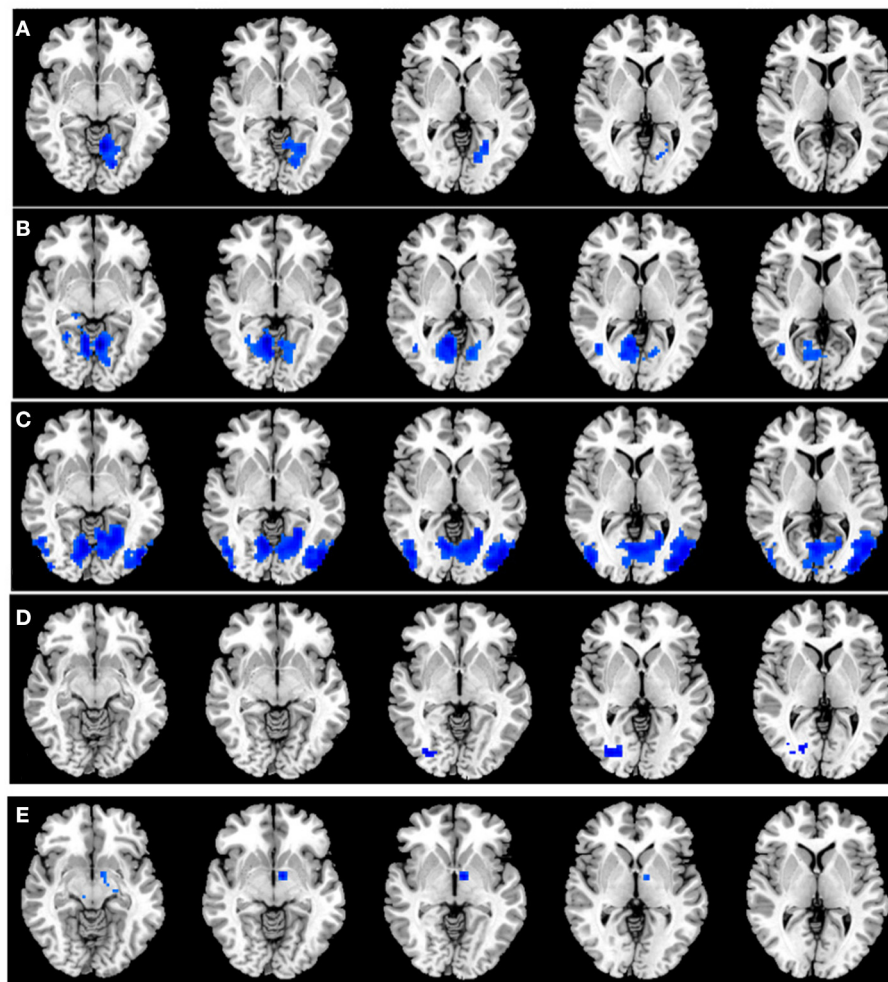
**TABLE 3 |** Significant differences in seed-based FC between TAO patients and HCs.

Seed region	Regions	Cluster size	MNI coordination			P value
			X	Y	Z	
R-PostCG/LING/CAL	L-LING	282	−12	−60	−12	−4.5011
	L-CUN	163	3	−93	24	−3.9564
	L-SOG	90	−24	−72	18	−3.8977
L-PostCG/LING/CAL	R-LING	852	−6	−60	−6	−4.7800
	R-MTG	29	42	−63	3	−3.3359
R-MTG	L-CER-8	129	−36	−57	−51	−3.4584
	L-LING	3542	3	−90	27	−4.4815
	L-SMA	775	−3	0	60	−4.3930
L-MTG	L-MOG	294	24	−81	15	−3.8720
R-MOG/ANG	L-MTP	732	0	−30	−33	−4.7765

TAO, thyroid-associated ophthalmopathy; HC, healthy control; MNI, Montreal Neurological Institute; FC, functional connectivity; PostCG, postcentral gyrus; LING, lingual gyrus; CAL, calcarine; MTG, middle temporal gyrus; MOG, middle occipital gyrus; ANG, angular gyrus; CUN, cuneus; SOG, superior occipital gyrus; CER, cerebellum; SMA, supplementary motor area; MTP, middle temporal pole.

with TAO were reported to show decreased degree centrality in the PostCG, which suggested an aberrant degree of its functional connectivity in the parietal lobe (Chen et al., 2021b). Moreover, patients with TAO had significant thinning of the gray matter sheet in the PostCG, which might offer the neuroanatomical basis for psychological and ocular disturbances in the TAO cohort (Wu et al., 2020). The supplementary motor complex consists of the SMA, supplementary eye field,



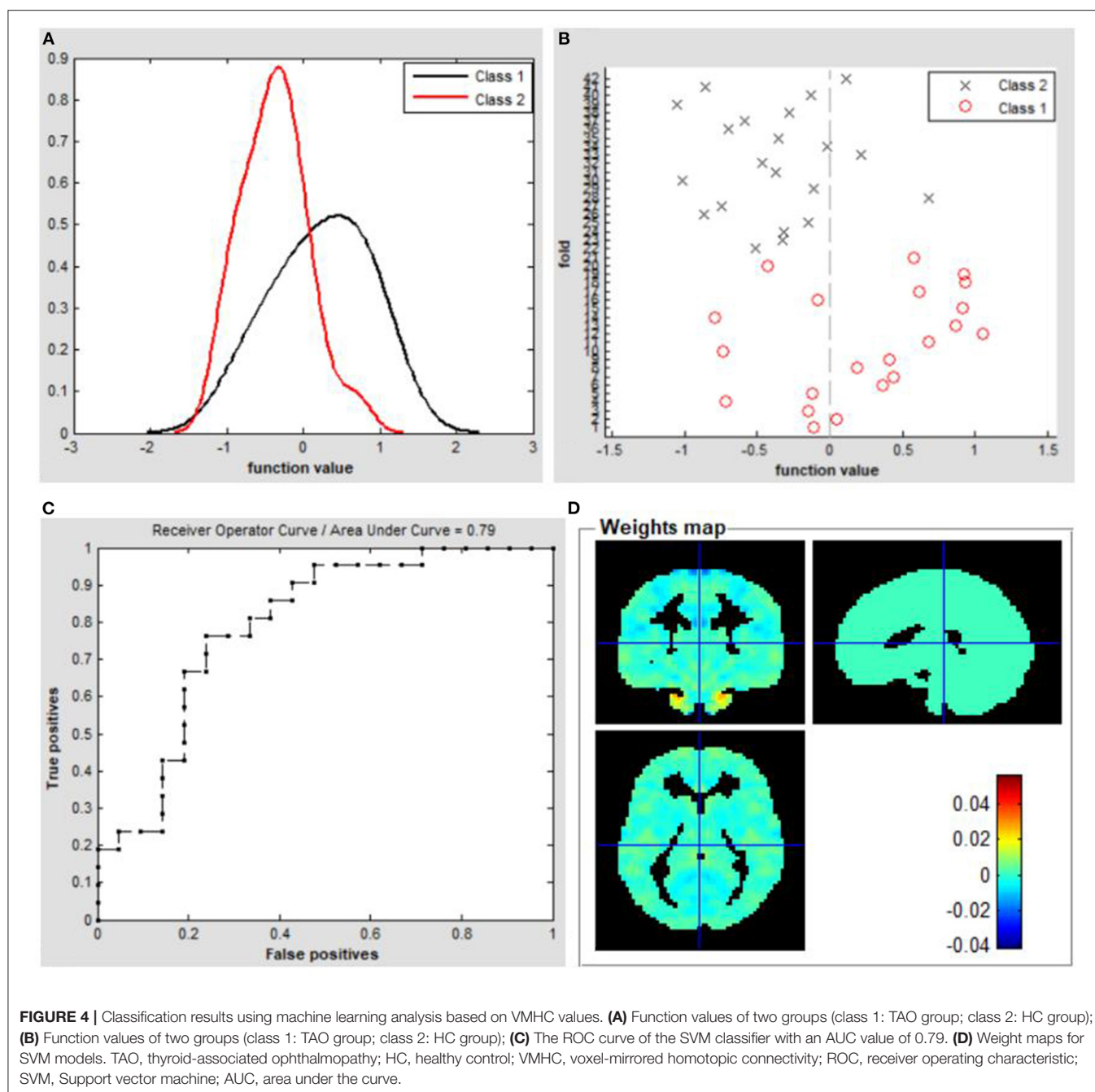


**FIGURE 3 | (A)** Significant FC differences between the right PostCG/LING/CAL and left LING/CUN/SOG. **(B)** Significant FC differences between the left PostCG/LING/CAL and right LING/MTG. **(C)** Significant FC differences between the right MTG and left CER-8/LING/MOG/SMA. **(D)** Significant FC differences between the left MTG and right MOG. **(E)** Significant FC differences between the right MOG/ANG and left MTP. TAO, thyroid-associated ophthalmopathy; FC, functional connectivity; PostCG, postcentral gyrus; LING, lingual gyrus; CAL, calcarine; MTG, middle temporal gyrus; MOG, middle occipital gyrus; CUN, cuneus; SOG, superior occipital gyrus; CER, cerebellum; SMA, supplementary motor area; MTP, middle temporal pole.

and pre-SMA; these areas are crucial for linking cognition to action (Hupfeld et al., 2017; Ruan et al., 2018). The SMA is located in the dorsomedial frontal cortex; it is involved in several functions related to motor sequence processing, planning, execution and inhibition (Li et al., 2006; Cona et al., 2017). Furthermore, the SMA is crucial for sensorimotor integration involved in generating actions (Ruan et al., 2018). Notably, a recent fMRI study revealed that, during silent lipreading, brain activity in the SMA decreased when an additional visual stimulus was included (Plata Bello et al., 2019). Consistent with these findings, we observed that patients with TAO had decreased interhemispheric FC within the sensorimotor network, which suggests impaired sensorimotor function in these patients.

Another important result in our study was that patients with TAO showed reduced interhemispheric FC strength in brain

areas associated with cognitive function. The CER is located in the posterior fossa; it has important roles in visuospatial processing and eye movement (Stoodley and Schmahmann, 2010). Recent researches have revealed a critical role for the CER in higher cognitive functions (Izawa et al., 2012; Tong et al., 2021). Here, we demonstrated that patients with TAO had abnormal spontaneous neuronal activity in the CER; this activity was associated with cognitive impairment (Qi et al., 2021). We also found that patients with TAO showed lower interhemispheric FC in the bilateral ANG, compared with HCs. The ANG, located immediately above the Wernicke area, is an important connection area at the back of the brain. Because of its position, the ANG is presumably critical for integrating information among multiple input modalities and brain networks (Seghier, 2013). There is increasing evidence that the ANG is involved in reading, comprehension, visuospatial



attention, spatial cognition, and episodic memory (Wang et al., 2010; Rugg and King, 2018). Humphreys et al. (2021) proposed a unifying model to explain complicated cognitive functions in the ANG; they suggested that the ANG served as an integrative dynamic buffer to combine information from local regions and brain networks. In addition, the ANG is a constituent part of the default mode network (DMN), which has been associated with spontaneous activity in rest situations; it is also involved in the unconscious processing of working memory tasks and implicit memory (Zuber et al., 2021). Thus, decreased interhemispheric FC in the ANG and

CER might contribute to diverse cognition deficits in patients with TAO.

The MTG and MTP, core components of the temporal lobe, receive visual information input from the occipital lobe; they may constitute the higher areas of visual processing (Vedaei et al., 2021). Neural activity in the temporal region is associated with semantic processing including memory, visual, verbal, and executive functioning (Kang et al., 2021). The MTG is a critical component of the task positive network and the DMN, which is associated with externally oriented attention (Hu et al., 2020). Patients with TAO commonly complain of cognitive

changes and emotional regulation deficits during the active stage. Patients with TAO reportedly have a predisposition to anxiety and attention disorder (Matos-Santos et al., 2001; Tsatsoulis, 2006). In the present study, we found decreased interhemispheric interactions in the MTG of patients with TAO. Therefore, integrating the neuroimaging findings with the cortical functions and the clinical psychiatric basis of the disease, we speculated that TAO might cause the MTG impairment, resulting in dysfunctions of visual attention, and visual processing.

An understanding of visual pathway lesions and cognitive deficits in TAO is important for the diagnosis and interventional treatment of the disease; combined VMHC and SVM assessments of TAO are thus meaningful. At present, the clinical diagnosis of TAO mainly depends on specific symptoms and computed tomography findings, but some patients lack specific symptoms. Therefore, we adopted an objective approach, SVM, to obtain a more reliable diagnosis for TAO. We also generated an ROC curve to assess the classification efficiency of the SVM approach. The overall identification accuracy of the SVM classifier was 73.81%; the AUC was 0.79, based on the LOOCV technique. These findings strongly support the hypothesis that the VMHC index can serve as a classification feature for distinguishing between the two groups through the application of supervised ML. Because of its robust objectivity and sensitivity, ML combined with multiparametric neuroimaging data might provide physicians with a powerful diagnostic tool in the near future.

However, the research had some potential limitations that should be ameliorated in the following studies. The first one is the relatively small sample size, although the results were encouraging. Due to the small sample size in the study, the generalizability of the findings was uncertain. Secondly, our study should include both the active and inactive patients with TAO and collect detailed clinical information scores and cognitive scales, which help understanding the neurological mechanisms underlying visual and cognitive disorders in these patients. Thirdly, a 73.81% accurate classification was not high enough. And we will expand the sample size and combine various machine learning methods including random forest or deep neural network to improve the accuracy in the next study. Additionally, the effect of physiological noise when performing rs-fMRI scanning was not completely eliminated, which might interfere with BOLD signals. Therefore, a combination of structural MRI, electroencephalogram, diffusion tensor imaging and fMRI might make the findings more convincing.

## REFERENCES

- Bhatara, V. S., Tripathi, R. P., Sankar, R., Gupta, A., and Khushu, S. (1998). Frontal lobe proton magnetic-resonance spectroscopy in Graves' disease: a pilot study. *Psychoneuroendocrinology*. 23, 605–612. doi: 10.1016/S0306-4530(98)00028-6
- Chen, L., Li, S., Cai, F., Wu, L., Gong, H., Pei, C., et al. (2019b). Altered functional connectivity density in primary angle-closure glaucoma patients at resting-state. *Quant. Imaging Med. Surg.* 9, 603–614. doi: 10.21037/qims.2019.04.13
- Chen, W., Wu, Q., Chen, L., Zhou, J., Chen, H. H., Xu, X. Q., et al. (2021a). Disrupted spontaneous neural activity in patients with thyroid-associated ophthalmopathy: a resting-state fMRI study using amplitude

## CONCLUSION

We found that patients with TAO showed significant dysfunctional interhemispheric FC in the visual network, sensorimotor network, and brain areas associated with cognitive function. VMHC variability has potential value for accurately and specifically distinguishing patients with TAO from HCs. These findings may provide novel insights into the neurological mechanisms that underlie visual and cognitive disorders in patients with TAO.

## DATA AVAILABILITY STATEMENT

The raw data supporting the conclusions of this article will be made available by the authors, without undue reservation.

## ETHICS STATEMENT

The studies involving human participants were reviewed and approved by Ethics Committee of Jiangxi Provincial People's Hospital. The patients/participants provided their written informed consent to participate in this study. Written informed consent was obtained from the individual(s) for the publication of any potentially identifiable images or data included in this article.

## AUTHOR CONTRIBUTIONS

C-XQ, ZW, and XH contributed to data collection, statistical analyses, and wrote the manuscript. All authors contributed to the article and approved the submitted version.

## ACKNOWLEDGMENTS

We acknowledge the assistance provided by the Natural Science Foundation of Jiangxi Province (20212BAB216058) and Jiangxi Provincial Health Technology Project (SKJP\_202210012).

## SUPPLEMENTARY MATERIAL

The Supplementary Material for this article can be found online at: <https://www.frontiersin.org/articles/10.3389/fnhum.2022.882114/full#supplementary-material>

of low-frequency fluctuation. *Front. Hum. Neurosci.* 15, 676967. doi: 10.3389/fnhum.2021.676967

- Chen, W., Wu, Q., Chen, L., Zhou, J., Chen, H. H., Xu, X. Q., et al. (2021b). Aberrant brain voxel-wise resting state fMRI in patients with thyroid-associated ophthalmopathy. *J. Neuroimaging*. 31, 773–783. doi: 10.1111/jon.12858
- Chen, Y., Meng, Z., Zhang, Z., Zhu, Y., Gao, R., Cao, X., et al. (2019a). The right thalamic glutamate level correlates with functional connectivity with right dorsal anterior cingulate cortex/middle occipital gyrus in unmedicated obsessive-compulsive disorder: a combined fMRI and <sup>1</sup>H-MRS study. *Aust. n Z J. Psychiatry*. 53, 207–218. doi: 10.1177/0004867418806370



- Cona, G., Marino, G., and Semenza, C. (2017). TMS of supplementary motor area (SMA) facilitates mental rotation performance: evidence for sequence processing in SMA. *Neuroimage*. 146, 770–777. doi: 10.1016/j.neuroimage.2016.10.032
- Coulter, I., Frewin, S., Krassas, G. E., and Perros, P. (2007). Psychological implications of Graves' orbitopathy. *Eur. J. Endocrinol.* 157, 127–131. doi: 10.1530/EJE-07-0205
- Cui, Q., Sheng, W., Chen, Y., Pang, Y., Lu, F., Tang, Q., et al. (2020). Dynamic changes of amplitude of low-frequency fluctuations in patients with generalized anxiety disorder. *Hum. Brain Mapp.* 41, 1667–1676. doi: 10.1002/hbm.24902
- Du, B., Wang, Y., Yang, M., and He, W. (2021). Clinical features and clinical course of thyroid-associated ophthalmopathy: a case series of 3620. *Chinese cases. Eye (Lond)*. 35, 2294–2301. doi: 10.1038/s41433-020-01246-7
- El Mohamad, A. R., Tatu, L., Moulin, T., Fadoul, S., and Vuillier, F. (2019). Main anatomical features of the calcarine sulcus: a 3D magnetic resonance imaging at 3T study. *Surg. Radiol. Anat.* 41, 181–186. doi: 10.1007/s00276-018-2118-x
- Flores, L. P. (2002). Occipital lobe morphological anatomy: anatomical and surgical aspects. *Arq. Neuropsiquiatr.* 60, 566–571. doi: 10.1590/S0004-282X2002000400010
- Foubert, L., Bennequin, D., Thomas, M. A., Droulez, J., and Milleret, C. (2010). Interhemispheric synchrony in visual cortex and abnormal postnatal visual experience. *Front. Biosci.* 15, 681–707. doi: 10.2741/3640
- Hu, G., Hu, X., Yang, K., Liu, D., Xue, C., Liu, Y., et al. (2020). Restructuring of contralateral gray matter volume associated with cognition in patients with unilateral temporal lobe glioma before and after surgery. *Hum. Brain Mapp.* 41, 1786–1796. doi: 10.1002/hbm.24911
- Huang, X., Dan, H. D., Zhou, F. Q., Deng, Q. Q., and Shen, Y. (2019). Abnormal intrinsic functional network hubs and connectivity following peripheral visual loss because of inherited retinal degeneration. *Neuroreport*. 30, 295–304. doi: 10.1097/WNR.0000000000001200
- Humphreys, G. F., Lambon Ralph, M. A., and Simons, J. S. (2021). A unifying account of angular gyrus contributions to episodic and semantic cognition. *Trends Neurosci.* 44, 452–463. doi: 10.1016/j.tins.2021.01.006
- Hupfeld, K. E., Ketcham, C. J., and Schneider, H. D. (2017). Transcranial direct current stimulation (tDCS) to the supplementary motor area (SMA) influences performance on motor tasks. *Exp. Brain. Res.* 235, 851–859. doi: 10.1007/s00221-016-4848-5
- Izawa, J., Criscimagna-Hemminger, S. E., and Shadmehr, R. (2012). Cerebellar contributions to reach adaptation and learning sensory consequences of action. *J. Neurosci.* 32, 4230–4239. doi: 10.1523/JNEUROSCI.6353-11.2012
- Jiang, Y. P., Yang, Y. C., Tang, L. Y., Ge, Q. M., Shi, W. Q., Su, T., et al. (2021). Altered spontaneous brain activity patterns in dysthyroid optic neuropathy: a resting-state fMRI study. *J. Integr. Neurosci.* 20, 375–383. doi: 10.31083/j.jin2002037
- Kang, B. X., Ma, J., Shen, J., Xu, H., Wang, H. Q., Zhao, C., et al. (2021). Altered brain activity in end-stage knee osteoarthritis revealed by resting-state functional magnetic resonance imaging. *Brain Behav.* 29, e2479. doi: 10.1002/brb3.2479
- Klaver, P., Latal, B., and Martin, E. (2015). Occipital cortical thickness in very low birth weight born adolescents predicts altered neural specialization of visual semantic category related neural networks. *Neuropsychologia*. 67:41–54. doi: 10.1016/j.neuropsychologia.2014.10.030
- Leopold, D. A. (2012). Primary visual cortex: awareness and blindsight. *Ann. Rev. Neurosci.* 35, 91–109. doi: 10.1146/annurev-neuro-062111-150356
- Li, C. S., Huang, C., Constable, R. T., and Sinha, R. (2006). Gender differences in the neural correlates of response inhibition during a stop signal task. *Neuroimage*. 32, 1918–1929. doi: 10.1016/j.neuroimage.2006.05.017
- Liang, M., Xie, B., Yang, H., Yin, X., Wang, H., Yu, L., et al. (2017). Altered interhemispheric functional connectivity in patients with anisometropic and strabismic amblyopia: a resting-state fMRI study. *Neuroradiology*. 59, 517–524. doi: 10.1007/s00234-017-1824-0
- Liu, P., Luo, B., Zhai, L. H., Wu, H. Y., Wang, Q. X., Yuan, G., et al. (2022). Multi-Parametric Diffusion Tensor Imaging of The Optic Nerve for Detection of Dysthyroid Optic Neuropathy in Patients With Thyroid-Associated Ophthalmopathy. *Front. Endocrinol. (Lausanne)*. 13:851143. doi: 10.3389/fendo.2022.851143
- Matos-Santos, A., Nobre, E. L., Costa, J. G., Nogueira, P. J., Macedo, A., Galvão-Teles, A., et al. (2001). Relationship between the number and impact of stressful life events and the onset of Graves' disease and toxic nodular goitre. *Clin. Endocrinol. (Oxf)*. 55, 15–19. doi: 10.1046/j.1365-2265.2001.01332.x
- Meylakh, N., and Henderson, L. A. (2022). Exploring alterations in sensory pathways in migraine. *J. Headache Pain*. 23, 5. doi: 10.1186/s10194-021-01371-y
- Plata Bello, J., García-Peña, C., Modroño, C., Hernández-Martín, E., Pérez-Martín, Y., Marcano, F., et al. (2019). Visual inputs decrease brain activity in frontal areas during silent lipreading. *PLoS One*. 14, e0223782. doi: 10.1371/journal.pone.0223782
- Qi, C. X., Wen, Z., and Huang, X. (2021). Spontaneous brain activity alterations in thyroid-associated ophthalmopathy patients using amplitude of low-frequency fluctuation: a resting-state fMRI study. *Neuroreport*. 32, 1416–1422. doi: 10.1097/WNR.0000000000001745
- Reddy, V., Taha, W., Kundumadam, S., and Khan, M. (2017). Atrial fibrillation and hyperthyroidism: a literature review. *Indian Heart J.* 69, 545–550. doi: 10.1016/j.ihj.2017.07.004
- Ruan, J., Bludau, S., Palomero-Gallagher, N., Caspers, S., Mohlberg, H., Eickhoff, S. B., et al. (2018). Cytoarchitecture, probability maps, and functions of the human supplementary and pre-supplementary motor areas. *Brain Struct. Funct.* 223, 4169–4186. doi: 10.1007/s00429-018-1738-6
- Rugg, M. D., and King, D. R. (2018). Ventral lateral parietal cortex and episodic memory retrieval. *Cortex*. 107, 238–250. doi: 10.1016/j.cortex.2017.07.012
- Seghier, M. L. (2013). The angular gyrus: multiple functions and multiple subdivisions. *Neuroscientist*. 19, 43–61. doi: 10.1177/1073858412440596
- Shao, Y., Bao, J., Huang, X., Zhou, F. Q., Ye, L., Min, Y. L., et al. (2018). Comparative study of interhemispheric functional connectivity in left eye monocular blindness versus right eye monocular blindness: a resting-state functional MRI study. *Oncotarget*. 9, 14285–14295. doi: 10.18632/oncotarget.24487
- Stoodley, C. J., and Schmahmann, J. D. (2010). Evidence for topographic organization in the cerebellum of motor control versus cognitive and affective processing. *Cortex*. 46, 831–844. doi: 10.1016/j.cortex.2009.11.008
- Teng, C., Zhou, J., Ma, H., Tan, Y., Wu, X., Guan, C., et al. (2018). Abnormal resting state activity of left middle occipital gyrus and its functional connectivity in female patients with major depressive disorder. *BMC Psychiatr.* 18, 370. doi: 10.1186/s12888-018-1955-9
- Tong, Y., Huang, X., Qi, C. X., and Shen, Y. (2021). Altered functional connectivity of the primary visual cortex in patients with iridocyclitis and assessment of its predictive value using machine learning. *Front. Immunol.* 12, 660554. doi: 10.3389/fimmu.2021.660554
- Tsatsoulis, A. (2006). The role of stress in the clinical expression of thyroid autoimmunity. *Ann. n Y Acad. Sci.* 1088, 382–395. doi: 10.1196/annals.1366.015
- Tu, S., Qiu, J., Martens, U., and Zhang, Q. (2013). Category-selective attention modulates unconscious processes in the middle occipital gyrus. *Conscious Cogn.* 22, 479–485. doi: 10.1016/j.concog.2013.02.007
- Tu, Y., Huang, P., Mao, C., Liu, X., and Gao, J. (2020). Abnormal functional connectivity density in patients with dysthyroid optic neuropathy. *Ophthalmic Res.* 7, 21. doi: 10.1159/000512755
- Vedaei, F., Newberg, A. B., Alizadeh, M., Muller, J., Shahrpour, S., Middleton, D., et al. (2021). Resting-state functional MRI metrics in patients with chronic mild traumatic brain injury and their association with clinical cognitive performance. *Front. Hum. Neurosci.* 15, 768485. doi: 10.3389/fnhum.2021.768485
- Wang, J., Conder, J. A., Blitzer, D. N., and Shinkareva, S. V. (2010). Neural representation of abstract and concrete concepts: a meta-analysis of neuroimaging studies. *Hum. Brain Mapp.* 31, 1459–1468. doi: 10.1002/hbm.20950
- Wu, Q., Hu, H., Chen, W., Chen, H. H., Chen, L., Xu, X. Q., et al. (2020). Morphological and microstructural brain changes in thyroid-associated ophthalmopathy: a combined voxel-based morphometry and diffusion tensor imaging study. *J. Endocrinol. Invest.* 43, 1591–1598. doi: 10.1007/s40618-020-01242-4
- Wu, Q., Hu, H., Chen, W., Chen, H. H., Chen, L., Zhou, J., et al. (2021). Disrupted topological organization of the brain structural network in patients with thyroid-associated ophthalmopathy. *Invest. Ophthalmol. Vis. Sci.* 62, 5. doi: 10.1167/iov.62.4.5
- Zah-Bi, G., Abeillon-du Payrat, J., Vie, A. L., Bournaud-Salinas, C., Jouanneau, E., and Berhouma, M. (2019). Minimal-access endoscopic endonasal management of dysthyroid optic neuropathy: the dysthone study. *Neurosurgery*. 85, E1059–E1067. doi: 10.1093/neuros/nyz268



- Zhang, P., Li, Y., Fan, F., Li, C. R., Luo, X., Yang, F., et al. (2018). Resting-state brain activity changes associated with tardive dyskinesia in patients with schizophrenia: fractional amplitude of low-frequency fluctuation decreased in the occipital lobe. *Neuroscience*. 385, 237–245. doi: 10.1016/j.neuroscience.2018.06.014
- Zhu, Y., Feng, Z., Xu, J., Fu, C., Sun, J., Yang, X., et al. (2016). Increased interhemispheric resting-state functional connectivity after sleep deprivation: a resting-state fMRI study. *Brain Imag. Behav.* 10, 911–919. doi: 10.1007/s11682-015-9490-5
- Zuber, P., Gaetano, L., Griffa, A., Huerbin, M., Pedullà L., Bonzano, L., et al. (2021). Additive and interaction effects of working memory and motor sequence training on brain functional connectivity. *Sci. Rep.* 11, 23089. doi: 10.1038/s41598-021-02492-9
- Zuo, X. N., Kelly, C., Di Martino, A., Mennes, M., Margulies, D. S., Bangaru, S., et al. (2010). Growing together and growing apart: regional and sex differences in the lifespan developmental trajectories of functional homotopy. *J. Neurosci.* 30, 15034–15043. doi: 10.1523/JNEUROSCI.2612-10.2010

**Conflict of Interest:** The authors declare that the research was conducted in the absence of any commercial or financial relationships that could be construed as a potential conflict of interest.

**Publisher's Note:** All claims expressed in this article are solely those of the authors and do not necessarily represent those of their affiliated organizations, or those of the publisher, the editors and the reviewers. Any product that may be evaluated in this article, or claim that may be made by its manufacturer, is not guaranteed or endorsed by the publisher.

Copyright © 2022 Qi, Wen and Huang. This is an open-access article distributed under the terms of the Creative Commons Attribution License (CC BY). The use, distribution or reproduction in other forums is permitted, provided the original author(s) and the copyright owner(s) are credited and that the original publication in this journal is cited, in accordance with accepted academic practice. No use, distribution or reproduction is permitted which does not comply with these terms.



# Altered Temporal Dynamics of the Amplitude of Low-Frequency Fluctuations in Comitant Exotropia Patients

Ri-Bo Chen<sup>1</sup>, Shu-Yuan Ye<sup>2</sup>, Chong-Gang Pei<sup>2\*</sup> and Yu-Lin Zhong<sup>3\*</sup>

<sup>1</sup> Department of Radiology, Jiangxi Provincial People's Hospital, The First Affiliated Hospital of Nanchang Medical College, Nanchang, China, <sup>2</sup> Department of Ophthalmology, The First Affiliated of Nanchang University, Nanchang, China, <sup>3</sup> Department of Ophthalmology, Jiangxi Provincial People's Hospital, The First Affiliated Hospital of Nanchang Medical College, Nanchang, China

## OPEN ACCESS

### Edited by:

Zhi Wen,  
Renmin Hospital of Wuhan  
University, China

### Reviewed by:

Xiuxiu Qin,  
Southern Medical University, China  
Yan Tong,  
Renmin Hospital of Wuhan  
University, China

### \*Correspondence:

Yu-Lin Zhong  
804722489@qq.com  
Chong-Gang Pei  
peichonggang11@163.com

### Specialty section:

This article was submitted to  
Brain Imaging and Stimulation,  
a section of the journal  
Frontiers in Human Neuroscience

**Received:** 14 May 2022

**Accepted:** 20 June 2022

**Published:** 13 July 2022

### Citation:

Chen R-B, Ye S-Y, Pei C-G and  
Zhong Y-L (2022) Altered Temporal  
Dynamics of the Amplitude of  
Low-Frequency Fluctuations in  
Comitant Exotropia Patients.  
Front. Hum. Neurosci. 16:944100.  
doi: 10.3389/fnhum.2022.944100

**Purpose:** Growing evidence reported that patients with comitant exotropia (CE) were accompanied by static cerebral neural activity changes. However, whether the dynamic time-varying of neural activity changes in patients with CE remains unknown.

**Methods:** A total of 36 patients with CE (25 men and 11 women) and 36 well-matched healthy controls are enrolled in the study. The dynamic amplitude of low-frequency fluctuation (dALFF) combined with the sliding window method was used to assess the dynamic neural activity changes in patients with CE.

**Results:** Compared with HCs, patients with CE had decreased dALFF values in the right superior parietal lobule (SPL) and right precuneus gyrus (PreCUN). Moreover, we found that the dALFF maps showed an accuracy of 48.61% and an area under the curve of .54 for distinguishing the patients with CE from HCs.

**Conclusion:** Our study demonstrated that patients with CE showed altered dynamic neural activity changes in the right SPL and right PreCUN, which might indicate the neuropathological mechanism of stereoscopic dysfunction in patients with CE.

**Keywords:** comitant exotropia, functional magnetic resonance imaging, dynamic amplitude of low-frequency fluctuation, stereoscopic vision, support vector machine

## INTRODUCTION

Comitant exotropia (CE) is a common ophthalmic disease. Patients with CE were associated with impaired stereoscopic vision. At present, the surgical treatment of strabismus correction is an important treatment for patients with CE. However, there are some strabismus patients who cannot reconstruct the stereoscopic vision completely, which had a bad influence on their daily life of these patients. Recent studies have shown that strabismus patients are more likely to be accompanied by emotional and psychological abnormalities (Lin et al., 2014; McBain et al., 2014; Lee et al., 2022). However, the exact mechanism of brain pathology in strabismus patients remains unclear.

Recently, the fMRI technology can be successfully used to detect static cerebral neural activity changes. Moreover, fMRI has been widely used to detect neural activity changes in strabismus patients. Shi et al. (2019) reported that constant exotropia patients had lower regional homogeneity (ReHo) values in the right secondary visual cortex (V2). Xi et al. (2020) also found that patients

with concomitant exotropia had decreased ALFF in the parieto-occipital regions. Li et al. (2016) reported that intermittent exotropia patients showed increased neural activities in the parietal lobule during fusion stimulus. He et al. (2021) found that the intermittent exotropia patients showed decreased functional connectivity (FC) between the primary visual cortex and right cuneus and right postcentral gyrus. Yu et al. (2022) reported that strabismus patients had increased FC within the visual network and sensorimotor network. Peng et al. (2021) demonstrated that the strabismus group showed significantly decreased homotopic connectivity values in the cerebellum and frontal superior orbital. Meanwhile, the visual cortex plays an important role in the formation of stereovision. The medial temporal (MT+) plays an important role in stereoscopic depth processing. Meanwhile, the dorsal visual pathway is involved in stereoscopic depth processing. Thus, the abovementioned studies evidenced that strabismus patients were accompanied by cerebral neural activity changes in several brain regions related to vision and vision-related eye movements. However, these studies have mainly focused on static neural activities changes in strabismus patients. Recent studies reported that human brain showed dynamic neural activity. Growing neuroimaging studies demonstrated that human brain showed dynamic spontaneous neural activity, which is involved in a variety of neurophysiological functions (Liu and Duyn, 2013; Zalesky et al., 2014). However, the effect of impaired stereoscopic vision on dynamic spontaneous neural activity in patients with CE remains unknown.

The human brain shows dynamic neural activity. Dynamic neural activity is involved in higher cognitive functions, such as consciousness (Cavanna et al., 2018) and cognition (Gonzalez-Castillo et al., 2019). The ALFF method is used to assess the local intrinsic brain activity (Zang et al., 2007). The dALFF method can be used to calculate the variance of ALFF with sliding-window approaches. A sliding-window correlation analysis, where the correlation is estimated for brain activity during multiple, shows possibly overlapping temporal segments. A dALFF method is a sensitive approach for investigating dynamic brain activity (Liao et al., 2019). Previous neuroimaging studies demonstrated that the dALFF method has been successfully applied to assess the dynamic neural mechanisms of diabetic retinopathy (Huang et al., 2021), primary dysmenorrhea pain (Gui et al., 2021), and blindness (Huang et al., 2020). Thus, we hypothesized that CE may be accompanied by abnormal dynamic brain activity changes.

Based on this assumption, the purpose of the study is to investigate the dynamic neural activity changes in patients with CE. Moreover, the support vector machine (SVM) method was applied to investigate the classification efficiency using dALFF as a feature.

## MATERIALS AND METHODS

### Participants

A total of 36 patients with CE and 36 healthy controls were recruited. The diagnostic criteria of patients with CE were as follows: (1) congenital CE, exodeviation angles between 15 and 80°. The exclusion criteria of CE individuals in the study were as follows: (1) with other ocular-related complications; (2) sensory exotropia, fixed exotropia.

### Ethical Statement

All research methods followed the Declaration of Helsinki and were approved by the Ethical Committee for Medicine of Jiangxi Provincial People's Hospital.

### MRI Acquisition

The MRI scanning was performed on a 3-tesla magnetic resonance scanner (Discovery MR 750 W system; GE Healthcare, Milwaukee, WI, USA) with the eight-channel head coil.

### FMRI Data Analysis

All preprocessing was performed using the toolbox for Data Processing & Analysis of Brain Imaging (DPABI, <http://www.rfmri.org/dpabi>), the more detailed steps refer to a previous study (Yan et al., 2016).

### DALFF Analysis

The dALFF method was performed using Temporal Dynamic Analysis (TDA) toolkits based on DPABI. Specifically, the R-fMRI indices mentioned above were computed with the hamming windows (window length = 30 TR, window step = 1 TR and window length = 70 TR, window step = 1). The CV (CV = SD/mean) of ALFF maps were prepared for further statistical analysis.

### SVM Analysis

The support vector machine algorithm was applied to investigate the classification. The following steps were followed: (1) the dALFF maps were selected as a classification feature. (2) Then, the SVM method was applied to classifier validation based on dALFF values in two groups. The receiver operating characteristic (ROC) curves and area under the curve (AUC) were also computed to evaluate the classification efficiency.

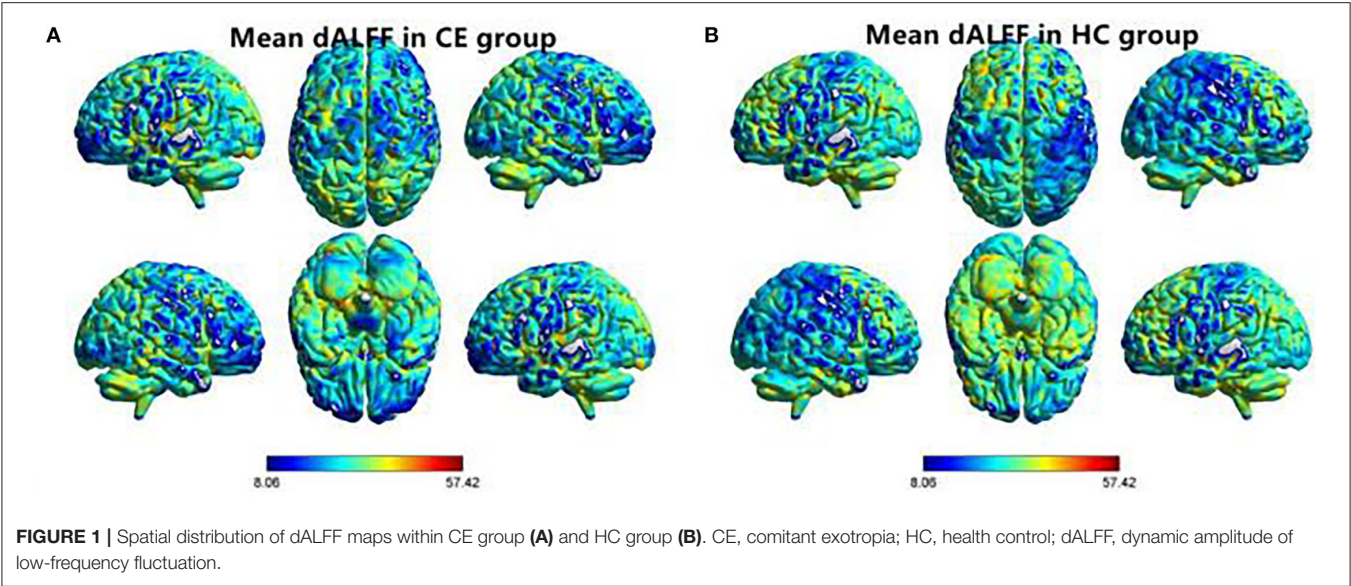
### Statistical Analysis

The independent sample *t*-test was used to assess the clinical scales between the two groups. The one-sample *t*-test was used to assess the spatial distribution of dALFF maps between two groups. Meanwhile, the two-sample *t*-test was applied to compare different dALFF values between the two groups (two-tailed,

**TABLE 1 |** Clinical indicates between two groups.

Condition	CE group	HC group	T-values	P-values
Gender (male/female)	(25/11)	(25/11)	N/A	N/A
Comitant category	Congenital exotropia	N/A	N/A	N/A
Age (years)	15.80 ± 2.46	16.00 ± 2.68	−0.240	0.812
Handedness	36 R	36 R	N/A	N/A

Independent *t*-test for clinical data (means ± SD). CE, comitant exotropia; HC, health control.

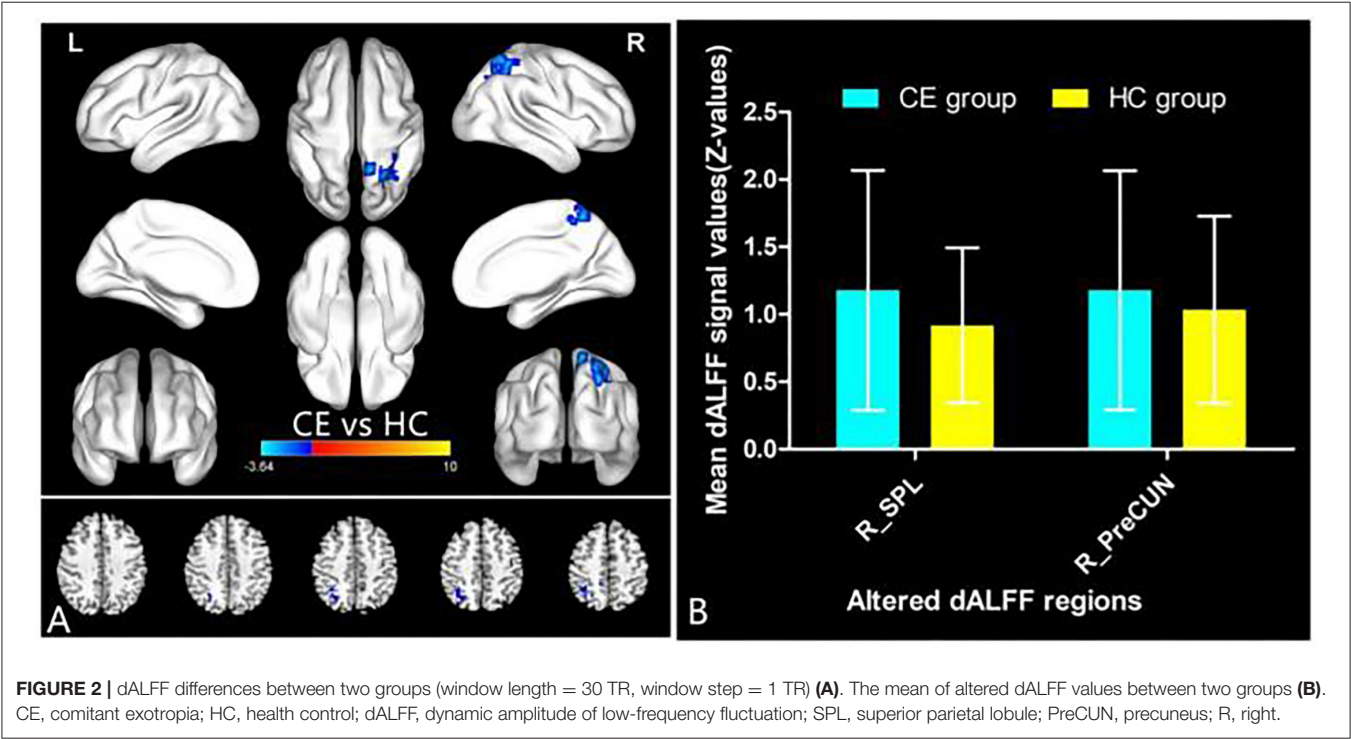


**FIGURE 1 |** Spatial distribution of dALFF maps within CE group (A) and HC group (B). CE, comitant exotropia; HC, health control; dALFF, dynamic amplitude of low-frequency fluctuation.

**TABLE 2 |** Different dALFF (window length = 30 TR, window step = 1 TR) values between two groups.

Condition	Brain regions	BA	Peak T-scores	MNI coordinates (x,y,z)	Cluster size (voxels)
CE<HC	R_SPL	–	–3.6382	39 –51 60	93
CE<HC	R_PreCUN	–	–3.4934	12 –54 66	46

CE, comitant exotropia; HC, health control; MNI: montreal neurological Institute; dALFF, dynamic amplitude of low-frequency fluctuation.



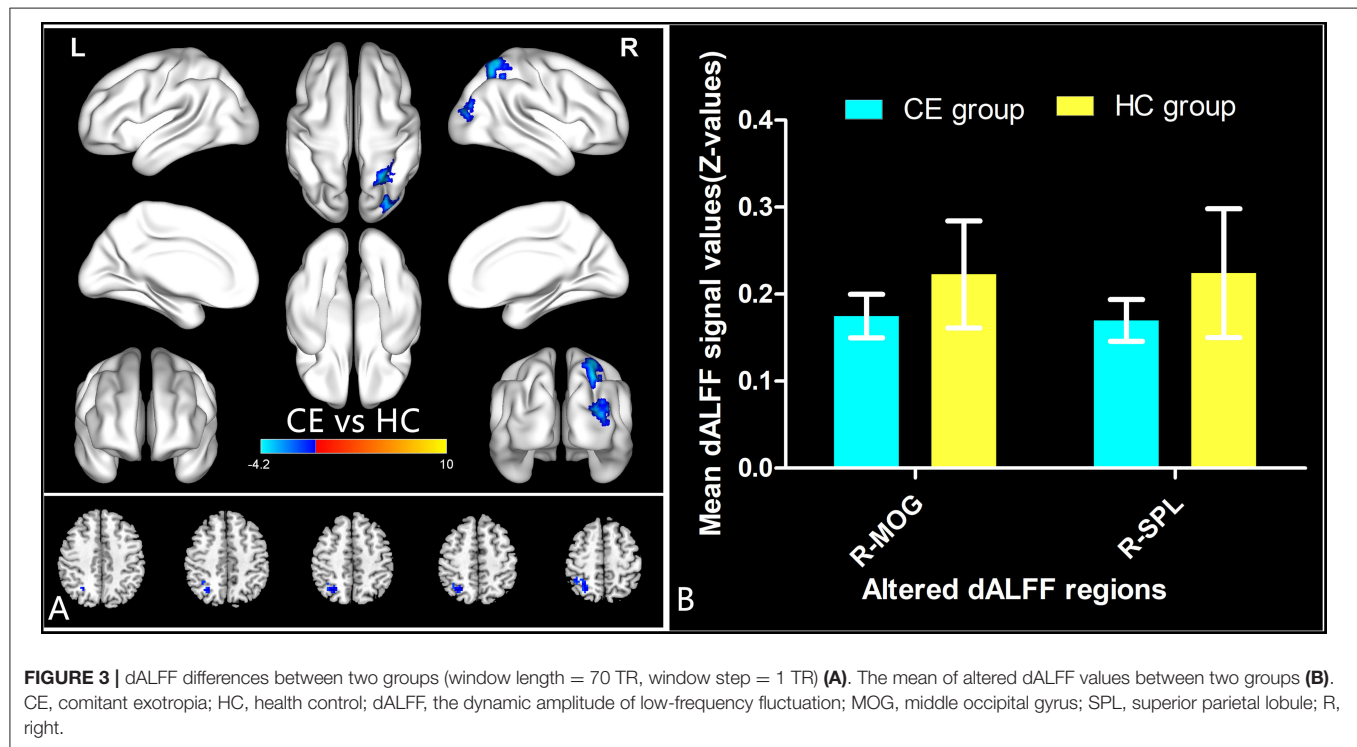
**FIGURE 2 |** dALFF differences between two groups (window length = 30 TR, window step = 1 TR) (A). The mean of altered dALFF values between two groups (B). CE, comitant exotropia; HC, health control; dALFF, dynamic amplitude of low-frequency fluctuation; SPL, superior parietal lobule; PreCUN, precuneus; R, right.



**TABLE 3** | Different dALFF (window length = 70 TR, window step = 1 TR) values between two groups.

Condition	Brain regions	BA	Peak T-scores	MNI coordinates (x, y, z)	Cluster size (voxels)
CE<HC	R-MOG	–	–4.1992	36 –78 9	76
CE<HC	R-SPL	–	–3.9941	27 –57 60	82

CE, comitant exotropia; HC, health control; MNI: montreal neurological Institute; dALFF, dynamic amplitude of low-frequency fluctuation.



voxel-level  $P < 0.01$ , Gaussian random field correction, cluster-level  $P < 0.05$ ).

## RESULTS

### Demographics and Disease Characteristics

The results of these clinical data were summarized in Table 1.

### Different DALFF Values Between Two Groups

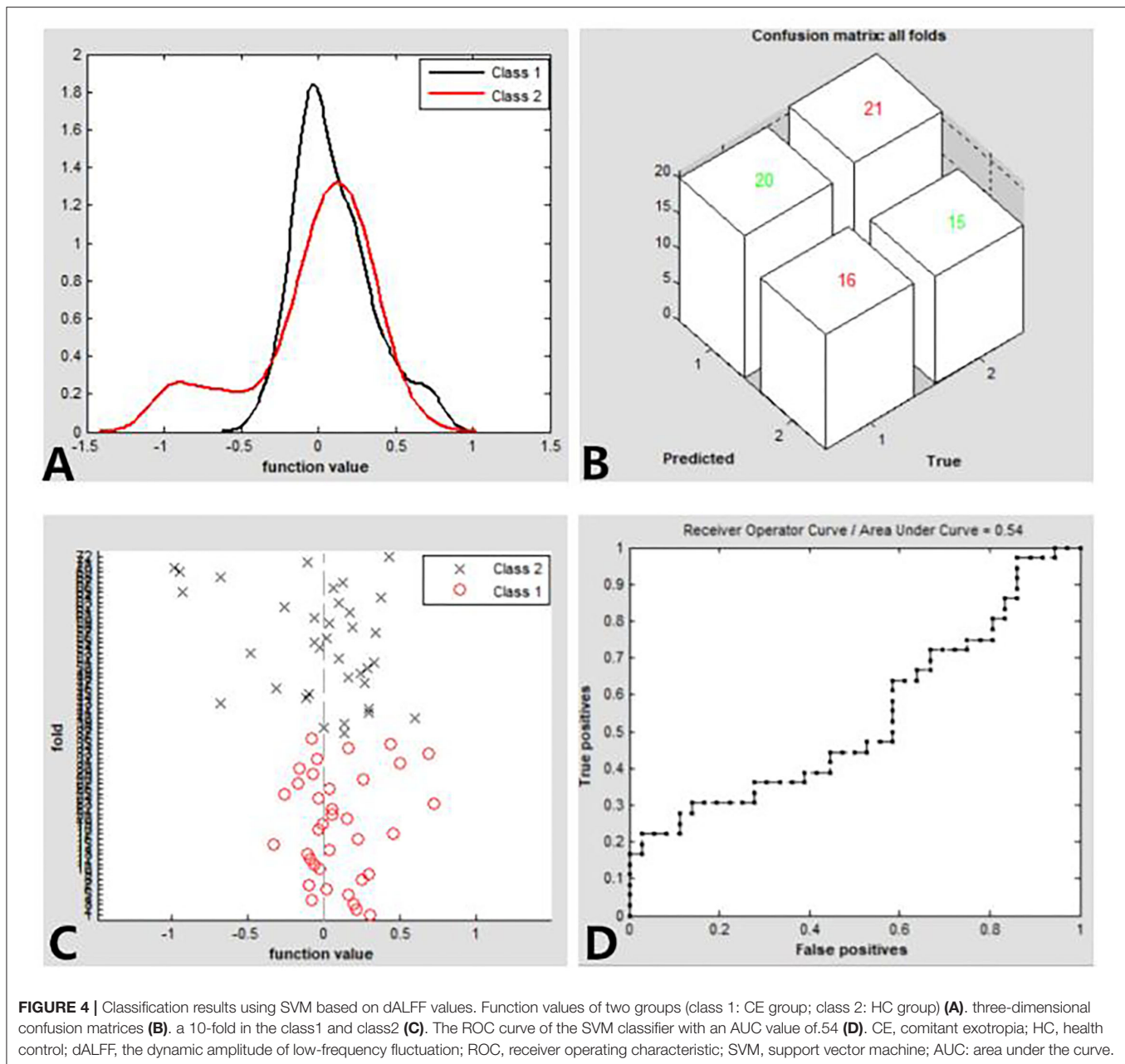
The spatial distribution of dALFF maps in two groups is shown in Figures 1A,B. Compared with the HCs, patients with CE showed decreased dALFF values in the R\_SPL and R\_PreCUN (Table 2 and Figure 2A). The mean values of different dALFF values were shown with a histogram (Figure 2B). Compared with the HCs, patients with CE showed decreased dALFF values in the R\_MOG and R\_SPL (Table 3 and Figure 3A). The mean values of different dALFF values were shown with a histogram (Figure 3B).

### SVM Results

We found that the dALFF maps showed an accuracy of 48.61% and an area under a curve of 0.54 for distinguishing the patients with CE from HCs. Figure 3 shows the classification results using SVM based on dALFF values. The function values of two groups (class 1: CE group; class 2: HC group; Figure 4A) had three-dimensional confusion matrices from machine learning analysis (Figure 4B) which have a 10-fold in class 1 and class 2 (Figure 4C). The ROC curve of the SVM classifier with an AUC value of 0.54 (Figure 4D).

## DISCUSSION

In our study, the dALFF method was applied to investigate the dynamic neural activity changes in patients with CE. Compared with the HCs, patients with CE showed decreased dynamic neural activity changes in the right SPL and right PreCUN, which might mirror the neuropathological mechanism of stereoscopic dysfunction in patients with CE. Our study demonstrated the decreased temporal variability of dALFF in the right SPL and right PreCUN, indicating lower flexibility of these cerebral neural



activities, which might reflect impaired stereoscopic vision in patients with CE.

Binocular vision can fuse visual images from the retinas of both eyes. The image is processed by the brain and formation of the stereoscopic image. The binocular disparity enables us to achieve depth perception. Thus, stereoscopic vision depends upon good vision in both eyes and good cortical mechanisms for sensory fusion. Previous neuroimaging studies demonstrated that several brain regions are involved in stereoscopic information processing related to the visual cortex (Likova and Tyler, 2007), parieto-occipital regions (Shikata et al., 1996), and the middle temporal (Uka and DeAngelis, 2004).

In our study, we found that patients with CE showed decreased dynamic neural activity changes in the right superior parietal lobule, which is involved in the discrimination of pure stereo-optic disparity information (Gulyas and Roland, 1994). Svetlana S et al. demonstrated that there were several brain regions (inferior temporal gyrus, lateral occipital sulcus) related to stereoscopic vision (Georgieva et al., 2008). Thus, our studies demonstrated that patients with CE had decreased temporal variability of dALFF in the right superior parietal lobule, which might reflect the stereoscopic dysfunction in patients with CE.

Another important finding is that patients with CE showed decreased dynamic neural activity changes in the right precuneus.

The precuneus is the core component of the default mode network (DMN). The DMN is involved in emotion and cognition. Previous studies found that strabismus patients showed emotion and depression. Thus, the decreased temporal variability of dALFF in the right precuneus might reflect mood disorders in patients with CE.

There are some limitations to this study. First, we only selected 30 and 70 TR as the window length in the study. Second, our study used relatively small sample sizes. Third, the patients with CE were associated with different exotropia angles, which might be a bad influence on the result of our study.

## CONCLUSION

Our results showed that patients with CE had increased altered dynamic neural activity changes in the right SPL and right PreCUN, indicating lower flexibility of these cerebral neural activities, which might reflect impaired stereoscopic vision in patients with CE.

## REFERENCES

- Cavanna, F., Vilas, M. G., Palmucci, M., and Tagliazucchi, E. (2018). Dynamic functional connectivity and brain metastability during altered states of consciousness. *Neuroimage* 180(Pt B), 383–395. doi: 10.1016/j.neuroimage.2017.09.065
- Georgieva, S. S., Todd, J. T., Peeters, R., and Orban, G. A. (2008). The extraction of 3D shape from texture and shading in the human brain. *Cereb. Cortex* 18, 2416–2438. doi: 10.1093/cercor/bhn002
- Gonzalez-Castillo, J., Caballero-Gaudes, C., Topolski, N., Handwerker, D. A., Pereira, F., and Bandettini, P. A. (2019). Imaging the spontaneous flow of thought: distinct periods of cognition contribute to dynamic functional connectivity during rest. *Neuroimage* 202:116129. doi: 10.1016/j.neuroimage.2019.116129
- Gui, S. G., Chen, R. B., Zhong, Y. L., and Huang, X. (2021). Machine learning analysis reveals abnormal static and dynamic low-frequency oscillations indicative of long-term menstrual pain in primary dysmenorrhea patients. *J. Pain Res.* 14, 3377–3386. doi: 10.2147/JPR.S332224
- Gulyas, B., and Roland, P. E. (1994). Binocular disparity discrimination in human cerebral cortex: functional anatomy by positron emission tomography. *Proc. Natl. Acad. Sci. U.S.A.* 91, 1239–1243. doi: 10.1073/pnas.91.4.1239
- He, X., Hong, J., Liu, Z., Wang, Q., Li, T., Qu, X., et al. (2021). Decreased functional connectivity of the primary visual cortex and the correlation with clinical features in patients with intermittent exotropia. *Front. Neurol.* 12:638402. doi: 10.3389/fneur.2021.638402
- Huang, X., Wen, Z., Qi, C. X., Tong, Y., Dan, H. D., Xie, B. J., et al. (2020). Altered temporal dynamic intrinsic brain activity in late blindness. *Biomed. Res. Int.* 2020:1913805. doi: 10.1155/2020/1913805
- Huang, X., Wen, Z., Qi, C. X., Tong, Y., and Shen, Y. (2021). Dynamic changes of amplitude of low-frequency fluctuations in patients with diabetic retinopathy. *Front. Neurol.* 12:611702. doi: 10.3389/fneur.2021.611702
- Lee, Y. H., Repka, M. X., Borlik, M. F., Velez, F. G., Perez, C., Yu, F., et al. (2022). Association of strabismus with mood disorders, schizophrenia, and anxiety disorders among children. *JAMA Ophthalmol.* 140, 373–381. doi: 10.1001/jamaophthalmol.2022.0137
- Li, Q., Bai, J., Zhang, J., Gong, Q., and Liu, L. (2016). Assessment of cortical dysfunction in patients with intermittent exotropia: an fMRI study. *PLoS ONE* 11:e0160806. doi: 10.1371/journal.pone.0160806

## DATA AVAILABILITY STATEMENT

The data analyzed in this study is subject to the following licenses/restrictions: The raw data supporting the conclusions of this article will be made available by the authors, without undue reservation. Requests to access these datasets should be directed to Y-LZ, 804722489@qq.com.

## ETHICS STATEMENT

This study conformed with the Declaration of Helsinki and was approved by the Medical Ethics Committee of the Jiangxi Provincial People's Hospital. The patients/participants provided their written informed consent to participate in this study.

## AUTHOR CONTRIBUTIONS

R-BC, S-YY, C-GP, and Y-LZ contributed to data collection, statistical analyses, and wrote the manuscript. All authors contributed to the article and approved the submitted version.

- Liao, W., Li, J., Ji, G. J., Wu, G. R., Long, Z., Xu, Q., et al. (2019). Endless fluctuations: temporal dynamics of the amplitude of low frequency fluctuations. *IEEE Trans. Med. Imaging* 38, 2523–2532. doi: 10.1109/TMI.2019.2904555
- Likova, L. T., and Tyler, C. W. (2007). Stereomotion processing in the human occipital cortex. *Neuroimage* 38, 293–305. doi: 10.1016/j.neuroimage.2007.06.039
- Lin, S., Congdon, N., Yam, J. C., Huang, Y., Qiu, K., Ma, D., et al. (2014). Alcohol use and positive screening results for depression and anxiety are highly prevalent among Chinese children with strabismus. *Am. J. Ophthalmol.* 157, 894–900.e1. doi: 10.1016/j.ajo.2014.01.012
- Liu, X., and Duyn, J. H. (2013). Time-varying functional network information extracted from brief instances of spontaneous brain activity. *Proc. Natl. Acad. Sci. U.S.A.* 110, 4392–4397. doi: 10.1073/pnas.1216856110
- McBain, H. B., MacKenzie, K. A., Au, C., Hancox, J., Ezra, D. G., Adams, G. G., et al. (2014). Factors associated with quality of life and mood in adults with strabismus. *Br. J. Ophthalmol.* 98, 550–555. doi: 10.1136/bjophthalmol-2013-304220
- Peng, J., Yao, F., Li, Q., Ge, Q., Shi, W., Su, T., et al. (2021). Alternations of interhemispheric functional connectivity in children with strabismus and amblyopia: a resting-state fMRI study. *Sci. Rep.* 11:15059. doi: 10.1038/s41598-021-92281-1
- Shi, H., Wang, Y., Liu, X., Xia, L., Chen, Y., Lu, Q., et al. (2019). Cortical alterations by the abnormal visual experience beyond the critical period: a resting-state fMRI study on constant exotropia. *Curr. Eye Res.* 44, 1386–1392. doi: 10.1080/02713683.2019.1639767
- Shikata, E., Tanaka, Y., Nakamura, H., Taira, M., and Sakata, H. (1996). Selectivity of the parietal visual neurones in 3D orientation of surface of stereoscopic stimuli. *Neuroreport* 7, 2389–2394. doi: 10.1097/00001756-199610020-00022
- Uka, T., and DeAngelis, G. C. (2004). Contribution of area MT to stereoscopic depth perception: choice-related response modulations reflect task strategy. *Neuron* 42, 297–310. doi: 10.1016/S0896-6273(04)00186-2
- Xi, S., Yao, J., Zhang, S., Liu, R., Wu, L., Ye, X., et al. (2020). Disrupted neural signals in patients with concomitant exotropia. *Ophthalm. Physiol. Opt.* 40, 650–659. doi: 10.1111/opo.12715
- Yan, C. G., Wang, X. D., Zuo, X. N., and Zang, Y. F. (2016). DPABI: data processing and analysis for (resting-state) brain imaging. *Neuroinformatics* 14, 339–351. doi: 10.1007/s12021-016-9299-4
- Yu, K., Lin, Q., Ge, Q. M., Yu, C. Y., Li, Q. Y., Pan, Y. C., et al. (2022). Measuring functional connectivity in patients with strabismus using stationary functional

- magnetic resonance imaging: a resting-state network study. *Acta Radiol.* 63, 110–121. doi: 10.1177/0284185120983978
- Zalesky, A., Fornito, A., Cocchi, L., Gollo, L. L., and Breakspear, M. (2014). Time-resolved resting-state brain networks. *Proc. Natl. Acad. Sci. U.S.A.* 111, 10341–10346. doi: 10.1073/pnas.1400181111
- Zang, Y. F., He, Y., Zhu, C. Z., Cao, Q. J., Sui, M. Q., Liang, M., et al. (2007). Altered baseline brain activity in children with ADHD revealed by resting-state functional MRI. *Brain Dev.* 29, 83–91. doi: 10.1016/j.braindev.2006.07.002

**Conflict of Interest:** The authors declare that the research was conducted in the absence of any commercial or financial relationships that could be construed as a potential conflict of interest.

**Publisher's Note:** All claims expressed in this article are solely those of the authors and do not necessarily represent those of their affiliated organizations, or those of the publisher, the editors and the reviewers. Any product that may be evaluated in this article, or claim that may be made by its manufacturer, is not guaranteed or endorsed by the publisher.

Copyright © 2022 Chen, Ye, Pei and Zhong. This is an open-access article distributed under the terms of the Creative Commons Attribution License (CC BY). The use, distribution or reproduction in other forums is permitted, provided the original author(s) and the copyright owner(s) are credited and that the original publication in this journal is cited, in accordance with accepted academic practice. No use, distribution or reproduction is permitted which does not comply with these terms.





## OPEN ACCESS

## EDITED BY

Xin Huang,  
Jiangxi Provincial People's Hospital,  
China

## REVIEWED BY

Yu Lin Zhong,  
Jiangxi Provincial People's Hospital,  
China  
Chen-Xing Qi,  
Renmin Hospital of Wuhan University,  
China

## \*CORRESPONDENCE

Xiao-rong Wu  
wxr98021@126.com

†These authors have contributed  
equally to this work

## SPECIALTY SECTION

This article was submitted to  
Brain Imaging and Stimulation,  
a section of the journal  
Frontiers in Human Neuroscience

RECEIVED 01 June 2022

ACCEPTED 12 July 2022

PUBLISHED 05 August 2022

## CITATION

Ji Y, Cheng Q, Fu W-w, Zhong P-p,  
Huang S-q, Chen X-l and Wu X-r  
(2022) Exploration of abnormal  
dynamic spontaneous brain activity  
in patients with high myopia via  
dynamic regional homogeneity  
analysis.  
*Front. Hum. Neurosci.* 16:959523.  
doi: 10.3389/fnhum.2022.959523

## COPYRIGHT

© 2022 Ji, Cheng, Fu, Zhong, Huang,  
Chen and Wu. This is an open-access  
article distributed under the terms of  
the [Creative Commons Attribution  
License \(CC BY\)](#). The use, distribution  
or reproduction in other forums is  
permitted, provided the original  
author(s) and the copyright owner(s)  
are credited and that the original  
publication in this journal is cited, in  
accordance with accepted academic  
practice. No use, distribution or  
reproduction is permitted which does  
not comply with these terms.

# Exploration of abnormal dynamic spontaneous brain activity in patients with high myopia via dynamic regional homogeneity analysis

Yu Ji†, Qi Cheng†, Wen-wen Fu, Pei-peí Zhong,  
Shui-qin Huang, Xiao-lin Chen and Xiao-rong Wu\*

Department of Ophthalmology, The First Affiliated Hospital of Nanchang University, Nanchang, China

**Aim:** Patients with high myopia (HM) reportedly exhibit changes in functional brain activity, but the mechanism underlying such changes is unclear. This study was conducted to observe differences in dynamic spontaneous brain activity between patients with HM and healthy controls (HCs) via dynamic regional homogeneity (dReHo) analysis.

**Methods:** Resting-state functional magnetic resonance imaging (rs-fMRI) scans were performed on 82 patients with HM and 59 HCs who were closely matched for age, sex, and weight. The dReHo approach was used to assess local dynamic activity in the human brain. The association between mean dReHo signal values and clinical symptoms in distinct brain areas in patients with HM was determined via correlation analysis.

**Results:** In the left fusiform gyrus (L-FG), right inferior temporal gyrus (R-ITG), right Rolandic operculum (R-ROL), right postcentral gyrus (R-PoCG), and right precentral gyrus (R-PreCG), dReHo values were significantly greater in patients with HM than in HCs.

**Conclusion:** Patients with HM have distinct functional changes in various brain regions that mainly include the L-FG, R-ITG, R-ROL, R-PoCG, and R-PreCG. These findings constitute important evidence for the roles of brain networks in the pathophysiological mechanisms of HM and may aid in the diagnosis of HM.

## KEYWORDS

high myopia, brain function, brain region, resting-state functional magnetic resonance imaging, dynamics regional homogeneity

## Introduction

High myopia (HM), a common ophthalmic disease, is the state of myopia with a refractive error of  $-6$  diopters or worse (Flitcroft et al., 2019). In East Asia, approximately 80–90% of young people have myopia, and one-fifth of these people have HM (Wu et al., 2016). It is estimated that, by 2050, there will be 938 million individuals with HM (9.8% of the global population) (Holden et al., 2016). High academic pressures and limited time outdoors are regarded as key risk factors for myopia (Morgan et al., 2021). The high prevalence of myopia leads to an increased incidence of HM because of the relationship between these two diseases (Morgan et al., 2018). Excessive axial elongation is the most important pathological change in patients with HM; it can cause retinal detachment, choroidal neovascularization, macular hemorrhage, and retinal ischemia, all of which lead to impaired visual function (Piao et al., 2021). In clinical practice, resting-state functional magnetic resonance imaging (rs-fMRI) has recently received considerable attention. Some studies have shown that patients with HM exhibit changes in brain function, mainly in terms of cognitive function (Zhang et al., 2020), but the differences in dynamic spontaneous brain activity between patients with HM and healthy controls (HCs) remain unknown.

Resting-state functional magnetic resonance imaging is an emerging neuroimaging modality that provides a new non-invasive technique to study the relationship between spontaneous brain activity and clinical manifestations. Compared with other fMRI methods, rs-fMRI has the advantages of direct signal acquisition and the detection of functional regions in various patient populations (Smitha et al., 2017). Patients with HM reportedly exhibit significantly decreased functional connectivity (FC) between the supramarginal gyrus and rostrolateral prefrontal cortex, as well as between the ventral attention and frontoparietal control networks (Zhai et al., 2016). Huang et al. (2016) demonstrated that the amplitude of low-frequency fluctuation (ALFF) in the bilateral inferior frontal gyrus was considerably lower in patients with HM than in HCs. The above studies provide a neuroimaging basis for a better understanding of attentional control problems in patients with HM. Nevertheless, most rs-fMRI studies show that functional brain activity is stationary throughout the resting scan, but they overlook the time-dependent nature of spontaneous neuronal activity fluctuation in the brain (Calhoun et al., 2014; Liao et al., 2015, 2019). Regional homogeneity (ReHo) can only reflect the static characteristics of human spontaneous brain activity, which contradicts the notion that resting-state spontaneous neurocerebral activity has time-dependent dynamic characteristics. Thus, there has been an increasing focus on dynamic processes in spontaneous brain activity. Recently, dynamic regional homogeneity (dReHo) has been used in studies of various diseases to investigate the dynamic variability of spontaneous neuronal brain activity.

Dynamic regional homogeneity is a commonly used analysis in rs-fMRI, which can show the dynamic temporal consistency of spontaneous brain activity between neighboring voxels, describe similarities in local brain activity, and explore the functional coordination of spontaneous neural activity (Zang et al., 2004). Dynamics amplitude of low frequency fluctuation (dALFF) is an analytical method that combines the ALFF and a sliding window (Cui et al., 2020); this method measures the intensity of low-frequency oscillation in spontaneous neural activity, which can represent the intensity of neural activity in a single acceleration and demonstrate excitability in specific regions of the cerebral cortex (Zang et al., 2007). Thus far, ALFF technology has been used to study functional changes in spontaneous brain activity in patients with HM (Huang et al., 2016). In contrast to ReHo, dReHo involves the use of a sliding window method; areas with large fluctuations in dReHo are generally functional centers of the brain (Hutchison et al., 2013). dReHo has been used in studies of neuropsychiatric diseases, such as brain networks involved in bipolar disorder, clinical depression, trigeminal neuralgia, and other diseases (Yan et al., 2019; Sun et al., 2021). To our knowledge, no study has explored dReHo abnormalities in patients with HM. There is increasing evidence that patients with HM have a greater cognitive impairment as compared to HCs (Zhang et al., 2020). Here, we investigated whether dReHo values differ between patients with HM and HCs, which may be related to the cognitive changes caused by HM.

## Participants and methods

### Participants

From August 2021 to December 2021, 82 patients with HM and 59 HCs were examined in the Department of Ophthalmology at Nanchang University's First Affiliated Hospital. For each participant, age, sex, and educational background were all met. People with brain disorders were excluded based on their clinical findings and physical assessment. All participants were examined in the same clinic and provided written informed consent to participate in the study. All procedures were conducted in accordance with the Declaration of Helsinki, and ethical approval was granted by the Nanchang University's First Affiliated Hospital's Medical Ethics Committee (Jiangxi Province, China).

The inclusion criteria for patients with HM were the binocular vision of  $-6$  diopters or worse; corrected decimal visual acuity better than 1.0; and the completion of MRI-related tests, optical coherence tomography, ultrasonography, and other ophthalmic examinations. The exclusion criteria

for patients with HM were binocular vision better than -6 diopters, retinal detachment, maculopathy, choroidal neovascularization, retinal pigment epithelial disease, history of ocular trauma or ophthalmic surgery, neurological disease, and/or cerebral infarction.

Healthy controls were randomly selected from Nanchang City according to their age, sex, and educational background. The inclusion criteria for HCs were no ocular disease; no major illness (e.g., neurological illness or cerebral infarction); uncorrected decimal visual acuity better than 1.0; and the completion of MRI-associated tests, optical coherence tomography, ultrasonography, and other ophthalmic examinations.

## fMRI data acquisition

A 3-T Trio Magnetic Resonance Imaging Scanning System (Trio Tim, Siemens Medical Systems, Erlangen, Germany) was used to collect all MRI data. During image acquisition, we asked participants to close their eyes, minimize motion, and avoid falling asleep. We also asked participants to use earplugs to reduce the effects of head motion and machine noise during scanning. The following three-dimensional high-resolution T1WI parameters were used: repetition time = 1,900 ms, echo time = 2.26 ms, thickness = 1, no intersection gap, acquisition matrix =  $256 \times 256$ , field of view =  $240 \times 240 \text{ mm}^2$ , and flip angle =  $12^\circ$ .

## fMRI data processing

In the brain imaging data processing and analysis toolbox (Data Processing and Analysis of Brain Imaging; DPABI),<sup>1</sup> the sliding time window method was used to calculate the dReHo index. In accordance with a previously described method, the minimum window length of the sliding time window was set at  $\geq 1/f_{\min}$  (the minimum frequency of the time series) because a shorter window length would increase the risk of false fluctuations in the time series (Leonardi and Van De Ville, 2015).

## Sliding time window analysis

In this study, the window length was 30 repetition time (TR) and the step size was 1 TR. In each time window, the ReHo indices of all brain voxels were calculated. Next, the standard deviations (SDs) of these ReHo brain maps were calculated to characterize the dynamics of ReHo. Finally, the smoothing kernel was set at  $8 \times 8 \times 8 \text{ mm}^3$  to smooth dReHo images.

<sup>1</sup> <http://rfmri.org/dpabi>

## Statistical analysis

Two-sample *t*-tests were performed on the fMRI data using SPM8 software (two-tailed voxel-level:  $p < 0.01$ , glomerular filtration rate (GRF) correction, cluster-level:  $p < 0.05$ ), which allows the assessment of differences in zReHo maps between two groups *via* the GRF method. The GRF method was used to compensate for multiple comparisons and to adjust for age and sex.

Based on the dReHo calculations, some brain regions showed differences in signals between patients with HM and HCs. Thus, the mean dReHo value in each region was obtained by averaging all voxels within that region.

## Results

### Demographics

This study contained 82 patients with HM (43 men and 39 women, mean age  $26.53 \pm 5.291$  years) and 59 HCs (24 men and 35 women, mean age  $25.67 \pm 3.102$  years). Demographic characteristics are shown in **Table 1**.

### Group differences in dynamic regional homogeneity

**Figure 1** shows comparisons between the HM and HC groups. dReHo values in the left fusiform gyrus (L-FG), right inferior temporal gyrus (R-ITG), right Rolandic operculum (R-ROL), right postcentral gyrus (R-PoCG), and right precentral gyrus (R-PreCG) were significantly higher in patients with HM than in HCs. The mean values of differences in dReHo between the two groups are shown in **Figure 2**. The mean differences in dReHo values between HM patients and HCs are shown in **Table 2**.

## Discussion

To our knowledge, this is the first study to use the dReHo method for the estimation of the effect of HM on dynamic spontaneous brain activity. The dReHo method can help to provide a greater understanding of HM-related functional

TABLE 1 Demographic characteristics of patients with HM and HCs.

Characteristic	HM	HC
Sex (male/female)	43/39	24/35
Age (years)	$26.53 \pm 5.291$	$25.67 \pm 3.102$

HM, high myopia; HC, healthy control.

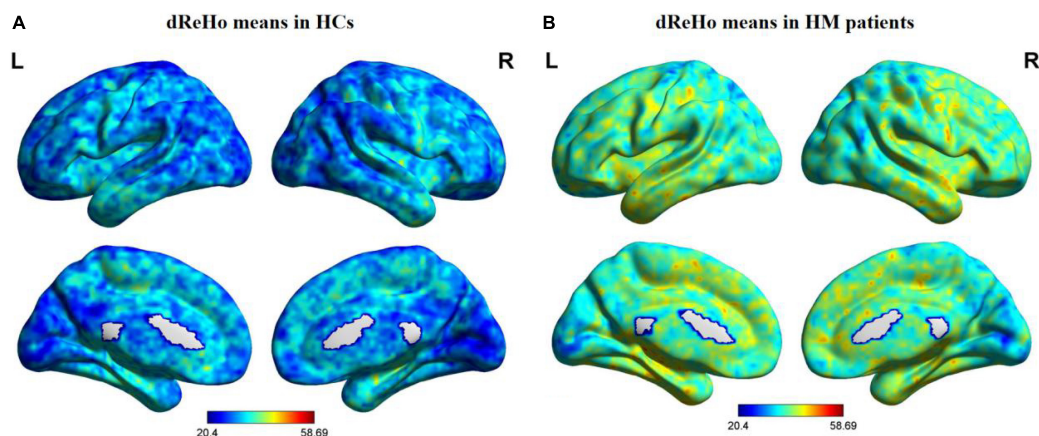


FIGURE 1

Distribution patterns of dReHo values are observed at the group level in HCs and patients with HM. Note: One-sample  $t$ -tests were used to compare dReHo maps between HCs (A) and patients with HM (B) ( $p < 0.01$ ). HCs, healthy controls; HM, high myopia; dReHo, dynamic regional homogeneity analysis; L, left; R, right.

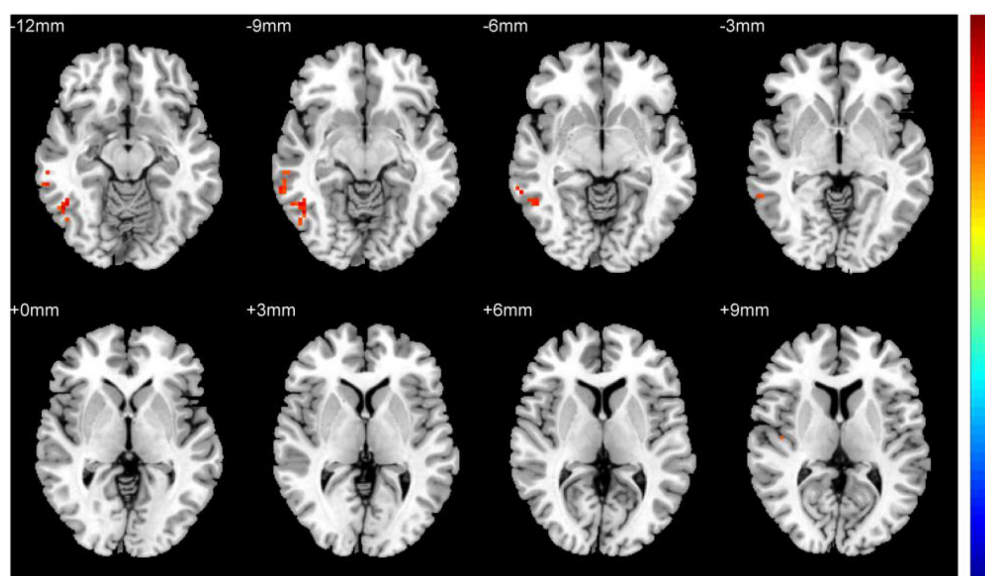


FIGURE 2

Comparison of differences in dReHo values between HCs and patients with HM. Significant differences in dReHo values are observed in the L-FG, R-ITG, R-ROL, R-PoCG, and R-PreCG. L-FG, left fusiform gyrus; R-ITG, right inferior temporal gyrus; R-ROL, right Rolandic operculum; R-PoCG, right postcentral gyrus; R-PreCG, right precentral gyrus.

remodeling in the brain. We found that patients with HM had significantly increased dReHo values in the L-FG, R-ITG, R-ROL, R-PoCG, and R-PreCG, which suggested a degree of synchronization in dynamic spontaneous brain activity among those regions. These changes could be linked to the activity of various areas in the brain.

The L-FG has a significant impact on language morphological processing (Zou et al., 2015), lexical processing of real words, and grapheme-to-phoneme processing of pseudo-words (Krishnamurthy et al., 2019). The FG has

spatially separated regions: the right side is more sensitive to facial recognition, while the left side is more sensitive to language recognition (Harris et al., 2016). Zu et al. (2022) found that patients with persistent generalized tonic-clonic seizures (GTCS) had increased ALFF values in the bilateral FG, which may be useful as a novel neurological marker for persistent seizures in patients with GTCS. Jung et al. (2021) reported that L-FG volume was associated with the recognition of emotional intensity and facial emotion by people with schizophrenia spectrum psychosis. Chen B. et al. (2021) revealed that patients



**TABLE 2** Mean differences in dReHo values between patients with HM and HCs.

Brain region	BA	Peak t-score	MNI coordinates (x, y, z)	Cluster size (voxels)
L-FG	20	3.4825	-33, -39, -24	13
R-ITG	–	3.4744	66, -39, -15	24
R-ROL	–	4.5164	42, -24, 15	18
R-PoCG	–	4.6369	54, -12, 39	40
R-PreCG	–	4.6523	18, -27, 78	38

Two-tailed voxel-level:  $p < 0.01$ , GRF correction, cluster-level:  $p < 0.05$ . BA, Brodmann area; MNI, Montreal Neurological Institute; L-FG, left fusiform gyrus; R-ITG, right inferior temporal gyrus; R-ROL, right Rolandic operculum; R-PoCG, right postcentral gyrus; R-PreCG, right precentral gyrus.

with late-life depression (LLD) and odor identification (OI) dysfunction showed significantly increased ReHo values in the L-FG. Therefore, increased ReHo values in the L-FG may indicate an increased risk of OI dysfunction in patients with LLD. Moreover, a previous study showed that patients with HM have decreased FC in the L-FG, which may cause differences in tactile function between patients with HM and HCs (Wu et al., 2020). Consistent with the previous findings, we demonstrated that patients with HM had significantly increased dReHo values in the L-FG, which suggests that behaviors in this brain area are reinforced. Thus, we speculate that increased dReHo values in the L-FG are related to dysfunctional language morphological processing in patients with HM; in such patients, the increased dReHo values in the L-FG may compensate for the decline in language morphological processing function.

The R-ITG plays an important role in higher cognitive functions, such as visual and language comprehension, as well as emotional regulation (Lin et al., 2020). Wei et al. (2021) demonstrated that FC in the ITG was increased in patients who had migraine without aura. They noted that the ITG is regarded as a component of the default mode network (DMN) (Liu et al., 2017) and has been associated with worsening pain. Li H. et al. (2021) reported that ReHo values in the bilateral ITG were greater in patients with obstructive sleep apnea (OSA). They showed that increased ReHo values in the bilateral ITG were positively correlated with the apnea-hypopnea index (AHI). Yuan et al. (2016) found that patients with amnesic moderate cognitive impairment (aMCI) had considerably lower ReHo values in the ITG when compared with HCs. Such a change in ReHo values could serve as a sensitive functional imaging biomarker for aMCI. Furthermore, Tu et al. (2018) revealed that ReHo values in the R-ITG were significantly higher in alcohol-dependent individuals than in HCs; notably, this region is responsible for the representation and detection of complex object features. In support of the previous findings, our study showed that patients with HM had significantly greater dReHo levels in the R-ITG. Thus, we presume that increased dReHo values in the R-ITG may be indicative of deficits in higher cognitive functions and vision in patients with HM; they might represent a functional activity to compensate for such deficits.

The R-ROL is involved in the processing of integrated exteroceptive-interoceptive information (Blefari et al., 2017). During the perception of pleasant auditory information, motor-related circuitry in the ROL may facilitate the formation of vocal representations (Koelsch et al., 2006). Zhang et al. (2021) demonstrated that individuals with addiction-related disorders had common decreases in gray matter (GM) volume in the R-ROL. They discovered similar structural changes in the prefrontal and insular areas of the brain among patients with different subtypes of addiction. Furthermore, Wollman et al. (2017) found that length of opioid use was negatively associated with GM in the R-ROL, which suggested that opioid addiction could lead to the disintegration of strongly overlapping structural and functional systems. Additionally, Li L. et al. (2021) reported that in the R-ROL, patients with Crohn's disease (CD) had considerably increased FC intensity. This could be a positive feedback mechanism for increased sensitivity to visceral sensory information, which modulates the brain's response to such information and may exacerbate inflammation. In a separate study, Li J. et al. (2021) revealed that, compared with HCs, patients with Parkinson's disease (PD) had considerably lower ReHo values in the R-ROL; this suggested a negative relationship between ReHo values and cognition. Indeed, the R-ROL has been associated with the severity of alterations in psychological domains, such as apathy, despair, and anxiety (Sutoko et al., 2020). Expanding upon the prior findings, this study showed that patients with HM had considerably higher dReHo values in the R-ROL, which suggests that behaviors in this brain area are reinforced. Thus, we speculate that HM leads to increased R-ROL activity, which can cause deficits in the processing of integrated exteroceptive-interoceptive signals in patients with HM; the increased dReHo values in the R-ROL may compensate for the reduced integration of exteroceptive-interoceptive signals.

The R-PoCG contributes to the processing of sensory data from various parts of the body (Kropf et al., 2019). Additionally, the PoCG is the main sensory reception area for touch, proprioception, pain, and temperature (Cauda et al., 2009). Hu et al. (2018) demonstrated that patients with HM had significantly decreased degree centrality (DC) values in the R-PoCG, which confirmed sensorimotor network (SMN) remodeling in such patients. Huang et al. (2016) reported that patients with HM showed higher ALFF values in the R-PoCG. Furthermore, Chen W. et al. (2021) found that patients with thyroid-associated ophthalmopathy (TAO) had significantly decreased DC values in the R-PoCG; the duration of illness was negatively correlated with DC values in the PoCG. Additionally, Zhen et al. (2018) revealed that patients with aMCI had considerably higher ReHo values in the R-PoCG. Such localized changes in FC imply that these networks simultaneously experience functional deficiencies and compensation. In the present study, we found that patients with HM had considerably higher dReHo values in the R-PoCG, which suggests that

behaviors in this brain area are reinforced. Thus, we speculate that HM leads to increased R-PoCG activity, which may broadly impair the processing of sensory information in patients with HM. However, the increased dReHo value in the R-PoCG may compensate for this reduced sensory processing ability.

The R-PreCG plays a critical role in sensorimotor processing (Desmurget et al., 2014). Tong et al. (2021) demonstrated that patients with iridocyclitis had significantly decreased ALFF in the R-PreCG. Wang et al. (2021) reported that patients with primary angle-closure glaucoma showed significantly decreased fractional ALFF in the R-PreCG. Furthermore, Jiang et al. (2021) revealed that, compared with HCs, patients with diabetic optic neuropathy had significantly higher ALFF values in the R-PreCG; they suggested that ALFF could be used to distinguish patients with diabetic optic neuropathy from individuals without the disease. Additionally, Duan et al. (2014) found that patients with neuromyelitis optica (NMO) had significantly decreased white matter volumes in the R-PreCG, which indicated the presence of subtle white matter damage to the motor, visual, and cognitive systems in such patients. Our present findings indicated that the HM group had considerably higher dReHo values in the R-PreCG, which suggests that behaviors in this brain area are reinforced. Therefore, we speculate that increased dReHo values in the R-PreCG lead to deficits in the sensorimotor processing of patients with HM; the increased dReHo values in the R-PreCG may compensate for this reduced sensorimotor processing ability.

Importantly, this study had some limitations. First, patients with HM in this trial were mostly young adults. Second, the data were frequently affected by some unavoidable factors in the fMRI environment (e.g., heartbeat, muscle beat, and respiratory motion). Finally, the patients had various lengths of HM history, which may have affected the accuracy of the findings. In future studies, we plan to focus on including participants of all ages and improving the test environment.

## Conclusion

Our results suggest that, compared with HCs, patients with HM have altered dReHo values in various brain regions, which implies that HM causes extensive changes in dynamic spontaneous brain activity; these changes presumably lead to the corresponding clinical manifestations. Our findings offer new insights into the causes and neural mechanisms of HM, and they may serve as guidance for its diagnosis.

## Data availability statement

The raw data supporting the conclusions of this article will be made available by the authors, without undue reservation.

## Ethics statement

The studies involving human participants were reviewed and approved by Nanchang University's First Affiliated Hospital's Medical Ethics Committee. The patients/participants provided their written informed consent to participate in this study. Written informed consent was obtained from the individual(s) for the publication of any potentially identifiable images or data included in this article.

## Author contributions

YJ was responsible for writing the manuscript. QC was in charge of proofreading and refining the manuscript's wording. W-WF, P-PZ, S-QH, and X-LC contributed to data collection and statistical analyses. YJ and QC designed the protocol and contributed to the MRI analysis. YJ, QC, and X-RW designed the study, oversaw all clinical aspects of study conduct, and manuscript preparation. All authors contributed to the article and approved the submitted version.

## Funding

The authors acknowledge the assistance provided by the National Nature Science Foundation of China (grant nos. 82160207, 81760179, and 81360151), the Health Development Planning Commission Science Foundation of Jiangxi Province (grant no. 20185118), the Key Research Plan of Jiangxi Provincial Science and Technology Department (grant no. 20192BBG70042), and the Key Projects of Jiangxi Youth Science Fund (grant no. 20202ACBL216008).

## Conflict of interest

The authors declare that the research was conducted in the absence of any commercial or financial relationships that could be construed as a potential conflict of interest.

## Publisher's note

All claims expressed in this article are solely those of the authors and do not necessarily represent those of their affiliated organizations, or those of the publisher, the editors and the reviewers. Any product that may be evaluated in this article, or claim that may be made by its manufacturer, is not guaranteed or endorsed by the publisher.

# References

- Blefari, M. L., Martuzzi, R., Salomon, R., Bello-Ruiz, J., Herbelin, B., Serino, A., et al. (2017). Bilateral Rolandic operculum processing underlying heartbeat awareness reflects changes in bodily self-consciousness. *Eur. J. Neurosci.* 45, 1300–1312. doi: 10.1111/ejn.13567
- Calhoun, V. D., Miller, R., Pearson, G., and Adali, T. (2014). The chronnectome: Time-varying connectivity networks as the next frontier in fMRI data discovery. *Neuron* 84, 262–274. doi: 10.1016/j.neuron.2014.10.015
- Cauda, F., Sacco, K., Duca, S., Cocito, D., D'Agata, F., Geminiani, G. C., et al. (2009). Altered resting state in diabetic neuropathic pain. *PLoS One* 4:e4542. doi: 10.1371/journal.pone.0004542
- Chen, B., Zhong, X., Zhang, M., Mai, N., Wu, Z., Chen, X., et al. (2021). The additive effect of late-life depression and olfactory dysfunction on the risk of dementia was mediated by hypersynchronization of the hippocampus/fusiform gyrus. *Transl. Psychiatry* 11:172. doi: 10.1038/s41398-021-01291-0
- Chen, W., Wu, Q., Chen, L., Zhou, J., Chen, H. H., Xu, X. Q., et al. (2021). Aberrant brain voxel-wise resting state fMRI in patients with thyroid-associated ophthalmopathy. *J. Neuroimaging* 31, 773–783. doi: 10.1111/jon.12858
- Cui, Q., Sheng, W., Chen, Y., Pang, Y., Lu, F., Tang, Q., et al. (2020). Dynamic changes of amplitude of low-frequency fluctuations in patients with generalized anxiety disorder. *Hum. Brain Mapp.* 41, 1667–1676. doi: 10.1002/hbm.24902
- Desmurget, M., Richard, N., Harquel, S., Baraduc, P., Szathmari, A., Mottolese, C., et al. (2014). Neural representations of ethologically relevant hand/mouth synergies in the human precentral gyrus. *Proc. Natl. Acad. Sci. U.S.A.* 111, 5718–5722. doi: 10.1073/pnas.1321909111
- Duan, Y., Liu, Y., Liang, P., Jia, X., Ye, J., Dong, H., et al. (2014). White matter atrophy in brain of neuromyelitisoptica: A voxel-based morphometry study. *Acta Radiol.* 55, 589–593.
- Flitcroft, D. I., He, M., Jonas, J. B., Jong, M., Naidoo, K., Ohno-Matsui, K., et al. (2019). IMI - Defining and Classifying Myopia: A Proposed Set of Standards for Clinical and Epidemiologic Studies. *Invest. Ophthalmol. Vis. Sci.* 60:M20–M30. doi: 10.1167/iovs.18-25957
- Harris, R. J., Rice, G. E., Young, A. W., and Andrews, T. J. (2016). Distinct but Overlapping Patterns of Response to Words and Faces in the Fusiform Gyrus. *Cereb. Cortex* 26, 3161–3168. doi: 10.1093/cercor/bhv147
- Holden, B. A., Fricke, T. R., Wilson, D. A., Jong, M., Naidoo, K. S., Sankaridurg, P., et al. (2016). Global Prevalence of Myopia and High Myopia and Temporal Trends from 2000 through 2050. *Ophthalmology* 123, 1036–1042.
- Hu, Y. X., He, J. R., Yang, B., Huang, X., Li, Y. P., Zhou, F. Q., et al. (2018). Abnormal resting-state functional network centrality in patients with high myopia: Evidence from a voxel-wise degree centrality analysis. *Int. J. Ophthalmol.* 11, 1814–1820. doi: 10.18240/ijo.2018.11.13
- Huang, X., Zhou, F. Q., Hu, Y. X., Xu, X. X., Zhou, X., Zhong, Y. L., et al. (2016). Altered spontaneous brain activity pattern in patients with high myopia using amplitude of low-frequency fluctuation: A resting-state fMRI study. *Neuropsychiatr. Dis. Treat* 12, 2949–2956. doi: 10.2147/NDT.S118326
- Hutchison, R. M., Womelsdorf, T., Allen, E. A., Bandettini, P. A., Calhoun, V. D., Corbetta, M., et al. (2013). Dynamic functional connectivity: Promise, issues, and interpretations. *Neuroimage* 80, 360–378.
- Jiang, Y. P., Liu, W. F., Pan, Y. C., Shu, H. Y., Zhang, L. J., Li, Q. Y., et al. (2021). The abnormal fractional amplitude of low-frequency fluctuation changes in patients with diabetic optic neuropathy: A steady-state fMRI study. *J. Integr. Neurosci.* 20, 885–893. doi: 10.31083/jjin2004090
- Jung, S., Kim, J. H., Kang, N. O., Sung, G., Ko, Y. G., Bang, M., et al. (2021). Fusiform gyrus volume reduction associated with impaired facial expressed emotion recognition and emotional intensity recognition in patients with schizophrenia spectrum psychosis. *Psychiatry Res. Neuroimaging* 307:11226. doi: 10.1016/j.pscychres.2020.111226
- Koelsch, S., Fritz, T., Dy, V. Cramon, Müller, K., and Friederici, A. D. (2006). Investigating emotion with music: An fMRI study. *Hum. Brain Mapp.* 27, 239–250.
- Krishnamurthy, L. C., Krishnamurthy, V., Crosson, B., Rothman, D. L., Schwam, D. M., Greenberg, D., et al. (2019). Strength of resting state functional connectivity and local GABA concentrations predict oral reading of real and pseudo-words. *Sci. Rep.* 9:11385. doi: 10.1038/s41598-019-47889-9
- Kropf, E., Syan, S. K., Minuzzi, L., and Frey, B. N. (2019). From anatomy to function: The role of the somatosensory cortex in emotional regulation. *Braz. J. Psychiatry* 41, 261–269.
- Leonardi, N., and Van De Ville, D. (2015). On spurious and real fluctuations of dynamic functional connectivity during rest. *Neuroimage* 104, 430–436. doi: 10.1016/j.neuroimage.2014.09.007
- Li, H., Li, L., Kong, L., Li, P., Zeng, Y., Li, K., et al. (2021). Frequency-Specific Regional Homogeneity Alterations and Cognitive Function in Obstructive Sleep Apnea Before and After Short-Term Continuous Positive Airway Pressure Treatment. *Nat. Sci. Sleep* 13, 2221–2238. doi: 10.2147/NSS.S344842
- Li, J., Liao, H., Wang, T., Zi, Y., Zhang, L., Wang, M., et al. (2021). Alterations of Regional Homogeneity in the Mild and Moderate Stages of Parkinson's Disease. *Front. Aging Neurosci.* 13:676899. doi: 10.3389/fpsy.2022.847366
- Li, L., Ma, J., Xu, J. G., Zheng, Y. L., Xie, Q., Rong, L., et al. (2021). Brain functional changes in patients with Crohn's disease: A resting-state fMRI study. *Brain Behav.* 11:e2243.
- Liao, X., Yuan, L., Zhao, T., Dai, Z., Shu, N., Xia, M., et al. (2015). Spontaneous functional network dynamics and associated structural substrates in the human brain. *Front. Hum. Neurosci.* 9:478. doi: 10.3389/fnhum.2015.00478
- Liao, W., Li, J., Ji, G. J., Wu, G. R., Long, Z., Xu, Q., et al. (2019). Endless Fluctuations: Temporal Dynamics of the Amplitude of Low Frequency Fluctuations. *IEEE Trans. Med. Imaging* 2019, 2523–2532. doi: 10.1109/TMI.2019.2904555
- Lin, Y. H., Young, I. M., Conner, A. K., Glenn, C. A., Chakraborty, A. R., Nix, C. E., et al. (2020). Anatomy and White Matter Connections of the Inferior Temporal Gyrus. *World Neurosurg* 143:e656–e666.
- Liu, P., Liu, Y., Wang, G., Yang, X., Jin, L., Sun, J., et al. (2017). Aberrant default mode network in patients with primary dysmenorrhea: A fMRI study. *Brain Imaging Behav.* 11, 1479–1485.
- Morgan, I. G., French, A. N., Ashby, R. S., Guo, X., Ding, X., He, M., et al. (2018). The epidemics of myopia: Aetiology and prevention. *Prog. Retin Eye Res.* 62, 134–149.
- Morgan, I. G., Wu, P. C., Ostrin, L. A., Tideman, J., Yam, J. C., Lan, W., et al. (2021). IMI Risk Factors for Myopia. *Invest. Ophthalmol. Vis. Sci.* 62:3.
- Piao, H., Guo, Y., Zhang, H., Sung, M. S., and Park, S. W. (2021). Acircularity and circularity indexes of the foveal avascular zone in high myopia. *Sci. Rep.* 11:16808.
- Smitha, K. A., Akhil Raja, K., Arun, K. M., Rajesh, P. G., Thomas, B., Kapilamoorthy, T. R., et al. (2017). Resting state fMRI: A review on methods in resting state connectivity analysis and resting state networks. *Neuroradiol. J.* 30, 305–317.
- Sun, F., Liu, Z., Yang, J., Fan, Z., and Yang, J. (2021). Differential Dynamical Pattern of Regional Homogeneity in Bipolar and Unipolar Depression: A Preliminary Resting-State fMRI Study. *Front. Psychiatry* 12:764932. doi: 10.3389/fpsy.2021.764932
- Sutoko, S., Atsumori, H., Obata, A., Funane, T., Kandori, A., Shimomaga, K., et al. (2020). Lesions in the right Rolandic operculum are associated with self-rating affective and apathetic depressive symptoms for post-stroke patients. *Sci. Rep.* 10:20264. doi: 10.1038/s41598-020-77136-5
- Tong, Y., Huang, X., Qi, C. X., and Shen, Y. (2021). Assessment of spontaneous brain activity patterns in patients with iridocyclitis: A resting-state study. *Neuroreport* 32, 612–620. doi: 10.1097/WNR.0000000000001631
- Tu, X., Wang, J., Liu, X., and Zheng, J. (2018). Aberrant regional brain activities in alcohol dependence: A functional magnetic resonance imaging study. *Neuropsychiatr. Dis. Treat* 14, 847–853.
- Wang, R., Tang, Z., Liu, T., Sun, X., Wu, L., and Xiao, Z. (2021). Altered spontaneous neuronal activity and functional connectivity pattern in primary angle-closure glaucoma: A resting-state fMRI study. *Neurol. Sci.* 42, 243–251. doi: 10.1007/s10072-020-04577-1
- Wei, H. L., Li, J., Guo, X., Zhou, G. P., Wang, J. J., Chen, Y. C., et al. (2021). Functional connectivity of the visual cortex differentiates anxiety comorbidity from episodic migraineurs without aura. *J. Headache Pain* 22:40. doi: 10.1186/s10194-021-01259-x
- Wollman, S. C., Alhassoon, O. M., Hall, M. G., Stern, M. J., Connors, E. J., Kimmel, C. L., et al. (2017). Gray matter abnormalities in opioid-dependent patients: A neuroimaging meta-analysis. *Am. J. Drug Alcohol Abuse* 43, 505–517. doi: 10.1080/00952990.2016.1245312
- Wu, P. C., Huang, H. M., Yu, H. J., Fang, P. C., and Chen, C. T. (2016). Epidemiology of Myopia. *Asia Pac. J. Ophthalmol.* 5, 386–393.
- Wu, Y. J., Wu, N., Huang, X., Rao, J., Yan, L., Shi, L., et al. (2020). Evidence of cortical thickness reduction and disconnection in high myopia. *Sci. Rep.* 10:16239. doi: 10.1038/s41598-020-73415-3
- Yan, J., Li, M., Fu, S., Li, G., Wang, T., Yin, Y., et al. (2019). Alterations of Dynamic Regional Homogeneity in Trigeminal Neuralgia: A Resting-State fMRI Study. *Front. Neurol.* 10:1083. doi: 10.3389/fneur.2019.01083

- Yuan, X., Han, Y., Wei, Y., Xia, M., Sheng, C., Jia, J., et al. (2016). Regional homogeneity changes in amnesic mild cognitive impairment patients. *Neurosci. Lett.* 629, 1–8.
- Zang, Y., Jiang, T., Lu, Y., He, Y., and Tian, L. (2004). Regional homogeneity approach to fMRI data analysis. *Neuroimage* 22, 394–400.
- Zang, Y. F., He, Y., Zhu, C. Z., Cao, Q. J., Sui, M. Q., Liang, M., et al. (2007). Altered baseline brain activity in children with ADHD revealed by resting-state functional MRI. *Brain Dev.* 29, 83–91.
- Zhai, L., Li, Q., Wang, T., Dong, H., Peng, Y., Guo, M., et al. (2016). Altered functional connectivity density in high myopia. *Behav. Brain Res.* 303, 85–92.
- Zhang, M., Gao, X., Yang, Z., Wen, M., Huang, H., Zheng, R., et al. (2021). Shared gray matter alterations in subtypes of addiction: A voxel-wise meta-analysis. *Psychopharmacology* 238, 2365–2379.
- Zhang, X. W., Dai, R. P., Cheng, G. W., Zhang, W. H., and Long, Q. (2020). Altered amplitude of low-frequency fluctuations and default mode network connectivity in high myopia: A resting-state fMRI study. *Int. J. Ophthalmol.* 13, 1629–1636. doi: 10.18240/ijo.2020.10.18
- Zhen, D., Xia, W., Yi, Z. Q., Zhao, P. W., Zhong, J. G., Shi, H. C., et al. (2018). Alterations of brain local functional connectivity in amnesic mild cognitive impairment. *Transl. Neurodegener.* 7:26.
- Zou, L., Packard, J. L., Xia, Z., Liu, Y., and Shu, H. (2015). Neural Correlates of Morphological Processing: Evidence from Chinese. *Front. Hum. Neurosci.* 9:714. doi: 10.3389/fnhum.2015.00714
- Zu, M., Fu, L., Hu, M., Cao, X., Wang, L., Zhang, J., et al. (2022). Amplitude of Low-Frequency Fluctuation With Different Clinical Outcomes in Patients With Generalized Tonic-Clonic Seizures. *Front. Psychiatry* 13:847366.





## OPEN ACCESS

EDITED BY  
Dongrong Xu,  
Columbia University, United States

REVIEWED BY  
Yu Ji,  
The First Affiliated Hospital  
of Nanchang University, China  
Wenqing Xia,  
Nanjing No. 1 Hospital, China

\*CORRESPONDENCE  
Xin Huang  
2017103020035@whu.edu.cn

†These authors have contributed  
equally to this work

SPECIALTY SECTION  
This article was submitted to  
Brain Imaging and Stimulation,  
a section of the journal  
Frontiers in Human Neuroscience

RECEIVED 03 May 2022  
ACCEPTED 19 July 2022  
PUBLISHED 24 August 2022

CITATION  
Chen R-B, Zhong Y-L, Liu H and  
Huang X (2022) Machine learning  
analysis reveals abnormal functional  
network hubs in the primary  
angle-closure glaucoma patients.  
*Front. Hum. Neurosci.* 16:935213.  
doi: 10.3389/fnhum.2022.935213

COPYRIGHT  
© 2022 Chen, Zhong, Liu and Huang.  
This is an open-access article  
distributed under the terms of the  
Creative Commons Attribution License  
(CC BY). The use, distribution or  
reproduction in other forums is  
permitted, provided the original  
author(s) and the copyright owner(s)  
are credited and that the original  
publication in this journal is cited, in  
accordance with accepted academic  
practice. No use, distribution or  
reproduction is permitted which does  
not comply with these terms.

# Machine learning analysis reveals abnormal functional network hubs in the primary angle-closure glaucoma patients

Ri-Bo Chen<sup>1†</sup>, Yu-Lin Zhong<sup>2†</sup>, Hui Liu<sup>2</sup> and Xin Huang<sup>2\*</sup>

<sup>1</sup>Department of Radiology, Jiangxi Provincial People's Hospital, The First Affiliated Hospital of Nanchang Medical College, Nanchang, China, <sup>2</sup>Department of Ophthalmology, Jiangxi Provincial People's Hospital, The First Affiliated Hospital of Nanchang Medical College, Nanchang, China

**Background:** Primary angle-closure glaucoma (PACG) is a serious and irreversible blinding eye disease. Growing studies demonstrated that PACG patients were accompanied by vision and vision-related brain region changes. However, whether the whole-brain functional network hub changes occur in PACG patients remains unknown.

**Purpose:** The purpose of the study was to investigate the brain function network hub changes in PACG patients using the voxel-wise degree centrality (DC) method.

**Materials and methods:** Thirty-one PACG patients (21 male and 10 female) and 31 healthy controls (HCs) (21 male and 10 female) closely matched in age, sex, and education were enrolled in the study. The DC method was applied to investigate the brain function network hub changes in PACG patients. Moreover, the support vector machine (SVM) method was applied to distinguish PACG patients from HC patients.

**Results:** Compared with HC, PACG patients had significantly higher DC values in the right fusiform, left middle temporal gyrus, and left cerebellum\_4\_5. Meanwhile, PACG patients had significantly lower DC values in the right calcarine, right postcentral gyrus, left precuneus gyrus, and left postcentral gyrus. Furthermore, the SVM classification reaches a total accuracy of 72.58%, and the ROC curve of the SVM classifier has an AUC value of 0.85 ( $r = 0.25$ ).

**Conclusion:** Our results showed that PACG patients showed widespread brain functional network hub dysfunction relative to the visual network, auditory network, default mode network, and cerebellum network, which might shed new light on the neural mechanism of optic atrophy in PACG patients.

## KEYWORDS

PACG, degree centrality, fMRI, SVM, brain network

## Introduction

Primary angle-closure glaucoma (PACG) is a serious and irreversible blinding eye disease worldwide. Angle closure is a key pathological process in PACG patients. The main clinical manifestations of PACG are elevated intraocular pressure, eye pain, and vision loss. There are multiple risk factors for PACG, such as genetic predisposition (Wiggs and Pasquale, 2017), hypertension (Lowry and Sanders, 2021), diabetes mellitus (Song et al., 2016), and autonomic dysfunction (Na et al., 2010). Elevated intraocular pressure leads to retinal ganglion cell apoptosis in PACG patients, which is an important pathological feature of PACG. Visual field examination is important for the assessment of visual function in glaucoma patients (De Moraes et al., 2017). However, recent studies have shown that glaucoma causes optic nerve atrophy as well as trans-synaptic degeneration of visual pathways (Lawlor et al., 2018).

Magnetic resonance imaging (MRI) techniques have been successfully applied to identify changes in neural function and structure within the visual cortex of glaucoma patients. Zhou et al. (2017) demonstrated an expanded representation of parafoveal areas in the visual cortex of primary open-angle glaucoma (POAG) patients, compared with healthy controls (HCs). Duncan et al. (2012) demonstrated that POAG patients had differences in cerebral blood flow (CBF) between ventral V1 and dorsal V1. These differences were correlated with visual function in the superior and inferior visual fields. Wang et al. (2017) reported that the POAG patients had decreased functional connectivity within the visual network. Moreover, glaucoma patients exhibited structural changes in the brain. Using diffusion kurtosis imaging, Li et al. (2020) demonstrated that patients with normal-tension glaucoma had microstructural abnormalities in bilateral BA17, BA18, and BA19. Hernowo et al. (2011) found reduced visual pathway volumes in glaucoma patients; affected areas included the optic nerves, optic chiasm, optic tract, and optic radiations. The above studies indicated that patients with glaucoma have functional and structural changes in the visual pathways and visual cortex. To our knowledge, there have been few studies of whole-brain network changes in PACG patients.

The human brain is a complex functional connectome (Sporns, 2011) that plays important roles in physiological processes such as visual function (Wang et al., 2018) and auditory function (Gurtubay-Antolin et al., 2021). Previous neuroimaging studies demonstrated that brain functional network hubs are involved in the integration of information from network elements. Hubs enable the integration of diverse sources of information; they also balance opposing pressures during the evolution of segregated networks. Increased degree centrality (DC) values indicate the enhanced local network information transmission. Meanwhile, the decreased DC values indicate the impaired local network information transmission. The voxel-wise DC method is a graph-based technique

that measures the functional relationships of specific voxels throughout the connectivity matrix of the brain, rather than in specific nodes or networks (Zuo et al., 2012). The advantage of the DC method is that the functional network of the whole brain voxel can be calculated without presupposition experimental hypothesis. Machine learning methods combined with the fMRI method have provided a systematic approach for developing an automatic, objective, and sophisticated classification of diseases. The support vector machine (SVM) method is the most commonly used supervised machine learning algorithm for MRI classification that enables individual-level classification and detects biomarkers on the basis of neuroimaging data. Glaucoma is not only associated with functional abnormalities in the visual area but has also been associated with neurodegenerative diseases. However, the effects of optic atrophy on whole-brain network hubs in PACG patients remain unclear. Thus, we hypothesized that PACG patients are accompanied by brain functional network hub changes.

Based on this hypothesis, the present study was performed to determine whether PACG patients exhibited abnormal changes in brain function network hubs. Moreover, the SVM method was used to assess classification power using the DC map as a feature.

## Materials and methods

### Participants

In total, thirty-one patients with PACG (21 males and 10 females) were enrolled from the Department of Ophthalmology, Jiangxi Provincial People's Hospital. The diagnostic criteria of PACG were: (1) the intraocular pressure was greater than 21 mmHg in both eyes; (2) optic disc/cup area > 0.6; (3) typical vision field defect (paracentric obscura, arcuate obscura, nasal ladder, fan-shaped field defect, and peripheral field defect); (4) without any other ocular diseases.

The exclusion criteria of PACG were: (1) advanced PACG patients are associated with severe eye pain; (2) PACG patients with a history of surgery; (3) PACG patients with glaucoma-related eye complications, including neovascular glaucoma, high myopia, optic neuritis, cataracts, eye atrophy, and corneal edema; and (4) PACG patients with psychiatric disorders, brain trauma, and other diseases.

Thirty-one HCs (21 males and 10 females) were also recruited for this study. The inclusion criteria were: (1) without any ocular disease with uncorrected visual acuity (VA) > 1.0; (2) no cardiovascular system diseases; and no psychiatric disorders.

### Ethical statement

All research methods followed the Declaration of Helsinki and were approved by the Ethical Committee for Medicine of Jiangxi Provincial People's Hospital. Participants enrolled

in the study of their own accord and were informed of the purpose, methods, as well as potential risks before signing an informed consent form.

## Clinical evaluation

The VA of all subjects was measured by using the logMAR table and Intraocular pressure was assessed by using automatic intraocular pressure measurement. The best-corrected VA of both eyes was measured in each group.

## Magnetic resonance imaging data acquisition

MRI scanning was performed on a 3-Tesla MR scanner (750W GE Healthcare, Milwaukee, WI, United States) with an eight-channel head coil. All participants were required to close their eyes without falling asleep when undergoing MRI scanning. The subjects should be kept calm and not engaged in specific thoughts.

## Data pre-processing

All preprocessing was performed using the toolbox for Data Processing & Analysis of Brain Imaging (DPABI)<sup>1</sup> (Yan et al., 2016) and briefly following the steps: (1) the first ten volumes of BOLD maps were removed. (2) Slice timing and head motion correction were conducted. (4) Normalized fMRI data were re-sliced with a resolution of  $3 \times 3 \times 3 \text{ mm}^3$ . (5) Data detrends; (6) Linear regression analysis was applied to regress out several covariates (mean framewise displacement, global brain signal, and averaged signal from cerebrospinal fluid and white matter). (7) Temporal band-pass filtering was performed (0.01–0.08 Hz).

## Voxel-wise degree centrality analysis

According to previous studies, we analyzed the different degree of centrality values with a correlation threshold of ( $r = 0.15, 0.2, 0.25, 0.3$ ) in this study (Zuo et al., 2012). The voxel-wise functional network was generated for each subject, for which we took each voxel as a node and inter-voxel correlations as the edge. Within the default brain mask provided by DPABI (in the MNI-152 standard space with  $3 \times 3 \times 3 \text{ mm}^3$  voxel size and resolution of  $61 \times 73 \times 61$ ), we used the preprocessed functional images to perform a voxel-wise correlation analysis. From the  $n \times n$  Pearson's correlation coefficient matrix, a map

of the degree of the connectivity was computed by counting for each voxel the number of voxels it was correlated to above a threshold of  $r > 0.25$ . A high threshold was chosen to eliminate counting voxels that had low temporal correlation attributable to signal noise. The  $z$ -score map was smoothed with a 6-mm full-width-half-maximum Gaussian kernel.

## Support vector machine analysis

The SVM algorithm was performed by using the Pattern Recognition for Neuroimaging Toolbox (PRoNTo) software Cyclotron Research Centre, University of Liège, Belgium (Schrouff et al., 2013). The following steps were followed: (1) the DC maps ( $r = 0.15, 0.2, 0.25, 0.3$ ) were used as classification feature. (2) Then, the leave-one-out cross-validation (LOOCV) technique was applied to classifier validation. (3) The total accuracy, specificity, sensitivity, and area under the receiver operating characteristic curve (AUC) were calculated.

## Statistical analysis

The chi-square test was used to calculate the sex and handedness and independent sample  $t$ -test was used for age, education, and BCVA between the two groups.

The one-sample  $t$ -test was conducted to assess the group mean of DC maps ( $r = 0.15, 0.2, 0.25, 0.3$ ). The two-sample  $t$ -test was used to compare the two group differences in the DC maps ( $r = 0.15, 0.2, 0.25, 0.3$ ) using the Gaussian random field (GRF) method. (two-tailed, voxel-level  $P < 0.01$ , GRF correction, cluster-level  $P < 0.05$ ).

## Results

### Demographics and disease characteristics

There were no statistically significant differences between the PACG and HC groups in gender, education, or age, but significant differences in BCVA of right eye ( $p < 0.001$ ), left eye ( $p < 0.001$ ). The results of these data are listed in **Table 1**.

### Different degree centrality between primary angle-closure glaucoma and healthy control group

The group means of DC maps of the PACG and HC [**Figure 1A** ( $r = 0.15$ ) **Figure 1B** ( $r = 0.20$ ), **Figure 1C** ( $r = 0.25$ ) and **Figure 1D** ( $r = 0.3$ )]. Compared with HC, PACG patients had significantly higher DC values in the left cerebellum\_Crus2,

<sup>1</sup> <http://www.rfmri.org/dpabi>

**TABLE 1** Demographic and clinical measurements between patients with PACG and HCs.

Condition	PACG group	HC group	T-value	P-value
Age (years)	50.96 ± 4.85	50.82 ± 6.76	0.727	0.470
Sex (male/female)	21/10	21/10	<0.001	1.000
Handness (right/left)	29/2	28/3	0.218	0.641
Education (years)	12.61 ± 5.88	11.46 ± 6.86	0.670	0.506
BCVA-OD	0.15 ± 0.10	1.18 ± 0.12	0.626	<0.001
BCVA-OS	0.30 ± 0.12	1.14 ± 0.10	0.538	<0.001

Chi-square test for sex and handedness. An independent t-test was used for age, education, and BCVA. Data are displayed as mean ± SD.

HC, healthy control; BCVA, best-corrected visual acuity; OD, oculus dexter; OS, oculus sinister; N/A, not applicable; R, right.

left cerebelum\_4\_5, right para hippocampal, and left thalamus. Meanwhile, PACG patients had significantly lower DC values in the right postcentral, left precuneus, and right postcentral ( $r = 0.15$ ) (**Table 2** and **Figure 2A**).

Compared with HC, PACG patients had significantly higher DC values in the right fusiform, left middle temporal gyrus, and left Cerebelum\_4\_5. Meanwhile, PACG patients had significantly lower DC values in the right calcarine, right postcentral gyrus, left precuneus gyrus, and left postcentral gyrus ( $r = 0.20$ ) (**Table 3** and **Figure 2B**).

Compared with HC, PACG patients had significantly higher DC values in the right fusiform, left middle temporal gyrus, and left Cerebelum\_4\_5. Meanwhile, PACG patients had significantly lower DC values in the right calcarine, right postcentral gyrus, left precuneus gyrus, and left postcentral gyrus ( $r = 0.25$ ) (**Table 4** and **Figure 2C**).

Compared with HC, PACG patients had significantly higher DC values in the right fusiform gyrus, left middle temporal gyrus, left cerebelum\_4\_5, and right cerebelum\_4\_5. Meanwhile, PACG patients had significantly lower DC values in the right calcarine, right postcentral, left precuneus, left postcentral and left paracentral\_lobule ( $r = 0.30$ ) (**Table 5** and **Figure 2D**).

## Support vector machine results

The SVM classification reaches a total accuracy of 72.58% and the ROC curve of the SVM classifier with an AUC value of 0.85 ( $r = 0.15$ ); (**Figure 3A**). The SVM classification reaches a total accuracy of 75.81% and the ROC curve of the SVM classifier with an AUC value of 0.85 ( $r = 0.20$ ); (**Figure 3B**). The SVM classification reaches a total accuracy of 74.19% and the ROC curve of the SVM classifier with an AUC value of 0.85 ( $r = 0.25$ ); (**Figure 3C**). The SVM classification reaches a total accuracy of 77.42% and the ROC

curve of the SVM classifier with an AUC value of 0.85 ( $r = 0.30$ ); (**Figure 3D**).

## Discussion

In this study, compared with HCs, PACG patients had significantly higher DC values in the right fusiform gyrus, left middle temporal gyrus, and left cerebellum\_4\_5. Conversely, PACG patients had significantly lower DC values in the right calcarine sulcus, right postcentral gyrus, left precuneus, and left postcentral gyrus. The SVM classifier had an overall accuracy of 72.58%; the ROC curve of the SVM classifier had an AUC value of 0.85 ( $r = 0.25$ ). These results demonstrated that PACG patients had widespread brain functional network hub dysfunction that affected the visual, auditory, default mode, and cerebellar networks. The findings might provide insights into the neural mechanism that underlies optic atrophy in PACG patients.

Notably, we found that PACG patients had significantly lower DC values in the right calcarine sulcus. The calcarine sulcus is a core component of the visual cortex; it plays an important role in transmitting visual information to the higher visual cortex. Previous neuroimaging studies showed visual dysfunction and vision-related cortex dysfunction in PACG patients. Colbert et al. (2021) found that glaucomatous mice with elevated intraocular pressure had decreased fractional anisotropy and increased radial diffusivity along the optic nerves and optic tract. Fujishiro et al. (2022) reported that ocular hypertension could lead to reduced cytochrome oxidase expression in the visual cortex. Pankowska et al. (2022) found that normal-tension glaucoma patients had reduced thickness in the right lateral occipital gyrus and left lingual gyrus. Consistent with these findings, we observed significantly lower DC values in the right calcarine sulcus in PACG patients, which suggested abnormal functional connectivity within the visual network.

Another important finding in this study was that PACG patients had significantly lower DC values in the right postcentral gyrus and left postcentral gyrus. The postcentral gyrus has an important role in sensorimotor function. There are two possible reasons for the phenomenon observed in our study. First, PACG patients exhibit visual loss associated with optic atrophy. Using diffusion tensor MRI, Yang et al. (2018) demonstrated that glaucomatous mice had extensive deterioration of visuomotor function by 9 months of age. Zwierko et al. (2022) reported differences in visuomotor task performance among older adults with moderate and advanced glaucoma. Dive et al. (2016) demonstrated visuomotor behavior in patients with glaucoma-related peripheral field reduction during the completion of natural movements. Thus, decreased DC values in the postcentral gyrus might indicate visuomotor dysfunction in PACG patients. Second, the postcentral gyrus plays an important role in nociceptive



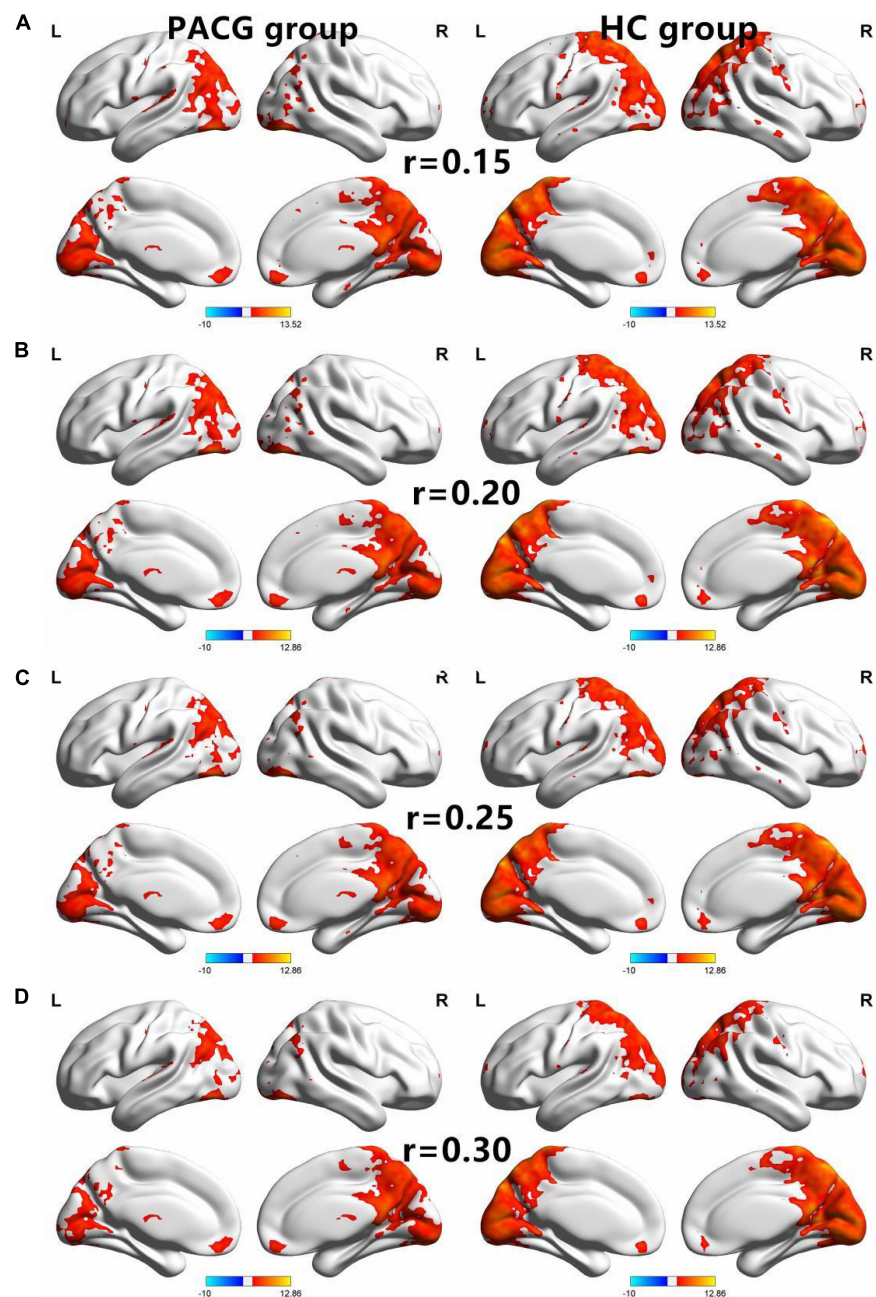


FIGURE 1

The spatial of the DC within the PACG and HC with different correlation thresholds ( $r = 0.15, 0.2, 0.25, 0.3$ ). The group means DC maps of the PACG and HC [(A) ( $r = 0.15$ ), (B) ( $r = 0.20$ ), (C) ( $r = 0.25$ ), and (D) ( $r = 0.30$ )]. PACG patients showed remarkably similar altered degree of centrality brain areas relative to healthy control in the different correlation thresholds ( $r = 0.15, 0.2, 0.25, 0.3$ ) (FDR correction  $p < 0.001$ ). DC, degree centrality; PACG, primary angle-closure glaucoma; HC, health control; L, left hemisphere; R, right hemisphere.

processing. Glaucoma patients experience painful swelling in both eyes. Dong et al. (2019) demonstrated that patients with eye pain had decreased voxel-mirrored homotopic connectivity in the precentral/postcentral gyrus. Additionally, Pan et al. (2018) reported that eye pain patients had a lower amplitude of low-frequency fluctuation in the left and right precentral/postcentral

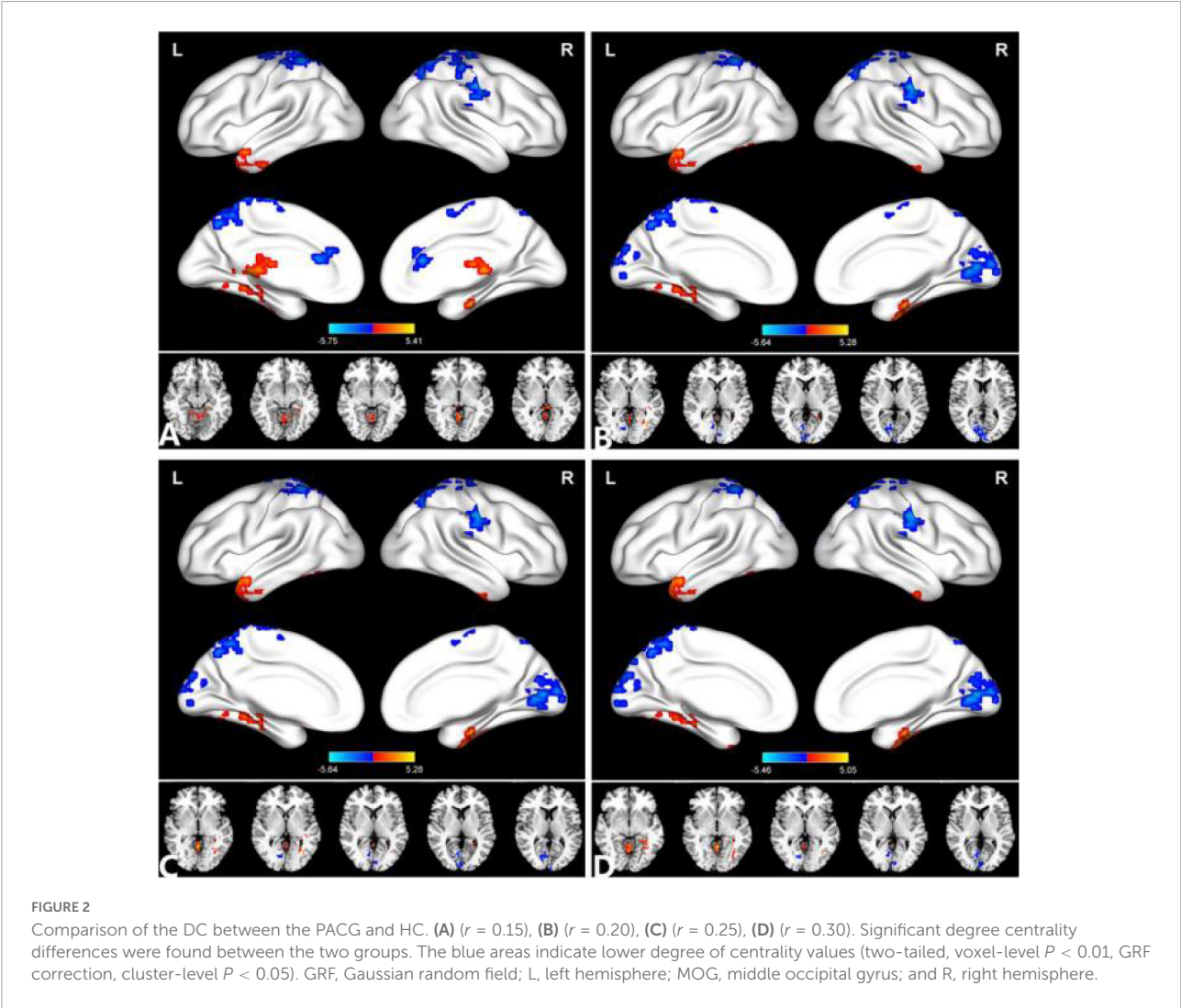
gyrus and left precuneus. Consistent with these findings, our study revealed that PACG patients had lower DC values in the postcentral gyrus, which might reflect visuomotor dysfunction and eye pain in PACG patients.

Finally, we found that PACG patients had significantly lower DC values in the left precuneus and increased DC values in the

TABLE 2 Significant differences in the DC between the two groups ( $r = 0.15$ ).

Condition	Brain regions	MNI			Peak <i>T</i> -scores	Cluster size (voxels)
		x	y	z		
<i>r</i> = 0.15						
PACG > HC	Cerebelum_Crus2_L	3	−51	−42	4.4289	178
PACG > HC	Cerebelum_4_5_L	0	−45	−18	5.4097	341
PACG > HC	ParaHippocampal_R	6	−15	−24	4.4358	44
PACG > HC	Thalamus_L	−6	−36	9	4.0191	56
PACG < HC	Postcentral_R	54	−15	39	−4.2974	76
PACG < HC	Precuneus_L	−12	−57	63	−5.7517	395
PACG < HC	Postcentral_R	39	−33	63	−4.4613	277

x, y, and z are the locations of the peak voxels in standard MNI coordinates.  
DC, degree centrality; PACG: primary angle-closure glaucoma; HC: healthy control; MNI, Montreal Neurological Institute; R, right; L, left.



left middle temporal gyrus. The precuneus and middle temporal gyrus are core components of the default mode network (DMN). The DMN is an endogenous neural network that shows consistently higher blood oxygenation level-dependent activity during rest. It plays an important role in self-referential thought and introspection; these actions involve various higher cognitive

TABLE 3 Significant differences in the DC between the two groups ( $r = 0.20$ ).

Condition	Brain regions	MNI			Peak <i>T</i> -scores	Cluster size (voxels)
		x	y	z		
r = 0.20						
PACG > HC	Fusiform_R	39	−3	−39	3.8686	54
PACG > HC	Middle temporal gyrus_L	−39	9	−36	4.3994	67
PACG > HC	Cerebelum_4_5_L	0	−45	−18	5.2788	607
PACG < HC	Calcarine_R	3	−72	24	−4.4152	158
PACG < HC	Postcentral_R	54	−15	36	−4.4885	81
PACG < HC	Precuneus_L	−12	−57	63	−5.6443	120
PACG < HC	Postcentral_R	39	−33	63	−4.2005	198
PACG < HC	Postcentral_L	−27	−42	66	−4.2295	174

x, y, and z are the locations of the peak voxels in standard MNI coordinates.

DC, degree centrality; PACG, primary angle-closure glaucoma; HC, healthy control; MNI, Montreal Neurological Institute; R, right; L, left.

TABLE 4 Significant differences in the DC between the two groups ( $r = 0.25$ ).

Condition	Brain regions	MNI			Peak T-scores	Cluster size (voxels)
		x	y	z		
		r = 0.25				
PACG > HC	Fusiform_R	39	−3	−39	3.8686	54
PACG > HC	Middle temporal gyrus_L	−39	9	−36	4.3994	67
PACG > HC	Cerebelum_4_5_L	0	−45	−18	5.2788	607
PACG < HC	Calcarine_R	3	−72	24	−4.4152	158
PACG < HC	Postcentral_R	54	−15	36	−4.4885	81
PACG < HC	Precuneus_L	−12	−57	63	−5.6443	120
PACG < HC	Postcentral_R	39	−33	63	−4.2005	198
PACG < HC	Postcentral_L	−27	−42	66	−4.2295	174

x, y, and z are the locations of the peak voxels in standard MNI coordinates.

DC, degree centrality; PACG, primary angle-closure glaucoma; HC, healthy control; MNI, Montreal Neurological Institute; R, right; L, left.

TABLE 5 Significant differences in the DC between the two groups ( $r = 0.30$ ).

Condition	Brain regions	MNI			Peak <i>T</i> -scores	Cluster size (voxels)
		x	y	z		
<i>r</i> = 0.30						
PACG > HC	Fusiform_R	39	−3	−39	3.7733	55
PACG > HC	Middle temporal gyrus_L	−39	9	−36	4.2944	75
PACG > HC	Cerebelum_4_5_L	0	−54	−3	5.0452	487
PACG > HC	Cerebelum_4_5_R	18	−39	−27	4.6504	47
PACG < HC	Calcarine_R	3	−72	24	−4.4721	187
PACG < HC	Postcentral_R	54	−15	36	−4.6369	85
PACG < HC	Postcentral_R	24	−30	75	−4.1747	178
PACG < HC	Precuneus_L	−12	−57	63	−5.4584	107
PACG < HC	Postcentral_L	−27	−42	66	−4.1125	86
PACG < HC	Paracentral_Lobule_L	−9	−27	78	−3.9634	57

x, y, and z are the locations of the peak voxels in standard MNI coordinates.

DC, degree centrality; PACG, primary angle-closure glaucoma; HC, healthy control; MNI, Montreal Neurological Institute; R, right; L, left.

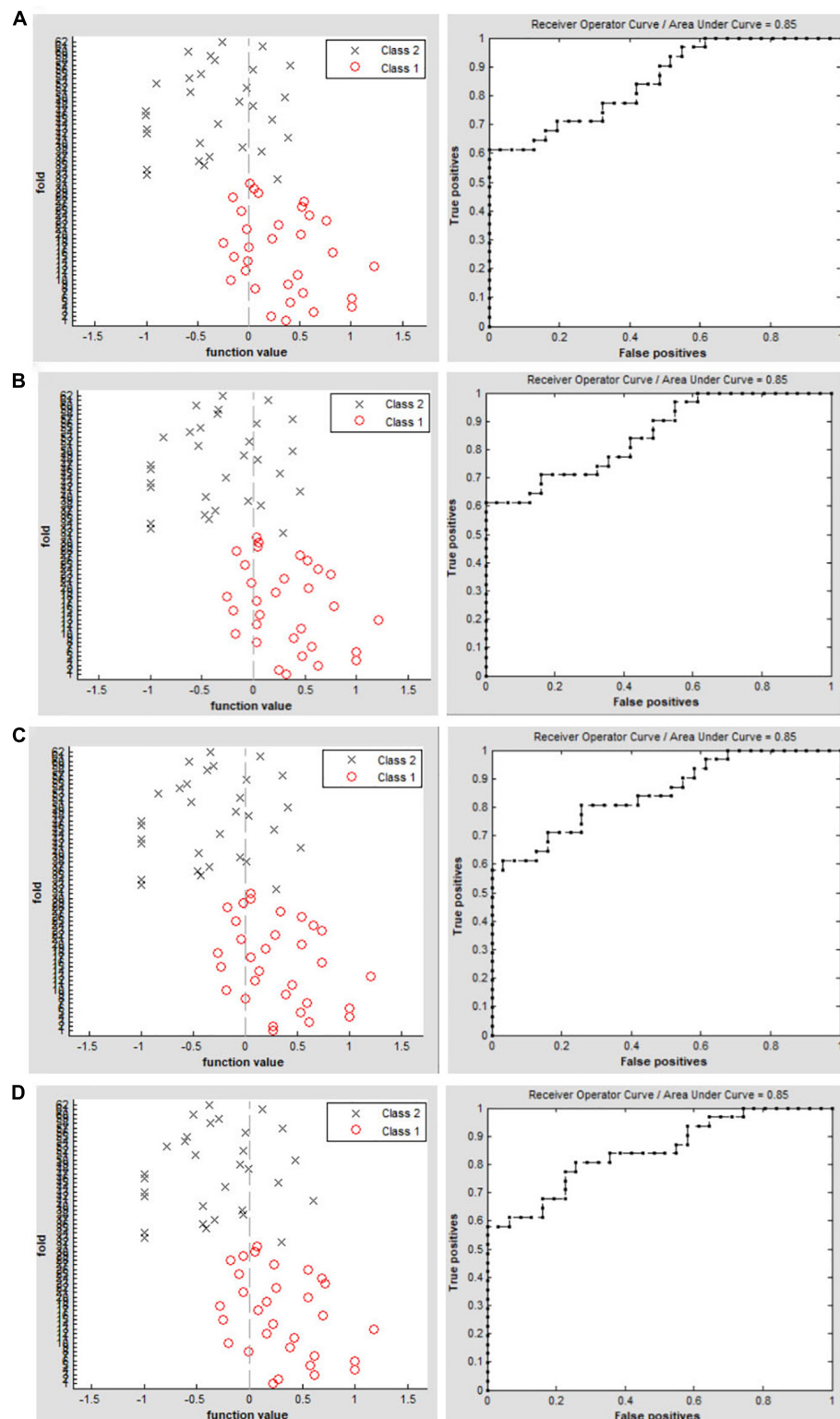


FIGURE 3

Classification results using machine learning analysis based on DC values. Function values of two groups (class 1: PACG group; class 2: HC group); The ROC curve of the SVM classifier with an AUC value of 0.85 ( $r = 0.15$ ). (A) Function values of two groups (class 1: PACG group; class 2: HC group); the ROC curve of the SVM classifier with an AUC value of 0.85 ( $r = 0.20$ ). (B) Function values of two groups (class 1: PACG group; class 2: HC group); The ROC curve of the SVM classifier with an AUC value of 0.85 ( $r = 0.25$ ). (C) Function values of two groups (class 1: PACG group; class 2: HC group); The ROC curve of the SVM classifier with an AUC value of 0.85 ( $r = 0.30$ ) (D).



functions such as memory, prospection, and self-processing (Raichle et al., 2001). Wang et al. (2017) demonstrated that POAG patients had decreased functional connectivity in the DMN. Giorgio et al. (2020) reported that ocular hypertension patients had decreased functional connectivity in key cognitive networks [DMN and frontoparietal working memory network (WMN)]. Our finding of significantly lower DC values in the DMN of PACG patients suggests that those patients are experiencing cognitive decline.

In our study, we used the DC maps as a feature. The SVM model was applied to investigate the SVM classification reaches a total accuracy of 72.58%–77.42% and the ROC curve of the SVM classifier with an AUC value of 0.85. The SVM model showed a high sensitivity for distinguishing the two groups. The DC maps could be sensitive biomarkers for distinguishing patients with PACG from HCs.

Some limitations should be mentioned in the study. First, the sample size of the study is relatively small. Second, the DC values are based on blood oxygen levels dependent (BOLD) on signals, which might be affected by physiological noise. Third, no multimodal MRI methods were used to verify the results of this study.

## Conclusion

Our results showed that PACG patients showed widespread brain functional network hub dysfunction relative to the visual network, auditory network, default mode network, and cerebellum network, which might shed new light on the neural mechanism of optic atrophy in PACG patients. Thus, the DC maps could be sensitive biomarkers for distinguishing patients with PACG from HCs. It provides an important imaging reference for clinicians in early diagnosis.

## Data availability statement

The raw data supporting the conclusions of this article will be made available by the authors, without undue reservation.

## References

- Colbert, M. K., Ho, L. C., van der Merwe, Y., Yang, X., McLellan, G. J., Hurley, S. A., et al. (2021). Diffusion tensor imaging of visual pathway abnormalities in five glaucoma animal models. *Invest. Ophthalmol. Vis. Sci.* 62:21. doi: 10.1167/iovs.62.10.21
- De Moraes, C. G., Liebmann, J. M., and Levin, L. A. (2017). Detection and measurement of clinically meaningful visual field progression in clinical trials for glaucoma. *Prog. Retin. Eye Res.* 56, 107–147. doi: 10.1016/j.preteyeres.2016.10.001
- Dive, S., Rouland, J. F., Lenoble, Q., Szaffarczyk, S., McKendrick, A. M., and Boucart, M. (2016). Impact of peripheral field loss on the execution

## Ethics statement

The studies involving human participants were reviewed and approved by the Medical Ethics Committee of the Jiangxi Provincial People's Hospital. The patients/participants provided their written informed consent to participate in this study.

## Author contributions

R-BC, Y-LZ, HL, and XH contributed to data collection and statistical analyses, wrote the manuscript, designed the protocol, contributed to the MRI analysis, designed the study, oversaw all the clinical aspects of study conduct, and prepared the manuscript. All authors contributed to the article and approved the submitted version.

## Acknowledgments

We acknowledge the assistance provided by the Natural Science Foundation of Jiangxi Province (20212BAB216058) and the Jiangxi Provincial Health Technology Project (202210012).

## Conflict of interest

The authors declare that the research was conducted in the absence of any commercial or financial relationships that could be construed as a potential conflict of interest.

## Publisher's note

All claims expressed in this article are solely those of the authors and do not necessarily represent those of their affiliated organizations, or those of the publisher, the editors and the reviewers. Any product that may be evaluated in this article, or claim that may be made by its manufacturer, is not guaranteed or endorsed by the publisher.

of natural actions: a study with glaucomatous patients and normally sighted people. *J. Glaucoma* 25, e889–e896. doi: 10.1097/IJG.0000000000000402

Dong, Z. Z., Zhu, F. Y., Shi, W. Q., Shu, Y. Q., Chen, L. L., Yuan, Q., et al. (2019). Abnormalities of interhemispheric functional connectivity in individuals with acute eye pain: a resting-state fMRI study. *Int. J. Ophthalmol.* 12, 634–639. doi: 10.18240/ijo.2019.04.18

Duncan, R. O., Sample, P. A., Bowd, C., Weinreb, R. N., and Zangwill, L. M. (2012). Arterial spin labeling fMRI measurements of decreased blood flow

in primary visual cortex correlates with decreased visual function in human glaucoma. *Vision Res.* 60, 51–60. doi: 10.1016/j.visres.2012.03.012

Fujishiro, T., Honjo, M., Kawasaki, H., and Aihara, M. (2022). Visual cortex damage in a ferret model of ocular hypertension. *Jpn. J. Ophthalmol.* 66, 205–212. doi: 10.1007/s10384-022-00901-8

Giorgio, A., Zhang, J., Costantino, F., De Stefano, N., and Frezzotti, P. (2020). Altered large-scale brain functional connectivity in ocular hypertension. *Front. Neurosci.* 14:146. doi: 10.3389/fnins.2020.00146

Gurtubay-Antolin, A., Battal, C., Maffei, C., Rezk, M., Mattioni, S., Jovicich, J., et al. (2021). Direct structural connections between auditory and visual motion-selective regions in humans. *J. Neurosci.* 41, 2393–2405. doi: 10.1523/JNEUROSCI.1552-20.2021

Hernowo, A. T., Boucard, C. C., Jansonius, N. M., Hooymans, J. M., and Cornelissen, F. W. (2011). Automated morphometry of the visual pathway in primary open-angle glaucoma. *Invest. Ophthalmol. Vis. Sci.* 52, 2758–2766. doi: 10.1167/iovs.10-5682

Lawlor, M., Danesh-Meyer, H., Levin, L. A., Davagnanam, I., Vita, E. De, and Plant, G. T. (2018). Glaucoma and the brain: trans-synaptic degeneration, structural change, and implications for neuroprotection. *Surv. Ophthalmol.* 63, 296–306. doi: 10.1016/j.survophthal.2017.09.010

Li, T., Qu, X., Chen, W., Wang, Q., Wang, H., Wang, Y., et al. (2020). Altered information flow and microstructure abnormalities of visual cortex in normal-tension glaucoma: evidence from resting-state fMRI and DKI. *Brain Res.* 1741:146874. doi: 10.1016/j.brainres.2020.146874

Lowry, E. A., and Sanders, D. S. (2021). Hypertension management and glaucoma: hypothesizing causes in correlational data. *Ophthalmology* 128, 401–402. doi: 10.1016/j.optha.2020.10.020

Na, K. S., Lee, N. Y., Park, S. H., and Park, C. K. (2010). Autonomic dysfunction in normal tension glaucoma: the short-term heart rate variability analysis. *J. Glaucoma* 19, 377–381. doi: 10.1097/IJG.0b013e3181c4ae58

Pan, Z. M., Li, H. J., Bao, J., Jiang, N., Yuan, Q., Freeberg, S., et al. (2018). Altered intrinsic brain activities in patients with acute eye pain using amplitude of low-frequency fluctuation: a resting-state fMRI study. *Neuropsychiatr. Dis. Treat.* 14, 251–257. doi: 10.2147/NDT.S150051

Pankowska, A., Matwiejczuk, S., Koziol, P., Zarnowski, T., Pietura, R., and Kosior-Jarecka, E. (2022). Visual tract degradation in bilateral normal-tension glaucoma-cortical thickness maps and volumetric study of visual pathway areas. *J. Clin. Med.* 11:1907. doi: 10.3390/jcm11071907

Raichle, M. E., MacLeod, A. M., Snyder, A. Z., Powers, W. J., Gusnard, D. A., and Shulman, G. L. (2001). A default mode of brain function. *Proc. Natl. Acad. Sci. U.S.A.* 98, 676–682. doi: 10.1073/pnas.98.2.676

Schrouff, J., Rosa, M. J., Rondina, J. M., Marquand, A. F., Chu, C., Ashburner, J., et al. (2013). PRoNTTo: pattern recognition for neuroimaging toolbox. *Neuroinformatics* 11, 319–337. doi: 10.1007/s12021-013-9178-1

Song, B. J., Aiello, L. P., and Pasquale, L. R. (2016). Presence and risk factors for glaucoma in patients with diabetes. *Curr. Diab. Rep.* 16:124. doi: 10.1007/s11892-016-0815-6

Sporns, O. (2011). The human connectome: a complex network. *Ann. N.Y. Acad. Sci.* 1224, 109–125. doi: 10.1111/j.1749-6632.2010.05888.x

Wang, J., Li, T., Zhou, P., Wang, N., Xian, J., and He, H. (2017). Altered functional connectivity within and between the default model network and the visual network in primary open-angle glaucoma: a resting-state fMRI study. *Brain Imaging Behav.* 11, 1154–1163. doi: 10.1007/s11682-016-9597-3

Wang, Z., Zeljcic, K., Jiang, Q., Gu, Y., Wang, W., and Wang, Z. (2018). Dynamic network communication in the human functional connectome predicts perceptual variability in visual illusion. *Cereb. Cortex* 28, 48–62. doi: 10.1093/cercor/bhw347

Wiggs, J. L., and Pasquale, L. R. (2017). Genetics of glaucoma. *Hum. Mol. Genet.* 26, R21–R27. doi: 10.1093/hmg/ddx184

Yan, C. G., Wang, X. D., Zuo, X. N., and Zang, Y. F. (2016). DPABI: data processing & analysis for (resting-state) brain imaging. *Neuroinformatics* 14, 339–351. doi: 10.1007/s12021-016-9299-4

Yang, X. L., van der Merwe, Y., Sims, J., Parra, C., Ho, L. C., Schuman, J. S., et al. (2018). Age-related changes in eye, brain and visuomotor behavior in the dba/2j mouse model of chronic glaucoma. *Sci. Rep.* 8:4643. doi: 10.1038/s41598-018-22850-4

Zhou, W., Muir, E. R., Naji, K. S., Chalfin, S., Rodriguez, P., and Duong, T. Q. (2017). Retinotopic fmri reveals visual dysfunction and functional reorganization in the visual cortex of mild to moderate glaucoma patients. *J. Glaucoma* 26, 430–437. doi: 10.1097/IJG.0000000000000641

Zuo, X. N., Ehmke, R., Mennes, M., Imperati, D., Castellanos, F. X., Sporns, O., et al. (2012). Network centrality in the human functional connectome. *Cereb. Cortex* 22, 1862–1875. doi: 10.1093/cercor/bhr269

Zwierko, T., Jedziniak, W., Florkiewicz, B., Lesiakowski, P., Sliwiak, M., Kirkiewicz, M., et al. (2022). Physical activity is associated with improved visuomotor processing in older adults with moderate and advanced glaucomatous visual field defect: a cross-sectional study. *Int. J. Environ. Res. Public Health* 19:1760. doi: 10.3390/ijerph19031760



## OPEN ACCESS

## EDITED BY

Xin Huang,  
Jiangxi Provincial People's Hospital,  
China

## REVIEWED BY

Betina Ip,  
University of Oxford, United Kingdom  
Toshihiro Kitama,  
University of Yamanashi, Japan

## \*CORRESPONDENCE

Sujeevini Sujanthan  
sujeevini.sujanthan@mail.mcgill.ca

## SPECIALTY SECTION

This article was submitted to  
Brain Imaging and Stimulation,  
a section of the journal  
Frontiers in Human Neuroscience

RECEIVED 13 May 2022

ACCEPTED 01 August 2022

PUBLISHED 09 September 2022

## CITATION

Sujanthan S, Shmuel A and Mendola JD  
(2022) Visually driven functional MRI  
techniques for characterization of  
optic neuropathy.  
Front. Hum. Neurosci. 16:943603.  
doi: 10.3389/fnhum.2022.943603

## COPYRIGHT

© 2022 Sujanthan, Shmuel and  
Mendola. This is an open-access article  
distributed under the terms of the  
[Creative Commons Attribution License  
\(CC BY\)](#). The use, distribution or  
reproduction in other forums is  
permitted, provided the original  
author(s) and the copyright owner(s)  
are credited and that the original  
publication in this journal is cited, in  
accordance with accepted academic  
practice. No use, distribution or  
reproduction is permitted which does  
not comply with these terms.

# Visually driven functional MRI techniques for characterization of optic neuropathy

Sujeevini Sujanthan<sup>1\*</sup>, Amir Shmuel<sup>2</sup>  
and Janine Dale Mendola<sup>1</sup>

<sup>1</sup>Department of Ophthalmology and Visual Sciences, McGill University, Montreal, QC, Canada,

<sup>2</sup>Departments of Neurology, Neurosurgery, Physiology and Biomedical Engineering, Montreal Neurological Institute, McGill University, Montreal, QC, Canada

Optic neuropathies are conditions that cause disease to the optic nerve, and can result in loss of visual acuity and/or visual field defects. An improved understanding of how these conditions affect the entire visual system is warranted, to better predict and/or restore the visual loss. In this article, we review visually-driven functional magnetic resonance imaging (fMRI) studies of optic neuropathies, including glaucoma and optic neuritis (ON); we also discuss traumatic optic neuropathy (TON). Optic neuropathy-related vision loss results in fMRI deficit within the visual cortex, and is often strongly correlated with clinical severity measures. Using predominantly flickering checkerboard stimuli, glaucoma studies indicated retinotopic-specific cortical alteration with more prominent deficits in advanced than in early glaucoma. Some glaucoma studies indicate a reorganized visual cortex. ON studies have indicated that the impacted cortical areas are briefly hyperactive. For ON, brain deficits are greater in the acute stages of the disease, followed by (near) normalization of responses of the LGN, visual cortex, and the dorsal visual stream, but not the ventral extrastriate cortex. Visually-driven fMRI is sensitive, at least in ON, in discriminating patients from controls, as well as the affected eye from the fellow eye within patients. The use of a greater variety of stimuli beyond checkerboards (e.g., visual motion and object recognition) in recent ON studies is encouraging, and needs to continue to disentangle the results in terms of change over time. Finally, visually-driven fMRI has not yet been applied in TON, although preliminary efforts suggest it may be feasible. Future fMRI studies of optic neuropathies

**Abbreviations:** BOLD, Blood oxygenation level-dependent signal; fMRI, functional magnetic resonance imaging; LGN, Lateral geniculate nucleus; LOC, Lateral occipital cortex; MT/V5, Middle temporal visual area; ON, optic neuritis; OCT, Optical coherence tomography; POAG, Primary open-angle glaucoma; RAPD, Relative afferent pupillary defect; RNFL, Retinal nerve fiber layer; TON, traumatic optic neuropathy; VEP, Visually evoked potentials; V1, Primary visual cortex; V2, Secondary visual cortex; V3, Tertiary visual cortex.

should consider using more complex visual stimuli, and inter-regional analysis methods including functional connectivity. We suggest that a more systematic longitudinal comparison of optic neuropathies with advanced fMRI would provide improved diagnostic and prognostic information.

#### KEYWORDS

glaucoma, optic neuritis, traumatic optic neuropathy, visually-driven fMRI, LGN, visual cortex, MT, LOC

## Introduction

The term *optic neuropathy* refers broadly to injury to the optic nerve. It is a serious condition that may result in loss of visual acuity and/or deficits to the visual field (partial or even full blindness). This type of injury can develop acutely or chronically. Acute optic neuropathies such as optic neuritis (ON) and traumatic optic neuropathy (TON) have a rapid onset and are typically caused by inflammation and trauma, respectively, whereas chronic optic neuropathies such as glaucoma are characterized by slow progression (Behbehani, 2007). The aim of this review is to determine how visually-driven functional MRI (fMRI) can be used to assess optic neuropathy-related effects on the entire visual system and potentially provide differential diagnostic or prognostic value in clinical settings. In a separate review, we review resting-state fMRI studies for the same patient groups. By comparing and contrasting glaucoma and ON we can begin to identify common or differential abnormalities induced by chronic vs. acute optic neuropathy. Glaucoma is a prominent example of a disease with progressive effects within the brain as a result of persistent impairment to visual input. In contrast, ON, quickly and severely disrupts normal retinal input but subsequently stabilizes, and recovery of function is common. These well-studied diseases can serve as an important benchmark for comparison and indication of what might be possible for a related optic neuropathy, TON, for which there are no fMRI studies thus far. In addition, ON studies will aid in understanding brain abnormalities specifically due to central visual field loss, which is what is expected—at least initially—in TON patients. We aim in particular to suggest that visually-driven fMRI techniques might contribute to further characterize TON and subsequently aid in the diagnosis, especially in the case of bilateral trauma when the diagnosis is most challenging. We first define some terminology related to the current standard methods of diagnosis and staging of neuropathies. Next, we define the fMRI technique that allows measurement of visual system function. Subsequent sections offer a critical review of published studies that used visually-driven fMRI to assess optic neuropathy-related abnormalities in thalamic and visual cortical areas. Glaucoma, ON and TON are each discussed separately.

## Ophthalmologic assessment tools

In this section, we briefly catalog measures from common ophthalmological tools that are often considered in fMRI literature as covariates that may relate neuroimaging markers to levels of disease severity. A summary figure lists these tools in relation to applicable levels of the visual system (Figure 1). The primary tools used for determining the extent of visual function loss in optic neuropathies evaluate structural defects in the retina and optic disc, and/or functional impairments in vision. Aspects of retinal anatomy such as the retinal nerve fiber layer (RNFL) thickness, or morphology of the optic nerve head (e.g., rim area and volume, as well as cup-disc ratio) are measured using optical coherence tomography (OCT), confocal scanning laser ophthalmoscopy, or scanning laser polarimetry. These tools currently provide valuable information about the severity of the disease but do not differentiate well between different optic neuropathies. Physical examination is accompanied with visual field testing, typically conducted with automated static perimetry, where sensitivity to light is evaluated using a small white flash on a dim background. Both focal and global visual field loss are often utilized for determining the pattern of visual field loss (i.e., predominantly central or peripheral) and the progression of the disease (Susanna and Vessani, 2009; Yaqub, 2012). Due to the retinotopic nature of these tests, there is a strong potential for direct correlation with fMRI measurement of the retinotopic maps in the visual cortex. These behavioral tests are also clinically important but do have limitations (Wilhelm and Schabet, 2015; Wu and Medeiros, 2018). The testing can be subjective, challenging for patients, and has poor sensitivity (e.g., to detect glaucomatous peripheral field loss). Some specific perimetric tests have been developed that attempt to isolate specific types of retinal ganglion cells, such as magnocellular or short-wavelength cell types which are biased in number in the peripheral or central retinal, respectively (Sharma et al., 2008). Although these could again be attractive as potential covariates for neuroimaging measures, they have not been widely successful clinically in identifying all individuals at risk for developing glaucoma (Havvas et al., 2013). Visual acuity, an eye's ability to resolve high spatial resolution, is often a critical measure obtained with Snellen or Early Treatment



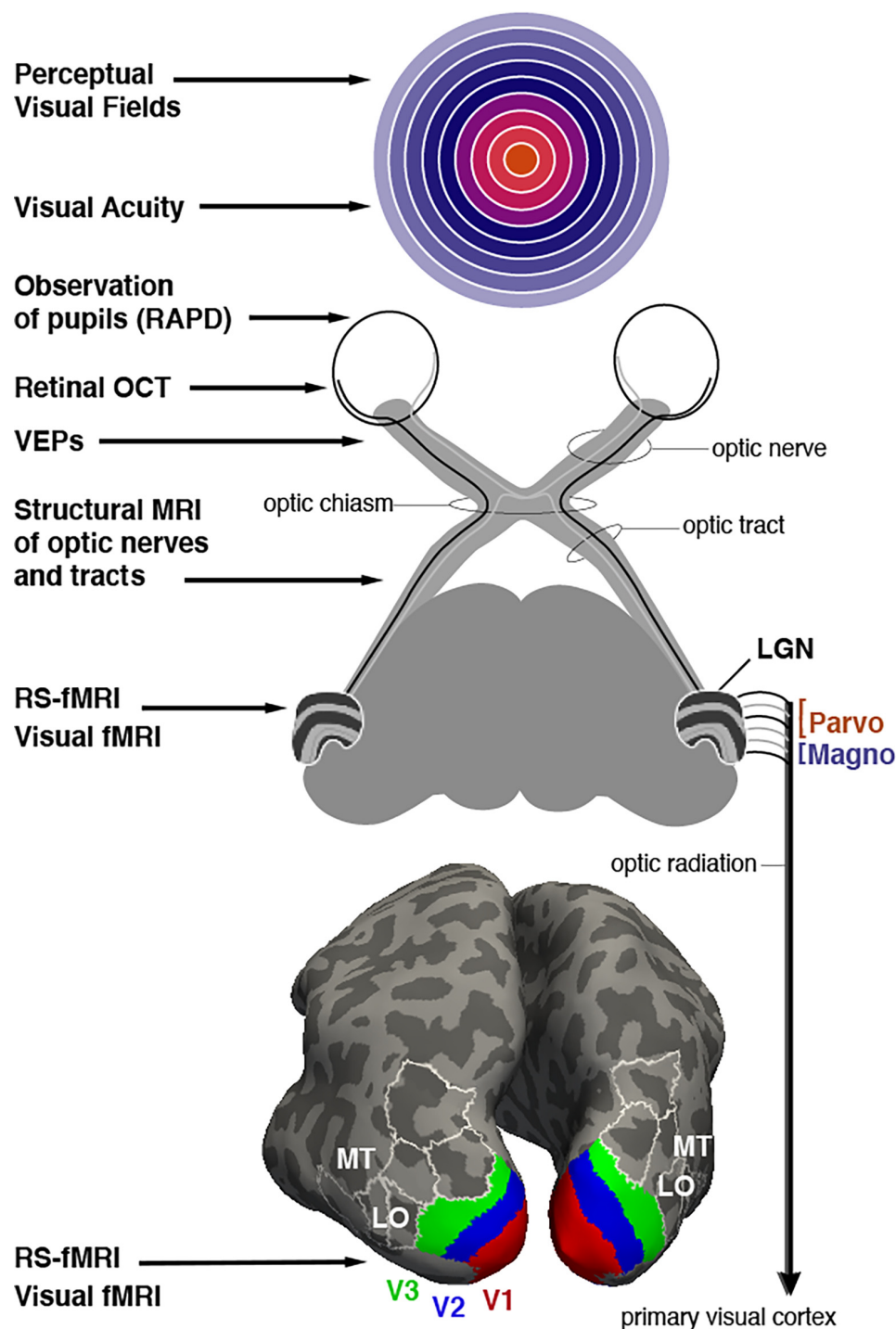


FIGURE 1

Assessment of optic neuropathy at different levels of the visual system. Potential ophthalmological tools are listed that rely on behavioral testing, clinical observation, microscopy, electrophysiology or MRI imaging (on left). **Top image:** Representation of the visual field with (foveal) central vision colored orange, mid-eccentricities colored with cooler hues, and peripheral locations colored with increasingly light purple. White rings represent eccentricities spanning from 10 to 90 degrees in 10 degree increments. **Middle image:** Schematic description of retinal projections to the thalamic lateral geniculate nucleus (LGN). LGN is shown with layers 1–6 that segregate input from each eye (contra, ipsi, ipsi, contra, ipsi, contra). Layers 1 and 2 form the magnocellular projections to V1 while layers 3–6 comprise the parvocellular input. **Bottom image:** Inflated depiction of cerebral cortex, posterior view. A probabilistic brain atlas (Wang et al., 2015) is used to show the location of several retinotopically organized visual areas. Lower-tier areas V1, V2, and V3 are shown with red, blue, and green, respectively. Some additional higher-tier areas are indicated as well, in particular areas MT and LO (LO1 and LO2) mentioned in the text as well. White outlines, included for context, localize area V3A, V3B, IP0 (dorsally), and V4v, VO1, VO2 (ventrally).

Diabetic Retinopathy Study charts. It can quickly estimate the quality of central vision, which to some extent serves as a measure of disease severity in optic neuropathies (Toosy et al., 2014). Traditionally, results from multiple longitudinal eye examinations are utilized for diagnosis and staging of patients. Furthermore, there are also other functional vision measures that provide valuable information about certain optic neuropathies. For example, visually evoked potentials (VEPs), a measure of the integrity of the retino-geniculate-cortical pathways, is strongly associated with the deficits in motion perception observed in ON patients. The relative afferent pupillary defect (RAPD) is another important and widely used ophthalmological assessment to determine asymmetry in reflexive pupillary response when light is alternately applied to each eye. The objective nature of the test makes it convenient to use, especially in trauma patients with limited responsiveness. However, it is only useful in identifying optic neuropathies that are unilateral or asymmetric in nature (Broadway, 2012). Correlation analysis between functional neuroimaging variables and these key clinical measures can help identify the most clinically relevant fMRI markers of injury for each optic neuropathy.

## Functional MRI techniques

fMRI is a non-invasive method to measure neuronal activity across the brain. Changes in neuronal activity are measured indirectly with the blood oxygenation level-dependent signal (BOLD; Kwong et al., 1992; Ogawa et al., 1992). fMRI is useful to vision science because we can address fundamental questions such as the location of the multiple representations of the retinal “map” in the occipital, posterior parietal, and posterior temporal lobes of the brain (e.g., V1, V2, V3, etc., as shown in Figure 1). It is also possible for subjects to perform a wide array of visual detection or discrimination tasks so that the most actively recruited cortical regions are visualized. Questions such as the degree of specialization of certain cortical areas can be addressed. Since fMRI has no known risk to subjects, they can be scanned repeatedly to monitor change over time. This can be exploited to study perceptual learning in healthy controls, for example. fMRI offers a wide field of view, and can easily cover the entire brain, although a trade-off exists between spatial resolution and field of view. In other words, to achieve the smallest voxels possible, a smaller volume of the brain is imaged. In this sense, the field is still limited by a finite spatial and temporal resolution. Using very advanced MRI scanners at ultra-high field strengths (like 7 Tesla) helps achieve even better spatial resolution (Chaimow et al., 2018). The temporal resolution of fMRI is inherently limited to approximately 1–2 seconds; it does not compete with electrophysiological techniques such as VEPs measured in milliseconds. Those techniques are thus complementary.

There are other practical limitations to fMRI that derive from experimental design and analysis. For example, should the

visual stimuli remain identical, or should the levels of visual performance remain identical across a range of subjects? In addition, in the context of clinical studies, it is very desirable to be able to make reliable fMRI measures in individual subjects so as to discriminate a patient from healthy controls. This is already possible, but sensitivity may be limited compared to comparisons at group level. All the studies reviewed here made comparisons at the group level. Emerging advances in data analysis may prove beneficial for improving single-subject analyses. For example, probabilistic atlases (from normal healthy subjects) can be applied to an individual subject's data to estimate the retinotopic boundaries of many visual areas, even if retinotopic mapping has not been performed for that particular subject. In the future, we expect that even more powerful analysis methods from the machine learning field can be employed to maximize sensitivity for classification (e.g., of diagnosis) of visual impairment and prediction (e.g., of prognosis) of recovery in an individual patient.

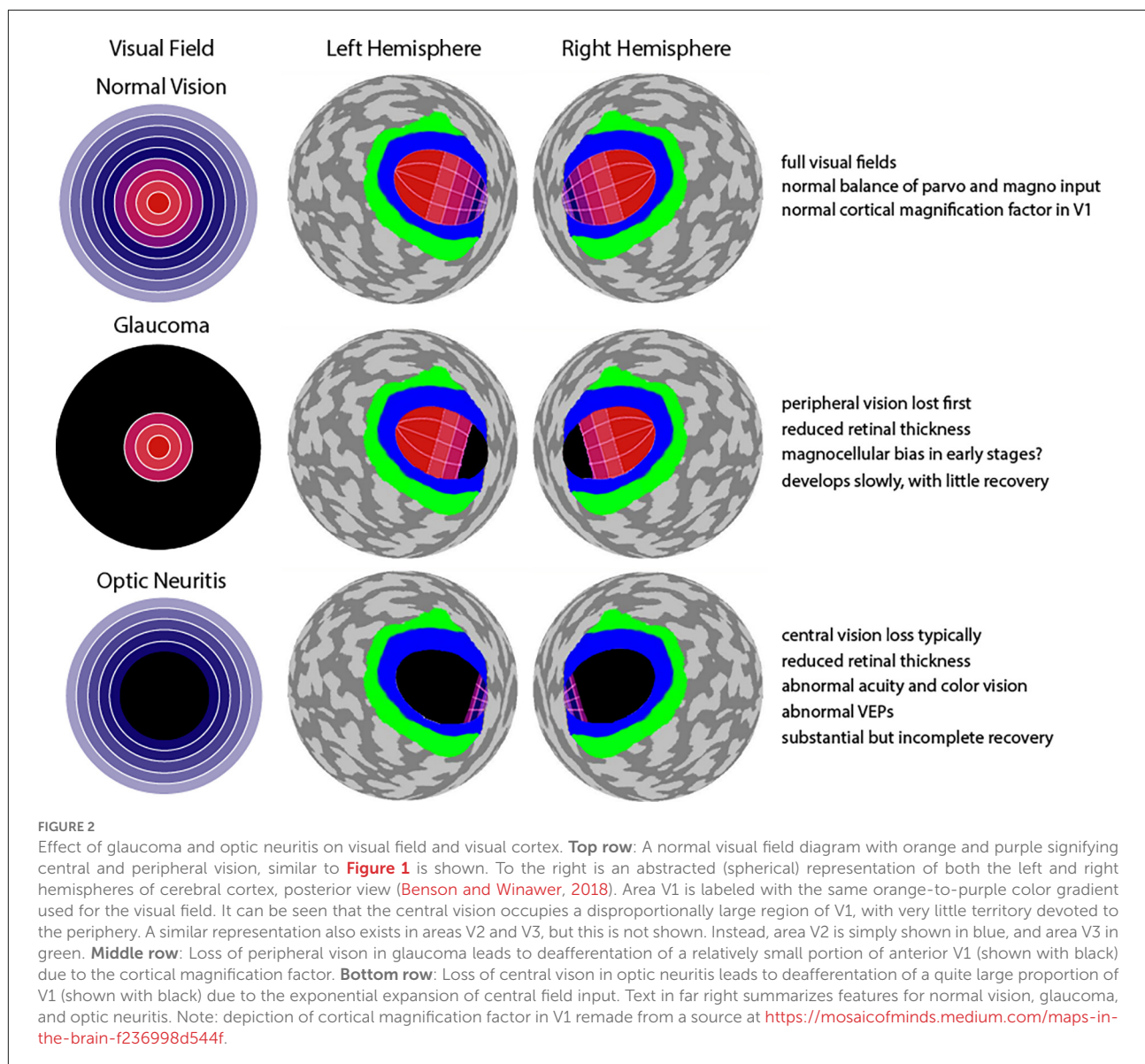
It is pertinent to this clinically-oriented review that some features of fMRI have been a persistent limitation when translation to clinical ophthalmological settings is considered. Importantly, stimulation of the peripheral field can be challenging inside the bore of MRI machines. In most studies the stimuli remain within the central 20 degrees. Specialized equipment is needed to reach the far periphery. In order to circumvent this limitation, one probabilistic atlas has cleverly estimated the locations of V1–V3 out to 90 degrees (Benson and Winawer, 2018). Moreover, specialized hardware is also required to allow separate images to be shown to each eye during fMRI sessions (i.e., dichoptic stimulation). Currently, there are multiple products on the market for dichoptic presentation of visual stimuli and thus allow for fMRI responses of each eye to be directly correlated with eye specific clinical measures. fMRI experiments typically require 1–2 hours with little to no movement, which may be considered demanding for patients. Visually-driven fMRI requires subjects to remain alert with eyes open, and usually subjects should avoid eye movements by fixating their gaze on a central mark for several minutes at a time. Finally, there is a serious commitment of time and expertise required to analyze and interpret the results.

Retinotopic mapping, the process of determining the visual receptive field properties of neuronal populations in the visual pathway (i.e., how the brain maps our visual field), is possible with BOLD fMRI, and is a useful technique to investigate the differences in visual system organization of healthy individuals and patients. Retinotopic mapping typically uses expanding ring stimuli to measure eccentricity and rotating wedge stimuli to measure polar angle (Sereno et al., 1995). The brain contains multiple, topographically organized, maps of visual space in the early visual areas, e.g., V1, V2, and V3, where neighboring visual space is represented in neighboring regions in visual cortex. Central foveal vision in particular is represented in

multiple regions including the occipital pole, as well as the lateral occipital cortex (LOC; Wandell et al., 2007). Another important feature is cortical magnification: a large portion of the visual cortex is dedicated to processing information from the central visual field, and as the distance from the fovea increases, cortical volume decreases exponentially (Wandell et al., 2007). Importantly, any changes to this normal pattern of cortical activation may suggest an impairment, compensatory effect (i.e., higher activity than normal), or even cortical reorganization. Moreover, compared to damage to peripheral vision, damage to central vision is expected to result in abnormal representation across a much larger expanse of visual cortical areas (Figure 2). This is a dramatic effect that would apply to many different visual areas, but this is depicted only for V1 in Figure 2.

## Methods

We searched PubMed using keywords specific to these optic neuropathies and selected peer-reviewed articles in English with relevant titles and abstracts for further review. Search terms included glaucoma, primary open-angle glaucoma, optic neuritis, optic neuropathy, optic damage, traumatic optic neuropathy or open globe injury, and keywords related to fMRI. After the initial selection, the full text was assessed for eligibility. We included studies containing patient groups affected by POAG, acute ON or clinically isolated syndrome of ON, as well as vision loss due to trauma to the optic nerve (i.e., open globe injury or TON). We specifically focused on typical idiopathic ON. Other related inflammatory diseases of the visual system (e.g., neuromyelitis optica spectrum disorder, MOG-antibody



ON, lupus, or GPA) were excluded as there are no visually-driven fMRI studies for such patients. Moreover, ON studies consisting primarily of MS patients were excluded. More details about the clinical profiles of ON patients utilized in the studies we reviewed can be found in **Supplementary Table 1**. Studies that focused on any other optic neuropathy, hereditary vision damage, animal research, molecular work, and clinical studies (i.e., case reports, randomized controlled trials and clinical trials) were also omitted. In addition, in this review we only included studies using visually-driven fMRI to investigate responses in cortical and subcortical visual areas of the brain. We chose to focus exclusively on the visual system in order to better isolate those findings and examine the untapped potential for improved sensitivity to the direct effects of deafferentation in this system.

## Glaucoma

Glaucoma is a leading cause of permanent blindness worldwide and has blinded about 3.2 million people as of 2020 (Broadway and Cate, 2015). This chronic and generally bilateral neurodegenerative optic disease leads to progressive visual field loss, typically with the peripheral visual field affected in the early stages, followed by central visual field loss. Partial regions of blindness develop gradually such as nasal step scotoma, inferior or superior arcuate scotoma, paracentral scotoma or generalized depression (Weinreb and Khaw, 2004; Jonas et al., 2017). This is a result of damaged retinal ganglion cells and degeneration of the optic nerve, producing characteristic changes to the optic nerve head known as “cupping” (Cohen and Pasquale, 2014). It may or may not be associated with high intraocular eye pressure, but this is currently the only modifiable risk factor for managing glaucomatous symptoms, and glaucoma may continue to progress following treatment. One of the most common types of glaucoma and the one that will be discussed in this paper is POAG.

Progressively, glaucoma results in optic nerve “rim” loss, increased cup to disc ratio, disc hemorrhage, retinal nerve fiber damage, and enlarged visual field defects. However, the biological mechanisms and sequela underlying these clinical presentations are poorly understood. Moreover, although these features are important in the diagnosis and follow-up of glaucoma, they cannot be used to define glaucoma with high sensitivity and specificity (Cohen and Pasquale, 2014). POAG is asymptomatic (i.e., normal visual field) until a substantial number (i.e., 25%–35%) of retinal ganglion cells have been permanently lost and visual deficits start to form within the central visual field (10°–20° degrees from fixation; Qing et al., 2010). Therefore, individuals are recommended to have their eyes examined periodically to detect structural changes to the optic disc, one of the first signs of glaucoma detectable in clinical eye examinations.

With the increasingly wide availability of functional MRI techniques, recent studies have started to examine the structure and function of the lateral geniculate nucleus (LGN), and visual cortex in glaucoma patients to observe any other signs of alterations that may provide new knowledge about the disease and serve as promising avenues to detect and halt vision loss. Indeed, many studies have documented injury to the optic nerve, and tract, as well as abnormalities in visual and even non-visual subcortical and cortical regions and networks (Lawlor et al., 2018). Degeneration along the visual pathway is believed to be triggered by the loss of retinal ganglion cells in a process called transsynaptic degeneration, where injured neurons subsequently impair their projection targets, depriving them of input connections. Investigating the changes in brain activity in the visual areas of glaucoma patients may help further understand the pathophysiology of the disease, and potentially aid in the development of interventions.

## Visually driven functional brain measures

We identified 10 cross-sectional visually-driven fMRI studies investigating the effect of glaucoma on the visual system. The stimulus parameters utilized and results reported in these studies are summarized in **Figure 3**. Unless otherwise indicated in column *Stimulus: Type* in **Figure 3**, the studies monocularly presented a standard checkerboard stimulus which consists of central fixation, black and white checkers with 100% contrast, and contrast reversing at 8 Hz to the affected eye. The stimulus is generally presented in a block design where it is alternated with a blank background with the same luminance as the mean luminance in the stimulus period. The fellow eye is generally patched in all studies except in Duncan et al. (2007a,b) where it was voluntarily closed, and fellow eye status is unknown for in Jiang et al. (2017). All glaucoma studies scanned patients at 3 Tesla and the resolution of the functional scans across the studies ranged from 2 to 3.4 mm<sup>3</sup>. Moreover, visual areas seem to be delineated using retinotopy (Duncan et al., 2007a,b; Borges et al., 2015; Zhang et al., 2016; Zhou et al., 2017) or an automated anatomical labeling system (Gerente et al., 2015; Jiang et al., 2017), and data were analyzed in Talairach (Borges et al., 2015) or Montreal Neurological Institute (Qing et al., 2010; Zhang et al., 2015, 2016; Murphy et al., 2016; Jiang et al., 2017) reference space.

The current literature indicates that visually driven fMRI has the ability to distinguish glaucoma patients from healthy subjects. For example, Borges et al. (2015) observed a reduction in activity in the bilateral occipital lobe in response to stimulation of the glaucomatous eye in POAG patients compared to healthy controls. In addition, it is interesting to note that the functional loss was only evident for the medium and high contrast stimuli and not for low contrast stimuli (Borges et al., 2015). Furthermore, eccentricity-specific reduction in the



Author, Year, Subject Groups (#)	Stimulus: Type	Stimulus: Location & Span	Stimulus: SF, Contrast & Flicker, Motion	Main Findings: Visual Cortex Deficit	Other Findings: LGN or Cortex Deficit
1. Zhang et al., 2015 <i>POAG (23) vs. HC (29)</i>	Checkerboard on black background vs. unknown baseline	Central upper or lower (preserved) hemifield; 3° diameter		Advanced patients vs. controls & early-moderate	
2. Qing et al., 2015 <i>POAG (6)</i>	Checkerboard on black background vs. black baseline	Central (preserved) upper or lower hemifield; 5° diameter		Affected eye vs. fellow eye <sup>^</sup> (asymmetric)	
3. Jiang et al., 2017 <i>POAG (13) vs. HC (13)</i>	Checkerboard vs. background (same mean luminance)	Unknown		Left cuneus <sup>#</sup>	Patients <i>higher</i> than controls; wide spread regions
4. Murphy et al., 2016 <i>Glaucoma (26) vs. HC (9)</i>	Checkerboard	Upper and lower hemifield alternated; unknown span		Advanced patients vs. controls <sup>#</sup> <sup>^</sup> *	Patients vs. controls (small effect)
5. Borges et al., 2015 <i>POAG (9) vs. HC (4)</i>	Checkerboard	Full-field; 18°x 16° diameter (horiz x vert)	Contrast at 5% (magn), 25%, and 80% (parvo)	Affected eye vs. fellow eye, esp. med/high contrast {No remapping}	
6. Zhang et al., 2016 <i>POAG (18) vs. HC (18)</i>	Checkerboard	Full field; 24° diameter	Low SF pattern at 30% contrast; 10 Hz (magn) 24°/s rotation	None	Early patients vs. controls, M layers LGN <sup>^</sup> ; LGN volume
	Checkerboard	Full field; 24° diameter	High SF, isolum red/green, 0.5 Hz (parvo) 2.4°/s rotation	None	None
7. Duncan et al., 2007a <i>POAG (6)</i>	Checkerboard	Quadrant of visual space with greatest visual loss; peripheral fixation; 30° diameter		Affected eye vs. fellow eye <sup>^</sup> (asymmetric)	
8. Duncan et al., 2007b <i>POAG (6)</i>					
9. Gerente et al., 2015 <i>POAG (17) vs. HC (8)</i>	Binocular Checkerboard	Polar wedge; 30° diameter	Rotating wedge	Advanced patients vs. controls & early patients <sup>#</sup> (asymmetric, per quadrant)	
10. Zhou et al., 2017 <i>POAG (9) vs. HC (9)</i>	Binocular Checkerboard for Mapping	Wide field; 110° diameter	6°/s wedge rotation; 1.8°/s ring Expansion-Contraction	Patients (advanced/moderate) vs. controls (peripheral VF) <sup>#</sup> (per quadrant) {Remapping}	

FIGURE 3

Summary of visual stimuli utilized and findings in visually-driven fMRI studies of glaucoma. The studies are listed in increasing order of the size of the checkerboard stimulus utilized. Left: Images of visual stimuli, similar to the ones utilized in each of the studies, have been provided. Note: Images in row 1, 2, 4, 9, and 10 are created with a figure licensed under a Creative Commons Attribution 4.0 International (<https://creativecommons.org/licenses/by/4.0/>, <https://creativecommons.org/licenses/by/4.0/legalcode>). It is attributed to Biological Psychiatry (<https://www.sciencedirect.com/science/article/pii/S0006322307012413?via%3Dihub#fig1>). Cropped in various shapes from original. Images in row 6 is obtained from Zhang et al. (2016) © 2015 Wiley Periodicals, Inc. <sup>^</sup>Deficit indicated by correlation with visual sensitivity measures (i.e., BOLD activity declines with increasing severity measure). \*Compensation indicated by correlation with visual sensitivity measures (i.e., BOLD activity increases with increasing severity measure). <sup>#</sup>Deficit indicated by correlation with retinal thickness (i.e., BOLD activity declines with increasing severity measure). <sup>##</sup>Compensation indicated by correlation with retinal thickness (i.e., BOLD activity increases with increasing severity measure). SF, spatial frequency; VF, visual field; POAG, primary open-angle glaucoma; HC, healthy controls.

activity of the bilateral occipital lobe has been reported. Zhou et al. (2017) utilized task-based fMRI and confirmed that the

stimulation of the peripheral visual field resulted in a lower BOLD percent change compared to control subjects. However,

the results have been mixed regarding the degree of abnormality in the *central* visual field. Zhou et al. (2017) found no difference in central-field visual regions between a cohort of POAG patients with various levels of disease severity and controls. However, on the contrary, presenting a central checkerboard stimulus to a relatively preserved central visual field did result in a reduction of BOLD percent change in asymmetric glaucoma patients (Qing et al., 2010), and did show compromised cerebral blood flow in central field visual cortex of advanced POAG patients (Zhang et al., 2015). Although the reason for these discrepant results is uncertain, one likely source would be variability in the staging and severity of disease in the respective patient groups studied.

There is more direct evidence that the extent of change in visual pathways and cortical activation is dependent on glaucoma severity across the spectrum from early to advanced disease. In early stages, visual field score seems to remain relatively normal despite reductions in RNFL thickness (Bowd et al., 2001), and indeed BOLD percent response in the visual cortex of the early to moderate POAG participants was not significantly abnormal (Gerente et al., 2015; Zhang et al., 2015; Zhou et al., 2017). Likewise, Zhang et al. (2016) reported a similar phenomenon but also suggested that early POAG patients may have a biased loss of *magnocellular* input compared to controls, which is consistent with the early loss of peripheral vision where magnocellular input dominates. In particular, early-stage glaucoma patients showed a reduced fMRI response in LGN to transient achromatic stimuli compared to sustained chromatic stimuli, suggesting loss of the magnocellular channel. While these findings seem promising, it is important to replicate these results using even newer methods that provide the high spatial resolution required to confidently isolate BOLD signal in individual layers of the LGN. When severe stages of glaucoma are studied, activation in the calcarine and occipital cortex is low compared to healthy controls particularly in the anterior calcarine sulcus where the representation of peripheral field is expected (Zhang et al., 2015; Murphy et al., 2016). Murphy et al. (2016) suggest that this retinotopic pattern of functional loss is more strongly observed in the primary visual cortex in comparison to higher visual areas, but the data is still lacking to show this clearly. It remains to be determined if extrastriate retinotopic visual cortices could ever be more sensitive to subtle alterations in visual function than any of the clinical parameters currently used for diagnosis with appropriately tailored stimuli and optimized fMRI protocols.

We conclude this section by mentioning that, despite the consistent reduction in functional brain activity as a result of POAG, some authors have argued that the visual cortex may actively compensate for the loss of visual input via specific reorganization. In particular, remapping may occur in early visual cortices to compensate for the reduced vision in the peripheral visual field. In other words, the foveal or parafoveal representations may be strengthened, possibly by recruiting deafferented cortical territory formerly representing

more peripheral eccentricities. Indeed, parafoveal regions in the visual cortex were found to be enlarged in mild to moderate POAG patients compared to controls in V1 and V2, but not V3 (Zhou et al., 2017). However, Borges et al. (2015) reported that they noticed a lack of remapping in affected regions of V1 and V2 in glaucoma in patients with *unilateral* POAG. This might suggest that reorganization does not occur until cortical circuits (which are primarily binocular) are consistently deafferented from both eyes. Finally, we note that Jiang et al. (2017) used a checkerboard stimulus and reported compensatory-like activity (i.e., higher BOLD signal) in various structures involved in the limbic network, default mode network, the dorsal visual pathway, and frontal gyri, of patients compared to controls. This seems to suggest that the effects of glaucoma are widespread, however this needs to be further explored with stimuli that specifically and maximally drive the specialized visual and extrastriate regions.

## Correlation with specific ophthalmological measures

Consistent with the strong relationship between fMRI results and overall measures of disease severity, many, but not all, studies report the expected significant correlations between more specific clinical measures and BOLD response in certain cortical areas. BOLD response in visual cortical areas of POAG patients showed a strong, positive correlation with RNFL thickness measured with OCT (Duncan et al., 2007a; Gerente et al., 2015) in the corresponding quadrant (Zhou et al., 2017), but not GDx nerve fiber layer analyzer, and mean disc height contour measured with Heidelberg retina tomograph II (Duncan et al., 2007a). Specifically, deterioration of peripapillary RNFL and macular ganglion cell-inner plexiform layer was shown to be strongly associated with lower activity in the primary visual cortex (Murphy et al., 2016) and less strongly associated with the BOLD signal from secondary and tertiary visual cortices (Murphy et al., 2016). Surprisingly, in one study of early glaucomatous stages, BOLD signals from the left cuneus were negatively correlated with relative RNFL (Jiang et al., 2017), suggesting compensatory activity. Also, in one exceptional study, the difference in BOLD response of the glaucomatous and healthy eye as a result of stimulating the *preserved* central visual field of asymmetric POAG patients did *not* correlate to the corresponding RNFL thickness values (Qing et al., 2010). Although the authors speculate that functional changes in the visual cortex may appear before clinical retinal signs, this remains unproven.

Unlike measures of the retina and optic nerve, behavioral perimetry scores from visual detection tests can estimate the output of the entire visual system and may be an even better measure of function. Indeed, the visual deficits determined by sensitivity differences between a glaucomatous and healthy eye

per visual field location (Duncan et al., 2007a), or per quadrant (Zhou et al., 2017) have been shown to correlate with reduced BOLD amplitudes in the corresponding calcarine and occipital cortex areas (Gerente et al., 2015). However, in contrast, Borges et al. (2015) reported no correlation between BOLD activation in the lesion projection zones in V1 and V2 of unilateral POAG patients and the corresponding visual field mean deviation scores. Even more surprising, Qing et al. (2010) report an inverse correlation between BOLD response and visual field scores, suggesting compensation. The difference in the results reported might be attributed to the various types of POAG included in the studies mentioned above including bilateral patients with varying degrees of asymmetry and the rare unilateral cases. It may also be relevant that the studies mentioned above employ slightly different methods such as performing visual field testing monocularly (Borges et al., 2015) vs. estimating binocular visual field using monocular tests (Qing et al., 2010; Gerente et al., 2015; Zhou et al., 2017), or stimulating the peripheral (Duncan et al., 2007a; Gerente et al., 2015; Zhou et al., 2017) vs. the *preserved* central visual field (Qing et al., 2010 and Borges et al., 2015). More work is required to disentangle all these factors.

## Visual stimuli

Eight of the 10 reviewed studies focused mainly on the visual cortex and reported significant changes in BOLD activity within V1. This can be attributed to the type of visual stimuli chosen and the subgroup of POAG patients in these studies. BOLD activity within visual cortices was not significantly altered in studies ( $n = 2$ ) that solely used early POAG patients. For all studies, the visual stimuli were predominantly black and white checkerboard stimuli with 100% contrast and contrast reversing at 8 Hz (see Figure 3). These stimulus parameters are known to maximally drive V1 (Fox and Raichle, 1984; Singh et al., 2000). Amongst the studies, the stimulus varied slightly in terms of size, the number of quadrants covered, and whether it was presented to the most preserved or the most affected area (see Figure 3). Nevertheless, BOLD activity in V1 or other occipital ROIs was consistently lower for POAG patients with at least mild-to-moderate severity.

Two of the 10 studies also used more complex checkerboard stimuli, i.e., concentric eccentricity rings or rotating polar wedges (see Figure 3). These were particularly useful in making specific conclusions about a potential reorganization of the visual cortex in different subgroups of POAG patients. Distinctions between early and severe POAG subgroups were successfully made with retinotopic mapping stimuli that spanned 30 degrees in diameter (Gerente et al., 2015). Zhou et al. (2017) studied this more systematically with retinotopic stimuli that spanned up to 110 degrees. Consistent with the previous study, differences between glaucoma patients and controls were seen when a visual field of around 20 degrees eccentricity

was stimulated. Nevertheless, it is important to note that the sensitivity to differentiate (at least mild to moderate) patients from controls increases with stimuli that span greater than 24 degrees eccentricity.

## Optic neuritis

ON is an acute demyelinating optic neuropathy resulting in a temporary vision loss due to inflammation of the optic nerve. The annual incidence of ON in the world is estimated to be 0.94–2.18 per 100,000 (Toosy et al., 2014). The most common form of ON is associated with multiple sclerosis and therefore is often linked to it. However, ON can present in isolation (Toosy et al., 2014). ON usually occurs in young adults and is characterized by mild to severe unilateral visual loss which develops rapidly and is accompanied by pain during eye movements, followed by spontaneous improvement. Initially, the affected eye in ON has diffuse abnormalities in the central visual field leading to reduced visual acuity; an early clinical sign of ON (Keltner et al., 1999; Toosy et al., 2014). However, patterns of visual field loss alone are of limited value in the differential diagnosis of ON and other optic neuropathies (Pau et al., 2011). The Optic Neuritis Treatment Trial also revealed that the fellow eye typically shows minimal to moderate deficits in the majority of ON patients (Keltner et al., 1993). Finally, other aspects of vision that are usually compromised include color vision; both blue-yellow and red-green defects.

The diagnosis of (unilateral) ON often involves assessing the relative afferent pupillary defect (RAPD) to determine asymmetry in an otherwise symmetric reflexive pupillary response. However, this test fails in cases of bilateral and symmetric visual loss (Broadway, 2012), or if there was previous episode of ON. RAPD assesses the function of one eye in comparison to the other eye. Therefore, the test requires patients to have one eye unaffected by optic neuropathies. In the case both eyes are or have been, affected, the test loses sensitivity. Diagnosis is also assisted by imaging the optic nerve with contrast-enhanced MRI to detect inflammation-mediated breakdown of the blood-nerve barrier (Toosy et al., 2014), and OCT retinal measurements of the thickness of the peripapillary nerve fiber layer (Wilhelm and Schabet, 2015). At disease onset, the optic nerve may appear normal, or RNFL thickness may be higher than normal due to the presence of edema, but a reduction in thickness has been identified as ON progresses (Toosy et al., 2014).

Since visual acuity and visual field are reported to eventually recover (almost) completely even after significant structural loss, it is difficult to gauge the permanent visual consequences of inflammation and predict the extent of subsequent recovery with these diagnostic techniques. Indeed, deficits in contrast sensitivity, color vision, and stereopsis, as well as delayed visual evoked potentials (VEP) may continue after recovery,

and are thought to persistently deliver an abnormal visual input to the visual cortex (Beck et al., 1992). There is some evidence that shows, regardless of the degree of optic nerve degeneration and/or demyelination after ON, inter-eye VEP amplitude differences start to decrease 3–6 months from disease onset (Brusa et al., 2001). This suggests neural plasticity of posterior visual pathways contributes to the recovery of visual function in ON patients (Chan, 2012). Therefore, analyzing the impact of ON in post-optic nerve structures longitudinally using visually-driven fMRI could provide a better understanding of the consequences of ON at each stage of the visual pathway and may help us explain the observed deficits. It has been noted that functional vision measures (i.e., visual acuity, contrast sensitivity, etc.) at 1 month, not within the first week of ON onset, are good indicators of visual performance at 6 months (Kupersmith et al., 2007). As such, longitudinal fMRI findings from post-optic nerve structures can be of value in developing more accurate predictions about the progression of ON. ON patients are considered to be in the acute phase within 1 month of disease onset, recovery phase at around 3–4 months, and recovered to normal or near-normal at 1-year from disease onset. Patient demographics and clinical characteristics included in the studies reviewed in this article are reported in the supplemental information (see **Supplementary Table 1**).

## Visually driven functional brain measures

We identified 12 visually-driven fMRI studies investigating the effect of ON on the visual system. Of these, there are cross-sectional studies of ON patients in the acute stage ( $n = 1$ ), after recovery ( $n = 3$ ), and a few studies with a mixed group of ON patients with a wide range of time since onset ( $n = 3$ ), including unknown time since disease onset ( $n = 1$ ), as well as four longitudinal studies. The stimulus parameters utilized and results reported in these studies are summarized in **Figure 4**. Unless otherwise indicated in column *Stimulus: Type vs. Baseline; Fellow Eye Status*, the stimulus is generally presented in a block design where it is alternated with no visual stimulation (i.e., darkness) to both eyes as the baseline condition. Likewise, the fellow eye is patched or occluded with the use of light-proof goggles in all studies, unless specified in **Figure 4**. Some studies utilized red/green stimuli, as indicated in column *Stimulus: Color, Contrast and Flicker, Motion*, with red/green filter glasses for monocular stimulation. All ON studies scanned patients at 1.5 Tesla (Rombouts et al., 1998; Werring et al., 2000; Langkilde et al., 2002; Russ et al., 2002; Toosy et al., 2002; Levin et al., 2006; Jenkins et al., 2010; Mascioli et al., 2012) or 3 (Korsholm et al., 2007; Benoliel et al., 2017). The resolution of the functional scans are not clearly reported in the majority of the ON studies. In the reported studies, the in-plane resolution ranged from 0.9–3 mm with a slice thickness of 2–5 mm. Finally, visual areas seem to be delineated using retinotopy (Levin et al., 2006;

Benoliel et al., 2017), anatomic landmarks (Langkilde et al., 2002; Korsholm et al., 2007), cytoarchitectonic maps (Korsholm et al., 2007), and/or a semi-automated contouring technique (Toosy et al., 2002), and data were analyzed in Talairach and Tournoux (Werring et al., 2000; Toosy et al., 2002; Levin et al., 2006; Mascioli et al., 2012; Benoliel et al., 2017) or Montreal Neurological Institute (Toosy et al., 2005; Korsholm et al., 2007; Jenkins et al., 2010) reference space.

fMRI studies of *acute* unilateral ON patients revealed that activity in their visual cortex is greatly reduced for monocular stimulation of the affected eye (Russ et al., 2002; Korsholm et al., 2007; Jenkins et al., 2010; Mascioli et al., 2012), and to a lesser extent the fellow eye (Toosy et al., 2005) compared to the control group. In addition to a reported 40% reduction in BOLD responses in the visual cortex from the affected eye (Russ et al., 2002), BOLD signals from LGN were also reduced (Korsholm et al., 2007), when compared to the fellow eye and to controls. Moreover, the affected eye in ON patients showed a greater deficit to a rapidly changing stimulus, meant to engage the magnocellular channel, than to slowly contrast reversing stimuli (Russ et al., 2002). This is most likely an indication that, in addition to parvocellular-dominated loss associated with central vision in early ON, both visual pathways may be affected in the setting of diverse patterns of visual field deficits.

Several studies further emphasize that abnormalities for the affected eye in the acute phase of the disease extend beyond the early visual cortex (V1/V2). The activity in the *ventral visual processing stream*, i.e., area LOC is consistently reported to be reduced at baseline (Korsholm et al., 2007; Raz et al., 2011). However, the results have been quite mixed regarding the BOLD responses in the *dorsal stream*, including the middle temporal visual area (MT/V5) in acute ON patients. Raz et al. (2011) reported that stimulating the affected eye with visual-motion stimuli revealed a deficit in MT from the onset of the disease, although the exact timepoint since onset during data collection is unknown. In contrast, another study found no difference in the pattern of BOLD activity within MT (but not so in V1) in response to stimulation of the affected eye in comparison to fellow eye (Mascioli et al., 2012). This apparent robustness of MT to acute visual deficits, or perhaps to low visual contrast, in the affected eye is intriguing, but the generality of this finding is still quite unclear. This study utilized sub-optimal stimuli (i.e., a central stationary checkerboard) and a small cohort ( $n = 6$ ) with mixed causes of optic nerve damage. Finally, a separate study of acute ON reported that in response to flickering checkerboard stimulation the *fellow eye* produced abnormally *high* BOLD activation in dorsal regions of bilateral cuneus (Jenkins et al., 2010). In this case, the interpretation is suggestive of cortical compensatory mechanisms. Indeed, this effect remained significant even after adjusting for covariates that reflect afferent input such as optic nerve lesion length, VEP amplitudes and demographic characteristics (Jenkins et al., 2010). So, with regard to the




















	Author, Year, Subject (#)	Stimulus: Type vs. Baseline; Fellow Eye Status	Stimulus: Location & Span	Stimulus: Color, Contrast & Flicker, Motion	Main Findings: Visual Cortex Deficit	Other Findings: LGN or Cortex Deficit
	1. Rombouts et al., 1998 <i>ON (9); HC (8)</i>	Monoc/Binocular Light; unknown	Full field	Red 8Hz	Patients, affected eye/fellow eye vs. controls	
	2. Werring et al., 2000 <i>ON (7); HC (7)</i>	Monocular Light	Full field	Red 8 Hz	R: Affected eye vs. controls	R: Affected/fellow eye higher than controls; wide spread regions
	3. Toosy et al., 2002 <i>ON (8); HC (8)</i>	Monocular Light	Full field	Red 8 Hz	R: Affected eye vs. fellow eye and controls	R: Affected/fellow eye higher than controls; wide spread regions
	2. Toosy et al., 2005 <i>ON (21); HC (46, 11 longitudinal)</i>	Monocular Light	Full field	Red 8 Hz	A: Affected eye/fellow eye% {Baseline fMRI not prognostic of recovery}	A: Affected/fellow eye (LOC)^ A: Affected eye (ventral)%* R: Affected/fellow eye (ventral stream)% Fellow eye (frontal)%*
	5. Jenkins et al., 2010 <i>ON (28); HC (10)</i>	Checkerboard vs. grey background	Central fixation; span unknown	Red/green	Affected eye vs. controls^	Fellow eye higher than controls (dorsal stream)
	6. Mascioli et al., 2012 <i>ON (8)</i>	Monocular Chessboard vs. no stimuli; unknown	Central visual field; Central fixation; 6°	Black/white	Affected eye vs. fellow eye	Affected eye vs. fellow; wide spread (NOT MT & FEF)
	7. Korsholm et al., 2007 <i>ON (19)</i>	Monocular Checkerboard	Full field; Circular; 12° x 18° diameter (horiz x vert)	Black/white 100% contrast Reversal at 8Hz	A: Affected eye vs. fellow eye^~ R: Affected eye normalized	A: Affected eye vs. fellow (LGN)^ (LOC)^~ R: Affected eye normalized (LOC & LGN)
	8 Langkilde et al., 2002 <i>ON (9); HC (10)</i>	Monoc/Binocular Checkerboard vs. black screen	Full field; 27.5° diameter	Black/white 100% contrast Reversal at 8Hz	Patients vs. controls^	
	9. Russ et al., 2002 <i>ON (20); HC (20)</i>	Monocular Checkerboard vs. unknown	Full field; 34° x 21° diameter (horiz x vert)	Black/white 100% contrast 1,2,4, and 8 Hz	A: Affected eye vs. fellow eye^ ~* R: Affected eye normalize	
	10. Levin et al., 2006 <i>ON (8); HC (4)</i>	Checkerboard vs. no stimuli	Full field; 15° diameter	Red or green on black background	Affected eye vs. fellow (only V1)	
		Scrambled Object vs. no stimuli	Full field; 15° diameter	Red or green on black background	Affected eye vs. fellow (only V1, V2)	
		Object vs. no stimuli	Full field; 15° diameter	Red or green line objects on black		Affected eye higher than fellow (LOC)
	11. Raz et al., 2011 <i>ON (21); HC (21)</i>	Monocular Checkerboard vs. unknown; unknown	Unknown	Unknown	A: Affected eye vs. controls (V1) R: NOT normalized	
		Monocular Motion vs. unknown; unknown	Unknown	Expand/contract array of dots		R: Affected eye vs. controls (MT)
		Monocular Object Naming vs. unknown; unknown	Unknown	Static luminance defined objects	A: Affected eye vs. controls (trend) R: Affected eye normalized	A: Affected eye vs. fellow (LOC- trend) R: Affected eye normalized
		Monocular Object Naming vs. unknown; unknown	Unknown	Motion-defined objects Moving	A: Affected eye vs. fellow & controls R: NOT normalized	A: Affected eye vs. fellow & controls (LOC and MT) R: NOT normalized
	12. Benoliel et al., 2017 <i>ON (11); HC (11)</i>	Monocular Object vs. unknown; unknown	Unknown	Motion-defined objects Moving	R: Affected/fellow eye vs. controls for (V1)	R: Affected eye vs. fellow, connectivity (V1, V2, V3 → MT) (V2, V3 → LOC) R: Affected eye (MT)~ Fellow Eye (V3, V4h, V3a, LOC & MT)~

FIGURE 4

Summary of visual stimuli utilized and findings in visually-driven fMRI studies of ON. The studies are listed based on the type of stimulus utilized. Left: Images of visual stimuli, similar to the ones utilized in each of the studies, have been provided. Note: Image in row 7 is licensed under a Creative Commons Attribution 4.0 International (<https://creativecommons.org/licenses/by/4.0/>, <https://creativecommons.org/licenses/by/4.0/legalcode>). It is attributed to Biological Psychiatry (<https://www.sciencedirect.com/science/article/pii/S0006322307012413?via%3Dihub#fig1>). A: Findings from ON patients in acute stage of disease (i.e., <1 month from disease onset); R: Findings from ON patients in recovery or recovered stage of disease (i.e., >3 months from disease onset); otherwise, results are obtained from mixed group of ON patients or time since onset unknown. ^Deficit indicated by correlation with visual sensitivity measures (i.e., BOLD activity declines with increasing severity measure). %Deficit indicated by correlation with optic nerve structural integrity (i.e., BOLD activity declines with increasing severity measure). \*\*Compensation indicated by correlation with optic nerve structural integrity (i.e., BOLD activity increases with increasing severity measure). ~Deficit indicated by correlation with optic nerve conduction measures (shorter VEP latency/ higher amplitude) (i.e., BOLD activity declines with increasing severity measure). ~\*Compensation indicated by correlation with optic nerve conduction measures (shorter VEP latency/ higher amplitude; i.e., BOLD activity increases with increasing severity measure). Note: studies mentioned in rows 5–9 did not provide stimulus figures. We have added reference figures based on stimulus description. ON, optic neuritis; HC, healthy controls.

dorsal visual cortex, the findings for acute ON remain unclear and become even harder to explain when considering the longitudinal deficits reported in these dorsal regions (considered below). Clearly, to resolve these contradictory findings, more studies need to focus on investigating the pattern of activation in extrastriate areas in response to stimuli these areas have a preferential bias for, such as stimuli with motion (i.e., for MT) and color, natural objects or scenes, and movies (i.e., for LOC).

Several longitudinal studies exist, and they suggest that the adaptive plasticity of the visual pathway as a whole is important for facilitating the spontaneous recovery of vision in ON patients. For example, fMRI measurement from the LGN and cortical visual areas (V1, V2, LOC) was reported at onset, as well as 3 months and 6 months from onset (Korsholm et al., 2007). The inter-eye difference in activation was shown to diminish (i.e., the fMRI signal of the affected eye increased) during recovery (Korsholm et al., 2007; Raz et al., 2011), with the affected eye showing normal visual acuity as early as 4 months from onset of the disease (Raz et al., 2011). However, since the VEP amplitude of the affected eye improved as the BOLD signal in LGN improved, the authors attributed this effect to the resolution of inflammation in the optic nerve rather than the emergence of compensatory activity within LGN or other visual areas (i.e., rewiring in areas receiving altered visual input). Similarly, the recovery of BOLD activity in early visual areas and LOC at 6 months is suggested to be a result of reduced inflammation of the optic nerve and the subsequent improvement in BOLD signal in LGN and VEP amplitude (Korsholm et al., 2007). Nevertheless, the mechanisms underlying VEP amplitude recovery despite progressive post-inflammatory degeneration and demyelination of the optic nerve is unclear. By contrast, other patterns of activity do suggest the existence of compensatory mechanisms within LGN to preserve visual function after insult to the optic nerve. The LGN of ON patients was seen to perform *above* normal upon stimulation of the fellow eye at baseline, but this disappears as BOLD activity in the affected eye normalizes, around 4–6 months from disease onset (Korsholm et al., 2007). In the same vein, Toosy et al. (2005) suggest a compensatory cortical activity to account for the improvement of *ventral stream* extrastriate regions (i.e., lateral temporal, fusiform) at 3 months from disease onset. The normalized BOLD measures correlated with clinical improvement, even after accounting for optic nerve structural deficits.

Despite the substantial recovery of vision in the months following disease onset, it is important to note that certain aspects of vision remain impaired. For example, the affected eye of ON patients 1 year after disease onset still shows ~20% reduction in BOLD amplitude in early visual areas (Langkilde et al., 2002; Russ et al., 2002; Levin et al., 2006; Benoliel et al., 2017). Also, delays in VEP latencies last for a prolonged, perhaps indefinite, period of time (Korsholm et al., 2007). In addition,

a persistent deficit within MT (Raz et al., 2011), as well as weaker functional connectivity between early visual areas and MT/LOC are reported for the affected eye in comparison to fellow eye and controls (Benoliel et al., 2017). Although this needs to be further clarified, the findings outlined above imply that abnormally high activity in the *acute* stages of the disease (e.g., in MT or elsewhere in the dorsal stream) may actually predict a *lack* of recovery. Alternatively, the prolonged MT abnormalities could also reasonably be related to delayed VEPs, given the importance of temporal precision for visual motion processing.

Finally, the exact time points at which MRI and other brain measures improve for ON patients remains to be determined. For example, due to the lack of studies that investigate the activity of MT at systematic intervals from disease onset, it is difficult to determine the critical time points of disease progression within MT. More generally, it is still unclear exactly where, when, and if visual areas normalize, as some studies report it to take place within 1 month whereas others suggest 6 months. Moreover, the pattern of activation in extra-occipital regions, brain areas outside of the early visual areas, may be non-linear during the course of the disease. In other words, at one time point, an abnormally high activity in an extra-occipital region correlates with clinical deficit whereas at another time point it shows a BOLD deficit that is consistent with the reported clinical deficits. Therefore, further work needs to be conducted to understand the sequelae of BOLD alterations, and whether they are temporary (i.e., diminishes as visual function improves) or permanent (appears after the attack and remains during recovery and post-recovery phase) by regressing out the structural and functional optic nerve changes from the percent BOLD change we observe in visual areas.

## Correlation with specific ophthalmological measures

As was seen with glaucoma, the brain activity of ON patients often correlates with specific ophthalmologic indices of severity and allows us to better understand the factors influencing the changes in cortical activation. As such, in multiple studies, visual perimetry scores of the affected eye are highly correlated with fMRI responses from the early visual cortex (Russ et al., 2002; Korsholm et al., 2007; Jenkins et al., 2010), LGN (Korsholm et al., 2007), as well as LOC and peristriate cortex (Toosy et al., 2005) from the onset of disease. Correlations seen within LOC and peristriate cortex are regarded as true cortical alterations, and not evidence of separate defects, as they remained even after accounting for the structural deficit of the optic nerve (Toosy et al., 2005). BOLD activity from the visual cortex of recovered patients also corresponds to the residual deficit reported in perimetry scores (Langkilde et al., 2002). Finally, contrast sensitivity and Snellen visual acuity are also typically correlated

with BOLD signal change in the visual cortex (Langkilde et al., 2002; Russ et al., 2002).

Moreover, optic nerve structural measures also correlate moderately well with fMRI responses in the affected eye of recovered ON patients, suggesting it is a good marker for chronic changes in the visual pathway of ON patients. A longitudinal study showed that BOLD activity in the visual cortex of acute ON patients at baseline corresponded with the optic nerve structural abnormalities (gadolinium-enhanced lesion length; Toosy et al., 2005). Surprisingly, at 3 months, reduced integrity of the optic nerve produced greater activity in extra-striate regions. However, by 12 months, residual abnormality in the optic nerve once again predicted a BOLD deficit in these extra-striate regions. Due to the constantly changing status of the optic nerve, at least in the early stages of ON, interpreting the biological meaning of the correlation of RNFL thinning/OCT measures with brain activity is difficult (i.e., are the discrepancies in the correlation pattern due to the lag of brain atrophy to RNFL thinning or robustness of visual cortex to alterations of the anterior visual pathway). Likewise, functional measures such as VEP latency and amplitude also show a low, but significant correlation with BOLD variables (Russ et al., 2002). Particularly, slow VEP latencies through the optic nerve in the affected eye, but not the fellow eye, of recovered unilateral ON patients were associated with decreased activation of the motion-related visual cortices such as V3 and MT (Benoliel et al., 2017).

## Visual stimuli

The importance of the choice of stimuli in revealing ON-related abnormalities in the occipital cortex and the related cerebral cortices is quite evident from the findings reviewed (Figure 4). In the acute phase of the disease, stimulating the affected eye resulted in a deficit in visual and extra-occipital regions with any of the following stimuli: checkerboard, static luminance-defined objects, or motion-defined objects (see Figure 4). Longitudinally, checkerboard or static luminance-defined objects subsequently showed recovery of BOLD signal from the early visual cortex, LGN, and LOC, as early as 1 month from disease onset. However, with the use of checkerboard and more complex motion-related stimuli, Raz and colleagues reported reduced activity within the visual cortex (especially V1) and MT, as well as abnormalities in connectivity between early visual areas and LOC to persist even after 12 months of disease onset. Hence, it is evident that the sensitivity of fMRI in detecting the deficits in optic neuropathies such as ON is partially limited by the stimuli and the fMRI paradigm chosen for the study.

Many of the early studies use simple photic stimulation (see Figure 4). This is not an ideal visual paradigm as often these studies report activity observed in widespread regions in the striate and extra-striate cortex and it becomes difficult to understand what the reported deficit and/or compensatory

activity within these areas means in terms of visual function. The majority of the studies resorted to black and white checkerboards, particularly in the central visual field. However, ON can produce widespread and diffuse patterns of visual field loss, especially in the acute stages, and therefore utilizing standard full-field checkerboard stimuli may be more beneficial in identifying the deficits. It is also a reliable stimulus to activate the primary visual cortices but needs to be supplemented with other types of stimuli in order to study the activity of higher-order visual areas. Indeed, some studies used more complex stimuli to test aspects of central visual function such as object and motion perception. However, given that such stimuli were found only in 2 of the 12 articles we reviewed, results are hard to generalize. Moreover, no studies have used truly natural stimuli with objects and scenes. Although the reason is unclear, it may be these stimuli are relatively more difficult to use, or incompatible with dichoptic stimulation of the eyes. Of course, equally important is to consider the stimuli utilized during the baseline condition and the status of the fellow eye in dichoptic stimulation paradigms (see column *Stimulus: Type vs. Baseline; Fellow Eye Status* in Figure 4). Neither of these parameters are consistently controlled within the studies we reviewed. Emerging evidence suggests that the status of the untested eye can significantly impact the fMRI BOLD signal obtained due to potential inhibitory effects from that eye (e.g., Chadnova et al., 2018). Therefore, future studies should consider these issues more carefully.

## Traumatic optic neuropathy

TON is a rare but serious acute optic neuropathy resulting in partial or complete visual loss as a result of a lesion to the optic nerve due to trauma (i.e., a direct hit to the head or orbit in for example accidents or falls). It can be present unilaterally or bilaterally. TON can be classified as direct, via a penetrating injury, or more commonly indirect, when the force of the impact from head trauma is transferred to the optic nerve (Miliaras et al., 2013). The mechanical shearing of optic nerve axons and/or ischemia is thought to be the underlying mechanisms.

In TON, the affected eye(s) shows atrophy of the optic disc along with a severe reduction in visual acuity, visual field defects, and impaired color perception (Miliaras et al., 2013). Reduced RNFL and ganglion cell/inner plexiform layer thickness (Kyncl et al., 2019) are also seen at about 3–6 weeks following injury (Miliaras et al., 2013). These ophthalmological findings are generally normal for the fellow eye (Kyncl et al., 2019). However, pattern electroretinogram and pattern visual evoked potential, an electrophysiological measure of the function of ganglion cells and optic nerve, respectively, has been reported to be abnormal for both the affected and fellow eye for at least 3 years since onset. Despite the usefulness of these measures, there are limitations for

use in TON. Due to the traumatic nature of the condition, TON patients are often unconscious or cognitively challenged in these assessments. Consequently, diagnosis and intervention for early loss can be delayed for days.

As a result, recent studies are employing MRI to study TON as it allows us to directly investigate the impact on the optic nerve irrespective of the cognitive status of the patient. There has been some progress in applying modern structural MRI techniques (Takehara et al., 1994; Kyncl et al., 2019), including diffusion tensor imaging to characterize the optic nerve in closed head trauma (Yang et al., 2011; Bodanapally et al., 2013, 2015; Li et al., 2014). However, the results are too sparse to allow meaningful generalization. Also, the effect of the structural alternations observed in the optic nerve on the activity of subsequent visual brain activity needs to be studied.

## Visually driven functional brain measures

Unlike glaucoma and ON, TON has barely been studied using visually-driven fMRI. However, visually-driven fMRI has been utilized in a single case report of an individual with an optic nerve lesion due to an injury to the orbit. fMRI scans utilizing a checkerboard stimulus performed on the fellow eye of an individual ~9–10 months since TON onset revealed a reduction in the activity of the visual cortex. Cortical activity is reported to gradually increase but does not recover completely as deficits persist even 4 years after onset (Kyncl et al., 2019). It is important to note that the affected eye was not stimulated due to the extent of damage and inability to maintain fixation on the chosen stimulus. Finally, there are a few studies that have employed functional MRI to study a clinical manifestation similar to TON called open globe injury, but at rest. Cortical brain activity in acute open globe injury patients studied with various resting-state fMRI techniques revealed functional network dysfunction in the bilateral visual cortex/calcarine/lingual/cuneus, temporal and dorsal visual pathway (Tan et al., 2016; Ye et al., 2018), as well as in numerous higher-level brain regions such as supplementary motor area (Wang et al., 2017), frontal area and cerebellum (Huang et al., 2016). Currently, it is impossible to distinguish whether the resulting brain activity is a result of poor visual input or compensatory activity due to the reorganization of cortical networks.

Although it remains to be shown that visually-driven fMRI is a useful methodology for studying TON patients, preliminary fMRI results suggest that it is possible to employ this technique to study unilateral and bilateral TON over time. Moreover, measuring spontaneous BOLD signals during the resting state may be especially valuable in this context. The minimal demands placed on patients during resting-state scans make this technique very feasible. Nevertheless, the lack of visually-driven TON studies can also be attributed to the rarity of the condition. It is difficult to recruit a sufficient number of patients and to ensure

that the patients are at a similar stage of disease progression as TON is a rapidly changing condition. Moreover, the lack of consciousness in TON patients can make it difficult to instruct patients about the task they may be expected to perform while in the scanner. It is necessary to design visual stimuli carefully and test the MRI protocol extensively before use in TON patients to ensure smooth functioning without patient input. Finally, MRI is an expensive tool with reduced accessibility. Therefore, unless a well-thought-out system is in place, diagnosing and assessing the severity of a rapidly changing optic neuropathy like TON may be difficult.

Despite the challenges, TON results in severe consequences, and an improved understanding of the functional alterations in the visual pathway over time is needed since there is no treatment for TON at this time. Furthermore, correlating the functional brain responses to clinical measures longitudinally may provide prognostic insights. Importantly, this could be useful in identifying the factors that predict recovery of vision in some TON patients and support any future developments in drug treatment options. Clinicians could then better choose a treatment plan (e.g., natural recovery or intervention).

## Discussion

Despite some inconsistencies and the low sample size of some of the studies reviewed here, visually-driven fMRI has been shown to be sensitive and reliable in identifying functional loss of brain activity as a result of glaucoma- or ON-specific visual impairment(s). fMRI also appears promising for studying TON-induced deficits. The visually-driven fMRI literature for glaucoma patients consistently reported reduced activity in the bilateral occipital lobe, especially for peripheral visual field stimulation. In association with that, there is evidence that the magnocellular layers of the LGN are affected early in glaucoma patients, and this seems to be the only parameter that successfully differentiates glaucoma patients in the early stages from healthy normal controls. BOLD signal within V1 in response to central field stimulation is heavily dependent on the severity of glaucoma. The effect of glaucoma on higher visual areas at onset and during the progression of the disease is still unclear.

In comparison, for ON patients, reduced BOLD activity has been reported in the LGN, visual cortex, LOC, and MT, although a study reports MT to be hyperactive in the acute phase. Also, the abnormalities are more pronounced in the acute stage of the disease. Brain activity, especially within LGN, visual cortex and LOC, is reported to increase and then normalize within 3–4 months of disease onset, and this is suspected to underly the spontaneous recovery in clinical visual function in ON patients, but more direct evidence is needed. It is notable that motion perception in particular appears to remain impaired in ON patients.



It appears that RNFL measures correlate better with brain activity in early glaucoma patients. This may be due to the high reproducibility of optic nerve measurements and the marked/rapid changes the retinal nerve fiber layer undergoes at the early stages of glaucoma. Whereas, perimetry seems better for ON, likely because of the better sensitivity of perimetry to central vs. peripheral vision.

Similar to glaucoma and ON, visually-driven fMRI results from a single TON patient suggest reduced activity within the visual cortex at disease onset, followed by minimal recovery of signal. Future studies of TON patients should take inspiration from the visually-driven fMRI work conducted with glaucoma and ON patients as they have shown that optic neuropathy-induced alterations can be seen in subcortical and cortical visual areas, including retinotopic-specific alterations where applicable, from the onset of the disease.

Compared to glaucoma, ON seems to have a stronger basis for functional cortical plasticity, however, it has not been extensively explored in either of the patient groups. This is yet to be studied in TON patients. Future studies should investigate the physiological basis for compensatory-like BOLD responses in higher-level visual areas, as reported for ON patients. The cortical circuitry underlying such activity and its role in resolving vision are unknown. We will also need to investigate whether the deafferented cortical regions are rewired to process information from intact regions of the retina (i.e., enlarged receptive fields), or whether the input of the fellow eye is strengthened in these regions to make up for the lack of input from the affected eye, or is it some combination of both. The documented “remapping” of parafoveal regions of V1 in POAG provides a precedent for these effects, at least in the context of slow progressive vision loss.

Moreover, there are still many other questions that need to be investigated in glaucoma, ON, and TON patients. For all conditions, future progress would be enhanced by comparison of multiple stimuli that maximally drive various subcortical channels, visual brain areas, and cortical pathways. In addition to the known association between central/peripheral vision and parvocellular/magnocellular input, it will be interesting to use more complex stimuli that are simply more effective at driving higher-tier areas. Testing directly for dysfunction of higher-order visual functions such as object recognition has already been achieved by a few studies of ON. Further, using the same set of stimuli to study multiple patient groups would allow direct comparison of activation patterns. In addition, to increase the feasibility of acquiring data from the affected and the fellow eye of patients with central vision loss like ON and TON, the stimuli utilized in these studies should be designed with care. Utilizing full-field stimuli, larger fixation point and/or long crosshairs, as well as eye-tracking could aid ON and TON patients maintain fixation with the affected eye for the duration of the scan. The potential role of fMRI for POAG is quite different than ON and TON for several reasons. The slow onset of peripheral field loss

poses a serious challenge for early detection, and fMRI does not seem likely to provide an easy solution to that issue. However, once patients are diagnosed with POAG it is conceivable that fMRI could be optimized for sensitivity by focusing on the magnocellular pathway, and relying on hardware to stimulate the peripheral field as much as possible. Nonetheless, the cortical magnification of the central field is a very important feature of fMRI data, suggesting that greater clinical impact is likely for conditions like ON and TON. This “enrichment” of sensitivity to central vision loss is a big advantage, as is the feasibility of scanning before, during and after recovery. Finally, for all conditions, since brain areas do not work in isolation, studying the functional connectivity in visually-driven activation patterns of the brain, in addition to BOLD patterns and strength, is crucial.

In conclusion, to obtain a more complete understanding of the optic neuropathies, it is important to continue investigating them using neuroimaging techniques that allow us to study the effect of the disease on the entire visual pathway. The potential remains for detecting early or subtle changes, possibly before structural or functional eye measures. Likewise, it may help identify reliable neuroimaging parameters that can serve as prognostic measures for visual function recovery rate in ON and TON patients. This may help promptly choose appropriate participants for additional drug therapy. Finally, it may allow us to identify neuroimaging biomarkers that differentiate acute optic neuropathies from chronic optic neuropathies. Hopefully other studies utilize visually-driven fMRI to investigate glaucoma, ON and TON in a novel way to obtain valuable information about these blinding diseases.

## Author contributions

JM and AS conceived the idea. JM, AS, and SS developed the idea. SS wrote the manuscript in consultation with JM. All authors provided feedback and helped shape the manuscript. All authors contributed to the article and approved the submitted version.

## Funding

This project was supported by funds from U.S. Department of Defense CDMRP Vision Research Program Grant # W81XWH1910853.

## Acknowledgments

We thank Dr. Leonard Levin for his support, advice, and suggested improvements to the manuscript. We thank Austin C. Cooper for assistance with figures.

## Conflict of interest

The authors declare that the research was conducted in the absence of any commercial or financial relationships that could be construed as a potential conflict of interest.

## Publisher's note

All claims expressed in this article are solely those of the authors and do not necessarily represent those of their affiliated

organizations, or those of the publisher, the editors and the reviewers. Any product that may be evaluated in this article, or claim that may be made by its manufacturer, is not guaranteed or endorsed by the publisher.

## Supplementary material

The Supplementary Material for this article can be found online at: <https://www.frontiersin.org/articles/10.3389/fnhum.2022.943603/full#supplementary-material>.

## References

- Beck, R. W., Cleary, P. A., Anderson, M. M. Jr, Keltner, J. L., Shults, W. T., Kaufman, D. I., et al. (1992). A randomized, controlled trial of corticosteroids in the treatment of acute optic neuritis. The optic neuritis study group. *N. Engl. J. Med.* 326, 581–588. doi: 10.1056/NEJM199202273260901
- Behbehani, R. (2007). Clinical approach to optic neuropathies. *Clin. Ophthalmol.* 1, 233–246.
- Benoliel, T., Raz, N., Ben-Hur, T., and Levin, N. (2017). Cortical functional modifications following optic neuritis. *Mult. Scler.* 23, 220–227. doi: 10.1177/1352458516649677
- Benson, N. C., and Winawer, J. (2018). Bayesian analysis of retinotopic maps. *eLife* 7:e40224. doi: 10.7554/eLife.40224
- Bodanapally, U. K., Kathirkamanathan, S., Geraymovych, E., Mirvis, S. E., Choi, A. Y., McMillan, A. B., et al. (2013). Diagnosis of traumatic optic neuropathy: application of diffusion tensor magnetic resonance imaging. *J. Neuroophthalmol.* 33, 128–133. doi: 10.1097/WNO.0b013e3182842553
- Bodanapally, U. K., Shanmuganathan, K., Shin, R. K., Dreizin, D., Katzman, L., Reddy, R. P., et al. (2015). Hyperintense optic nerve due to diffusion restriction: diffusion-weighted imaging in traumatic optic neuropathy. *Am. J. Neuroradiol.* 36, 1536–1541. doi: 10.3174/ajnr.A4290
- Borges, V. M., Danesh-Meyer, H. V., Black, J. M., and Thompson, B. (2015). Functional effects of unilateral open-angle glaucoma on the primary and extrastriate visual cortex. *J. Vis.* 15, 1–14. doi: 10.1167/15.15.9
- Bowd, C., Zangwill, L. M., Berry, C. C., Blumenthal, E. Z., Vasile, C., Sanchez-Galeana, C., et al. (2001). Detecting early glaucoma by assessment of retinal nerve fiber layer thickness and visual function. *Invest. Ophthalmol. Vis. Sci.* 42, 1993–2003.
- Broadway, D. C. (2012). How to test for a relative afferent pupillary defect (RAPD). *Community Eye Health* 25, 58–59.
- Broadway, D. C., and Cate, H. (2015). Pharmacotherapy and adherence issues in treating elderly patients with glaucoma. *Drugs Aging* 32, 569–581. doi: 10.1007/s40266-015-0282-9
- Brusa, A., Jones, S. J., and Plant, G. T. (2001). Long-term remyelination after optic neuritis: a 2-year visual evoked potential and psychophysical serial study. *Brain* 124, 468–479. doi: 10.1093/brain/124.3.468
- Chadnova, E., Reynaud, A., Clavagnier, S., Baker, D. H., Baillet, S., Hess, R. F., et al. (2018). Interocular interaction of contrast and luminance signals in human primary visual cortex. *Neuroimage* 167, 23–30. doi: 10.1016/j.neuroimage.2017.10.035
- Chaimow, D., Yacoub, E., Ugurbil, K., and Shmuel, A. (2018). Spatial specificity of the functional MRI blood oxygenation response relative to neuronal activity. *Neuroimage* 164, 32–47. doi: 10.1016/j.neuroimage.2017.08.077
- Chan, J. W. (2012). Early diagnosis, monitoring and treatment of optic neuritis. *Neurologist* 18, 23–31. doi: 10.1097/NRL.0b013e31823d7acd
- Cohen, L. P., and Pasquale, L. R. (2014). Clinical characteristics and current treatment of glaucoma. *Cold Spring Harb. Perspect. Med.* 4:a017236. doi: 10.1101/cshperspect.a017236
- Duncan, R. O., Sample, P. A., Weinreb, R. N., Bowd, C., and Zangwill, L. M. (2007a). Retinotopic organization of primary visual cortex in glaucoma: a method for comparing cortical function with damage to the optic disk. *Invest. Ophthalmol. Vis. Sci.* 48, 733–744. doi: 10.1167/iops.06-0773
- Duncan, R. O., Sample, P. A., Weinreb, R. N., Bowd, C., and Zangwill, L. M. (2007b). Retinotopic organization of primary visual cortex in glaucoma: comparing fMRI measurements of cortical function with visual field loss. *Prog. Retin. Eye Res.* 26, 38–56. doi: 10.1016/j.preteyeres.2006.10.001
- Fox, P. T., and Raichle, M. E. (1984). Stimulus rate dependence of regional cerebral blood flow in human striate cortex, demonstrated by positron emission tomography. *J. Neurophysiol.* 51, 1109–1120. doi: 10.1152/jn.1984.51.5.1109
- Gerente, V. M., Schor, R. R., Chaim, K. T., De Maria Felix, M., Ventura, D. F., Teixeira, S. H., et al. (2015). Evaluation of glaucomatous damage via functional magnetic resonance imaging and correlations thereof with anatomical and psychophysical ocular findings. *PLoS One* 10, 1–12. doi: 10.1371/journal.pone.0126362
- Havvas, I., Papaconstantinou, D., Moschos, M. M., Theodossiadi, P., Andreanos, V., Ekatomatis, P., et al. (2013). Comparison of SWAP and SAP on the point of glaucoma conversion. *Clin. Ophthalmol.* 7, 1805–1810. doi: 10.2147/OPHT.S50231
- Huang, X., Li, H. J., Ye, L., Zhang, Y., Wei, R., Zhong, Y. L., et al. (2016). Altered regional homogeneity in patients with unilateral acute open-globe injury: a resting-state functional MRI study. *Neuropsychiatr. Dis. Treat.* 12, 1901–1906. doi: 10.2147/NDT.S110541
- Jenkins, T., Ciccarelli, O., Toosy, A., Miszkil, K., Wheeler-Kingshott, C., Altmann, D., et al. (2010). Dissecting structure-function interactions in acute optic neuritis to investigate neuroplasticity. *Hum. Brain Mapp.* 31, 276–286. doi: 10.1002/hbm.20863
- Jiang, M. M., Zhou, Q., Liu, X. Y., Shi, C. Z., Chen, J., Huang, X. H., et al. (2017). Structural and functional brain changes in early- and mid-stage primary open-angle glaucoma using voxel-based morphometry and functional magnetic resonance imaging. *Medicine* 96, 1–7. doi: 10.1097/MD.00000000000006139
- Jonas, J. B., Aung, T., Bourne, R. R., Bron, A. M., Ritch, R., Panda-Jonas, S., et al. (2017). Glaucoma. *Lancet* 390, 2183–2193. doi: 10.1016/S0140-6736(17)31469-1
- Keltner, J. L., Johnson, C. A., Spurr, J. O., and Beck, R. W. (1993). Baseline visual field profile of optic neuritis. The experience of the optic neuritis treatment trial. Optic neuritis study group. *Arch. Ophthalmol.* 111, 231–234. doi: 10.1001/archophth.1993.01090020085029
- Keltner, J. L., Johnson, C. A., Spurr, J. O., and Beck, R. W. (1999). Comparison of central and peripheral visual field properties in the optic neuritis treatment trial. *Am. J. Ophthalmol.* 128, 543–553. doi: 10.1016/s0002-9394(99)00304-9
- Korsholm, K., Madsen, K. H., Frederiksen, J. L., Skimminge, A., and Lund, T. E. (2007). Recovery from optic neuritis: an ROI-based analysis of LGN and visual cortical areas. *Brain* 130, 1244–1253. doi: 10.1093/brain/awm045
- Kupersmith, M. J., Gal, R. L., Beck, R. W., Xing, D., Miller, N., Optic Neuritis Study Group, et al. (2007). Visual function at baseline and 1 month in acute optic neuritis: predictors of visual outcome. *Neurology* 69, 508–514. doi: 10.1212/01.wnl.0000267272.60714.42
- Kwong, K. K., Belliveau, J. W., Chesler, D. A., Goldberg, I. E., Weisskoff, R. M., Poncelet, B. P., et al. (1992). Dynamic magnetic resonance imaging of human brain activity during primary sensory stimulation. *Proc. Natl. Acad. Sci. U S A* 89, 5675–5679. doi: 10.1073/pnas.89.12.5675
- Kyncl, M., Lestak, J., Tintera, J., and Haninec, P. (2019). Traumatic optic neuropathy—a contralateral finding: a case report. *Exp. Ther. Med.* 17, 4244–4248. doi: 10.3892/etm.2019.7445

- Langkilde, A. R., Frederiksen, J. L., Rostrup, E., and Larsson, H. B. W. (2002). Functional MRI of the visual cortex and visual testing in patients with previous optic neuritis. *Eur. J. Neurol.* 9, 277–286. doi: 10.1046/j.1468-1331.2002.00399.x
- Lawlor, M., Danesh-Meyer, H., Levin, L. A., Davagnanam, I., De Vita, E., Plant, G. T., et al. (2018). Glaucoma and the brain: trans-synaptic degeneration, structural change and implications for neuroprotection. *Surv. Ophthalmol.* 63, 296–306. doi: 10.1016/j.survophthal.2017.09.010
- Levin, N., Orlov, T., Dotan, S., and Zohary, E. (2006). Normal and abnormal fMRI activation patterns in the visual cortex after recovery from optic neuritis. *Neuroimage* 33, 1161–1168. doi: 10.1016/j.neuroimage.2006.07.030
- Li, J., Shi, W., Li, M., Wang, Z., He, H., Xian, J., et al. (2014). Time-dependent diffusion tensor changes of optic nerve in patients with indirect traumatic optic neuropathy. *Acta Radiol.* 55, 855–863. doi: 10.1177/0284185113506900
- Mascioli, G., Salvolini, S., Cavola, G. L., Fabri, M., Giovannini, A., Mariotti, C., et al. (2012). Functional MRI examination of visual pathways in patients with unilateral optic neuritis. *Radiol. Res. Pract.* 2012:265306. doi: 10.1155/2012/265306
- Miliaras, G., Fotakopoulos, G., Asproudis, I., Voulgaris, S., Zikou, A., Polyzoidis, K., et al. (2013). Indirect traumatic optic neuropathy following head injury: report of five patients and review of the literature. *J. Neurol. Surg. A Cent. Eur. Neurosurg.* 74, 168–174. doi: 10.1055/s-0032-1330115
- Murphy, M. C., Conner, I. P., Teng, C. Y., Lawrence, J. D., Safiullah, Z., Wang, B., et al. (2016). Retinal structures and visual cortex activity are impaired prior to clinical vision loss in glaucoma. *Sci. Rep.* 6, 1–11. doi: 10.1038/srep31464
- Ogawa, S., Tank, D. W., Menon, R., Ellermann, J. M., Kim, S. G., Merkle, H., et al. (1992). Intrinsic signal changes accompanying sensory stimulation: functional brain mapping with magnetic resonance imaging. *Proc. Natl. Acad. Sci. U S A* 89, 5951–5955. doi: 10.1073/pnas.89.13.5951
- Pau, D., Al Zubidi, N., Yalamanchili, S., Plant, G. T., and Lee, A. G. (2011). Optic neuritis. *Eye* 25, 833–842. doi: 10.1038/eye.2011.81
- Qing, G., Zhang, S., Wang, B., and Wang, N. (2010). Functional MRI signal changes in primary visual cortex corresponding to the central normal visual field of patients with primary open-angle glaucoma. *Invest. Ophthalmol. Vis. Sci.* 51, 4627–4634. doi: 10.1167/iops.09-4834
- Raz, N., Dotan, S., Benoliel, T., Chokron, S., Ben-Hur, T., Levin, N., et al. (2011). Sustained motion perception deficit following optic neuritis: Behavioral and cortical evidence. *Neurology* 76, 2103–2111. doi: 10.1212/WNL.0b013e31821f4602
- Rombouts, S. A., Lazeron, R. H., Scheltens, P., Uitdehaag, B. M., Sprenger, M., Valk, J., et al. (1998). Visual activation patterns in patients with optic neuritis: an fMRI pilot study. *Neurology* 50, 1896–1899. doi: 10.1212/wnl.50.6.1896
- Russ, M. O., Cleff, U., Lanfermann, H., Schalnus, R., Enzensberger, W., Kleinschmidt, A., et al. (2002). Functional magnetic resonance imaging in acute unilateral optic neuritis. *J. Neuroimaging* 12, 339–350. doi: 10.1111/j.1552-6569.2002.tb00142.x
- Sereno, M. I., Dale, A. M., Reppas, J. B., Kwong, K. K., Belliveau, J. W., Brady, T. J., et al. (1995). Borders of multiple visual areas in humans revealed by functional magnetic resonance imaging. *Science* 268, 889–893. doi: 10.1126/science.7754376
- Sharma, P., Sample, P. A., Zangwill, L. M., and Schuman, J. S. (2008). Diagnostic tools for glaucoma detection and management. *Surv. Ophthalmol.* 53, S17–S32. doi: 10.1016/j.survophthal.2008.08.003
- Singh, K. D., Smith, A. T., and Greenlee, M. W. (2000). Spatiotemporal frequency and direction sensitivities of human visual areas measured using fMRI. *Neuroimage* 12, 550–564. doi: 10.1006/nimg.2000.0642
- Susanna, R. Jr., and Vessani, R. M. (2009). Staging glaucoma patient: why and how? *Open Ophthalmol. J.* 3, 59–64. doi: 10.2174/1874364100903020059
- Takehara, S., Tanaka, T., Uemura, K., Shinohara, Y., Yamamoto, T., Tokuyama, T., et al. (1994). Optic nerve injury demonstrated by MRI with STIR sequences. *Neuroradiology* 36, 512–514. doi: 10.1007/BF00593510
- Tan, G., Huang, X., Ye, L., Wu, A. H., He, L. X., Zhong, Y. L., et al. (2016). Altered spontaneous brain activity patterns in patients with unilateral acute open globe injury using amplitude of low-frequency fluctuation: a functional magnetic resonance imaging study. *Neuropsychiatr. Dis. Treat.* 12, 2015–2020. doi: 10.2147/NDT.S110539
- Toosy, A. T., Hickman, S. J., Miskiel, K. A., Jones, S. J., Plant, G. T., Altmann, D. R., et al. (2005). Adaptive cortical plasticity in higher visual areas after acute optic neuritis. *Ann. Neurol.* 57, 622–633. doi: 10.1002/ana.20448
- Toosy, A. T., Mason, D. F., and Miller, D. H. (2014). Optic neuritis. *Lancet Neurol.* 13, 83–99. doi: 10.1016/S1474-4422(13)70259-X
- Toosy, A. T., Werring, D. J., Bullmore, E. T., Plant, G. T., Barker, G. J., Miller, D. H., et al. (2002). Functional magnetic resonance imaging of the cortical response to photic stimulation in humans following optic neuritis recovery. *Neurosci. Lett.* 330, 255–259. doi: 10.1016/s0304-3940(02)00700-0
- Wandell, B. A., Dumoulin, S. O., and Brewer, A. A. (2007). Visual field maps in human cortex. *Neuron* 56, 366–383. doi: 10.1016/j.neuron.2007.10.012
- Wang, H., Chen, T., Ye, L., Yang, Q. C., Wei, R., Zhang, Y., et al. (2017). Network centrality in patients with acute unilateral open globe injury: a voxelwise degree centrality study. *Mol. Med. Rep.* 16, 8295–8300. doi: 10.3892/mmr.2017.7635
- Wang, L., Mruczek, R. E., Arcaro, M. J., and Kastner, S. (2015). Probabilistic maps of visual topography in human cortex. *Cerebral Cortex* 25, 3911–3931. doi: 10.1093/cercor/bhu277
- Weinreb, R. N., and Khaw, P. T. (2004). Primary open-angle glaucoma. *Lancet* 363, 1711–1720. doi: 10.1016/S0140-6736(04)16257-0
- Werring, D. J., Bullmore, E. T., Toosy, A. T., Miller, D. H., Barker, G. J., MacManus, D. G., et al. (2000). Recovery from optic neuritis is associated with a change in the distribution of cerebral response to visual stimulation: a functional magnetic resonance imaging study. *J. Neurol. Neurosurg. Psychiatry* 68, 441–449. doi: 10.1136/jnnp.68.4.441
- Wilhelm, H., and Schabet, M. (2015). The diagnosis and treatment of optic neuritis. *Dtsch. Arztebl. Int.* 112, 616–626. doi: 10.3238/arztebl.2015.0616
- Wu, Z., and Medeiros, F. A. (2018). Recent developments in visual field testing for glaucoma. *Curr. Opin. Ophthalmol.* 29, 141–146. doi: 10.1097/ICU.0000000000000461
- Yang, Q. T., Fan, Y. P., Zou, Y., Kang, Z., Hu, B., Liu, X., et al. (2011). Evaluation of traumatic optic neuropathy in patients with optic canal fracture using diffusion tensor magnetic resonance imaging: a preliminary report. *ORL J. Otorhinolaryngol. Relat. Spec.* 73, 301–307. doi: 10.1159/000330723
- Yaqub, M. (2012). Visual fields interpretation in glaucoma: a focus on static automated perimetry. *Community Eye Health* 25, 1–8.
- Ye, L., Wei, R., Huang, X., Shi, W. Q., Yang, Q. C., Yuan, Q., et al. (2018). Reduction in interhemispheric functional connectivity in the dorsal visual pathway in unilateral acute open globe injury patients: a resting-state fMRI study. *Int. J. Ophthalmol.* 11, 1056–1060. doi: 10.18240/ijo.2018.06.26
- Zhang, P., Wen, W., Sun, X., and He, S. (2016). Selective reduction of fMRI responses to transient achromatic stimuli in the magnocellular layers of the LGN and the superficial layer of the SC of early glaucoma patients. *Hum. Brain Mapp.* 37, 558–569. doi: 10.1002/hbm.23049
- Zhang, S., Wang, B., Xie, Y., Zhu, S. H., Thomas, R., Qing, G., et al. (2015). Retinotopic changes in the gray matter volume and cerebral blood flow in the primary visual cortex of patients with primary open-angle glaucoma. *Invest. Ophthalmol. Vis. Sci.* 56, 6171–6178. doi: 10.1167/iops.15-17286
- Zhou, W., Muir, E. R., Nagi, K. S., Chalfin, S., Rodriguez, P., Duong, T. Q., et al. (2017). Retinotopic fMRI reveals visual dysfunction and functional reorganization in the visual cortex of mild to moderate glaucoma patients. *J. Glaucoma* 26, 430–437. doi: 10.1097/IJG.0000000000000641



## OPEN ACCESS

## EDITED BY

Yan Tong,  
Renmin Hospital of Wuhan University,  
China

## REVIEWED BY

Tianming Huo,  
Wuhan University, China  
Fei Chen,  
First Affiliated Hospital of Zhengzhou  
University, China

## \*CORRESPONDENCE

Yu Lin Zhong  
804722489@qq.com

†These authors have contributed  
equally to this work

## SPECIALTY SECTION

This article was submitted to  
Brain Imaging and Stimulation,  
a section of the journal  
Frontiers in Human Neuroscience

RECEIVED 05 June 2022

ACCEPTED 12 August 2022

PUBLISHED 16 September 2022

## CITATION

Xiao YM, Gan F, Liu H and Zhong YL  
(2022) Altered synchronous neural  
activities in retinal vein occlusion  
patients: A resting-state fMRI study.  
*Front. Hum. Neurosci.* 16:961972.  
doi: 10.3389/fnhum.2022.961972

## COPYRIGHT

© 2022 Xiao, Gan, Liu and Zhong. This  
is an open-access article distributed  
under the terms of the [Creative  
Commons Attribution License \(CC BY\)](#).  
The use, distribution or reproduction in  
other forums is permitted, provided  
the original author(s) and the copyright  
owner(s) are credited and that the  
original publication in this journal is  
cited, in accordance with accepted  
academic practice. No use, distribution  
or reproduction is permitted which  
does not comply with these terms.

# Altered synchronous neural activities in retinal vein occlusion patients: A resting-state fMRI study

Yu Mei Xiao<sup>1†</sup>, Fan Gan<sup>2†</sup>, Hui Liu<sup>2</sup> and Yu Lin Zhong<sup>2\*</sup>

<sup>1</sup>Department of Operation, Jiangxi Provincial People's Hospital, The First Affiliated Hospital of Nanchang Medical College, Nanchang, China, <sup>2</sup>Department of Ophthalmology, Jiangxi Provincial People's Hospital, The First Affiliated Hospital of Nanchang Medical College, Nanchang, China

**Objective:** Retinal vein occlusion (RVO) is the second most common retinal vascular disorder after diabetic retinopathy, which is the main cause of vision loss. Retinal vein occlusion might lead to macular edema, causing severe vision loss. Previous neuroimaging studies of patients with RVO demonstrated that RVO was accompanied by cerebral changes, and was related to stroke. The purpose of the study is to investigate synchronous neural activity changes in patients with RVO.

**Methods:** A total of 50 patients with RVO and 48 healthy subjects with matched sex, age, and education were enrolled in the study. The ReHo method was applied to investigate synchronous neural activity changes in patients with RVO.

**Results:** Compared with HC, patients with RVO showed increased ReHo values in the bilateral cerebellum\_4\_5. On the contrary, patients with RVO had decreased ReHo values in the bilateral middle occipital gyrus, right cerebellum\_crus1, and right inferior temporal gyrus.

**Conclusion:** Our study demonstrated that patients with RVO were associated with abnormal synchronous neural activities in the cerebellum, middle occipital gyrus, and inferior temporal gyrus. These findings shed new insight into neural mechanisms of vision loss in patients with RVO.

## KEYWORDS

retinal vein occlusion, regional homogeneity, resting-state fMRI, brain activity, fMRI

## Introduction

Retinal vein occlusion (RVO) is a common ophthalmic disease, which is the second most common retinal vascular disorder after diabetic retinopathy and is the main cause of vision loss. Retinal vein occlusion can be classified as hemorrhagic. In recent years, growing evidences have demonstrated that there are several risk factors for the



occurrence of RVO such as hypertension, (Ponto et al., 2019) hyperlipidemia, (Kolar, 2014) and/or diabetes mellitus (Chang et al., 2021). The clinical manifestations of retinal vein occlusion are flame hemorrhages, dot and blot hemorrhages, cotton wool spots, hard exudates, retinal edema, and dilated tortuous veins (Jaulim et al., 2013). At present, the effective treatments of RVO mainly include injection of anti-VEGF drugs and retinal laser (Ciulla et al., 2021). However, there are still some patients with RVO with poor outcomes and recurrent macular edema. Recent studies have shown that RVO in patients, not only causes changes in the retina, but may also be accompanied by abnormalities in cerebral blood vessels (Park et al., 2015; Rim et al., 2015). Meanwhile, the RVO can be seen as a sign of cerebral disease. Nam et al. (2021) found that the patients with RVO had increased risks of dementia and Alzheimer's disease. Lee et al. (2021) demonstrated that patients with RVO with APOE $\epsilon$ 4 allele are at higher risk for vascular dementia. However, at present, recent studies showed the cerebral disease caused by RVO are all indirect evidence and lack direct evidence. The exact pathological mechanism of brain changes caused by RVO is not clear.

Magnetic resonance imaging (MRI) provides us with an important method to assess brain function and structural changes *in vivo*. Dong et al. (2021) reported that patients with RVO showed abnormal brain network hubs related to the right superior parietal lobule, middle frontal gyrus, and left precuneus. Su et al. (2020) found that patients with RVO had abnormal functional connectivity between the primary visual cortex, and visual-related and cognitive-related region. Cho et al. (2017) demonstrated that incidence of cerebral small vessel disease were higher in young patients with RVO. Zhang et al. (2022) reported that patients with RVO were associated with abnormal white matter bundle, which is located in the bilateral posterior thalamic, bilateral sagittal stratum. However, there are few studies on the cerebral functions and structure changes in patients with RVO. The exact synchronous neural activity changes in the patients with RVO remain unknown.

The human brain had synchronized neural activity at rest. The synchronized neural activity plays a critical role in the multiple neurophysiological functions. Piazza et al. (2021) demonstrated that child participants showed synchronized neural activity during book reading and showed a positive correlation between learning and intersubject neural synchronization in the parietal cortex. Grover et al. (2021) also demonstrated that synchronous electrophysiological rhythms are a core mechanism for cognitive function and its breakdown in neuropsychiatric disorders. Benedetto et al. (2021) reported that a synchronized neural rhythm will modulate cortical excitability rhythmically, which should be reflected in sensorimotor and visual areas coherence to encode sensory-motor timing. Regional homogeneity (ReHo) is a novel fMRI method, which is applied to calculate the coherence of blood oxygen levels depend on (BOLD) signals

(Zang et al., 2004). The ReHo values are reflected in the cerebral synchronized neural activity changes. The ReHo method has a high temporal and spatial resolution. Besides, the ReHo method is a data-driven technology, which can reflect the whole brain synchronized neural activity changes without beforehand region of interest. The ReHo method has been successfully applied to study the changes in the brain neural mechanisms in various neurological diseases such as depression, (Yan et al., 2021) mild cognitive impairment (Liu et al., 2021) and stroke (Zhao et al., 2018). However, the whole brain synchronized neural activity changes in patients with RVO remain unclear.

Based on these assumptions, our study is to determine whether the patients with RVO were associated with the whole brain synchronized neural activity changes. Our study will shed new light on the neural mechanism of visual loss in patients with RVO.

## Materials and methods

### Participants

In total, fifty patients with RVO (25 men, 25 women, 35 BRVO, and 15 RVO) and 48 HCs (24 men, 24 women) participated in the study. The diagnostic criteria of RVO were by fundus examination such as intraretinal hemorrhages, cotton wool spots, and vascular congestion.

The exclusion criteria of RVO in the study were: (1) RVO accompanied by arterial occlusion or ocular ischemic syndrome; and (2) with other eye diseases (glaucoma, amblyopia, high myopia, or optic neuritis).

All the HCs met the following criteria: (1) no ocular diseases (myopia, cataracts, glaucoma, optic neuritis, or retinal degeneration); (2) binocular visual acuity 1.0; (3) no ocular surgical history; and (4) no mental disorders.

Ethical statement: All the research methods followed the Declaration of Helsinki and were approved by the Ethical Committee for Medicine of Jiangxi Provincial People's Hospital.

TABLE 1 Clinical information for two groups.

	RVO group	HC group	T-values	P-values
Sex (male/female)	50	48	N/A	0.780
Mean age (years)	45.15 $\pm$ 14.95	45.30 $\pm$ 13.87	-0.038	0.970
Education (years)	10.96 $\pm$ 3.73	11.12 $\pm$ 2.86	-0.164	0.871
BCVA-OD	0.44 $\pm$ 0.27	1.16 $\pm$ 0.16	-11.474	< 0.001*
BCVA-OS	0.43 $\pm$ 0.37	1.19 $\pm$ 0.16	-9.352	< 0.001*

Chi-square test for sex.

Independent *t*-test was used for other normally distributed continuous data.

Data are presented as mean  $\pm$  standard deviation.

RVO, retinal vein occlusion; HC, healthy control; BCVA, best-corrected visual acuity; OD, oculus dexter; OS, oculus sinister.

\**p* < 0.05.

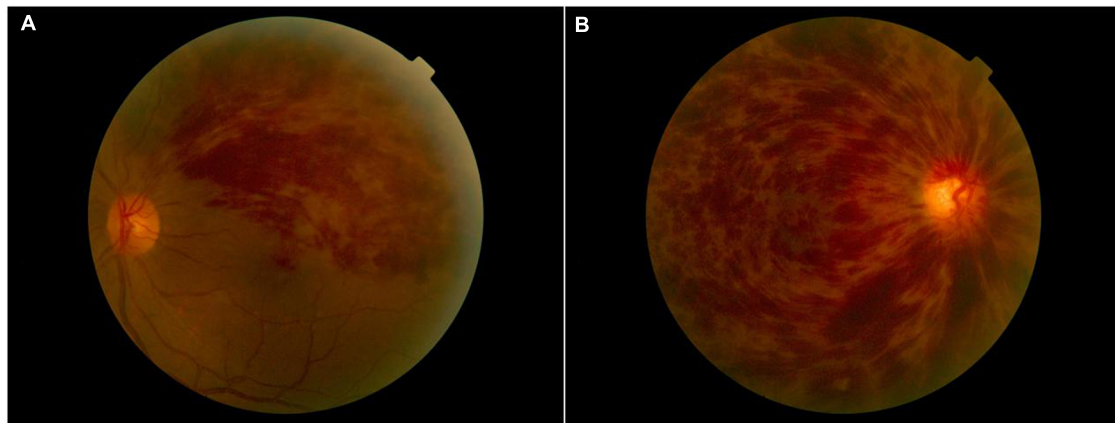


FIGURE 1

A typical fundus photograph of BRVO (A) and CRVO (B). BRVO, branch retinal vein occlusion; CRVO, central retinal vein occlusion.

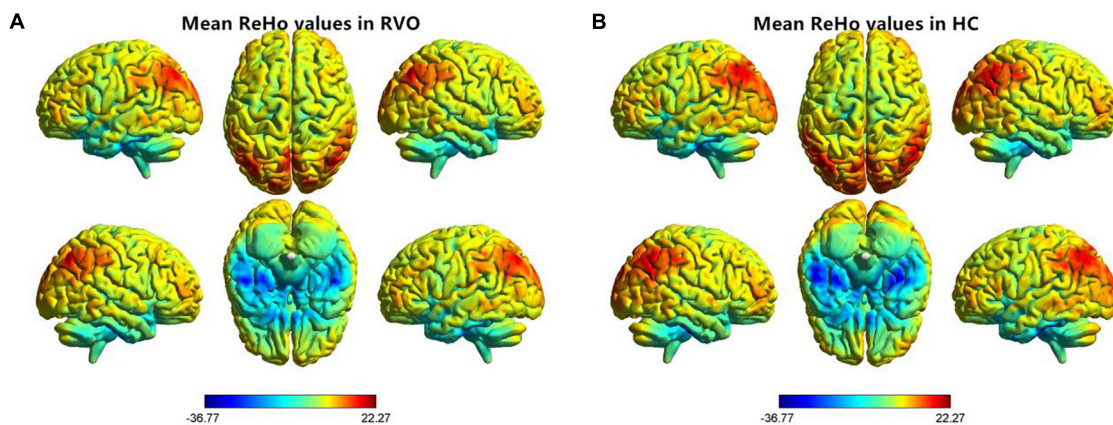


FIGURE 2

Distribution patterns of the ReHo value at the group level in patients with RVO and HCs. One-sample *t*-test result of ReHo maps within the RVO (A) and HCs (B). The color bar represents the *t* values. RVO, retinal vein occlusion; HC, health controls; ReHo, regional homogeneity; L, left; R, right.

## Clinical data analysis

The visual acuity of all subjects was measured using the logMAR table and intraocular pressure was assessed by automatic intraocular pressure measurement. The best-corrected VA and intraocular pressure of both eyes were measured in each group.

## MRI data acquisition

The MRI scanning was performed on a 3-Tesla MR scanner (750W GE Healthcare, Milwaukee, WI, United States) with an eight-channel head coil. All the participants were required to close their eyes without falling asleep when undergoing MRI scanning. In total, 240 functional images

parameters (repetition time = 2,000 ms, echo time = 25 ms, thickness = 3.0 mm, gap = 1.2 mm, acquisition matrix =  $64 \times 64$ , field of view =  $240 \times 240 \text{ mm}^2$ , flip angle =  $90^\circ$ , voxel size =  $3.6 \times 3.6 \times 3.6 \text{ mm}^3$ , and 35 axial slices) covering the whole brain were obtained.

## Data preprocessing

All the preprocessing was performed using the toolbox for Data Processing and Analysis of Brain Imaging (DPABI<sup>1</sup>) (Yan et al., 2016) and specific analysis steps were referred to previous researches (Chen et al., 2022; Wen et al., 2022). The

<sup>1</sup> <http://www.rfmri.org/dpabi>

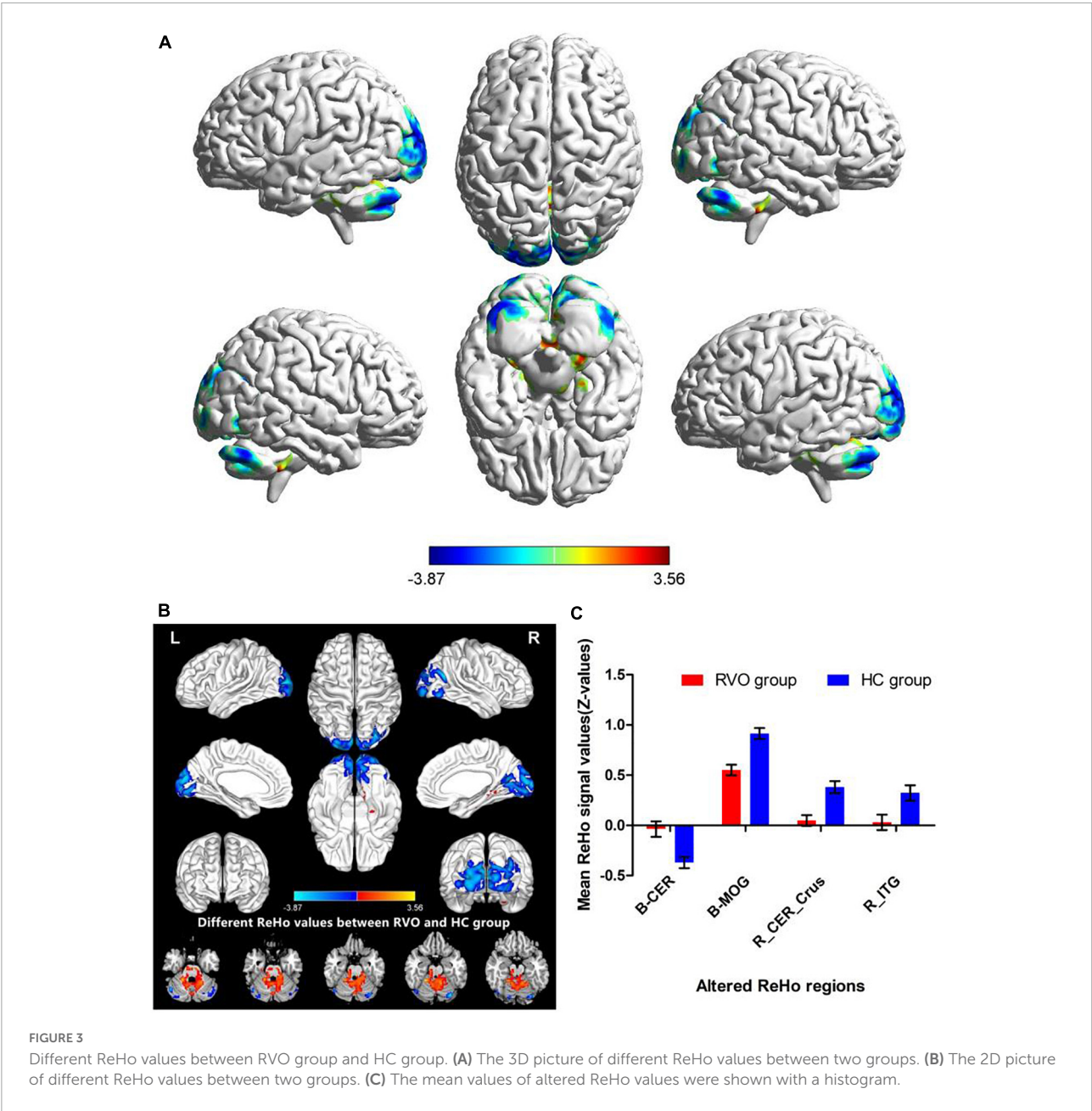


TABLE 2 Brain regions with significantly different ReHo signal values between two groups.

Conditions	Brain regions	Cluster size	MNI coordinates			t-score of peak voxel
			X	Y	Z	
RVO > HCs	B-Cerebelum_4_5	1128	27	−27	−51	3.5638
RVO < HCs	B-Middle Occipital Gyrus	1718	3	−99	3	−3.8721
RVO < HCs	R_Cerebelum_Crus1	203	48	−63	−30	−3.4208
RVO < HCs	R_Inferior Temporal Gyrus	26	48	−69	−6	−2.5795

x, y, and z are the locations of the peak voxels in standard MNI coordinates.  
The statistical threshold was set at (two-tailed, voxel-level  $P < 0.05$ , GRF correction, cluster-level  $P < 0.05$ ).  
RVO, retinal vein occlusion; ReHo, regional homogeneity; HC, healthy control; MNI, Montreal Neurological Institute; GRF, Gaussian random field; B, bilateral; R, right.

details steps were as follows: (1) Remove first 10-time points of each subject. (2) Slice timing effects, motion corrected, and realigned. (3) Individual T1-weighted images were registered to the mean fMRI data. (4) Normalized to the standard Montreal Neurological Institute (MNI) space. (5) Detrend of the time course was performed. (6) Linear regression analysis was used to remove nuisance covariates (such as white matter signal, six head motion parameters, and cerebrospinal fluid signal). (7) After that, the fMRI images were band pass-filtered (0.01–0.08 Hz) to reduce the effects of low-frequency drift and high-frequency signals.

## ReHo analysis

The ReHo index was calculated by DPABI software. All ReHo maps of each voxel were *z*-transformed with Fisher's *r*-to-*z* transformation to reduce the influence of individual variation for group statistical comparisons.

## Statistical analysis

The independent sample *t*-test was used to investigate the clinical features of the two groups.

The one-sample *t*-test was conducted to assess the group mean of ReHo maps. The two-sample *t*-test was used to compare the two group differences in the ReHo and FC maps using the Gaussian random field (GRF) method (two-tailed, voxel-level  $P < 0.05$ , GRF correction, cluster-level  $P < 0.05$ ).

## Results

### Demographics and disease characteristics

There were no statistically significant differences between the RVO and HC groups in gender, education, or age, but significant differences in BCVA of the right eye ( $p < 0.001$ ), left eye ( $p < 0.001$ ). The results of these data were listed in **Table 1**. A typical fundus photograph of BRVO (**Figure 1A**) and CRVO (**Figure 1B**).

### Comparisons of ReHo between patients with PACG and HC

The group means of ReHo maps of the RVO and HC are shown in **Figures 2A,B**. Compared with HC, patients with RVO showed increased ReHo values in the bilateral cerebellum\_4\_5. On the contrary, patients with RVO had decreased ReHo values in the bilateral middle occipital gyrus, right cerebellum\_crus1, and right inferior temporal gyrus

(**Table 2** and **Figures 3A,B**) The mean values of altered ReHo values were shown with a histogram (**Figure 3C**).

## Discussion

In our study, compared with HC, patients with RVO showed increased ReHo values in the bilateral cerebellum\_4\_5. On the contrary, patients with RVO had decreased ReHo values in the bilateral middle occipital gyrus, right cerebellum\_crus1, and right inferior temporal gyrus. Thus, the patients with RVO were associated with widespread cerebral neural activity changes related to the cerebellum, occipital gyrus, and temporal gyrus.

Our study demonstrated that patients with RVO showed a significant decrease in ReHo values in the bilateral middle occipital gyrus. The middle occipital gyrus is the location of the primary visual cortex, which receives visual signals from the retina and transfers these visual information into the higher visual cortex. The most important pathology of RVO is obstruction of retinal veins, accompanied by hemorrhage and exudation and macular edema, which can lead to the retinal ganglion cell dysfunction. Thus, the visual loss of RVO might be contributed to the decreased ReHo values. Meanwhile, previous neuroimaging studies demonstrated that patients with RVO were associated with visual cortex dysfunction (Su et al., 2020). Consistent with these findings, our study found that patients with RVO showed a significant decrease in ReHo values in the bilateral visual cortex, which might be reflect the visual dysfunction in patients with RVO.

Another important finding is that patients with RVO showed increased ReHo values in the bilateral cerebellum\_4\_5 and decreased ReHo values in the right cerebellum\_crus1.

The cerebellum is an important cerebral region, which responds to the controls of movement and balance perception. Previous neuroimaging studies have reported that cerebrovascular disease is associated with cerebellar dysfunction (Zhang et al., 2016; Koch et al., 2019). Dong et al. (2007) demonstrated that stroke patients showed fMRI activation in the perilesional primary motor cortex and cerebellum with training-related motor gains after stroke. Wei et al. (2020) found that ischemic pontine stroke patients showed significant gray matter volume (GMV) atrophy in the bilateral cerebellar posterior lobe. Thus, our study demonstrated that the patients with RVO showed abnormal ReHo values in the bilateral cerebellum, which might reflect that patients with RVO may have the same brain function changes as stroke.

Some limitations should be mentioned in the study. First, the sample size of this study is small. Second, in our study, patients with RVO were accompanied by hypertension and other diseases, which may have a certain impact on the results of the study. Third, during fMRI scanning, MRI machine noise and physiological noises (breathing and heart rate) can affect BOLD signals.



## Conclusion

Our study demonstrated that patients with RVO were associated with abnormal synchronous neural activities in the cerebellum, middle occipital gyrus, and inferior temporal gyrus. These findings shed new insight into neural mechanisms of vision loss in patients with RVO.

## Data availability statement

The raw data supporting the conclusions of this article will be made available by the authors, without undue reservation.

## Ethics statement

The studies involving human participants were reviewed and approved by the Ethical Committee for Medicine of Jiangxi Provincial People's Hospital. The patients/participants provided their written informed consent to participate in this study. Written informed consent was not obtained from the individual(s) for the publication of any potentially identifiable images or data included in this article.

## References

- Benedetto, A., Binda, P., Costagli, M., Tosetti, M., and Morrone, M. C. (2021). Predictive visuo-motor communication through neural oscillations. *Curr. Biol.* 31, 3401.e4–3408.e4. doi: 10.1016/j.cub.2021.05.026
- Chang, Y. S., Ho, C. H., Chu, C. C., Wang, J. J., and Jan, R. L. (2021). Risk of retinal vein occlusion in patients with diabetes mellitus: A retrospective cohort study. *Diabetes Res. Clin. Pract.* 171:108607. doi: 10.1016/j.diabres.2020.10.8607
- Chen, R. B., Zhong, Y. L., and Huang, X. (2022). The predictive value of local to remote functional connectivity changes in comitant exotropia patients. *Neuroreport* 33, 259–265. doi: 10.1097/WNR.0000000000001777
- Cho, K. H., Kim, C. K., Oh, K., Oh, S. W., Park, K. H., and Park, S. J. (2017). Retinal Vein Occlusion as the Surrogate Marker for Premature Brain Aging in Young Patients. *Invest. Ophthalmol. Vis. Sci.* 58, BIO82–BIO87. doi: 10.1167/iiov.17-21413
- Ciulla, T., Pollack, J. S., and Williams, D. F. (2021). Visual acuity outcomes and anti-VEGF therapy intensity in macular oedema due to retinal vein occlusion: a real-world analysis of 15 613 patient eyes. *Br. J. Ophthalmol.* 105, 1696–1704. doi: 10.1136/bjophthalmol-2020-317337
- Dong, W. J., Su, T., Li, C. Q., Shu, Y. Q., Shi, W. Q., Min, Y. L., et al. (2021). Altered brain network centrality in patients with retinal vein occlusion: a resting-state fMRI study. *Int. J. Ophthalmol.* 14, 1741–1747. doi: 10.18240/ijo.2021.11.14
- Dong, Y., Winstein, C. J., Albistegui-DuBois, R., and Dobkin, B. H. (2007). Evolution of FMRI activation in the perilesional primary motor cortex and cerebellum with rehabilitation training-related motor gains after stroke: a pilot study. *Neurorehabil. Neural Repair* 21, 412–428. doi: 10.1177/1545968306298598
- Grover, S., Nguyen, J. A., and Reinhart, R. M. G. (2021). Synchronizing Brain Rhythms to Improve Cognition. *Annu. Rev. Med.* 72, 29–43. doi: 10.1146/annurev-med-060619-022857
- Jaulim, A., Ahmed, B., Khanam, T., and Chatziralli, I. P. (2013). Branch retinal vein occlusion: epidemiology, pathogenesis, risk factors, clinical features, diagnosis, and complications. An update of the literature. *Retina* 33, 901–910. doi: 10.1097/IAE.0b013e3182870c15
- Koch, G., Bonni, S., Casula, E. P., Iosa, M., Paolucci, S., Pellicciari, M. C., et al. (2019). Effect of Cerebellar Stimulation on Gait and Balance Recovery in Patients With Hemiparetic Stroke: A Randomized Clinical Trial. *JAMA Neurol.* 76, 170–178. doi: 10.1001/jamaneurol.2018.3639
- Kolar, P. (2014). Risk factors for central and branch retinal vein occlusion: a meta-analysis of published clinical data. *J. Ophthalmol.* 2014:724780. doi: 10.1155/2014/724780
- Lee, C. S., Lee, M. L., Gibbons, L. E., Yanagihara, R. T., Blazes, M., Kam, J. P., et al. (2021). Associations Between Retinal Artery/Vein Occlusions and Risk of Vascular Dementia. *J. Alzheimers Dis.* 81, 245–253. doi: 10.3233/JAD-201492
- Liu, L., Jiang, H., Wang, D., and Zhao, X. F. A. (2021). study of regional homogeneity of resting-state Functional Magnetic Resonance Imaging in mild cognitive impairment. *Behav Brain Res.* 26:113103. doi: 10.1016/j.bbr.2020.113103
- Nam, G. E., Han, K., Park, S. H., Cho, K. H., and Song, S. J. (2021). Retinal Vein Occlusion and the Risk of Dementia: A Nationwide Cohort Study. *Am. J. Ophthalmol.* 221, 181–189. doi: 10.1016/j.ajo.2020.07.050
- Park, S. J., Choi, N. K., Yang, B. R., Park, K. H., Woo, S. J. (2015). Risk of stroke in retinal vein occlusion. *Neurology* 85, 1578–1584.
- Piazza, E. A., Cohen, A., Trach, J., and Lew-Williams, C. (2021). Neural synchrony predicts children's learning of novel words. *Cognition* 214:104752. doi: 10.1016/j.cognition.2021.104752
- Ponto, K. A., Scharrer, I., Binder, H., Korb, C., Rosner, A. K., Ehlers, T. O., et al. (2019). Hypertension and multiple cardiovascular risk factors increase the risk for retinal vein occlusions: results from the Gutenberg Retinal Vein Occlusion Study. *J. Hypertens.* 37, 1372–1383. doi: 10.1097/HJH.0000000000002057

## Author contributions

YX, FG, HL, and YZ contributed to data collection, statistical analyses, wrote the manuscript, designed the protocol, contributed to the MRI analysis, designed the study, oversaw all clinical aspects of study conduct, and manuscript preparation. All authors contributed to the article and approved the submitted version.

## Conflict of interest

The authors declare that the research was conducted in the absence of any commercial or financial relationships that could be construed as a potential conflict of interest.

## Publisher's note

All claims expressed in this article are solely those of the authors and do not necessarily represent those of their affiliated organizations, or those of the publisher, the editors and the reviewers. Any product that may be evaluated in this article, or claim that may be made by its manufacturer, is not guaranteed or endorsed by the publisher.

- Rim, T. H., Kim, D. W., Han, J. S., and Chung, E. J. (2015). Retinal vein occlusion and the risk of stroke development: a 9-year nationwide population-based study. *Ophthalmology* 122, 1187–1194. doi: 10.1016/j.ophtha.2015.01.020
- Su, T., Yuan, Q., Liao, X. L., Shi, W. Q., Zhou, X. Z., Lin, Q., et al. (2020). Altered intrinsic functional connectivity of the primary visual cortex in patients with retinal vein occlusion: a resting-state fMRI study. *Quant. Imaging Med. Surg.* 10, 958–969. doi: 10.21037/qims.2020.03.24
- Wei, Y., Wang, C., Liu, J., Miao, P., Wu, L., Wang, Y., et al. (2020). Progressive Gray Matter Atrophy and Abnormal Structural Covariance Network in Ischemic Pontine Stroke. *Neuroscience* 10, 255–265. doi: 10.1016/j.neuroscience.2020.08.033
- Wen, Z., Wan, X., Qi, C. X., and Huang, X. (2022). Local-to-Remote Brain Functional Connectivity in Patients with Thyroid-Associated Ophthalmopathy and Assessment of Its Predictive Value Using Machine Learning. *Int. J. Gen. Med.* 21, 4273–4283. doi: 10.2147/IJGM.S353649
- Yan, C. G., Wang, X. D., Zuo, X. N., and Zang, Y. F. D. P. A. B. I. (2016). Data Processing & Analysis for (Resting-State) Brain Imaging. *Neuroinformatics* 14, 339–351. doi: 10.1007/s12021-016-9299-4
- Yan, M., He, Y., Cui, X., Liu, F., Li, H., Huang, R., et al. (2021). Disrupted Regional Homogeneity in Melancholic and Non-melancholic Major Depressive Disorder at Rest. *Front. Psychiatry* 16:618805. doi: 10.3389/fpsyt.2021.618805
- Zang, Y., Jiang, T., Lu, Y., He, Y., and Tian, L. (2004). Regional homogeneity approach to fMRI data analysis. *Neuroimage* 22, 394–400. doi: 10.1016/j.neuroimage.2003.12.030
- Zhang, L., Sui, R., Zhang, L., and Zhang, Z. (2016). Morphological and Metabolic Alteration of Cerebellum in Patients with Post-Stroke Depression. *Cell Physiol. Biochem.* 40, 420–430. doi: 10.1159/000452557
- Zhang, M. X., Chen, M. J., Tang, L. Y., Yu, C. Y., Xu, Y. L., Xu, S. H., et al. (2022). Altered White Matter Integrity in Patients with Retinal Vein Occlusion: A Diffusion Tensor Imaging and Tract-Based Spatial Statistics Study. *Dis. Markers* 24:9647706. doi: 10.1155/2022/9647706
- Zhao, Z., Tang, C., Yin, D., Wu, J., Gong, J., Sun, L., et al. (2018). Frequency-specific alterations of regional homogeneity in subcortical stroke patients with different outcomes in hand function. *Hum. Brain Mapp.* 39, 4373–4384. doi: 10.1002/hbm.24277



## OPEN ACCESS

## EDITED BY

Ahmed Toosy,  
University College London,  
United Kingdom

## REVIEWED BY

Sasitorn Siritho,  
Bumrungrad International Hospital,  
Thailand

## \*CORRESPONDENCE

Sujeevini Sujanthan  
sujeevini.sujanthan@mail.mcgill.ca  
Amir Shmuel  
amir.shmuel@mcgill.ca  
Janine Dale Mendola  
janine.mendola@mcgill.ca

†These authors have contributed  
equally to this work

## SPECIALTY SECTION

This article was submitted to  
Brain Imaging and Stimulation,  
a section of the journal  
Frontiers in Human Neuroscience

RECEIVED 13 May 2022

ACCEPTED 15 September 2022

PUBLISHED 18 October 2022

## CITATION

Sujanthan S, Shmuel A and  
Mendola JD (2022) Resting-state  
functional MRI of the visual system  
for characterization of optic  
neuropathy.  
*Front. Hum. Neurosci.* 16:943618.  
doi: 10.3389/fnhum.2022.943618

## COPYRIGHT

© 2022 Sujanthan, Shmuel and  
Mendola. This is an open-access  
article distributed under the terms of  
the [Creative Commons Attribution  
License \(CC BY\)](#). The use, distribution  
or reproduction in other forums is  
permitted, provided the original  
author(s) and the copyright owner(s)  
are credited and that the original  
publication in this journal is cited, in  
accordance with accepted academic  
practice. No use, distribution or  
reproduction is permitted which does  
not comply with these terms.

# Resting-state functional MRI of the visual system for characterization of optic neuropathy

Sujeevini Sujanthan<sup>1\*†</sup>, Amir Shmuel<sup>2,3\*</sup> and  
Janine Dale Mendola<sup>1\*†</sup>

<sup>1</sup>Department of Ophthalmology & Visual Sciences, McGill University, Montreal, QC, Canada,

<sup>2</sup>Departments of Neurology, Neurosurgery, Physiology, and Biomedical Engineering, McGill University, Montreal, QC, Canada, <sup>3</sup>Montreal Neurological Institute, McGill University, Montreal, QC, Canada

Optic neuropathy refers to disease of the optic nerve and can result in loss of visual acuity and/or visual field defects. Combining findings from multiple fMRI modalities can offer valuable information for characterizing and managing optic neuropathies. In this article, we review a subset of resting-state functional magnetic resonance imaging (RS-fMRI) studies of optic neuropathies. We consider glaucoma, acute optic neuritis (ON), discuss traumatic optic neuropathy (TON), and explore consistency between findings from RS and visually driven fMRI studies. Consistent with visually driven studies, glaucoma studies at rest also indicated reduced activation in the visual cortex and dorsal visual stream. RS-fMRI further reported varying levels of functional connectivity in the ventral stream depending on disease severity. ON patients show alterations within the visual cortex in both fMRI techniques. Particularly, higher-than-normal RS activity is observed in the acute phase and decreases as the disease progresses. A similar pattern is observed in the visual cortex of TON-like, open globe injury (OGI), patients. Additionally, visually driven and RS-fMRI studies of ON patients show recovery of brain activity in the visual cortex. RS-fMRI suggests recovery of signals in higher-tier visual areas MT and LOC as well. Finally, RS-fMRI has not yet been applied to TON, although reviewing OGI studies suggests that it is feasible. Future RS-fMRI studies of optic neuropathies could prioritize studying the fine scale RS activity of brain areas that visually driven studies have identified. We suggest that a more systematic longitudinal comparison of optic neuropathies with advanced fMRI would provide improved diagnostic and prognostic information.

## KEYWORDS

glaucoma, optic neuritis, traumatic optic neuropathy, resting-state fMRI, visual cortex, dorsal visual stream, ventral visual stream, LGN

## Introduction

Optic neuropathy refers broadly to a disease of the optic nerve. It is a serious condition that may result in deficits in the visual field (partial or even full blindness). This type of injury can develop acutely or chronically. Acute optic neuropathies such as optic neuritis (ON) and traumatic optic neuropathy (TON) have a rapid onset and are typically caused by inflammation and/or trauma, whereas chronic optic neuropathies such as glaucoma are characterized by a slow onset (Behbehani, 2007). The aim of this selective review is to identify the reported optic neuropathy-related changes within the visual system as reported in resting-state functional MRI (RS-fMRI) studies, and assess the consistency between RS-fMRI and visually driven fMRI findings for each optic neuropathy. We strive to provide insights into the common and differential effects of chronic versus acute onset of optic neuropathies over the course of the disease along with central versus peripheral visual field defects on visual brain areas. A summary of visually driven fMRI results is provided for reference (Figure 1). This review is offered as a companion to the longer review of visually driven studies published in this same issue, with the same inclusion criteria (Sujanathan et al., 2022). We note that graph-theory analysis RS-fMRI papers were excluded as they have not been utilized to study all optic neuropathies we consider in this manuscript. In addition, they mainly focus on brain alternations outside the visual system, which is beyond the scope of this review.

## Resting-state functional magnetic resonance imaging

Resting-state functional magnetic resonance imaging is emerging as a powerful tool to non-invasively quantify brain activity at rest (i.e., spontaneous brain activity) of both intact visual brain regions and visual regions that have lost visual input (e.g., Cole et al., 2010). RS-fMRI allows for the study of local organization and functional connectivity (FC) of brain structures via temporal synchronization of neuronal activity. The resting BOLD (blood oxygen level-dependent) signal can be analyzed using various techniques. Below, we describe RS-fMRI analysis techniques employed in optic neuropathy studies.

Amplitude of low-frequency fluctuation (ALFF) and regional homogeneity (ReHo) are functional *segregation*

methods for identifying neural networks across the whole brain, where brain regions are divided according to their presumed shared function, and provides information about local neural activity rather than FC between different regions (Lv et al., 2018). ALFF evaluates the combined BOLD signal in a region of interest by measuring the brain signal variability of each voxel in a particular frequency domain. ReHo is a method to evaluate the synchrony or “similarity” of the time course of each voxel in a region of interest to its neighboring voxels in the time domain (Lv et al., 2018). Alternatively, the following methods measure temporal synchronization between separated brain regions to assess functional *integration*. Strong FC may arise from direct or indirect anatomic connections or by way of having common input. Seed-based methods determine the brain regions closely associated with the BOLD time-series of a seed region, i.e., any brain region determined in an *a priori* manner. In comparison, independent component analysis (ICA) is more data-driven and ideally detects all functionally connected networks within the brain. However, the number of networks that can be detected is limited by the number of independent components specified. A few commonly identified RS-networks include the default mode network, medial executive network, working memory, and visual network (Lv et al., 2018). Finally, voxel-mirrored homotopic connectivity (VMHC) is a specific voxel-wise analysis method in which the synchrony between geometrically corresponding interhemispheric regions at rest is quantified. It is yet to be determined what combination of RS-fMRI analysis methods could be most sensitive to detecting optic neuropathy-related brain deficits.

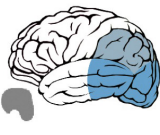

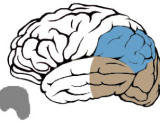
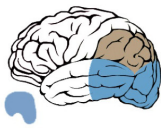
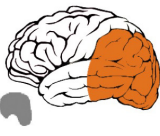
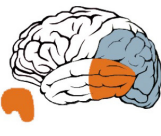

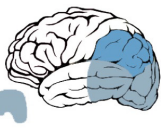
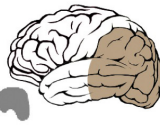

## Resting-state functional magnetic resonance imaging in glaucoma

Glaucoma is a chronic optic neuropathy resulting from the loss of retinal ganglion cells. It is characterized by reduced retinal thickness, peripheral vision loss in the early stages of the disease, followed by central visual field loss, and eventual low vision or blindness (Weinreb and Tee Khaw, 2004; Jonas et al., 2017). Here, we consider the most common form, primary open-angle glaucoma (POAG). The effects of the visual deficits on the FC of cortical networks are yet to be fully understood. We selectively identified 12 RS-fMRI peer-reviewed articles with patient groups that meet our inclusion criteria and findings relevant to the themes revealed in our analysis of the *visually driven* glaucoma literature (Sujanathan et al., 2022). We aim to explore here if RS-fMRI findings reveal results similar to those obtained with visually driven protocols. We thus expected to find: (1) reduced activity in lower visual areas, especially eccentricity-specific deficits, (2) disease severity-specific alterations in brain activity; for example biased loss of activity in LGN magnocellular layers in early POAG patients, and compromised cortical representation of central

---

Abbreviations: ALFF, amplitude of low-frequency fluctuation; BOLD, blood oxygenation level-dependent signal; FC, functional connectivity; ICA, independent component analysis; LGN, lateral geniculate nucleus; LOC, lateral occipital cortex; MT/V5, middle temporal visual area; OGI, open globe injury; ON, optic neuritis; POAG, primary open-angle glaucoma; ReHo, regional homogeneity; ROC, receiver operating characteristic; RS-fMRI, resting-state functional magnetic resonance imaging; TON, traumatic optic neuropathy; VEP, visually evoked potentials; VMHC, voxel-mirrored homotopic connectivity.



Glaucoma	Resting State	Visually Driven	Resting State	Visually Driven
LGN (magno)	X	✓✓		
LGN (parvo)	X	✓		
Lower-tier visual cortex (V1, V2)	✓✓	✓✓		
Ventral Stream	✓✓	X		
Dorsal Stream	✓	X		
Retinotopic remapping	X	✓*		
Acute ON	Resting State	Visually Driven		
LGN	X	✓✓		
Lower-tier visual cortex (V1, V2)	✓**	✓✓		
Ventral Stream	✓**	✓✓		
Dorsal Stream	✓✓	✓**		
Recovering ON	Resting State	Visually Driven		
LGN	X	✓*		
Lower-tier visual cortex (V1, V2)	✓*	✓		
Ventral Stream	✓*	✓*		
Dorsal Stream	✓*	✓		
Remote ON	Resting State	Visually Driven		
LGN	X	✓		
Lower-tier visual cortex (V1, V2)	X	✓		
Ventral Stream	X	✓		
Dorsal Stream	X	✓✓		
Acute OGI	Resting State	Visually Driven		
LGN	X	X		
Lower-tier visual cortex (V1, V2)	✓**	X		
Ventral Stream	✓**	X		
Dorsal Stream	✓**	X		

✓ = Some evidence for abnormality (reduced activity)

✓✓ = Consistent evidence for abnormality (reduced activity)

X = No data available

✓\* = Evidence for hyperactivity or strengthening

✓\*\* = Some evidence for both reduced and increased activity

FIGURE 1

Summary of resting-state and visually driven fMRI findings in Glaucoma, Optic Neuritis and Traumatic Optic Neuropathy. **Left:** fMRI findings of glaucoma, ON and (TON-like) OGI patients are summarized based on visual areas that were investigated and themes that were revealed in our analysis of visually driven and RS-fMRI literature of each optic neuropathy. Findings from rapidly changing optic neuropathies such as ON and OGI have been split into three stages of the disease: acute – within 1 month of disease onset, recovering – 3–4 months from disease onset, and remote – 1 year or more since disease onset. **Right:** pictorial representation of the fMRI findings within LGN and visual cortical areas, specifically lower visual areas, dorsal visual stream and ventral visual stream, for glaucoma patients, ON patients at different stages of the disease and OGI patients.

visual field only in advanced patients, and (3) remapping in visual cortices with enlarged parafoveal regions and/or higher-than-normal activity in visual association and higher-level cortical areas.

As expected, RS-studies utilizing functional *segregation* methods do in fact indicate poor local specialization in regions of the visual network of POAG patients. For instance, ALFF values were lower in the cuneus (Li et al., 2014) and

ReHo revealed lower synchrony between neighboring voxels in the bilateral calcarine cortex (Song et al., 2014). Likewise, functional *integration* methods noted dysconnectivity *between* lower-tier and higher-tier visual areas (Frezzotti et al., 2016; Giorgio et al., 2018). ICA and voxel-wise analyses revealed decreased FC between the primary and secondary visual cortices (Wang J. et al., 2017), and reduced interhemispheric synchronization of homotopic primary and secondary visual areas (Zhou et al., 2016; Wang et al., 2018). However, we note that there are no RS-fMRI studies that investigate retinotopy-specific functional alterations *within* primary visual areas in glaucoma patients at a fine scale. This has already been achieved in healthy controls (e.g., Dawson et al., 2013, 2016) as well as in amblyopia (Mendola et al., 2018), and could potentially identify the progression of glaucoma based on the representation of the central and peripheral eccentricities.

With regard to the higher-level visual cortex, we noted common reports of abnormally low resting connectivity in the ventral visual stream based on: (1) ALFF (Li et al., 2014; Liu and Tian, 2014), (2) ICA-based FC (Frezzotti et al., 2016), (3) cerebral blood flow-FC strength (Wang et al., 2021), (4) VMHC (Wang et al., 2018), and (5) voxel-wise analysis (Dai et al., 2013). In comparison, there are fewer reports of deficits in the dorsal stream (i.e., ReHo) (Song et al., 2014), or functional dysconnectivity between primary visual cortex and dorsal visual stream (i.e., VMHC and voxel-wise analysis) (Dai et al., 2013). While interesting, this moderate tendency for greater involvement of the ventral visual cortex was not evident in our review of studies using visually driven fMRI with glaucoma patients. Instead, that review hinted at the loss of magnocellular input – at least in early POAG – which is expected to most severely affect the dorsal visual stream. It thus remains to be understood if these tentative trends are reproduced, and exactly how such biases depend on severity.

As per our second hypothesis, the RS-fMRI literature shows that the pattern and extent of alterations are dependent on glaucoma severity. From the limited number of studies that report results in specific POAG subgroups, it can be noted that the areas in the ventral visual network show low resting FC in early POAG patients (inferior temporal gyrus and LOC) (Frezzotti et al., 2016; Wang et al., 2021), and a combination of low and high FC patterns in advanced POAG patients (Frezzotti et al., 2014). For example, FC of some areas in advanced POAG is lower (lingual gyrus), whereas others are unexpectedly higher (LOC and temporo-occipital fusiform cortex) compared to controls (Frezzotti et al., 2014). Although the abnormalities in the ventral visual stream could be consistent with the loss of central representation observed in advanced glaucoma patients, it is unclear why this effect is evident even in early POAG patients. Lastly, in comparison with visually driven fMRI, RS-fMRI studies emphasize functional alterations beyond visual areas in cortical areas proximal to the visual network from early stages of the disease (e.g., the memory and DMN networks) (e.g., Frezzotti et al., 2016).

Concerning our third hypothesis, regarding compensatory activity, RS-fMRI of glaucoma patients also reveals abnormally high brain activity, but generally in areas more distal from the visual network. For example, high resting FC can be observed within the medial executive network or other distant higher-level brain regions, as well as between these networks and the visual network (Dai et al., 2013; Frezzotti et al., 2014; Li et al., 2014; Liu and Tian, 2014; Song et al., 2014; Zhou et al., 2016; Giorgio et al., 2018; Zhang et al., 2019). This common type of observation is usually considered to reflect some unspecified state of “compensation.” Such concepts are poorly understood, but do at least document that bidirectional changes in activity are likely the result of localized damage to a complex network.

## Resting-state functional magnetic resonance imaging in optic neuritis

Optic neuritis is an acute optic neuropathy resulting from inflammation, and subsequent lesions of the optic nerve, followed by spontaneous recovery. In the acute stages of the disease (e.g., within 1 month of onset), the affected eye displays greatly delayed and decreased visually evoked potential (VEP) responses (i.e., demyelinated optic nerve), as well as poor visual acuity and color vision (Toosy et al., 2014). Subsequently, visual acuity begins to improve during the recovery phase at around 3–4 months and reaches normal or near-normal vision at 1-year from disease onset, although a reduction in retinal thickness and other abnormalities continue to exist (Beck et al., 1992). Here, we review 5 peer-reviewed articles studying RS-fMRI brain activity in ON patients that meet our inclusion criteria to explore commonalities in findings with visually driven fMRI studies (Table 1). Specifically, we would expect: (1) functional deficit within low-level visual cortex in the early stages of ON, (2) functional alterations within higher-tier areas, specifically decreased activity within the ventral visual stream (i.e., visual cortical region LOC) and a trend toward hyperactivity in the dorsal stream of early-stage ON patients, and (3) recovery of activity in LGN, visual cortex, and ventral visual stream, but persistent deficit likely in the dorsal stream (i.e., cortical area MT).

To our surprise, and contrary to visually driven fMRI reports, an increase in resting activity was observed in the occipital lobe immediately (i.e., within a week) after ON onset (Huang et al., 2015; Figure 1). Similarly, while visually driven fMRI studies reported reduced activity in the ventral visual stream, the majority of current RS-fMRI studies indicate increased ALFF values in many temporal lobe brain structures (Huang et al., 2015; Yan et al., 2022). However, in another study, ReHo analysis suggests an overall brain *deficit* at rest (Shao et al., 2015). Moreover, studies predominantly suggest a resting deficit within the dorsal cortical areas (i.e., fronto-parietal structures),

at least during the very early stages of the disease (Huang et al., 2015; Shao et al., 2015; Yan et al., 2022). Interestingly, a different pattern is evident for the visual cortex of patients scanned around 50 days from ON onset. Now in agreement with findings reported with visually driven fMRI, lower resting connectivity is observed from the visual cortex (Wu et al., 2015). RS-FC between the visual cortex and the fronto-parietal cortex remains impaired as reported in the acute stage of ON (Wu et al., 2015). However, the relationship between the activity of extra-striate regions and patients' visual function outcomes is unclear.

Consistent with the recovery of BOLD signals observed in the visually driven fMRI literature at 3–4 months from disease onset, one RS study with a majority of ON patients in the recovery phase revealed higher-than-normal resting FC within the visual network. For instance, abnormally high resting activity was reported in the lower (i.e., calcarine sulcus) and higher visual areas (i.e., LOC and MT) of the visual network (Backner et al., 2018). This might suggest that recovery of function is partially supported by adaptive changes in connectivity. Importantly, as expected, MT connectivity was seen to increase as the inter-eye VEP latency difference in ON patients decreased. As also concluded in the visually driven review, this suggests that the increased activity in the visual pathway is at least partly due to the reduced inflammation of the optic nerve. However, the abnormally high resting signal observed in the visual pathway raises the possibility for additional involvement by adaptive plasticity mechanisms.

Finally, the activity of LGN in ON patients has not been investigated with RS-fMRI yet, despite its ability to produce distinct levels of activity during the acute and recovery phase of ON and its potential use in objectively staging patients, as shown in visually driven fMRI. Likewise, RS-fMRI is yet to be utilized to study activity in subcortical and cortical visual regions of purely

recovered ON patients. This is a particularly important group to study as it would allow us to evaluate the extent of recovery possible in areas along the visual pathway, and determine the correlation to earlier time points of visual function and BOLD measures, potentially informing the prediction of prognosis.

## Resting-state functional magnetic resonance imaging in traumatic optic neuropathy

Traumatic optic neuropathy causes acute partial or complete, unilateral or bilateral visual loss following injury to the optic nerve and demyelination of afferent visual pathways due to trauma. It can be further categorized into direct and indirect trauma, depending on how the optic nerve was affected (Miliaras et al., 2013). Like ON, substantial recovery is generally observed to take place (Singman et al., 2016). Diagnosis of TON with current neuro-ophthalmological tools may be challenging as trauma patients could have cognitive impairments. TON is typically assessed using the afferent pupillary reflex, but this is insensitive to bilateral TON (Broadway, 2012). Thus, utilizing RS-fMRI, a non-demanding imaging technique, might provide real diagnostic and prognostic value in clinical settings. Similar to our review of TON using visually driven fMRI, we found no peer-reviewed articles that studied TON using RS-fMRI. Therefore, we reviewed four papers on patients with a similar trauma, called open globe injury (OGI) (Table 1). OGI results in injury to the eye-wall and is more readily diagnosed.

Resting changes of the whole brain in OGI patients were studied using voxel-wise degree centrality (Wang H. et al., 2017), ReHo (Huang et al., 2016), ALFF (Tan et al., 2016), and VMHC (Ye et al., 2018). Indeed, functional deficit was

**TABLE 1** Patient demographic and disease information from ON and (TON-like) OGI studies reviewed in this paper. Studies are listed in increasing order of average onset duration in patient population at the time of data collection. Unless stated, all studies included patients without other apparent cause of vision loss and retro geniculate diseases. ON = optic neuritis; OGI = open globe injury.

Author, Year	Number of patients	Age (Range/Mean) (± SD)	Stage & type of disease; # of occurrences	Mean time from onset at data collection
<b>ON</b>				
Shao et al., 2015	12	46.08 (± 7.91)	ON	5.3 days (± 3.2)
Huang et al., 2015	12	44.83 (± 10.71)	Acute ON	5.4 days (± 2.9)
Yan et al., 2022	21	44.83 (± 10.71)	ON	5.4 days (± 2.9)
Wu et al., 2015	15	24–56 (median: 35)	Acute; clinically isolated ON	50 days (± 25)
Backner et al., 2018	18	18 – 65	Clinically isolated ON	1–28 months (median: 3–4 months)
<b>OGI</b>				
Tan et al., 2016	18	44.6 (± 14.08)	Acute OGI	1.0 day (± 1.23)
Wang H. et al., 2017	18	44.17 (± 13.94)	Acute, <i>unilateral</i> OGI	1.0 day (± 1.23)
Huang et al., 2016	18	44.6 (± 14.08)	Acute OGI	1.1 day (± 0.4)
Ye et al., 2018	18	43.05 (± 8.79)	Acute OGI	6.6 days (± 3.4)

evident within and between the two hemispheres of the brain in patients with acute lesions to the anterior visual pathway. However, the direction of the effect is quite variable and highly dependent on time since onset. For example, resting cortical activity of OGI patients within 1–2 days of onset is higher-than-normal compared to controls, especially in the primary visual cortex and precuneus as shown by degree centrality (Wang H. et al., 2017) and ALFF (Tan et al., 2016) values, as well as in lingual gyrus as shown by ALFF values (Huang et al., 2016). Interestingly, a different pattern is revealed in patients that were tested 3 days after OGI onset. Those patients display *lower* VMHC values compared to controls in the brain regions such as bilateral calcarine, lingual and cuneus and structures in the dorsal visual pathway such as the middle occipital gyrus displayed (Ye et al., 2018). This is consistent with findings from a single TON-related case report discussed in our visually driven review (Sujanathan et al., 2022). Importantly, receiver operating characteristic (ROC) curves have been used to identify brain regions based on their resting FC measures that may be used as biomarkers to distinguish OGI patients from healthy controls. With a range of analysis techniques (VMHC, ALFF and mean ReHo), ROC values regularly show areas under the curve in the range of 0.7–0.9 for the visual cortex and non-visual cortex (Huang et al., 2016; Tan et al., 2016; Ye et al., 2018), suggesting activity within the reported regions may be useful as diagnostic markers.

Taken together, OGI and TON are rapidly changing conditions that require immediate attention and treatment. It appears that initially hyperactive brain regions show deficits as the disease progresses. However, this is difficult to assert, based on the limited number of studies available, all acute cross-sectional studies. It is evident that RS-fMRI could provide valuable insight into the pathogenesis and progression of acute optic neuropathies such as TON. Therefore, if fMRI techniques are employed more frequently and ambitiously, advancement in the diagnosis or prognosis of TON might be possible.

## Discussion

Overall, when considering the visual system specifically, both RS-fMRI and visually driven fMRI studies are often consistent in the reported findings in each optic neuropathy. In chronic diseases such as glaucoma, both fMRI modalities report reduced activity in visual networks. However, RS-fMRI more commonly suggests deficits in the ventral than the dorsal visual stream, and the ventral FC pattern becomes more diverse with increasing glaucoma severity. For acute diseases such as ON and (TON like) OGI, RS-activity reveals that higher-than-normal activity is briefly observed at onset, before it ultimately

shows a deficit as seen in visually driven fMRI studies. Both modalities report deficits within the dorsal pathway in ON from onset. So far, both visual streams are shown to be affected in acute OGI at rest, although no visually driven fMRI results exist.

We highlight here several important concluding points. Firstly, the resting activity of the LGN has not yet been investigated with RS-fMRI in any of the diseases we considered. This would be of particular interest given the LGN's proximity to the optic nerve and the fact that it conveniently maintains the segregation of inputs from each eye. In addition, if resolution allows, patterns of connectivity for magnocellular or parvocellular layers would provide additional information about the pathophysiology of these diseases. In fact, this has already been reported for one fMRI study of glaucoma that used parvo- or magno-biased visual stimuli (Zhang et al., 2016). In addition, visually driven fMRI studies of ON patients have noted distinct patterns of activity within LGN during the acute and recovery stage (Korsholm et al., 2007).

Secondly, we suggest that better use of regions of interest within the visual cortex based on *a priori* hypotheses would improve the sensitivity of RS-fMRI studies to the direct effects of deafferentation. Many distinct visual areas can now be defined based on retinotopic organization or other functional characteristics. The lateral occipital region (LOC) is quite important for object perception and contains a prominent representation of the central visual field (separate from the occipital pole). Another area that may be useful to better exploit is MT, a motion-sensitive region where the magnocellular LGN inputs are expected to have a strong impact. Future studies should examine RS-fMRI activation patterns within and between multiple visual areas, as this has the potential to increase sensitivity. Probabilistic atlases now allow the location of many extrastriate areas to be estimated, even without direct mapping in each subject (e.g., Wang et al., 2015; Benson and Winawer, 2018; Rosenke et al., 2021). In fact, it is even possible to use regions of interest *within* a single retinotopic visual area to study fine-scale resting networks, and document changes in central versus peripheral eccentricities (Dawson et al., 2016; Mendola et al., 2018).

Third, we found no obvious pattern regarding the sensitivity of the different RS-fMRI analysis methods reported here, but we remain convinced that different methods are likely to reveal distinct aspects of pathology. As such, future studies that directly compare multiple analysis methods would be of enormous value. Lastly, the cross-sectional design common to most of these studies is a clear limitation. Although there is great value in following the same group of patients longitudinally, as shown by a limited number of visually driven fMRI studies (Sujanathan et al., 2022), this is rarely done in RS-studies of optic neuropathies.



In summary, we suggest that RS-fMRI data could prove increasingly valuable for characterizing optic neuropathies, particularly in the case of TON, and for managing disease progression. Given that RS-fMRI does not utilize visual stimulation or a task-induced response, it is well-suited to study vision in cognitively challenged patients or patients that are unable to maintain fixation. Moreover, the high sensitivity of fMRI data to central vision loss due to the high cortical magnification of the central field could be hugely beneficial in studying TON. In combination with other MRI modalities, including structural MRI, it could be even more powerful. For future efforts to uncover basic mechanisms of functional loss and recovery, studies that compare visually driven and RS-fMRI findings from local visual areas and closely related brain networks in the same cohort of subjects would be most useful.

## Author contributions

JM and AS conceived the idea. JM, AS, and SS developed the idea. SS wrote the manuscript in consultation with JM. All authors provided feedback and helped shape the manuscript.

## References

- Backner, Y., Kuchling, J., Massarwa, S., Oberwahrenbrock, T., Finke, C., Bellmann-Strobl, J., et al. (2018). Anatomical Wiring and Functional Networking Changes in the Visual System Following Optic Neuritis. *JAMA Neurol.* 75, 287–295. doi: 10.1001/JAMANEUROL.2017.3880
- Beck, R. W., Cleary, P. A., Anderson, M. M. Jr., Keltner, J. L., Shults, W. T., Kaufman, D. L., et al. (1992). A randomized, controlled trial of corticosteroids in the treatment of acute optic neuritis. The Optic Neuritis Study Group. *N. Engl. J. Med.* 326, 581–588. doi: 10.1056/NEJM199202273260901
- Behbehani, R. (2007). Clinical approach to optic neuropathies. *Clin. Ophthalmol.* 1:233.
- Benson, N. C., and Winawer, J. (2018). Bayesian analysis of retinotopic maps. *eLife* 7:e40224. doi: 10.7554/eLife.40224
- Broadway, D. C. (2012). How to test for a relative afferent pupillary defect (RAPD). *Commun. Eye Health* 25:58.
- Cole, D. M., Smith, S. M., and Beckmann, C. F. (2010). Advances and pitfalls in the analysis and interpretation of resting-state FMRI data. *Front. Syst. Neurosci.* 4:8. doi: 10.3389/fnsys.2010.00008
- Dai, H., Morelli, J. N., Ai, F., Yin, D., Hu, C., Xu, D., et al. (2013). Resting-state functional MRI: Functional connectivity analysis of the visual cortex in primary open-angle glaucoma patients. *Hum. Brain Mapp.* 34, 2455–2463. doi: 10.1002/HBM.22079
- Dawson, D. A., Cha, K., Lewis, L. B., Mendola, J. D., and Shmuel, A. (2013). Evaluation and calibration of functional network modeling methods based on known anatomical connections. *NeuroImage* 67, 331–343. doi: 10.1016/j.NEUROIMAGE.2012.11.006
- Dawson, D. A., Lam, J., Lewis, L. B., Carbonell, F., Mendola, J. D., and Shmuel, A. (2016). Partial Correlation-Based Retinotopically Organized Resting-State Functional Connectivity Within and Between Areas of the Visual Cortex Reflects More Than Cortical Distance. *Brain Connect.* 6, 57–75. doi: 10.1089/BRAIN.2014.0331
- Frezzotti, P., Giorgio, A., Motolese, I., De Leucio, A., Iester, M., Motolese, E., et al. (2014). Structural and functional brain changes beyond visual system in patients with advanced glaucoma. *PLoS One* 9:e105931. doi: 10.1371/JOURNAL.PONE.0105931
- Frezzotti, P., Giorgio, A., Toto, F., De Leucio, A., and De Stefano, N. (2016). Early changes of brain connectivity in primary open angle glaucoma. *Hum. Brain Mapp.* 37, 4581–4596. doi: 10.1002/HBM.23330
- Giorgio, A., Zhang, J., Costantino, F., De Stefano, N., and Frezzotti, P. (2018). Diffuse brain damage in normal tension glaucoma. *Hum. Brain Mapp.* 39, 532–541. doi: 10.1002/HBM.23862
- Huang, X., Cai, F. Q., Hu, P. H., Zhong, Y. L., Zhang, Y., Wei, R., et al. (2015). Disturbed spontaneous brain-activity pattern in patients with optic neuritis using amplitude of low-frequency fluctuation: A functional magnetic resonance imaging study. *Neuropsychiatr. Dis. Treat.* 11, 3075–3083. doi: 10.2147/NDT.S92497
- Huang, X., Li, H. J., Ye, L., Zhang, Y., Wei, R., Zhong, Y. L., et al. (2016). Altered regional homogeneity in patients with unilateral acute open-globe injury: A resting-state functional MRI study. *Neuropsychiatr. Dis. Treat.* 12, 1901–1906. doi: 10.2147/NDT.S110541
- Jonas, J. B., Aung, T., Bourne, R. R., Bron, A. M., Ritch, R., and Panda-Jonas, S. (2017). Glaucoma. *Lancet* 390, 2183–2193. doi: 10.1016/S0140-6736(17)31469-1
- Korsholm, K., Madsen, K. H., Frederiksen, J. L., Skimminge, A., and Lund, T. E. (2007). Recovery from optic neuritis: An ROI-based analysis of LGN and visual cortical areas. *Brain* 130, 1244–1253. doi: 10.1093/BRAIN/AWM045
- Li, T., Liu, Z., Li, J., Liu, Z., Tang, Z., Xie, X., et al. (2014). Altered amplitude of low-frequency fluctuation in primary open-angle glaucoma: A resting-state FMRI study. *Investig. Ophthalmol. Vis. Sci.* 56, 322–329. doi: 10.1167/IOVS.14-14974
- Liu, Z., and Tian, J. (2014). “Amplitude of low frequency fluctuation in primary open angle glaucoma: A resting state fMRI study,” in *Annual International Conference of the IEEE Engineering in Medicine and Biology Society. IEEE Engineering in Medicine and Biology Society. Annual International Conference, 2014*, (Chicago, IL: IEEE), 6706–6709. doi: 10.1109/EMBC.2014.6945167
- Lv, H., Wang, Z., Tong, E., Williams, L. M., Zaharchuk, G., Zeineh, M., et al. (2018). Resting-State Functional MRI: Everything That Nonexperts Have Always Wanted to Know. *AJNR* 39, 1390–1399. doi: 10.3174/AJNR.A5527

## Funding

This project was supported by funds from United States Department of Defense CDMRP Vision Research Program Grant # W81XWH1910853.

## Conflict of interest

The authors declare that the research was conducted in the absence of any commercial or financial relationships that could be construed as a potential conflict of interest.

## Publisher's note

All claims expressed in this article are solely those of the authors and do not necessarily represent those of their affiliated organizations, or those of the publisher, the editors and the reviewers. Any product that may be evaluated in this article, or claim that may be made by its manufacturer, is not guaranteed or endorsed by the publisher.

- Mendola, J. D., Lam, J., Rosenstein, M., Lewis, L. B., and Shmuel, A. (2018). Partial correlation analysis reveals abnormal retinotopically organized functional connectivity of visual areas in amblyopia. *NeuroImage Clin.* 18, 192–201. doi: 10.1016/j.NICL.2018.01.022
- Miliaras, G., Fotakopoulos, G., Asproudis, I., Voulgaris, S., Zikou, A., and Polyzoidis, K. (2013). Indirect traumatic optic neuropathy following head injury: Report of five patients and review of the literature. *J. Neurol. Surg. Part A Cent. Eur. Neurosurg.* 74, 168–174. doi: 10.1055/S-0032-1330115
- Rosenke, M., van Hoof, R., van den Hurk, J., Grill-Spector, K., and Goebel, R. (2021). A Probabilistic Functional Atlas of Human Occipito-Temporal Visual Cortex. *Cerebr. Cortex* 31, 603–619. doi: 10.1093/CERCOR/BHAA246
- Shao, Y., Cai, F. Q., Zhong, Y. L., Huang, X., Zhang, Y., Hu, P. H., et al. (2015). Altered intrinsic regional spontaneous brain activity in patients with optic neuritis: A resting-state functional magnetic resonance imaging study. *Neuropsychiatr. Dis. Treat.* 11, 3065–3073. doi: 10.2147/NDT.S92968
- Singman, E. L., Daphalapurkar, N., White, H., Nguyen, T. D., Panghat, L., Chang, J., et al. (2016). Indirect traumatic optic neuropathy. *Mil. Med. Res.* 3:2. doi: 10.1186/S40779-016-0069-2
- Song, Y., Mu, K., Wang, J., Lin, F., Chen, Z., Yan, X., et al. (2014). Altered spontaneous brain activity in primary open angle glaucoma: A resting-state functional magnetic resonance imaging study. *PLoS One* 9:e89493. doi: 10.1371/JOURNAL.PONE.0089493
- Sujanthan, S., Shmuel, A., and Mendola, J. D. (2022). Visually driven functional MRI techniques for characterization of optic neuropathy. *Front. Hum. Neurosci.* 16:943603. doi: 10.3389/FNHUM.2022.943603
- Tan, G., Huang, X., Ye, L., Wu, A. H., He, L. X., Zhong, Y. L., et al. (2016). Altered spontaneous brain activity patterns in patients with unilateral acute open globe injury using amplitude of low-frequency fluctuation: A functional magnetic resonance imaging study. *Neuropsychiatr. Dis. Treat.* 12, 2015–2020. doi: 10.2147/NDT.S110539
- Toosy, A. T., Mason, D. F., and Miller, D. H. (2014). Optic neuritis. *Lancet Neurol.* 13, 83–99. doi: 10.1016/S1474-4422(13)70259-X
- Wang, H., Chen, T., Ye, L., Yang, Q. C., Wei, R., Zhang, Y., et al. (2017). Network centrality in patients with acute unilateral open globe injury: A voxel-wise degree centrality study. *Mol. Med. Rep.* 16, 8295–8300. doi: 10.3892/MMR.2017.7635
- Wang, J., Li, T., Zhou, P., Wang, N., Xian, J., and He, H. (2017). Altered functional connectivity within and between the default model network and the visual network in primary open-angle glaucoma: A resting-state fMRI study. *Brain Imaging Behav.* 11, 1154–1163. doi: 10.1007/S11682-016-9597-3
- Wang, L., Mruczek, R. E., Arcaro, M. J., and Kastner, S. (2015). Probabilistic Maps of Visual Topography in Human Cortex. *Cerebr. Cortex* 25, 3911–3931. doi: 10.1093/CERCOR/BHU277
- Wang, Q., Chen, W., Wang, H., Zhang, X., Qu, X., Wang, Y., et al. (2018). Reduced Functional and Anatomic Interhemispheric Homotopic Connectivity in Primary Open-Angle Glaucoma: A Combined Resting State-fMRI and DTI Study. *Investig. Ophthalmol. Vis. Sci.* 59, 1861–1868. doi: 10.1167/IOVS.17-23291
- Wang, Q., Qu, X., Chen, W., Wang, H., Huang, C., Li, T., et al. (2021). Altered coupling of cerebral blood flow and functional connectivity strength in visual and higher order cognitive cortices in primary open angle glaucoma. *J. Cerebr. Blood Flow Metab.* 41, 901–913. doi: 10.1177/0271678X20935274
- Weinreb, R. N., and Tee Khaw, P. (2004). Primary open-angle glaucoma. *Lancet* 363, 1711–1720. doi: 10.1016/S0140-6736(04)16257-0
- Wu, G. F., Brier, M. R., Parks, C. A., Ances, B. M., and Van Stavern, G. P. (2015). An Eye on Brain Integrity: Acute Optic Neuritis Affects Resting State Functional Connectivity. *Investig. Ophthalmol. Vis. Sci.* 56, 2541–2546. doi: 10.1167/IOVS.14-16315
- Yan, K., Shi, W. Q., Su, T., Liao, X. L., Wu, S. N., Li, Q. Y., et al. (2022). Brain Activity Changes in Slow 5 and Slow 4 Frequencies in Patients With Optic Neuritis: A Resting State Functional MRI Study. *Front. Neurol.* 13:823919. doi: 10.3389/FNEUR.2022.823919
- Ye, L., Wei, R., Huang, X., Shi, W. Q., Yang, Q. C., Yuan, Q., et al. (2018). Reduction in interhemispheric functional connectivity in the dorsal visual pathway in unilateral acute open globe injury patients: A resting-state fMRI study. *Int. J. Ophthalmol.* 11, 1056–1060. doi: 10.18240/IJO.2018.06.26
- Zhang, P., Wen, W., Sun, X., and He, S. (2016). Selective reduction of fMRI responses to transient achromatic stimuli in the magnocellular layers of the LGN and the superficial layer of the SC of early glaucoma patients. *Hum. Brain Mapp.* 37, 558–569. doi: 10.1002/HBM.23049
- Zhang, Q., Shu, Y., Li, X., Xiong, C., Li, P., Pang, Y., et al. (2019). Resting-state functional magnetic resonance study of primary open-angle glaucoma based on voxelwise brain network degree centrality. *Neurosci. Lett.* 712:134500. doi: 10.1016/J.NEULET.2019.134500
- Zhou, P., Wang, J., Ting, L., and Wang, N. (2016). “Abnormal interhemispheric resting-state functional connectivity in primary open-angle glaucoma,” in *Annual International Conference of the IEEE Engineering in Medicine and Biology Society. IEEE Engineering in Medicine and Biology Society. Annual International Conference, 2016*, (Orlando, FL: IEEE), 4055–4058. doi: 10.1109/EMBC.2016.7591617



## OPEN ACCESS

## EDITED BY

Xin Huang,  
Jiangxi Provincial People's Hospital,  
China

## REVIEWED BY

Xiaolai Zhou,  
Zhongshan Ophthalmic Center, Sun  
Yat-sen University, China  
Zizhong Hu,  
Nanjing Medical University, China

## \*CORRESPONDENCE

Quan-gang Xu  
xuquangang@126.com  
Shi-hui Wei  
weishihui706@hotmail.com

†These authors have contributed  
equally to this work

## SPECIALTY SECTION

This article was submitted to  
Brain Imaging and Stimulation,  
a section of the journal  
Frontiers in Human Neuroscience

RECEIVED 08 June 2022

ACCEPTED 20 September 2022

PUBLISHED 03 November 2022

## CITATION

Sun M-m, Zhou H-f, Sun Q, Li H-e,  
Liu H-j, Song H-l, Yang M, Teng D,  
Wei S-h and Xu Q-g (2022) Leber's  
hereditary optic neuropathy  
complicated with multiple-related  
diseases.  
*Front. Hum. Neurosci.* 16:964550.  
doi: 10.3389/fnhum.2022.964550

## COPYRIGHT

© 2022 Sun, Zhou, Sun, Li, Liu, Song,  
Yang, Teng, Wei and Xu. This is an  
open-access article distributed under  
the terms of the [Creative Commons  
Attribution License \(CC BY\)](#). The use,  
distribution or reproduction in other  
forums is permitted, provided the  
original author(s) and the copyright  
owner(s) are credited and that the  
original publication in this journal is  
cited, in accordance with accepted  
academic practice. No use, distribution  
or reproduction is permitted which  
does not comply with these terms.

# Leber's hereditary optic neuropathy complicated with multiple-related diseases

Ming-ming Sun<sup>1†</sup>, Huan-fen Zhou<sup>2†</sup>, Qiao Sun<sup>3†</sup>, Hong-en Li<sup>1</sup>,  
Hong-juan Liu<sup>4</sup>, Hong-lu Song<sup>1</sup>, Mo Yang<sup>5</sup>, Da Teng<sup>6</sup>,  
Shi-hui Wei<sup>2\*</sup> and Quan-gang Xu<sup>1\*</sup>

<sup>1</sup>Senior Department of Ophthalmology, The Third Medical Center of PLA General Hospital and Chinese PLA Medical School, Beijing, China, <sup>2</sup>Senior Department of Ophthalmology, The First Medical Center of PLA General Hospital and Chinese PLA Medical School, Beijing, China, <sup>3</sup>Department of Ophthalmology, Shanghai Aier Eye Hospital, Shanghai, China, <sup>4</sup>Beijing Ophthalmology and Visual Sciences Key Laboratory, Beijing Tongren Eye Center, Beijing Tongren Hospital, Capital Medical University, Beijing, China, <sup>5</sup>Department of Neuro-Ophthalmology, Eye Hospital, China Academy of Chinese Medical Sciences, Beijing, China, <sup>6</sup>Department of Ophthalmology, Beijing Tiantan Hospital, Beijing, China

**Objective:** To elucidate the clinical, radiologic characteristics of Leber's hereditary optic neuropathy (LHON) associated with the other diseases.

**Materials and methods:** Clinical data were retrospectively collected from hospitalized patients with LHON associated with the other diseases at the Neuro-Ophthalmology Department at the Chinese People's Liberation Army General Hospital (PLAGH) from December 2014 to October 2018.

**Results:** A total of 13 patients, 24 eyes (10 men and 3 women; mean age, 30.69 ± 12.76 years) with LHON mitochondrial DNA (mtDNA) mutations, were included in the cohort. 14502(5)11778(4)11778 & 11696(1)12811(1)11696(1)3460(1). One patient was positive for aquaporin-4 antibody (AQP4-Ab), and two were positive for myelin oligodendrocyte glycoprotein antibody (MOG-Ab). Three patients were associated with idiopathic optic neuritis (ON). Two patients were with compression optic neuropathy. Three patients were with the central nervous system (CNS) diseases. One patient was with proliferative diabetic retinopathy (PDR) and one with idiopathic orbital inflammatory syndrome (IOIS). At the onset, visual acuity (VA) in eighteen eyes was below 0.1, one eye was 0.5, five eyes were above 0.5, while VA in sixteen eyes was below a 0.1 outcome, three eyes experienced moderate vision loss. MRI images showed T2 lesions and enhancement in nine patients who received corticosteroids treatment; additional immune modulators treatment was performed on two patients. None of the patients had relapse during the follow-up time.

**Conclusion:** Leber's hereditary optic neuropathy can be accompanied with multiple-related diseases, especially different subtypes of ON, which were also

exhibited with IOIS and compression optic neuropathy for the first time in this cohort. This condition may be a distinct entity with an unusual clinical and therapeutic profile.

#### KEYWORDS

Leber's hereditary optic neuropathy, optic neuritis, aquaporin-4 antibody, myelin oligodendrocyte glycoprotein antibody, multiple sclerosis

## Introduction

Leber's hereditary optic neuropathy (LHON) is an inherited optic neuropathy characterized by subacute painless vision loss (Hudson et al., 2008). Retinal ganglion cells (RGCs) are preferentially affected, leading to optic nerve degeneration, but additional extraocular abnormalities have been described in LHON pedigrees. Previous studies suggest that LHON may be a systemic disorder with manifestations in organs other than the optic nerves (Nikoskelainen et al., 1995). These include non-neurological as well as neurological abnormalities. Since LHON was first described in 1926 by Mauksch and his colleagues; the association between CNS inflammatory demyelination and LHON was always controversial (Dujmovic et al., 2016). Until now, the relationship between LHON and the other diseases has not been clear, and whether the other organs may be involved in patients with LHON is unknown.

In clinical, we noticed 13 patients who carried mitochondrial DNA (mtDNA) mutations that were accompanied with the other diseases, including ocular disorders and systemic diseases. We conducted the current study to describe the clinical, laboratory, imaging presentations of MRI, and associated diseases at a single center, using data collected in a retrospective fashion.

## Patients and methods

The clinical records from December 2014 to October 2018 of hospitalized patients carried mtDNA mutations were selected from the Chinese People's Liberation Army General Hospital (PLAGH) in this study. The study protocol was approved by the institutional review board of the PLAGH and performed in accordance with the content of the Helsinki Declaration. All patients provided written informed consent to undergo examinations.

## Ophthalmologic and associated examinations

Ophthalmological examinations included a test for relative afferent pupillary defect (RAPD), and a direct and indirect

ophthalmoscopy to examine the retina. The best corrected visual acuity (BCVA) was tested using a Snellen chart, and a VA below 0.01 was documented with count finger (CF), hand motion (HM), perceived light, and no perceived light. The standard protocol for the Optic Disc Cube 200 × 200 circle scan and the Macular Cube 512 × 128 scan was performed using one of the two spectral-domain optic coherence tomography (SD-OCT) devices (Carl Zeiss Meditec, USA or Heidelberg Engineering, Germany). Blood was collected at the Rheumatologic Research Center in the PLAGH. Cerebrospinal fluid (CSF) samples were collected for the routine testing of white cell counts, total protein levels, and concentrations of IgG. Patients with LHON were diagnosed by screening for mtDNA. Cell-based assays (CBA) to detect the serum aquaporin-4 antibody (AQP4-Ab) and the myelin oligodendrocyte glycoprotein antibody (MOG-Ab) were performed for the patients with ON.

Magnetic resonance imaging was performed on a 3T system in eight patients with a T2-weighted image (T2WI) and a T1-weighted image (T1WI) sequences with fat suppression, and a gadolinium-enhanced T1. Proton Magnetic Resonance Spectroscopy (H-MRS) is performed when patients are accompanied with intracranial lesions.

The following data were analyzed: age, sex, age at the onset, the involved eye, time between two eyes, family history, laboratory findings, associated diseases, treatment, and prognosis.

## Results

### Demographics characteristics

**Table 1** summarizes their clinical characteristics, genotypes, and plus diseases. A total of 13 patients (10 males, 3 females; age range, 13–53 years) with genetically confirmed carried mtDNA mutations that were associated with the other diseases. Four patients carried the 11778 mutations, five patients carried the 14502 mutations, one patient carried the 12811 mutations, the 3460 mutations, the 11696 mutations, respectively. And, in one patient, the 11778 mutations were associated with 11696. Three patients had concomitant ION. Two patients complained with MOG-Ab positive; the titers were 1:10 and 1:100, respectively. One patient complained with AQP4-Ab



positive. Two patients were with compression optic neuropathy (hypophysoma and intracranial germinoma). Three patients with the central nervous system (CNS) diseases [multiple sclerosis (MS), leigh, and cranial neuropathy]. One patient with PDR and one with idiopathic orbital inflammatory syndrome (IOIS, orbital pseudotumor). Five patients were diagnosed with LHON prior, while eight patients were diagnosed with the other diseases prior. Two patients were confirmed in the maternal family.

## Clinical characteristics

A total of 182 patients (345 eyes) were diagnosed with LHON in our center, while 13 patients were diagnosed with LHON Plus; the frequency of LHON Plus in LHON was 7.14%. The age onset of LHON with other diseases and pure LHON were ( $25.9 \pm 3.1$ ) and ( $22.1 \pm 0.9$ ) years, respectively. In LHON Plus, 11 patients suffered simultaneous or sequential binocular involved, the time between two eyes from 1 month to 6 years; the average time was ( $30 \pm 17.16$ ) days. There was no significant difference between the age onset, involved eyes, and the time between two eyes of LHON Plus and pure LHON. The BCVA was significant difference between two groups; the visual function was better in LHON Plus than pure LHON, and we suspected the reason was the plus disease accepted effective treatment. The data between the two groups are listed in **Table 2**.

Four patients were RAPD positive. Approximately, 76.92% (10/13) patients had pale fundus, especially the temporal side. One patient had edema disk. Two patients had normal fundus. Nine patients (14 eyes) had distinctive visual field (VF)

**TABLE 2** The clinical characteristics between Leber's hereditary optic neuropathy (LHON) with other diseases and pure LHON.

	LHON plus	LHON	P
The age-onset (y)	$25.9 \pm 3.1$	$22.1 \pm 0.9$	0.28
Involved eyes (binocular)	11	163	0.64
The time between two eyes (d)	$30 \pm 17.16$	$48.26 \pm 12.74$	0.71
BCVA visual acuity	$0.51 \pm 0.13$	$0.90 \pm 0.03$	0.002

BCVA, best corrected visual acuity.

defection, which showed central or eccentric scotoma especially. The results of the VEP examination in 10 patients showed the delayed implicit period and lower amplitude. SD-OCT imaging of the peripapillary nerve fiber layer (pRNFL) showed diffuse thinning in eight patients (14 eyes); SD-OCT imaging of the macular retinal ganglion cell and inner plexiform layers (RGC-IPL) revealed ganglion cell atrophy, more severe in the nasal quadrants. **Figure 1** shows the images evidence and changes by fundus photography, humphrey VF testing, and SD-OCT images in different patients.

## Magnetic resonance imaging manifestation and cerebrospinal fluid tests

**Table 3** gives the orbit MRI and CSF test results. The 12 of 13 patients had optic nerve MRI scans in our hospital. T2WI images showed an increased signal of the optic nerve, and post-contrast T1WI with fat suppression showed abnormal enhancement of the optic nerve in six patients (**Figure 2**). Every

**TABLE 1** Clinical features data for 13 patients.

Case	Age at onset (years)	Involved eye(s)	Time between two eyes	Plus	Mutation	Family history	Visual acuity at onset		VA (outcome)	
							OD	OS	OD	OS
1/M/27	27	OU	/	MOG-ON	12811	/	0.6	0.6	1	0.8
2/M/23	22	OU	1 month	MOG-ON	14502	/	0.6	0.5	0.6	0.15
3/F/45	45	OU	/	NMO-ON	14502	/	CF	CF	CF	CF
4/M/27	26	OU	1 month	ION	11778	/	0.04	CF	0.08	0.02
5/M/17	17	OD	/	ION	11778	Positive	/	CF	/	CF
6/M/29	29	OU	/	ION	11696	/	0.8	0.04	0.8	0.5
7/M/33	33	OS	/	IGM	14502	/	/	HM	/	LP
8/M/19	19	OU	/	MS	14502	/	CF	CF	0.02	0.2
9/F/50	49	OU	6 month	IOIS	14502	/	0.8	0.02	1	0.02
10/M/23	23	OU	/	Hypophysoma	3460	/	CF	0.1	CF	0.1
11/F/13	7	OU	6 years	Leigh	11778	Positive	CF	CF	CF	CF
12/M/53	20	OU	/	Cranial neuropathy	11778	/	CF	CF	CF	CF
13/M/40	20	OU	3 month	PDR	11778, 11696	/	0.04	0.01	0.07	0.02

F, female; M, male; OD, oculus dexter; OS, oculus sinister; OU, oculus uterque; CF, counting fingers; HM, hand motion; ION, idiopathic optic neuritis; IGM, intracranial germinoma; MS, multiple sclerosis; IOIS, idiopathic orbital inflammatory syndrome; PDR, proliferative diabetic retinopathy.

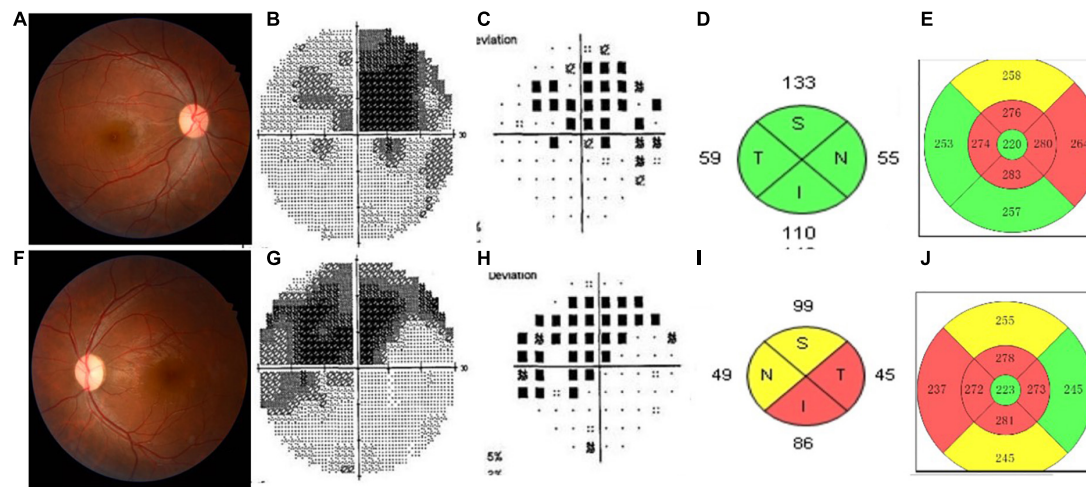


FIGURE 1

This shows the images evidence and changes in the patients with Leber's hereditary optic neuropathy (LHON). Color fundus photographs (A,F) demonstrate temporal optic nerve pallor OS (F). Humphrey visual field (VF) testing demonstrates a dense superior central scotoma OD (B,C) and a central scotoma with a superior arcuate defect OS (G,H), having mean deviations (MD) of  $-13.54$  and  $-12.73$ , respectively. SD-OCT imaging of the peripapillary nerve fiber layer (pRNFL) (D,I) showed diffuse thinning of the left eye (I). Spectral-domain optical coherence tomography (SD-OCT) imaging of the macular inner limiting membrane-retinal pigment epithelium (ILM-RPE) (E,J) revealed ganglion cell atrophy, more severe in the nasal quadrants involved left eye (J) than the right eye (E).

TABLE 3 The characteristics of MRI, treatment, and cerebrospinal fluid (CSF) with Leber's hereditary optic neuropathy (LHON) plus patients.

Case	MRI	Methylprednisolone, mg, initial		Prevention	CSF		
		Intravenous	Oral		WBC ( $10^6/L$ )	Total protein (mg/L)	IgG (mg/dl)
N					–	150~400	0~3.4
1/M/27	T2 lesions and enhancement (OS, Orbital) + T2 lesions (intracranial)	500	48	/	/	/	/
2/M/23	T2 lesions and enhancement (Optic chiasm)	1,000	48	Azathioprine	1	341.7	2.51
3/F/45	T2 lesions (Optic chiasm)	1,000	48	Azathioprine/ rituximab	0	321.1	2.79
4/M/27	T2 lesions and enhancement (OS, Orbital)	1,000	48	/	2	521.5	3.47
5/M/17	T2 lesions and enhancement (OS, Orbital + Canalicular)	1,000	48	/	2	382.1	2.74
6/M/29	T2 lesions and enhancement (OU, Orbital)	1,000	64	/	0	323.7	2.58
7/M/33	T2 lesions and enhancement (OS, Optic nerve + Optic chiasm)	1,000	64	/	12	527.9	5.33
8/M/19	T2 lesions (intracranial + Optic nerve + Optic chiasm)	250	48	/	1	292.2	1.04
9/F/50	T2 lesions and enhancement (OS, Orbital + Canalicular)	1,000	48	/	/	/	/
10/M/23	Postoperative changes of hypophysoma	/	/	/	/	/	/
11/F/13	T2 lesions (intracranial)	/	/	/	/	/	/
12/M/53	T2 lesions (intracranial)	/	/	/	/	/	/
13/M/40	/	/	/	/	/	/	/

OD, oculus dexter; OS, oculus sinister; OU, oculus uterque.

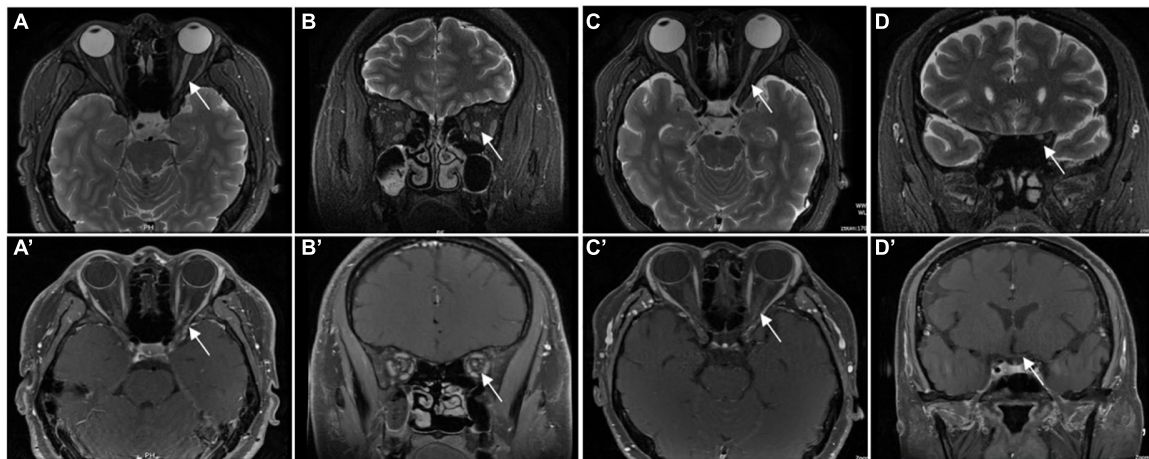


FIGURE 2

Orbital MRI images in patients who were diagnosed with ON. Panels (A,C) (axial) and (B,D) (coronal) showed the high signal of the left ON (the white arrow) in T2WI. Panels (C) (axial) and (D) (coronal) showed the enhancement of left ON (the white arrow) in gadolinium-enhanced T1. Panels (A') (axial) and (B') (coronal) showed the enhancement of left ON (white arrow) in gadolinium enhanced T1. Panels (C') (axial) and (D') (coronal) showed the normal signal of left ON (the white arrow) in gadolinium-enhanced T1.

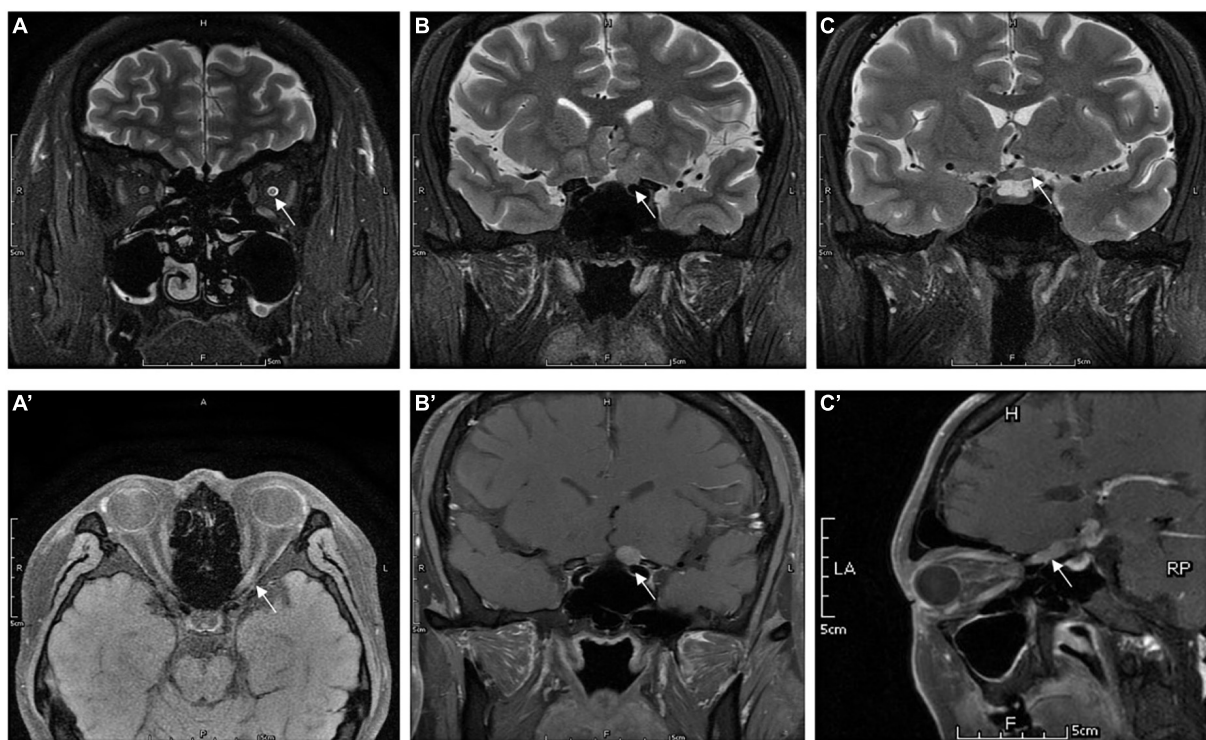


FIGURE 3

Orbital MRI images in patients who were diagnosed with IGM (case 7): panels (A) (axial), and (B,C) (coronal) showed the hypersignal of the optic nerve (the white arrow) extends to optic chiasm in T2WI. Panels (A') (axial), (B') (coronal), and (C') (sagittal) showed the enhancement of left ON (the white arrow) in gadolinium-enhanced T1.

segment of the optic nerve may be involved. In the patients with optic nerve tumor, T2WI images showed an increased signal, and post-contrast T1WI with fat suppression showed abnormal

enhancement of the enlarged optic nerve (Figure 3). The typical MRI characteristics of MS are as follows: periventricular lesions, which are arranged perpendicular to the ventricular margin,

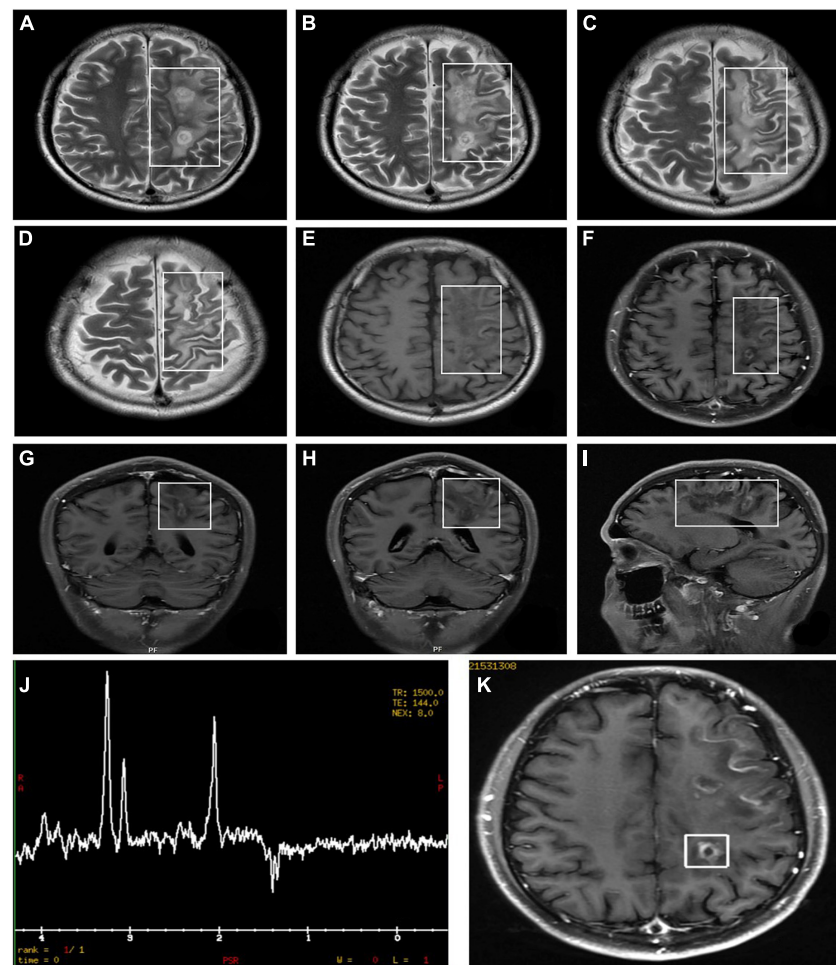


FIGURE 4

Orbital MRI images in patients who were diagnosed with LHON-MS (case 9). The figure showed multiple lesions presented with an abnormal signal (A–I). MRI findings (K) and Proton Magnetic Resonance Spectroscopy (H-MRS) findings (J) in the proband of Pedigree 1—multiple demyelinating lesions in the left cerebrum (MRI) and an inverted double peak of lactic acid (Lac) at 1.33 ppm (H-MRS).

Dawson's fingers (Figure 4). Axial and coronal T1WI with fat suppression and contrast showed left optic nerve enhancement at the level of the orbital apex, which diagnosed IOIS. T2WI images showed intracranial lesions without enhancement in four patients. H-MRS images showed lactic acid peak in one patient (Figure 4). Seven (7/13, 53.85%) of the patients had lumbar puncture and the CSF test; two had both elevated total protein concentration of 521.5 and 527.9 mg/l (normal range, 150–400 mg/l) and elevated IgG concentration of 3.47 mg/dl and 5.33 mg/dl in CSF (normal range, 0–3.4 mg/l, Table 3), respectively.

## Treatment and prognosis

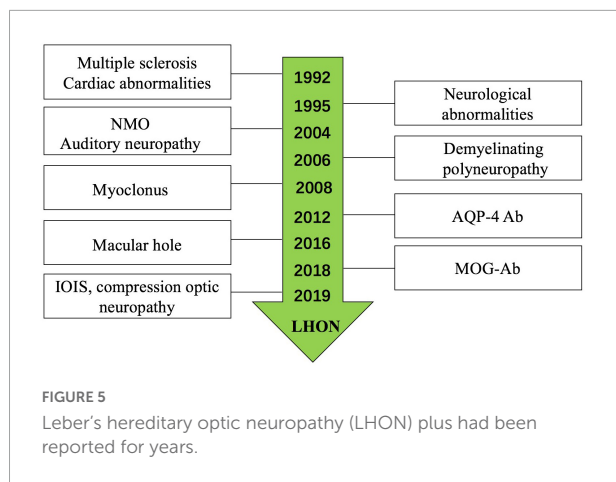
In this study cohort, 75% (18/24) of the eyes experienced severe vision loss ( $\leq 0.1$ ) at the onset, only one eye experienced

moderate vision loss (0.1–0.5), five eyes experienced mild vision loss ( $\geq 0.5$ ). Steroid therapy was performed for nine patients with MRI changes. Two patients received immune modification therapy (azathioprine/rituximab) with AQP-Ab or MOG-Ab positive. Vision improved in seven patients, unchanged in four patients, and worse in two patients (Table 1). The follow-up duration ranged from 12 to 58 months, with a mean time of ( $31 \pm 17.12$ ) months. One patient suffered from cranial surgery, and the pathological test revealed the IGM diagnosed. The other patients were with no recurrence.

## Discussion

Leber's hereditary optic neuropathy plus has been reported by many researchers; a systematic review of the literature was conducted on all publications on LHON plus since the





original description by [Harding et al. \(1992\)](#) (**Figure 5**; [Bower et al., 1992](#); [Harding et al., 1992](#); [Nikoskelainen et al., 1995](#); [Ceranić and Luxon, 2004](#); [McFarland et al., 2007](#); [La Morgia et al., 2008](#); [Shiraishi et al., 2014](#); [Shimada and Horiguchi, 2016](#); [Bittner et al., 2019](#)); the most common disease was LHON-MS (Harding disease) ([Harding et al., 1992](#); [Kellar-Wood et al., 1994](#); [Bhatti and Newman, 1999](#)). The last decade witnessed important discoveries in immune-mediated diseases of the optic nerve; the recognition of LHON plus is increasingly clear. There were studies reported LHON comorbidity with MOG-Ab ([Bittner et al., 2019](#)) and NMO ([Bhatti and Newman, 1999](#)). While in our single neuro-ophthalmology center, we found six (46.15%) patients who were comorbid with ON, in which two patients were with MOG-Ab positive ([Shiraishi et al., 2014](#)) and one patient with AQP4-Ab positive. The ratio of different subtypes of optic neuritis (ON) was higher than the other diseases; we analyzed the reason may be our center is the neuro-ophthalmology department, while the other centers are the neurology department. We also found LHON accompanied with IOIS and compression optic neuropathy, which were unreported before; only [Jones et al. \(2018\)](#) reported a case of saccular left renal artery aneurysm in a 27-year-old man with known LHON.

Approximately, 90% patients carry one of the three primary mtDNA mutations: 11778, 3460, or 14484 ([Harding et al., 1995](#); [Mackey et al., 1996](#); [Newman and Biousse, 2004](#)). While, in our study, the ratio of these three mutations was only 46.15% and none of the 14484 mutations were found. The clinical characteristics of LHON Plus may be varied. But the SD-OCT results show that more severe ganglion cell atrophy in the nasal quadrants is homogeneous, which reminds to test mtDNA mutations. The visual acuity of patients with LHON may be stable in a previous study; most patients may suffer low visual acuity ( $\leq 0.1$ ). Although most patients with LHON Plus suffer severe vision loss,

they will recover after accepted corrected and symptomatic treatment. According to the guideline, patients diagnosed with NMOSD should give immune modification therapy to involve relapse.

The most common disease in our study is CNS inflammatory demyelination disease; MRI is the modality of choice for investigating ON, compressive lesions, and the other diseases. An MRI can be performed to evaluate a patient's potential benefit from intravenous methylprednisolone and disease-modifying therapy. Eleven patients presented with optic nerve or intracranial T2 lesions and (or) enhanced T1 lesions; nine patients received intravenous methylprednisolone therapy, two patients. So we suggest the patients who had diagnosed LHON should perform MRI examination.

A few limitations existed in this cohort study. First, we only report the ratio of LHON Plus in-patients in a single neuro-ophthalmology center. Second, the study only found LHON accompanied with AQP4-Ab positive, but the pathogeny is unknown; we cannot clearly explain the reason of the visual loss. Another limitation was the follow-up timer was not enough; we cannot make sure whether the patients were diagnosed with LHON or carried mtDNA mutations, especially in some patients who had one eye involved.

## In summary

Leber's hereditary optic neuropathy plus may be a clinical syndrome associated with multiple diseases; even normal people will carry with mutations, which still need investigation. When field vision of the patient showed the blind spot in the temporal or SD-OCT imaging of the macular RGC-IPL revealed ganglion cell atrophy, more severe in the nasal quadrants; we suggested that the patient undergo LHON mutation examination. An MRI examination is necessary. The treatment should be dependent on the clinical and examination results; the prognosis is relatively ideal.

## Data availability statement

The original contributions presented in this study are included in the article/supplementary material, further inquiries can be directed to the corresponding authors.

## Ethics statement

Written informed consent was obtained from the individual(s), and minor(s)' legal guardian/next of kin, for

the publication of any potentially identifiable images or data included in this article.

## Author contributions

H-FZ and S-HW designed and conducted the study. M-MS, QS, H-EL, H-LS, H-JL, MY, and DT collected, analyzed, managed, and interpreted the data. M-MS and H-FZ prepared the manuscript and conducted the statistical analysis. H-FZ and Q-GX performed critical revision of the manuscript. All authors reviewed and approved the final version of the manuscript.

## Funding

This work was supported by a grant from the Key Program for International S&T Cooperation Projects of China project “The molecular mechanism research of ACT001

targeting microglia for neuromyelitis optica therapy” (No. 2018YFE0113900).

## Conflict of interest

The authors declare that the research was conducted in the absence of any commercial or financial relationships that could be construed as a potential conflict of interest.

## Publisher's note

All claims expressed in this article are solely those of the authors and do not necessarily represent those of their affiliated organizations, or those of the publisher, the editors and the reviewers. Any product that may be evaluated in this article, or claim that may be made by its manufacturer, is not guaranteed or endorsed by the publisher.

## References

- Bhatti, M., and Newman, N. J. (1999). A multiple sclerosis-like illness in a man harboring the mtDNA 14484 mutation. *J. Neuroophthalmol.* 19, 28–33.
- Bittner, F., Falardeau, J., and Spain, R. (2019). Myelin oligodendrocyte glycoprotein antibody-associated demyelination comorbid with leber hereditary optic neuropathy. *JAMA Neurol.* 76, 227–228. doi: 10.1001/jamaneurol.2018.3207
- Bower, S., Hawley, L., and Mackey, D. (1992). Cardiac arrhythmia and Leber's hereditary optic neuropathy. *Lancet* 339, 1427–1428. doi: 10.1016/0140-6736(92)91257-9
- Ceranić, B., and Luxon, L. (2004). Progressive auditory neuropathy in patients with Leber's hereditary optic neuropathy. *J. Neurol. Neurosurg. Psychiatry* 75, 626–630. doi: 10.1136/jnnp.2003.017673
- Dujmovic, I., Jancic, J., Dobricic, V., Jankovic, M., Novakovic, I., Comabella, M., et al. (2016). Are Leber's mitochondrial DNA mutations associated with aquaporin-4 autoimmunity? *Mult. Scler.* 22, 393–394. doi: 10.1177/1352458515590649
- Harding, A., Sweeney, M., Govan, G., and Riordan-Eva, P. (1995). Pedigree analysis in Leber hereditary optic neuropathy families with a pathogenic mtDNA mutation. *Am. J. Hum. Genet.* 57, 77–86.
- Harding, A., Sweeney, M., Miller, D., Mumford, C., Kellar-Wood, H., Menard, D., et al. (1992). Occurrence of a multiple sclerosis-like illness in women who have a Leber's hereditary optic neuropathy mitochondrial DNA mutation. *Brain* 115 (Pt 4), 979–989. doi: 10.1093/brain/115.4.979
- Hudson, G., Mowbray, C., Elson, J., Jacob, A., Boggild, M., Torroni, A., et al. (2008). Does mitochondrial DNA predispose to neuromyelitis optica (Devic's disease)? *Brain*. 131:e93. doi: 10.1093/brain/awm224
- Jones, R., Lee, J., and Ali, M. (2018). Renal artery aneurysm associated with Leber hereditary optic neuropathy. *J. Vasc. Surg. Cases Innov. Tech.* 4, 5–7. doi: 10.1016/j.jvscit.2017.10.001
- Kellar-Wood, H., Robertson, N., Govan, G., Compston, D., and Harding, A. (1994). Leber's hereditary optic neuropathy mitochondrial DNA mutations in multiple sclerosis. *Ann. Neurol.* 36, 109–112. doi: 10.1002/ana.410360121
- La Morgia, C., Achilli, A., Iommarini, L., Barboni, P., Pala, M., Olivieri, A., et al. (2008). Rare mtDNA variants in Leber hereditary optic neuropathy families with recurrence of myoclonus. *Neurology* 70, 762–770. doi: 10.1212/01.wnl.0000295505.74234.d0
- Mackey, D., Oostra, R., Rosenberg, T., Nikoskelainen, E., Bronte-Stewart, J., Poulton, J., et al. (1996). Primary pathogenic mtDNA mutations in multigeneration pedigrees with Leber hereditary optic neuropathy. *Am. J. Hum. Genet.* 59, 481–485.
- McFarland, R., Chinnery, P., Blakely, E., Schaefer, A., Morris, A., and Foster, S. (2007). Homoplasmy, heteroplasmy, and mitochondrial dystonia. *Neurology* 69, 911–916. doi: 10.1212/01.wnl.0000267843.10977.4a
- Newman, N., and Biousse, V. (2004). Hereditary optic neuropathies. *Eye (Lond)*. 18, 1144–1160. doi: 10.1038/sj.eye.6701591
- Nikoskelainen, E., Marttila, R., Huoponen, K., Juvonen, V., Lamminen, T., Sonninen, P., et al. (1995). Leber's “plus”: Neurological abnormalities in patients with Leber's hereditary optic neuropathy. *J. Neurol. Neurosurg. Psychiatry* 59, 160–164. doi: 10.1136/jnnp.59.2.160
- Shimada, Y., and Horiguchi, M. (2016). Leber hereditary optic neuropathy associated with bilateral macular holes. *Neuroophthalmology* 40, 125–129. doi: 10.3109/01658107.2016.1148744
- Shiraishi, W., Hayashi, S., Kamada, T., Isobe, N., Yamasaki, R., Murai, H., et al. (2014). A case of neuromyelitis optica harboring both anti-aquaporin-4 antibodies and a pathogenic mitochondrial DNA mutation for Leber's hereditary optic neuropathy. *Mult. Scler.* 20, 258–260. doi: 10.1177/1352458513513057

# Frontiers in Human Neuroscience

Bridges neuroscience and psychology to  
understand the human brain

The second most-cited journal in the field of  
psychology, that bridges research in psychology  
and neuroscience to advance our understanding  
of the human brain in both healthy and diseased  
states.

## Discover the latest Research Topics

See more →

### Frontiers

Avenue du Tribunal-Fédéral 34  
1005 Lausanne, Switzerland  
[frontiersin.org](https://frontiersin.org)

### Contact us

+41 (0)21 510 17 00  
[frontiersin.org/about/contact](https://frontiersin.org/about/contact)

